INFORMATION TO USERS

This manuscript has been reproduced from the microfilm master. UMI films the text directly from the original or copy submitted. Thus, some thesis and dissertation copies are in typewriter face, while others may be from any type of computer printer.

The quality of this reproduction is dependent upon the quality of the copy submitted. Broken or indistinct print, colored or poor quality illustrations and photographs, print bleedthrough, substandard margins, and improper alignment can adversely affect reproduction.

In the unlikely event that the author did not send UMI a complete manuscript and there are missing pages, these will be noted. Also, if unauthorized copyright material had to be removed, a note will indicate the deletion.

Oversize materials (e.g., maps, drawings, charts) are reproduced by sectioning the original, beginning at the upper left-hand corner and continuing from left to right in equal sections with small overlaps.

ProQuest Information and Learning
300 North Zeeb Road, Ann Arbor, MI 48106-1346 USA
800-521-0600

Transmembrane signalling and transport in *Escherichia coli*: Crystal structures of FhuA and liganded complexes

By

Andrew D. Ferguson

Department of Microbiology and Immunology
McGill University, Montréal
May 2000

A thesis submitted to the Faculty of Graduate Studies and Research in partial fulfilment of the requirements of the degree of Doctor of Philosophy

"It is not so very important for a person to learn facts. For that he does not really need a college. He can learn them from books. The value of an education is not the learning of many facts but the training of the mind to think something that cannot be learned from textbooks."

-Albert Einstein

Table of contents

Abstract

Ph.D. **Andrew D. Ferguson** **Microbiology and Immunology**

In *Escherichia coli*, FhuA, together with the energy-transducing TonB-ExbB-ExbD complex, mediates the uptake of hydroxamate-type siderophores across the outer membrane. In addition to transporting ferrichrome, FhuA functions as the primary receptor for several bacteriophages, antibiotics, and colicin M. To comprehend how FhuA binds its cognate ligands, and to establish the molecular basis of active transport, the three-dimensional structure must be determined. In pursuit of this goal, an affinity tag was inserted into the *fhuA* gene at a known surface-exposed location. The recombinant FhuA protein was overexpressed and purified by metal-chelate chromatography. Sparse matrix screening established parameters for the growth of well-ordered crystals of FhuA. The crystallographic structure of FhuA and its complex with ferricrocin were solved at 2.50 and 2.70 Å by multiwavelength anomalous dispersion. The crystallographic structure reveals that FhuA is a monomeric integral outer membrane protein that is composed of two domains. The C-terminal domain, a 22-stranded antiparallel β-barrel, spans the outer membrane. Positioned within the β-barrel is the N-terminal 'cork' domain, which is formed by a mixed four-stranded β-sheet with four interspersed α-helices. Upon binding of ferricrocin, conformational changes are propagated from the extracellular pocket to the periplasmic pocket of FhuA; a transmembrane signal indicating the liganded status of the receptor. Structural analysis combined with sequence homologies and mutagenesis data are used to propose a mechanism for TonB-dependent siderophore-mediated iron acquisition.

Noncovalently associated with the membrane-embedded surface of FhuA is a single lipopolysaccharide molecule. Following the examination of electrostatic protein-lipid contacts, a structure-based algorithm revealed a conserved four-residue LPS-binding motif that is present among known LPS-binding proteins.

An expansion of these structural studies was the solution of the crystallographic structures of additional liganded complexes. The three-dimensional structures of FhuA in

complex with the antibiotics albomycin and rifamycin CGP 4832 were determined at 3.10 and 2.90 Å, respectively. In addition to probing the plasticity and accessibility of the ligand-binding site, these results establish a structural platform for the design of novel antibiotics. Moreover, insights into the physical association of FhuA with TonB can be derived from these data.

Résumé

Ph.D. **Andrew D. Ferguson** **Microbiologie et Immunologie**

Chez *Escherichia coli*, FhuA, de concert avec le complexe TonB-ExbB-ExbD, médie l'importation des sidérophores à travers la membrane externe. En plus de transporter les ferricrocines, FhuA agit comme récepteur pour différents bactériophages, antibiotiques et pour la toxine bactérienne colicine M. Pour bien comprendre comment FhuA lie ses ligands et afin d'établir les bases moléculaires du transport actif, la structure tri-dimensionnelle devait être déterminée. Un peptide poly-histidine a été inséré dans la protéine FhuA à un endroit démontré être à la surface. La protéine recombinante a été surexprimée puis purifiée par chromatographie d'affinité pour le métal. Le criblage par matrice éparse a permis d'établir les paramètres pour la croissance de cristaux bien structurés. La structure cristallographique de FhuA et de celle de FhuA complexée avec le ferricrocine a été résolue à 2.50 et 2.70 Å par MAD. La structure cristallographique révèle que FhuA est une protéine monomérique intégrée à la membrane externe et composée de deux domaines. Le domaine C-terminal, un baril-β composé de 22 brins antiparallèles, traverse la membrane externe. Le domaine N-terminal est situé à l'intérieur du baril-β formant ainsi un 'bouchon'. Il est constitué d'un feuillet de 4 brins β, avec 4 hélices α intercalées. Suite à la liaison du ferricrocine, des changements conformationnels se propagent de la poche extracellulaire à la poche périplasmique de FhuA; ceci constituerait un signal transmembranaire indiquant l'état d'occupation du récepteur. L'analyse de la structure, combinée à des données de mutagenèse et d'homologie de séquences, est utilisée pour proposer un mécanisme pour l'acquisition du fer, médiée par les sidérophores, via TonB.

Une molécule de lipopolysaccharide est associée de façon non-covalente à la surface de FhuA enchassée dans la membrane. Suite à l'étude des contacts électrostatiques protéine-lipide, un algorithme basé sur la structure a révélé la présence d'un motif conservé de 4 résidus liant les LPS. Ce motif est également retrouvé chez d'autres proteines qui lient les LPS.

Nous avons ensuite déterminé la structure cristallographique de FhuA complexée avec d'autres ligands. La structure de la protéine liée aux antibiotiques albomycine et rifamycine CGP 4832 a été déterminée respectivement à 3.10 et 2.90 Å. En plus de démontrer la plasticité et l'accessibilité du site de liaison du ligand, ces résultats établissent une base structurale pour le design de nouveaux antibiotiques. De plus, ces données permettent de spéculer quant aux mécanismes d'interaction entre le baril-β de FhuA et TonB.

Acknowledgements

I wish to express my sincere thanks to my thesis supervisor, Dr. Ward. His kindness and scientific integrity allowed me to complete my graduate studies at McGill University under difficult circumstances. The constant support provided by Dr. Worobec, University of Manitoba is gratefully acknowledged. She taught me that you must have long-term goals to keep from being frustrated by short-term failures. The contributions of Drs. Boismenu, Butler, Crago, DuBow, and Mamer are appreciated. I also thank Martin Houle and Nathalie Bouchard for their assistance.

Drs. Diederichs and Welte, Universität Konstanz welcomed me into their laboratory. Dr. Diederichs taught me how to think critically, to conduct experimental work with patience and diligence, to explore all the possibilities, and to never, settle for second place. Dr. Welte showed me what it means to be a true scientist. His endless fascination, wisdom and generosity are truly inspirational. Drs. Breed and Hofmann, in different ways, made positive contributions to my studies at the Universität Konstanz. I also wish to thank Dr. Braun, Universität Tübingen for providing materials, stimulating discussions and support.

The assistance of Dr. Degano, beam line 5.2 R, ELETTRA; Dr. Gonzalez, beam line X31, DESY; Dr. Svensson, beam line I711, Max-Lab II; and in particular, Dr. Thompson, beam line BM14, ERSF; during data collection is gratefully acknowledged.

I wish to thank my family for their support and encouragement throughout my graduate program. I owe my greatest debt of gratitude to my partner and best friend, Deborah. Her selflessness, constant encouragement, patience, and understanding give me strength. Without her unconditional love and support, I would not have been able to complete this journey.

Finally, financial support from the CSA; Deutsche Forschungsgemeinschaft; DAAD; DESY; ELETTRA; EMBL; ERSF; McGill University; MRC of Canada; Max-Lab II; NSERC of Canada; and NATO is also acknowledged.

Claim of contribution to original knowledge

1. Conditions for the large-scale purification (under native conditions) of hexahistidine tagged FhuA proteins were established and optimized. This protocol proved to be essential for the growth of well-ordered protein crystals, and ultimately, the solution of the three-dimensional structure of FhuA. This unique method has broad applicability for the isolation of other affinity-labelled outer membrane proteins.

2. The sparse matrix screening method was implemented to identify crystal growth conditions for seven different hexahistidine tagged FhuA proteins solubilized with numerous primary detergents. Full-length recombinant proteins [FhuA321.H_6, FhuA405.H_6] and those with internal deletions [FhuA(Δ21-128)405.H_6, FhuA(Δ322-355)405.H_6, FhuA(Δ322-335)405.H_6, and FhuA(Δ335-355).H_6] were assessed. Variations in crystal growth parameters for one recombinant protein, FhuA405.H_6, overexpressed using various *E. coli* K-12 background strains (AW740, BL21, and DL41) were also characterized. This study produced the first published report of the growth of diffraction quality crystals of a TonB-dependent receptor.

3. Conditions for the growth of well-ordered crystals of FhuA in complex with a single LPS molecule were established and optimized. Purification and crystal growth parameters for the co-crystallization of any protein with LPS had not been described previously.

4. Expression and purification protocols for the isolation of a selenomethionine derivative of FhuA were established, and crystal growth conditions identified and refined. This represents the first example of the application of the multiwavelength anomalous dispersion phasing technique to the structural solution of an integral membrane protein.

5. A study describing the use of a novel additive termed *cis*-inositol for the growth of higher quality water-soluble and membrane protein crystals is presented. This detergent-based additive modulates crystal growth kinetics such that larger more regular crystals with increased internal order are obtained. When *cis*-inositol was included in the crystallization buffer, the observed diffraction limit for FhuA crystals was extended from 2.70 to 2.50 Å resolution. However, the broad applicability of this substance as a crystal growth additive remains to be established.

6. The three-dimensional structure of FhuA in complex with a single LPS molecule has been determined at 2.50 Å resolution. This study describes the first structure of a TonB-dependent receptor, and establishes a structural model for other high-affinity outer membrane receptors.

7. The crystal structure of FhuA in complex with ferricrocin has been determined at 2.70 Å resolution. This work describes the first structure of a liganded active outer membrane transporter. Ligand-induced conformational changes are propagated through the outer membrane from the extracellular pocket to the periplasmic pocket of the receptor. Using genetic, mutagenesis and structural data, a siderophore-mediated iron transport mechanism, applicable to all TonB-dependent receptors, has been proposed.

8. The three-dimensional structures of two *E. coli* K-12 LPS molecules have been solved at 2.50 and 2.70 Å, respectively. These structures represent the only LPS structures elucidated thus far, and describe the sole structures of a binary complex of an outer membrane protein with LPS. Using these structures a common four-residue LPS-binding motif that is conserved among known LPS-binding proteins of prokaryotic and eukaryotic origin has been identified. This system provides a foundation for the design of LPS-binding proteins with modified activities, the determination of the crystallographic structures of other LPS chemotypes, and may prove useful in isolating ternary complexes with LPS-binding proteins.

9. The crystallographic structure of FhuA in complex with phenylferricrocin has been elucidated at 2.95 Å resolution. This study provides the first structural description of this siderophore, and further probes the accessibility and plasticity of the ligand-binding site of FhuA.

10. The three-dimensional structure of FhuA in complex with the antibiotic albomycin has been solved at 3.10 Å resolution. This structure represents the first structure of the antibiotic albomycin, and provides the structural basis for the rational design of siderophore-antibiotic conjugates. Moreover, this structure describes the first example of an outer membrane transporter with an antibiotic bound in the ligand-binding site.

11. The crystal structure of FhuA in complex with the semi-synthetic rifamycin derivative CGP 4832 has been determined at 2.90 Å resolution. This study establishes the only three-dimensional structure of rifamycin CGP 4832, and the second example of an active outer membrane transporter in complex with an antibiotic. This crystallographic structure is similar to, yet distinct from, all previous liganded FhuA complexes elucidated thus far. Specifically, a third conformation of the cork domain has been identified. By consolidating the available genetic, biochemical and structural data, a TonB-dependent mechanism of ligand transport in which the TonB-box and one or more periplasmic turns of β-barrel form interactions with the energy-transducer TonB, is proposed. The crystallographic information derived from this study may also guide the design of receptor-specific antibiotics.

Manuscripts and authorship

In accord with the Faculty of Graduate Studies and Research, McGill University 'Guidelines Concerning Thesis Preparation', I have chosen to present the experimental portion of this thesis (chapters 2, 3, 4, 5, 6, and 7) in the form of manuscripts. A provision in these guidelines states:

"Candidates have the option of including, as part of the thesis, the text of one or more papers submitted, or to be submitted, for publication, or the clearly duplicated text (not the reprints) of one or more published papers. These texts must conform to the 'Guidelines for Thesis Preparation' with respect to font size, line spacing, and margin sizes, and must be bound together as an integral part of the thesis (reprints of the published papers can be included in appendices at the end of the thesis).

The thesis must be more than a collection of manuscripts. All components must be integrated into a cohesive unit with a logical progression from one chapter to the next. In order to ensure that the thesis has continuity, connecting texts that provide logical bridges between the different papers are mandatory.

The thesis must still conform to all other requirements of the 'Guidelines Concerning Thesis Preparation'. The thesis must include: a table of contents; an abstract in English and French; an introduction which clearly states the rationale and objectives of the research; a comprehensive review of the literature (in addition to that covered in the introduction to each paper); a final conclusion and summary; and a thorough bibliography or reference list.

As manuscripts for publication are frequently very concise documents, where appropriate, additional material must be provided (e.g. in appendices) in

sufficient detail to allow a clear and precise judgement to be made of the importance and originality of the research reported in the thesis.

In general, when co-authored papers are included in a thesis the candidate must have made a substantial contribution to all papers included in the thesis. In addition, the candidate is required to make an explicit statement in the thesis as to who contributed to such work and to what extent. This statement should appear in a single section entitled 'Contribution of Authors' as a preface to the thesis. The supervisor must attest to the accuracy of this statement at the doctoral oral defence. Since the task of examiners is made more difficult in these cases, it is in the candidate's interest to make perfectly clear the responsibilities of all authors of the co-authored papers."

Contribution of authors

The manuscripts that compose the experimental chapters of this thesis are listed below. The contributions of individual co-authors with respect to the experimental work are specified for each manuscript. I am responsible for the remainder of the presented work and composed the text of all the manuscripts, unless otherwise indicated. Drs. Braun, Breed, Coulton, Diederichs, Hofmann, Holst, Lindner, Ward, and Welte edited select manuscripts. This research was conducted under the co-supervision of Drs. Coulton, Diederichs, Ward, and Welte. Some experiments were performed in the laboratories of Drs. Braun, Fiedler, Hergetschweiler, Holst, and Lindner.

1. **Andrew D. Ferguson, Jason Breed, Kay Diederichs, Wolfram Welte & James W. Coulton** (1998). An internal affinity-tag for purification and crystallization of the ferrichrome-iron receptor FhuA, an integral outer membrane protein from *Escherichia coli* K-12. *Protein Science* 7:1636-1638 (presented as chapter two).

   Dr. Breed provided suggestions concerning the optimization of crystal growth strategies.
   Dr. Diederichs assisted in data collection and reduction.
   Dr. Welte granted access to laboratory equipment, computer facilities, and provided chemical reagents.
   Dr. Coulton provided *E. coli* K-12 strain AW740/pHX405.

2. **Andrew D. Ferguson, Kaspar Hergetschweiler, Bernd Morgenstern, Wolfram Welte & Jason Breed** (2000). *cis*-inositol: an additive for the growth of protein crystals. Submitted (presented as chapter three).

   Dr. Hergetschweiler provided *cis*-inositol.
   B. Morgenstern synthesized *cis*-inositol.

Dr. Welte granted access to laboratory equipment, computer facilities, and provided chemical reagents.

Dr. Breed initiated crystal growth experiments with *cis*-inositol as a crystal growth additive for water-soluble proteins. He also provided supplementary data concerning the effect of this additive for the growth of hen egg white lysozyme crystals. Dr. Breed contributed equally to the writing of this manuscript.

3. **Andrew D. Ferguson, Eckhard Hofmann, James W. Coulton, Kay Diederichs & Wolfram Welte** (1998). Siderophore-mediated iron transport: Crystal structure of FhuA with bound lipopolysaccharide. *Science* **282**:2215-2220 (presented as chapter four).

Dr. Hofmann assisted in experimental phase determination, and model building and structural refinement.

Dr. Coulton provided *E. coli* K-12 strains AW740 and DL41, harbouring plasmid-encoded recombinant FhuA.

Dr. Diederichs supervised all aspects of data collection and reduction, experimental phase determination, model building and structural refinement.

Dr. Welte granted access to laboratory equipment, computer facilities, and provided chemical reagents. He also participated in the development of a mechanism for TonB-dependent siderophore-mediated transport, and the writing of select portions of this manuscript.

4. **Andrew D. Ferguson, Wolfram Welte, Eckhard Hofmann, Buko Lindner, Otto Holst, James W. Coulton & Kay Diederichs** (2000). A conserved structural motif for lipopolysaccharide recognition by prokaryotic and eukaryotic proteins. *Structure* In press (presented as chapter five).

Dr. Welte granted access to laboratory equipment, computer facilities, and provided chemical reagents.

Dr. Hofmann assisted in the construction of structural models for LPS.

Dr. Lindner collected matrix assisted laser-desorption ionization mass spectrometry data from purified LPS.

Dr. Holst conducted chemical composition analysis and collected nuclear magnetic resonance data from purified LPS.

Dr. Coulton provided *E. coli* K-12 strain AW740/pHX405.

Dr. Diederichs applied the computational method that to identify a common LPS-binding motif. He also contributed equally to the writing of this manuscript.

5. **Andrew D. Ferguson, Volkmar Braun, Hans-Peter Fiedler, James W. Coulton, Kay Diederichs & Wolfram Welte** (2000). Crystal structure of the antibiotic albomycin in complex with the outer membrane transporter FhuA. *Protein Science* In press (presented as chapter six).

Dr. Braun provided phenylferricrocin.

Dr. Fiedler provided albomycin.

Dr. Coulton provided *E. coli* K-12 strain AW740/pHX405.

Dr. Diederichs assisted in data collection and reduction.

Dr. Welte granted access to laboratory equipment, chemical reagents, and computer facilities.

6. **Andrew D. Ferguson, Jiri Ködding, Georg Walker, James W. Coulton, Kay Diederichs, Volkmar Braun & Wolfram Welte** (2000). Crystal structure of a rifamycin derivative in complex with the active outer membrane transporter FhuA. To be submitted (presented as chapter seven).

J. Ködding assisted in the co-crystallization of FhuA with rifamycin CGP 4832.

G. Walker collected intrinsic tryptophan fluorescence data.

Dr. Coulton provided *E. coli* K-12 strain AW740/pHX405.

Dr. Diederichs carried out data reduction.

Dr. Braun arranged for the synthesis and purification of rifamycin CGP 4832. He also provided supplementary data and evaluated the bactericidal activity and FhuA-mediated uptake of this antibiotic.

Dr. Welte granted access to laboratory equipment, chemical reagents, and computer facilities.

7. **Andrew D. Ferguson, James W. Coulton, Kay Diederichs & Wolfram Welte** (2000). The ferric hydroxamate uptake receptor FhuA and related TonB-dependent transporters in the outer membrane of gram-negative bacteria. *Handbook of Metalloproteins*. K. Wieghardt, R. Huber, T.L. Poulos, A. Messerschmidt, (eds.), John Wiley & Sons, Chichester, UK (To minimize any repetition of material presented in chapter one of this thesis, this manuscript is not included).

Rationale and objectives of the thesis

The objective of this thesis is to provide a better understanding of the structure-function relationships of bacterial outer membrane transporters. To fully comprehend how these proteins bind their cognate ligands and to establish the molecular basis of energy-dependent transport, their three-dimensional structures must be determined. FhuA, the receptor for ferrichrome from *E. coli*, is a member of a family of integral outer membrane proteins, which, together with the energy-transducing protein TonB, mediate the active transport of siderophores and vitamin B_{12} across the outer membrane of gram-negative bacteria. This multifunctional receptor can serve as a model system to answer the following questions pertaining to energy-dependent ligand transport across the outer membrane. What regions of the FhuA polypeptide are involved in the binding of bacteriophages and the import of colicin M? What molecular architecture constitutes the binding-sites for ferrichrome, the antibiotics albomycin, rifamycin CGP 4832, and microcin J25? Do these structurally unrelated ligands induce distinct conformational changes in the receptor? Do the observed structural alterations establish the structural basis for transmembrane signalling and ligand transport? Can a unique mechanism of ligand transport and conformational dynamics, applicable to other TonB-dependent receptors, be derived from the crystallographic structure of unliganded FhuA and its liganded complexes? Where are the putative sites of interaction with associated proteins located? Can a plausible model for energy-dependent transport be inferred from crystallographic data? The answers to these questions will provide a structural platform to further probe the complex mechanism of TonB-coupled transport and signal transduction through the outer membrane.

In chapter one, a comprehensive review of bacterial strategies of iron acquisition is presented. Whenever possible, relevant structure-function relationships, including the discussion of available crystallographic structures, are used to propose a model for TonB-dependent ligand transport across the outer membrane. Chapter two describes the development and optimization of experimental methods for the isolation of affinity-tagged derivatives of FhuA. Sparse matrix screening was utilized to establish parameters

for the growth of well-ordered crystals of FhuA. The identification of crystal growth conditions was an essential prerequisite for the determination of the three-dimensional structure of FhuA. To optimize crystal growth conditions an amphipathic substance termed *cis*-inositol was synthesized and utilized as a crystal growth additive. By including this agent in the crystallization buffer the observed diffraction limit for crystals of FhuA was extended from 2.70 to 2.50 Å resolution. This work is presented in chapter three.

The focus of chapter four is the determination of the crystallographic structure of FhuA and its complex with ferricrocin at 2.50 and 2.70 Å resolution, respectively. This was accomplished by the construction of a methionine-requiring *E. coli* strain harbouring plasmid-encoded recombinant FhuA. The structure was solved with multiwavelength anomalous dispersion data collected from a single selenomethionine derivative crystal. FhuA is a β-barrel composed of 22 antiparallel β-strands: longer extracellular loops and shorter periplasmic turns connect adjacent β-strands. Located within the β-barrel is a structurally distinct domain, 'the cork', which consists of a four-stranded antiparallel β-sheet and interspersed α-helices and connecting segments. Upon binding of ferricrocin to FhuA, conformational changes are transduced through the outer membrane, and displayed by a periplasmic segment of the receptor. These structural alterations may constitute the structural basis for transmembrane signalling. Sequence homologies and mutagenesis data are used to propose a structural mechanism for TonB-dependent siderophore-mediated iron transport across the outer membrane.

An unexpected feature of these structural studies was the identification of a single LPS molecule noncovalently associated with the membrane-embedded surface of FhuA. Data derived from nuclear magnetic resonance, matrix assisted laser-desorption mass spectrometry, and compositional analyses were used to accurately model the three-dimensional structures of two LPS molecules. The placement of the glycolipid on the outer surface of the β-barrel precisely delineates the interface between the lipid bilayer and the external solvent. LPS is an immunomodulatory molecule that stimulates the innate immune response. Until now, precise structural details of LPS and its cognate binding proteins were unavailable. Eight positively charged side-chain residues of FhuA

provide specific electrostatic interactions with the negatively charged moieties of LPS. Three-dimensional arrangements similar to these residues were searched on all structurally known proteins with a fast template-matching algorithm, and a subset of four residues was identified which is common to known LPS-binding proteins. These four residues appear to provide the structural basis of pattern recognition in the innate immune response, which can be utilize in the design of LPS-binding properties with modified LPS-binding properties. This work is presented in chapter five.

Previous studies established that the antibiotic albomycin and the semi-synthetic rifamycin derivative CGP 4832 are actively pumped into the periplasm of *E. coli* cells by FhuA. Chapters six and seven present the three-dimensional structures of FhuA in complex with these antibiotics, respectively. Unexpectedly, these structurally unrelated antibiotics utilize a common binding site. Comparing the liganded structures of FhuA to the unliganded conformation identifies the structural basis for ligand recognition, and illustrates the conformational dynamics of the cork domain. Moreover, the structure of FhuA in complex with rifamycin CGP 4832 further advances the proposed mechanism of ligand transport, and strongly suggests that the β-barrel domain forms interactions with TonB. This structural data can also be used for the rational design of both novel siderophore-antibiotic conjugates and receptor-specific antibiotics.

1. Introduction

Iron has played an essential role in the evolution of life on earth. As the availability of this metal is extremely limited in an oxygen-rich atmosphere, microorganisms have evolved a diverse repertoire of high-affinity iron acquisition strategies to satisfy their nutritional requirement. The transport of iron into cells must be tightly regulated to avoid the detrimental effects associated with iron toxicity. Under iron limited conditions most bacteria secrete at least one siderophore. These low molecular weight compounds avidly scavenge iron from the external environment or host iron-containing proteins, and are subsequently bound by distinct receptors embedded within the bacterial cell envelope. The siderophore-mediated iron uptake pathways of gram-negative bacteria are arranged to ensure directed transport of siderophores across the outer membrane, periplasm, and the cytoplasmic membrane. The proteins needed for each phase of the transport process are localized to distinct compartments and have defined functions. The ferric hydroxamate uptake receptor, known as FhuA, is a member of a diverse family of integral membrane proteins, the TonB-dependent receptors, which actively pump siderophores and vitamin B_{12} across the outer membrane of gram-negative bacteria.

The focus of this thesis is an analysis of the relationship between the three-dimensional structure of FhuA from *Escherichia coli*, and its biological function as an energy-dependent transporter. FhuA, together with the energy-transducing TonB-ExbB-ExbD complex, mediates the uptake of hydroxamate-type siderophores into the periplasm. In addition to transporting ferrichrome, FhuA acts as the primary receptor for several bacteriophages, the antibiotics albomycin and rifamycin CGP 4832, the cyclic peptide antibiotic microcin J25, and the bacterial toxin colicin M. This review of recent literature is designed to place the experimental data presented in this thesis in relation to the current understanding of the molecular mechanisms of microbial iron acquisition. Emphasis will be placed on the structure-function relationships of TonB-dependent receptors and their unique energy-dependent mechanism of ligand transport.

2. Cell envelope of gram-negative bacteria

The cell wall performs two functions; it serves both as a mechanical device that allows bacterial cells to maintain their structural integrity, and as a permeability barrier. Selective permeability allows cells to accumulate and retain nutrients without compromising the protective properties of the cell wall. Functional roles can be assigned to the compartments that form the cell envelope of gram-negative bacteria and the proteins found within these distinct microenvironments (Figure 1).

2a. *Capsular polysaccharides and the enterobacterial common antigen*

Covalently linked to the extracellular leaflet of the outer membrane and in direct physical contact with the external medium are capsular polysaccharides (reviewed by Whitfield & Valvano, 1993; Rick & Silver, 1996). Repeating oligosaccharide units that differ in their constituents, branching, charge density and immunogenicity forms these structures. Enterobacteriaceae capsular or 'K'-antigens mediate interactions between the bacterium and its local environment, and are important determinants of bacterial virulence *in vivo*. Synthesis of capsular polysaccharides is one technique, utilized by *E. coli*, to evade detection by the immune systems of vertebrate hosts. By masking immunogenic cell envelope moieties, primarily lipopolysaccharide (LPS), and serving as a physical barrier, recognition by phagocytic host cells is accomplished.

Enterobacteriaceae possess an additional glycolipid covalently linked to the outer membrane and extending into the surrounding medium termed the enterobacterial common antigen (ECA; reviewed by Rick & Silver, 1996). Repeating trisaccharide units form this structure; the lipid moiety anchors the polysaccharide in the outer membrane. Immunogenic *E. coli* strains contain ECA polysaccharide chains that are linked to the outer cores of the LPS molecules that form the outer membrane (Holst, 1999). However, the immunogenicity of ECA is dependent upon its association with LPS, as purified ECA is not an immunogen (Kuhn et al., 1988).

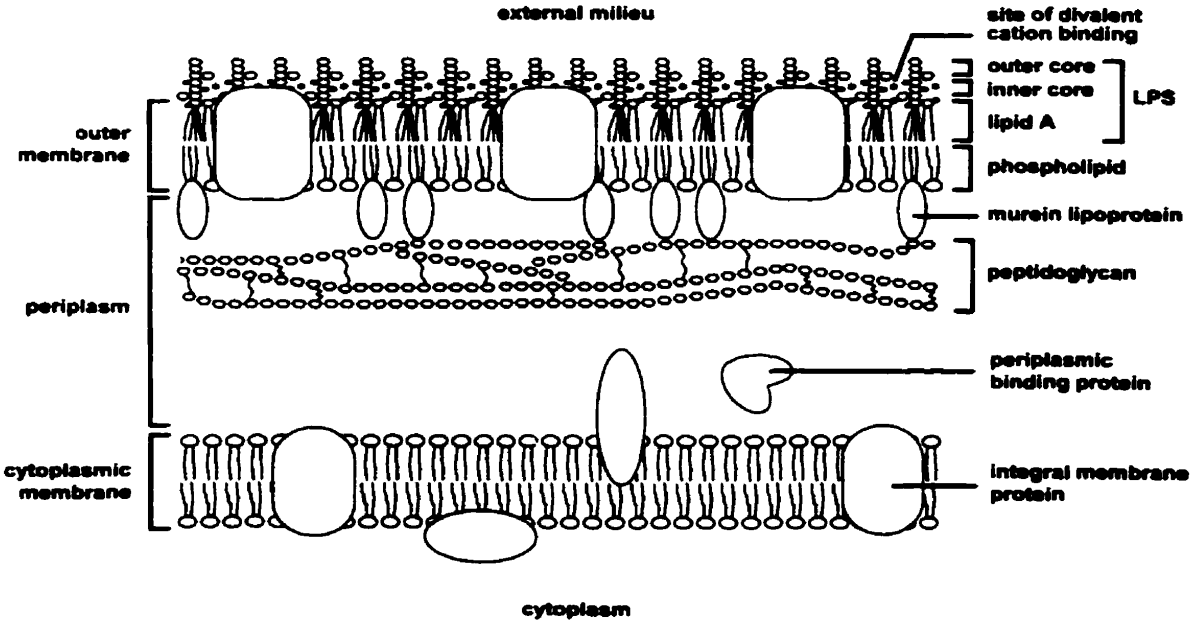

Figure 1. Schematic representation of the cell envelope of gram-negative bacteria. The enterobacterial common antigen and capsular polysaccharides are not shown. G. Moeck kindly provided this figure.

2b. *Outer membrane*

An asymmetric bilayer forms the outer membrane of gram-negative bacteria (reviewed by Nikaido, 1996). This structure functions as a molecular sieve that regulates the flow of hydrophobic solutes in and out of the cell. Channel-forming proteins regulate the permeability of the outer membrane to hydrophilic solutes. The extracellular leaflet of the lipid bilayer is comprised entirely of LPS molecules, whereas a mixture of phospholipids, including phosphatidylethanolamine and phosphatidylserine, form the periplasmic leaflet. LPS forms an effective barrier to harmful lipophilic solutes, and is essential to the structural integrity and protective properties of the outer membrane.

2c. *Lipopolysaccharide*

LPS is composed of three covalently linked domains that are differentiated by their

genetic organization, chemical structures and biological features (reviewed by Raetz, 1996; Figure 2). They are (i) lipid A, a glycolipid; (ii) the core, a nonrepeating heterooligosaccharide; and (iii) O-antigen, an immunogenic highly variable repeating polysaccharide that extends into the medium. Some bacterial strains, including *E. coli* K-12, have defects in the gene cluster responsible for the synthesis of O-antigen; they synthesize a truncated form of LPS consisting of lipid A and the core only. Lipid A anchors LPS in the outer membrane by hydrophobic and electrostatic forces. The chemical composition and conformation of enterobacterial lipid A are the determinants for endotoxic activity (Brandenburg et al., 1996). Bisphosphorylated hexa-acyl lipid A is the minimal LPS structure required to elicit the innate immune response (Zähringer et al., 1994). Five core types have been identified in *E. coli* by chemical, serological and genetic investigations (Holst, 1999). The core consists of a branched, nonrepeating oligosaccharide that can be divided into two structurally distinct components, the inner and outer core. The inner core is primarily formed by 3-deoxy-D-*manno*-oct-2-ulopyranosonate (Kdo), L-*glycero*-D-*manno*-heptopyranose (Hep) and phosphate residues. The outer core consists of hexose moieties, including galactose (Gal), glucose (Glc) and 2-amino-2-deoxy-D-glucose (glucosamine, GlcN).

2d. *X-ray structure of lipopolysaccharide*

The three-dimensional structures of two LPS molecules in complex with the outer membrane protein FhuA have been determined by X-ray crystallography (Ferguson et al., 2000a). Compositional analysis, matrix-assisted laser desorption mass spectrometry and nuclear magnetic resonance data on the chemical structure were consistent with the observed experimental electron density maps, and were used to build accurate crystallographic models for both LPS molecules (Figures 2 and 3). The glucosamine disaccharide of lipid A is bisphosphorylated at the O1-position of GlcN I and monophosphorylated at the O4'-position of GlcN II. In both FhuA-LPS complexes the line connecting the O1 and O4'-phosphate moieties is approximately perpendicular to the barrel axis. The glucosamine disaccharide is acylated with four 3-hydroxymyristate residues at the 2, 3, 2' and 3'-positions of GlcN I and GlcN II, respectively. The 3-

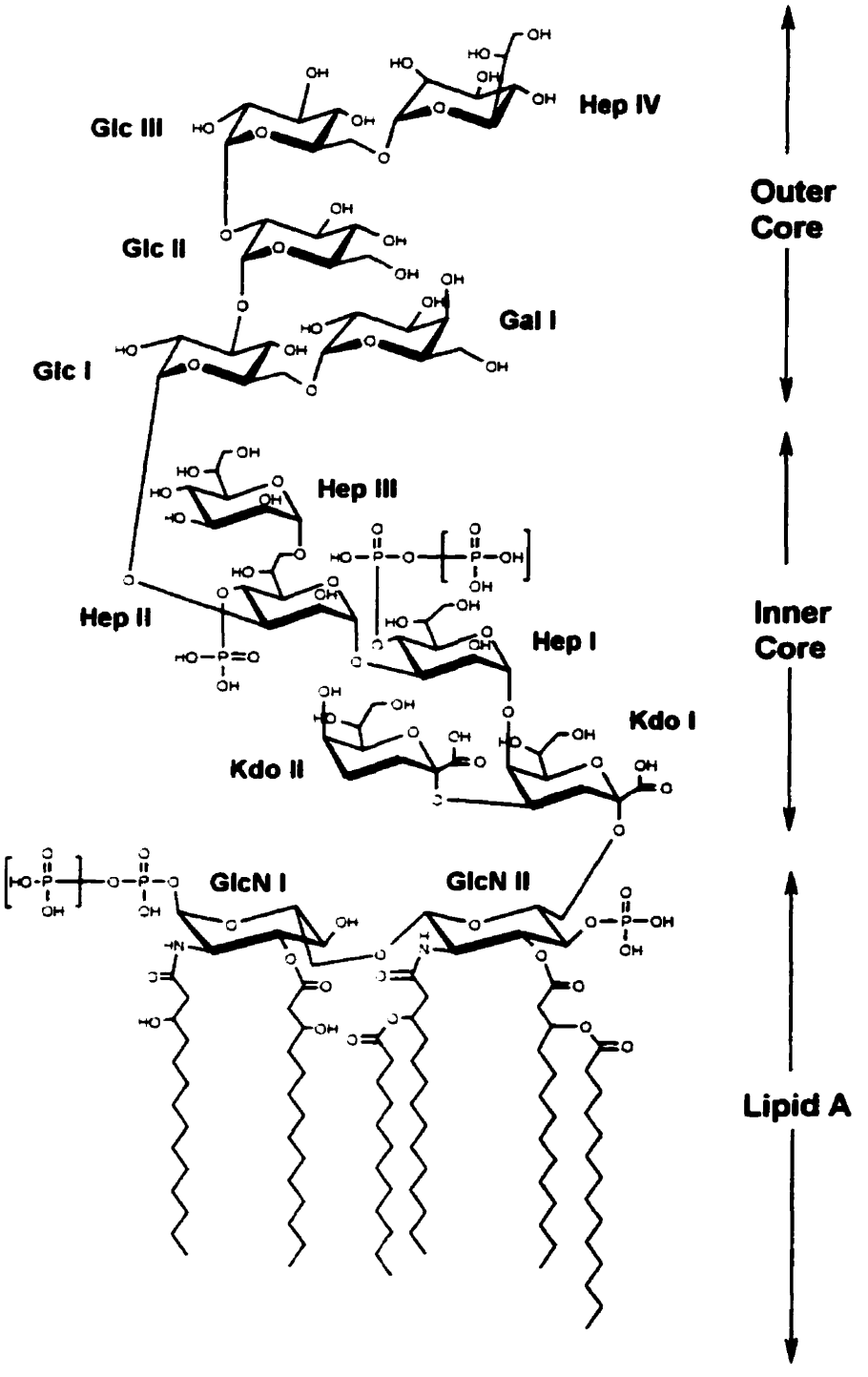

Figure 2. Schematic representation of the three-dimensional structure of LPS. Brackets indicate nonstoichiometric partial substitutions.

of the 2' and 3'-myristate residues are further acylated with laurate and myristate. Numerous van der Waals contacts with hydrophobic side-chain residues fix all acyl chains except the 3-myristate in a highly ordered conformation approximately parallel to the barrel axis. Two Kdo residues, two phosphorylated Hep residues, and one nonphosphorylated heptose residue form the inner core of both LPS molecules. Three glucose, one galactose, and a fourth disordered heptose residue form the outer core.

2e. *Lipopolysaccharide recognition and the innate immune response*

In humans, LPS stimulates the innate immune system to produce cytokines and other inflammatory mediators (reviewed by Medzhitov & Janeway, 1997). Low concentrations of LPS in the bloodstream lead to stimulation of this system, and thus enhance resistance to bacterial infections. However, high doses of LPS result in excessive release of inflammatory mediators that may cause septic shock. Septic shock and its associated pathophysiology are often fatal. In the treatment of bacterial sepsis, LPS represents a possible target for future drug development.

Lipid A, the highly conserved component of LPS with its multiple asymmetric carbon atoms, is well suited for specific recognition by LPS-binding proteins (Medzhitov & Janeway, 1997; Hoffmann et al., 1999). Proteins involved in the innate immune system have evolved specific LPS-binding sites, primarily for lipid A. The negatively charged phosphates of LPS form strong electrostatic interactions with positively charged side-chain residues of FhuA. To determine if the arrangement of side-chain residues identified in the LPS-binding site of FhuA was also found on surfaces of proteins of known structure, a structure-based search algorithm was implemented (Kleywegt, 1999). The α-carbon coordinates of all eight positively charged residues involved in LPS binding to FhuA, together with partial information about their side-chain conformations were used as search templates. One four-residue template (FhuA residues: Lys306, Lys351, Arg382 and Lys428) detected a small number of conformational matches in the Protein Data Bank, and has been denoted as the 'LPS-binding motif' (Ferguson et al., 2000a).

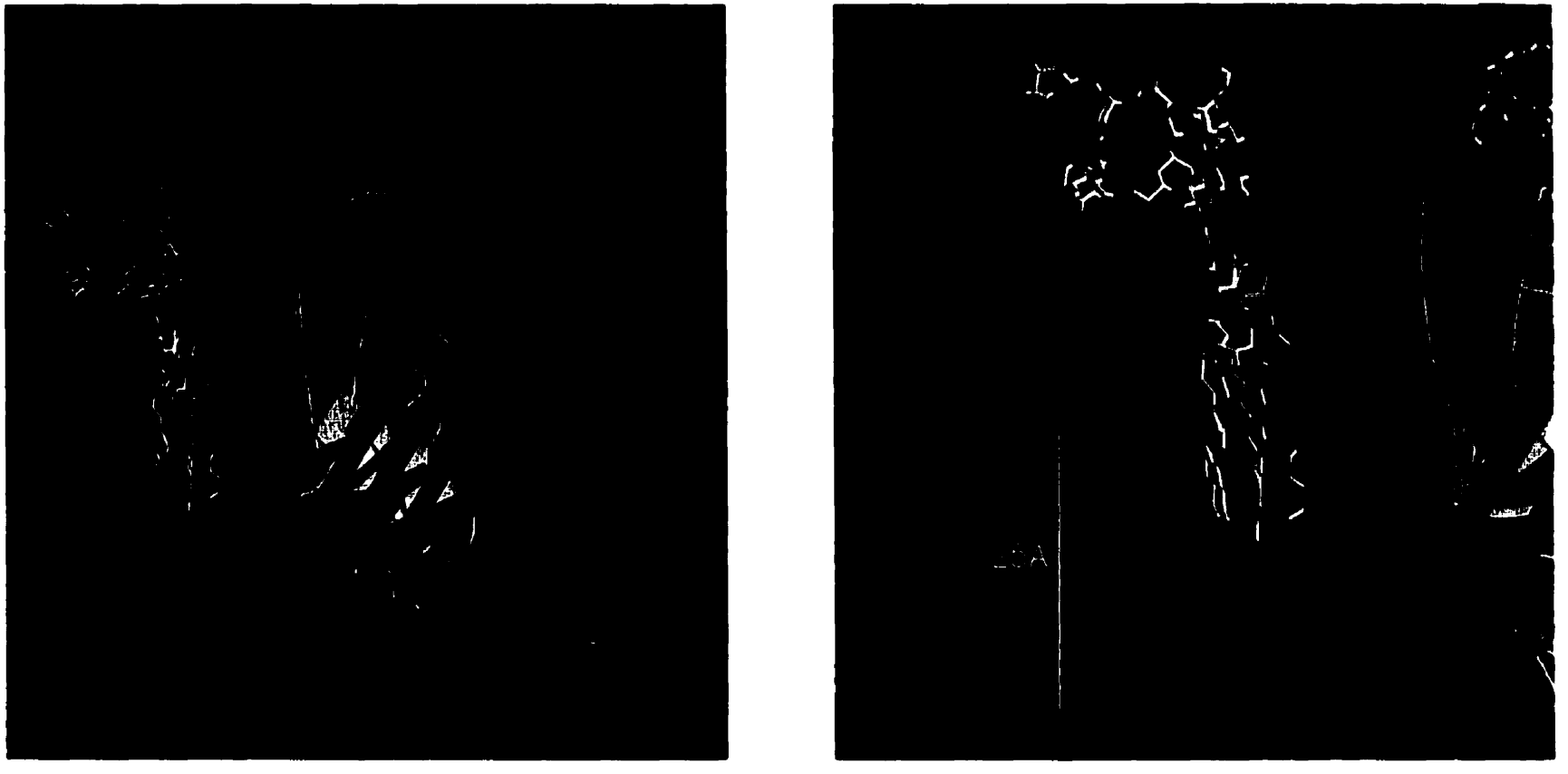

Figure 3. Ribbon representation of the crystallographic structure of LPS and its placement on the membrane-embedded surface of FhuA. The barrel and cork domains of FhuA are coloured blue and yellow, respectively. LPS is shown as a bond model with oxygen atoms red, nitrogen atoms blue, carbon atoms grey, and phosphorous atoms green. Select side-chain residues that compose the upper and lower aromatic girdles of FhuA are coloured green.

Several proteins that bind LPS and that mediate the LPS-induced immune response were identified by this search. The bactericidal permeability-inducer (BPI) is a cytoplasmic protein from polymorphonuclear neutrophils that targets endocytosed bacteria (Little et al., 1994). BPI downregulates the LPS-induced immune response by forming large LPS aggregates (Gazzano-Santoro et al., 1994). The three-dimensional structure of BPI consists of two similar, extended domains arranged in tandem to form a 'boomerang-shaped' molecule (Beamer et al., 1998). The BPI side-chain residues identified by this structural search [Lys42, Lys48, Lys92 and Lys99] are all located at the distal tip of the N-terminal end of the molecule. Assigned to these side-chain residues is a functional role in LPS binding and LPS detoxification (Taylor et al., 1995). Peptides derived from residues 17 to 45 and residues 65 to 99 of BPI are capable of inhibiting the LPS-induced inflammatory response.

Other proteins known to bind LPS and/or to act antagonistically to the LPS-induced immune response include lactoferrin and *Limulus* anti-LPS factor. Lactoferrin, an iron binding glycoprotein found at mucosal surfaces and in biological fluids, is released from neutrophil granules during the inflammatory response. This protein has both bacteriostatic and bactericidal activity. The three-dimensional structure of human lactoferrin is composed of two related globular lobes that are connected by a short α-helix (Anderson et al., 1989). The N-terminal and C-terminal lobes of the protein can be subdivided into two structurally distinct domains, each composed of a five or six-stranded antiparallel β-sheet and multiple α-helices. Two spatially distinct putative LPS-binding sites have been identified for this molecule (Appelmelk et al., 1994; Elass-Rouchard et al., 1995). Residues 2 to 4 in combination with residues 28 to 34 were found to be involved in LPS binding (Elass-Rouchard et al., 1995; 1998; Van Berkel et al., 1997). In accord with this data, a structural search using the putative LPS-binding motif identified two four-residue LPS-binding sites on the surface of lactoferrin. The first is formed by residues Arg2, Arg4, Arg24 and Arg27, and is located in the N-terminal lobe of the molecule. A second C-terminal LPS-binding site is composed of residues Arg356, Lys359, Lys633 and Lys637. Synthetic peptides containing residues 28 to 34 of lactoferrin possess bactericidal activity against gram-negative bacteria (Odell et al., 1996).

Horseshoe crabs (*Tachypleus tridentatus* and *Limulus phemus)* have a primitive circulatory system, hemolymph, that is composed of a single cell type, the hemocyte. Exposure of *Limulus* hemocytes to LPS induces an intracellular cascade that leads to coagulation; a defensive mechanism against bacterial infection (Tanaka et al., 1982). The *Limulus* antibacterial and anti-LPS factor (LALF) inhibits this coagulation cascade by binding LPS and neutralizing its endotoxic effects (Warren et al., 1992). The crystallographic structure of LALF contains a pair of antiparallel β-strands and a connecting amphipathic loop that confer a 'wedge-shape' to this molecule (Hoess et al., 1993). A cluster of positively charged side-chain residues is found on the amphipathic loop and on the adjacent residues of the β-strands. The structural search identified four basic side-chain residues (Arg40, Arg41, Lys47 and Lys64) that may compose the LPS-binding site. Synthetic cyclic peptides derived from residues 36 to 45 of LALF and similar peptides (residues 41 to 53) from *Tachypleus* anti-LPS factor have indeed been shown to bind and inhibit the LPS-induced immune response (Kloczewiak et al., 1994; Ried et al., 1996).

Taken together these findings suggest that the arrangement of FhuA side-chain residues Lys306, Lys351, Arg382 and Lys428 represent a conserved and specific LPS-binding motif. In all cases, the proposed LPS-binding sites found on the surfaces of the identified proteins are consistent with the functional and mutational data. Moreover, all side-chain residues that compose these proposed LPS-binding sites are surface-exposed and docking of LPS to these proteins is possible without steric clashes.

2f. *Outer membrane proteins: structural integrity, virulence factors and enzymes*

Embedded within the outer membrane of *E. coli* are proteins that contribute in different ways to the physiology of the bacterial cell. Five proteins (OmpA, OmpC, OmpF, PhoE, and murein lipoprotein) comprise approximately 80% of the total protein content of the lipid bilayer. Presented here are examples of outer membrane proteins with defined functions and known three-dimensional structures.

Outer membrane protein A

OmpA is an abundant, highly conserved protein that together with the murein lipoprotein, functions primarily to maintain the structural integrity of outer membrane (Sonntag et al., 1978; Nikaido & Vaara, 1985). Analogous to other outer membrane proteins, OmpA also functions as a bacteriophage and colicin receptor (Morona et al., 1984; 1985). The three-dimensional structure of the N-terminal domain of OmpA (residues 1 to 171) has been elucidated by X-ray crystallography (Pautsch & Schulz, 1998; reviewed by Gouaux, 1998). This monomeric integral membrane protein is formed by an antiparallel eight-stranded β-barrel; longer extracellular loops and shorter periplasmic turns connect adjacent β-strands. The surface-exposed loops are functionally important for conjugation and the adsorption of bacteriophages (Koebnik, 1999). Two girdles of aromatic side-chain residues delineate a 25 Å hydrophobic zone on the external surface of the barrel, indicating the placement of OmpA within the bilayer. In accord with the observation that OmpA does not significantly contribute to the permeability of the outer membrane, the interior of the barrel contains an intricate network of hydrogen bonds, and is physically occluded at its periplasmic end. A 'hinge' region connects the β-barrel to the C-terminal domain of OmpA, which is localized in the periplasm. The periplasmic domain of OmpA is postulated to mediate noncovalent interactions between the outer membrane and peptidoglycan (Koebnik, 1995). Murein lipoprotein molecules embedded within the periplasmic leaflet provide additional points of contact. Accordingly, murein lipoprotein-deficient mutants of *E. coli* possess 'leaky' outer membranes with increased permeability (Hirota et al., 1977; Nikaido et al., 1977).

Outer membrane protein X

The outer membrane protein OmpX mediates the entry of *E. coli* into mammalian cells and functions as a virulence factor that inhibits the host complement pathway. A high-resolution crystallographic structure of OmpX has recently become available (Vogt & Schulz, 1999). Analogous to OmpA, OmpX also consists of a slender, elliptical-shaped eight-stranded antiparallel β-barrel, with longer extracellular loops and shorter

periplasmic turns. Both proteins resemble an inverted micelle and have similar molecular dimensions. Analogous to other outer membrane proteins a zone of hydrophobic side-chain residues, flanked by phenylalanine, tyrosine and tryptophan moieties, extends into the bilayer. Given the extensive hydrogen bonding network observed within the barrel and the absence of any direct pathway connecting the extracellular and periplasmic ends of OmpX, it is improbable that this protein forms channels. Vogt & Schulz (1999) suggest that the edge of a protruding β-sheet may bind host proteins, and thus, promote cell adhesion and disruptions to the complement pathway.

Outer membrane phospholipase A

Outer membrane phospholipase A is one of the few enzymes that are embedded within the outer membrane (reviewed by Dekker, 2000). Disruptive changes in the structural integrity and fluidity of the outer membrane, such as those induced upon the binding of BPI during phagocytosis (Wright et al., 1990), activates this enzyme to degrade phospholipids. The structures of phospholipase A in the inactive monomeric and an inhibited dimeric form have been determined by X-ray crystallography (Snijder et al., 1999). Each monomer unit is formed by a 12-stranded antiparallel β-barrel; the 'flat sides' of each barrel form the monomer-monomer interface. The active sites of the homodimeric complex are located slightly above the extracellular leaflet of the outer membrane. In accord with the observation that calcium is required for enzymatic activity of phospholipase A (Ubarretxena-Belandia et al., 1998), a calcium ion is bound near the active site of each monomer unit. With this structural data a model for the activation of phospholipase A has been proposed (Snijder et al., 1999). Under normal physiological conditions the extracellular leaflet of the outer membrane contains only LPS molecules. If the outer membrane becomes perturbed, symmetric patches of phospholipids may insert into LPS monolayer (Nikaido & Vaara, 1985). This event triggers the dimerization of phospholipase A, which enzymatically degrades phospholipids in an effort to restore the structural integrity of the outer membrane.

2g. *Outer membrane transporters*

The outer membrane protects the bacterial cell from antibiotics, degradative enzymes and other deleterious agents. However, the presence of this highly effective permeability barrier restricts access to some larger essential nutrients, including siderophores and vitamin B_{12}. Thus, gram-negative bacteria have developed distinct transport mechanisms to solve this problem (reviewed by Postle, 1990; Welte et al., 1995; Nikaido, 1996). Three distinct classes of channel-forming transport proteins are involved in these processes (i) nonspecific porins, which facilitate the diffusion of small solutes; (ii) specific porins, which enhance the rate of passive diffusion at low solute concentrations; and (iii) energy-dependent receptors, which mediate the active transport of metabolites that are found in exceedingly low concentrations in the environment.

Nonspecific porins

Nonspecific porins possess large water-filled channels that facilitate the passive diffusion of ions and other small hydrophilic compounds across the outer membrane. The expression of nonspecific porins is often regulated by environmental conditions (Nikaido & Vaara, 1985). For example, when starved for phosphate *E. coli* expresses the anion selective porin PhoE, which mediates the passage of phosphate and phosphorylated compounds into the periplasm (Korteland et al., 1982; Bauer et al., 1989). Similarly, under conditions of high osmolarity and temperature, *E. coli* represses the synthesis of the cationic selective porin OmpF while upregulating the expression of the OmpC porin (Stock et al., 1989).

The three-dimensional structures of six nonspecific porins have been determined by X-ray crystallography [*Rhodobacter capsulatus* porin (Weiss et al., 1991); OmpF and PhoE from *E. coli* (Cowan et al., 1992); *Rhodopseudomonas blastica* porin (Kreusch & Schulz., 1994); *Paracoccus denitrificans* porin (Hirsch et al., 1997); and OmpK36 from *Klebsiella pneumoniae* - an OmpC homologue (Dutzler et al., 1999)]. While these structures share no significant sequence homology, they assume a similar fold, 16-stranded antiparallel β-barrels that form stable homotrimers. Each monomer unit

contains a single transmembrane channel (7 by 11 Å in diameter) that is open to both the external medium and the periplasm. The third extracellular loop, known as the 'constriction loop', of each monomer folds into the lumen of the channel. The channel conductance, ion selectivity and the exclusion limit of nonspecific porins have been characterized by (i) single channel conductivity measurements; (ii) measurements of the efflux of radiolabelled sugars; (iii) osmotic swelling assays; and (iv) analysis of the electrostatic distribution within the channel (reviewed by Welte et al., 1995). Ion selectivity (anionic *versus* cationic permeability) is primarily defined by the electrostatic potential of those side-chain residues that form the constriction loop. Selectivity can be reversed by mutating charged residues (Bauer et al., 1989; Przybylski et al., 1996). While the physical properties of the solute influence the rate of diffusion, influx is proportional to the external solute concentration.

It has been proposed that *E. coli* cells regulate the permeability of the outer membrane to hydrophilic solutes by a voltage-gating mechanism. When reconstituted in planar lipid bilayers nonspecific porins close upon the application of an external voltage. However, with the exception of the Donnan potential, no continuous potential can be maintained across the outer membrane (Nikaido & Vaara, 1985). Moreover, the Donnan potential does not induce porin channels to close (Sen et al., 1988). If a voltage-gating mechanism does exist, X-ray crystallographic data and molecular dynamic simulations suggest that it may involve the rearrangement of side-chain residues or the movement of the constriction loop toward the opposite side of the channel (Phale et al., 1997; Watanabe et al., 1997). Voltage-gating would be beneficial for the bacterial cell if porins or mutant porins with open channels were to become incorrectly inserted into the cytoplasmic membrane (Delcour, 1997).

Specific porins

Some metabolites are too large to diffuse through nonspecific porin channels. Thus, gram-negative bacteria have evolved specific porins to accelerate the rate of diffusion of these nutrients across the outer membrane. For example, in *E. coli*, LamB, Tsx, and ScrY mediate the uptake of maltose, nucleosides, and sucrose. These solutes diffuse passively

through specific porins with Michaelis-Menton saturation kinetics at high solute concentrations. However, the presence of stereospecific ligand-binding sites within the channel increases the rate of influx at low solute concentrations (Benz et al., 1987; Jordy et al., 1996).

The three-dimensional structures of two specific porins have been determined by X-ray crystallography [maltoporin (LamB; Schirmer et al., 1995); and sucrose porin (ScrY; Forst et al., 1998)]. Analogous to the nonspecific porins, LamB and ScrY form stable homotrimers in the outer membrane. The monomer units of LamB and ScrY are formed by 18-stranded antiparallel β-barrels. Longer extracellular loops and shorter periplasmic turns connect adjacent β-strands. The surface-exposed loops of both porins are involved in ligand binding and transport (Anderson et al., 1999; Ulmke et al., 1999). Similar to the constriction loop of nonspecific porins, the third extracellular loop of LamB and ScrY is attached by polar and apolar interactions to the inner barrel wall, and thus constricts the channel. Different from maltoporin, ScrY has a 70 residue N-terminal extension that is localized in the periplasm. Residues 4 to 45 are predicted to form a coiled-coil structure (Forst et al., 1998); however, no precise functional role has been assigned to this segment.

Electrostatic analysis illustrates the absence of charged residues within the constriction loops of specific porins. However, a series of six aromatic side-chain residues termed the 'greasy slide', extends from the extracellular to the periplasmic vestibules of both porins. This arrangement of aromatic residues is involved in the permeation of sugars through the channel. Indeed, the crystallographic structures of LamB and ScrY in complex with various carbohydrates revealed sugar molecules bound to the greasy slide (Schirmer et al., 1995; Dutzler et al., 1995; Forst et al., 1998).

High-affinity receptors

Outer membrane receptors are functionally different from nonspecific and specific porins. They bind their cognate ligands with high-affinity (K_D ~0.1 μM), thereby concentrating them at the cell surface. The concentration of siderophores and vitamin B_{12} in the solvent is insufficient to establish the required gradient across the outer membrane.

Thus, porin-mediated passive diffusion does not satisfy cellular requirements for these essential metal-containing complexes. The three-dimensional structure of the high-affinity receptor FhuA from *E. coli* is presented in section six of this thesis.

2h. *Periplasm*

Located between the outer and cytoplasmic membranes is the periplasm (reviewed by Oliver, 1996). Essential processes that are responsive to both intracellular and extracellular events, including the regulation of osmolarity, protein folding and translocation, disulphide-bond formation, chemotaxis, capsular polysaccharide and LPS synthesis, and the uptake of essential nutrients, occur within this compartment. Positioned within the periplasm is the peptidoglycan layer. Peptidoglycan is composed of repeating saccharide and amino acid units; adjacent glycan strands are cross-linked by peptide bonds (Park, 1996). However, this highly cross-linked structure is not rigid, but rather assumes a 'gel-like' form (Hobot et al., 1984). The degree of polymerization, hydration, and protein content of the periplasm, influence the mobility of soluble and membrane-associated periplasmic proteins (Dijkstra & Keck, 1996). Whereas the outer membrane functions primarily as a permeability barrier, the peptidoglycan layer contributes to the mechanical integrity and shape of the bacterial cell. For gram-positive bacteria, the surface-exposed peptidoglycan layer is multilayered and can be up to ten times as thick compared to the equivalent structure in gram-negative bacteria, and may also function as a permeability barrier.

2i. *Cytoplasmic membrane*

Analogous to the outer membrane, two opposed monolayers form the symmetric bilayer that is the cytoplasmic membrane (reviewed by Kadner, 1996). The lipid molecules that comprise this membrane establish a hydrophobic environment, which is conducive for the proper insertion and function of a diverse array of membrane-embedded protein complexes. The phospholipid composition regulates permeability, and the structure and function of those proteins embedded within the cytoplasmic membrane.

The protein constituents of this bilayer are involved in every aspect of cellular physiology, including energy-dependent import and export of metabolites, electron transport, protein and carbohydrate translocation, transmembrane signalling, cell motility and chemotaxis, and septum formation. The three-dimensional structures of cytoplasmic membranes proteins involved in aerobic [cytochrome *c* oxidase (Iwata et al., 1995)] and anaerobic respiration [fumarate reductase (Iverson et al., 1999; Lancaster et al., 2000)], and the synthesis of ATP are available [F_1F_0-ATPase (Stock et al., 1999)].

Two functions of the cytoplasmic membrane are of particular importance to this review. The uptake of siderophores and vitamin B_{12} across the gram-negative cell envelope requires energy. An electrochemical gradient maintained across the cytoplasmic membrane drives ligand transport into the periplasm. Moreover, the translocation of these nutrients into the cytoplasm is dependent upon specific ABC transporters that are embedded within the cytoplasmic membrane and the hydrolysis of ATP.

3. The biological importance of iron

Iron has played an essential role in the evolution of life on earth, and is required by all living organisms with the possible exception of a few microbes. As a transition element, iron can reversibly modify its oxidation state. The ability to lose or gain a single electron generates a wide range of favourable reduction-oxidation potentials. Accordingly, this metal is often an essential cofactor in central metabolic processes, including RNA synthesis and electron transport (Briat, 1992). In aqueous solution, iron can exist in two forms [ferrous (Fe^{II}) or ferric (Fe^{III})], and in spite of the reduction-oxidation potential within the bacterial cell, iron is stored in the ferric state. Despite its relative abundance in nature, atmospheric oxygen rapidly oxidizes iron to form stable, but sparingly soluble ferric oxyhydroxide polymers. In fact, the concentration of biologically available iron may be as low as 10^{-18} M at physiological pH (Neilands et al., 1987). However, unregulated intracellular iron metabolism causes lipid peroxidation, oxidation of sulphydryl groups, DNA-damaging lesions, membrane disruptions, and ultimately, cell death. The Fenton and Haber-Weis reactions coordinate the reduction of Fe^{III} to Fe^{II}, in

the presence of hydrogen peroxide, with the production molecular oxygen, hydroxyl anions, superoxide and hydroxyl radicals (Braun, 1997). Superoxide dismutases normally degrade superoxide radicals (Sehn & Meier, 1994). Peroxide anions are subsequently converted into molecular oxygen and water by the enzymatic activity of related catalases and peroxidases. These systems protect bacteria against potent oxidizing agents that are generated either endogenously during respiration or exogenously by host organisms (Farr & Kogoma, 1991).

4. Biological strategies for iron acquisition

To satisfy their nutritional iron requirement, prokaryotic and lower eukaryotic organisms have evolved a sophisticated repertoire of highly efficient iron acquisition strategies (reviewed by Guerinot, 1994; Braun et al., 1998).

4a. *Iron acquisition by plants*

Plants have adapted specific techniques to solubilize iron found in the rhizosphere (reviewed by Römheld, 1987). These mechanisms include (i) reduction of Fe^{III} by increasing the enzymatic activity of ferric reductases that are localized to the root surface (Chaney et al., 1972; Römheld & Marschner, 1986a); (ii) acidification of the rhizosphere also promotes the reduction of Fe^{III} to Fe^{II} (Römheld et al., 1984); and (iii) secreting Fe^{III}-chelating compounds termed phytosiderophores from their roots into the soil (Hether et al., 1984; Römheld & Marschner, 1986b). High-affinity uptake systems translocate these iron-chelates across the surface of the root (Römheld & Marschner, 1986b; Higuchi et al., 1999).

4b. *Iron acquisition by animals*

In the human body, haemoglobin and ferritin store the vast majority of iron. The remainder is bound to host iron-binding proteins, primarily transferrin in serum and lactoferrin in secretory fluids and on mucosal surfaces. These glycoproteins dramatically

restrict the availability of iron and thereby inhibit bacterial growth. Although precise structural details regarding the mechanisms of mammalian iron acquisition and homeostasis remain to be established, several crystal structures provide some insights into these essential processes.

Transferrin and the transferrin receptor

Mammalian transferrin is composed of two similar globular domains (N and C-lobe) that are connected by a flexible hinge; each lobe contains a single Fe^{III}-binding site (Bailey et al., 1988). The human transferrin receptor, embedded within the plasma membrane, is a transmembrane glycoprotein that binds holotransferrin, internalizes, and shuttles this molecule to an endosome. Each monomer unit of this homodimeric receptor is composed of three domains: the N-terminal cytoplasmic domain, the transmembrane domain, and the ectodomain, which contains the transferrin-binding site. Accordingly, one transferrin receptor binds two holotransferrin molecules. The three-dimensional structure of the ectodomain of the human transferrin receptor has recently been determined (Lawrence et al., 1999). Using structural data, a model for the interaction of holotransferrin with its cognate receptor, and the uptake of iron by receptor-mediated endocytosis have been proposed. The surface of transferrin and its receptor are complementary. There is a bowl-like depression at the top of the receptor, and two lateral-facing putative transferrin-binding clefts. The three domains that comprise the ectodomain contribute to this surface, which is believed to mediate protein-protein interactions with the holotransferrin molecule. Following the formation of a complex, conformational changes induce localized pH changes in the putative transferrin-binding clefts, such that the relative binding affinity for holotransferrin is altered. Upon acidification, both Fe^{III} ions disassociate from the carrier, presumably by interdomain rigid-body movements within the N and C-lobes of transferrin (MacGillivray et al., 1998). Following this event, the apotransferrin-receptor complex reinserts into the plasma membrane and is released.

Haemochromatosis protein HFE

In humans, there are no known regulated iron excretion mechanisms thus; iron homeostatis is achieved by controlling rate of intestinal iron absorption. Hereditary haemochromatosis is an autosomal recessive disorder that causes patients to absorb excess iron. As a result, intracellular iron stores can be up to ten times the normal level, with iron being deposited in virtually every organ in the body and leading to multiple organ failure, liver cancer, impaired intellectual development in children, and cardiovascular complications. The haemochromatosis protein HFE is a transmembrane glycoprotein that is related to the major histocompatibility complex (MHC) class I proteins. In contrast to class I MHC molecules, which present peptide antigens to T cells, HFE does not perform any known immune function (Lebrón et al., 1998). Consistent with its role in an iron-overload disorder, HFE forms a complex with the transferrin receptor (Feder et al., 1998). Biochemical assays showed that HFE and holotransferrin are capable of simultaneously binding the transferrin receptor on the same side of the plasma membrane, and that HFE can inhibit interactions between holotransferrin and its associated receptor (Lebrón et al., 1998; 1999). The three-dimensional structure of HFE in complex with the human transferrin receptor has been solved by X-ray crystallography (Bennett et al., 2000). The crystal structure shows that two HFE molecules are bound to a single transferrin receptor. Accordingly, mutations in HFE that affect the formation of this complex or the disassociation of the holotransferrin-transferrin receptor complex disrupt iron homeostasis (Andrews & Levy, 1998).

5. Iron acquisition by bacteria

To establish commensal or pathogenic relationships with host organisms or to survive as free-living organisms, bacteria must obtain iron from their local environment. Sequestration of iron is an extremely effective nonspecific host response to bacterial infection. To circumvent this defensive mechanism, bacterial strains that do not secrete siderophores have evolved a sophisticated repertoire of strategies to utilize host iron-

containing proteins as sources of iron (reviewed by Schryvers & Stojiljkovic, 1999; Table 1).

5a. *Regulation of gene transcription*

To proliferate within host organisms bacteria must scavenge essential nutrients. As the availability of iron is restricted within the fluids and tissues of the host, the presence of high-affinity iron acquisition systems increases bacterial virulence *in vivo* (Litwin & Calderwood, 1993). Under conditions of low iron bacteria increase the rate of transcription of genes involved in iron uptake and certain other virulence factors. However, the transport of iron across the outer membrane and its intracellular metabolism must be tightly regulated to avoid the detrimental effects associated with iron toxicity. Accordingly, iron-dependent repressors control the expression of most iron-responsive genes. When activated by a divalent transition metal, the transcriptional regulatory proteins Fur (ferric uptake regulation) from gram-negative and some gram-positive bacteria, and DtxR (diphtheria toxin repressor) of the remaining gram-positive bacteria, couple the intracellular Fe^{II} concentration with gene expression, and thus, provide an adaptive growth response (reviewed by Hennecke, 1990; Tao et al., 1994; Escolar et al., 1999).

In the presence of sufficient intracellular concentrations of iron, the protein DtxR from *Corynebacterium diphtheriae* represses a family of genes that encode diphtheria toxin, high-affinity iron acquisition systems, and other virulence factors. The three-dimensional structures of DtxR in the absence and presence of various transition metals have been determined (Qiu et al., 1995; Schiering et al., 1995; Ding et al., 1996; Qiu et al., 1996). The general architecture of the repressor shows that DtxR is a dimeric regulatory protein, which is composed of two similar globular lobes. Three domains form each lobe: an N-terminal DNA-binding domain; an interface domain, which contains two metal-binding sites; and a third flexible C-terminal domain. Each DNA-binding domain contains a helix-turn-helix motif that is formed by side-chain residues from the second and third α-helices of the protein. Glutamate, cysteine, histidine and methionine side-chain residues coordinate the metal ion; additional glutamate, aspartate

Table 1. Representative members of the TonB-dependent family of outer membrane transporters

Substrate	Organism	Outer Membrane Receptor
Ferric aerobactin	*Escherichia coli*	IutA
Ferrichrome, albomycin, rifamycin CGP 4832, microcin J25	*Escherichia coli*	FhuA
Coprogen, rhodoturulate	*Escherichia coli*	FhuE
Ferric enterobactin	*Escherichia coli*	FepA
Dihydroxybenzoate, catechol-substituted cephalosporins	*Escherichia coli*	Cir
Dihydroxybenzoylserine, dihydroxybenzoate, catechol-substituted cephalosporins	*Escherichia coli*	Fiu
Ferric citrate	*Escherichia coli*	FecA
Vitamin B_{12}	*Escherichia coli*	BtuB
Ferric pyoverdin	*Pseudomonas aeruginosa*	FpvA
Iron-loaded transferrin	*Neisseria menigitidis*, *Neisseria gonorrhoeae*	TbpA-TbpB
Iron-loaded lactoferrin	*Neisseria menigitidis*, *Neisseria gonorrhoeae*	LbpA-LbpB
Haem	*Vibrio cholerae*	HutA-HutB
Haem	*Serratia marcescens*	HasR
Haem	*Yersinia pestis*	HmuR
Haem	*Yersinia enterocolitica*	HemR
Haemglobin	*Neisseria menigitidis*, *Neisseria gonorrhoeae*	HmbR
Haemoglobin-haptoglobin complexes	*Haemophilus influenzae*	HhuA
Haemoglobin-haptoglobin complexes	*Neisseria menigitidis*, *Neisseria gonorrhoeae*	HpuB-HpuA

and arginine residues contribute to the stability of the metal binding site (Ding et al., 1996). The binding of a metal cofactor to the aporepressor triggers a 'calliper-like' conformational change in the relative orientation of the monomer units in the dimeric structure of DtxR. In this DNA-binding mechanism, the cation functions as the pin at the pivot points of the calliper. The three-dimensional structure of DtxR in complex with both a divalent corepressor and a 33-base pair synthetic oligonucleotide corresponding to the corynebacteriophage β-*tox* operator sequence has been determined (White et al., 1998). The structure shows that the oligonucleotide interacts with two dimers of activated DtxR that bind to opposite sides of the nucleic acid. DNase I protection assays and structural data revealed a 19-base pair footprint within the *tox* operator for activated DtxR (Tao & Murphy, 1992; Schmitt & Holmes, 1993). Residues from α-helices B and C of the helix-turn-helix motif interact with the major groove of DNA. Following metal ion-mediated activation, an N-terminal α-helix of DtxR undergoes a helix-to-coil transition. This conformational change occurs in the absence of DNA binding and is essential for recognition of the *tox* operator sequence.

The Fur protein from *E. coli* is a histidine-rich protein that negatively regulates the expression of genes responsible for iron acquisition (Schäffer et al., 1985). Although the *fur* and *dtxR* genes share modest sequence homology, their DNA-binding domains and metal-binding sites may assume similar three-dimensional structures. By analogy to the metal-binding sites of DtxR and given the frequent involvement of sulphydryl and other negatively charged groups in coordinating divalent metals, side-chain residues localized to the C-terminal domain of Fur are believed to bind Fe^{II}. The binding of a corepressor confers DNA-binding ability to Fur (DE Lorenzo et al., 1987; Escolar et al., 1997). While the DNA-binding domain has been localized to the N-terminal domain of the repressor, no classical helix-turn-helix motif has been identified (Stojiljkovic & Hantke, 1995). DNase I protection assays originally revealed a footprint for Fe^{II}-activated Fur within the promoter region of the aerobactin operator of plasmid ColV-K30 that spans a 19-base pair palindrome (DE Lorenzo et al., 1987; Escolar et al., 1997). This protected region has been termed the Fur-responsive regulatory region or the 'Fur-box' (DE Lorenzo et al., 1988a; 1988b). However, more recent data suggest that the consensus sequence which is recognized by Fur actually consists of three 6-base pair repeats rather than a single 19-

base pair palindrome (Escolar et al., 1998). Contacts between Fur and its corresponding operator sequence have been analyzed by site-directed mutagenesis and methylation-protection assays (DE Lorenzo et al., 1988a). These experiments suggest that two dimeric Fur molecules bind to opposite sides of the DNA template, as observed with DtxR (White et al., 1998). Fur homologues have been identified in a broad-spectrum of bacterial genera (Vasil & Ochsner, 1999). These regulatory proteins directly or indirectly regulate the expression of genes with diverse functions, including those involved in central metabolic processes, oxidative stress response mechanisms, siderophore-mediated iron acquisition, bacterial virulence, and the autoregulation of *fur*.

5b. ***Iron acquisition from transferrin and lactoferrin***

Neiserriaceae and Pasteurellaceae contain Fur-regulated genes that encode receptors for host holotransferrin and hololactoferrin molecules (reviewed by Cornelissen & Sparling, 1994; Gray-Owen & Schryvers, 1996). Bacterial transferrin and lactoferrin-mediated iron acquisition systems have an organization similar to those observed with the TonB-dependent siderophore and vitamin B_{12} uptake pathways, with analogous outer membrane, periplasmic and cytoplasmic membrane protein components. The energetic requirements and possibly mechanism of transport are also maintained. In contrast to other TonB-dependent transporters, these outer membrane transporters must extract Fe^{III} from the carrier molecule before pumping the ion across the outer membrane.

Transferrin and lactoferrin receptors consist of two proteins; transferrin-binding proteins TbpA and TbpB, and lactoferrin-binding proteins LbpA and LbpB (Schryvers & Morris, 1988; Legrain et al., 1993; Bonnah & Schryvers, 1998; Petterson et al., 1998). Comparing the primary structures of *tbpA* and *lbpA* to the gene sequences of TonB-dependent receptors from *E. coli* identifies some homologous regions (Cornelissen et al., 1992; Mazarin et al., 1995); suggesting these outer membrane receptors may possess similar three-dimensional structures. Accordingly, an outer membrane protein topology algorithm (Diederichs et al., 1998) predicts that LbpA forms a 22-stranded β-barrel. Assuming that LbpA assumes a similar three-dimensional structure as observed with FhuA and FepA, the N-terminal 150 amino acid residues of LbpA may form a globular

domain that is placed within a β-barrel (Prinz et al., 1999). TbpB and LbpB are surface-exposed lipoproteins that are anchored to the outer membrane by lipid moieties (Lissolo et al., 1994). While the presence of TbpB and LbpB increases the binding efficiency of holotransferrin and hololactoferrin, TbpA and LbpA can bind and utilize, albeit less effectively, these molecules as sources of iron in their absence (Anderson et al., 1994; Bonnah & Schryvers, 1998; Gómez et al., 1998; Retzer et al., 1998). The N and C-terminal lobes of TbpB share structural and functional similarities. Both contain residues that contribute to the preferential binding of holotransferrin and may participate in the initial capture and the catalytic extraction of Fe^{III} (Cornelissen & Sparling, 1996; Retzer et al., 1999). Similarly, LbpB preferentially binds hololactoferrin (Bonnah & Schryvers, 1998; Pettersson et al., 1998). Conformational changes may facilitate the release of iron from these iron carriers (Anderson et al., 1990; MacGillivray et al., 1998).

The precise mechanism of TbpA and LbpA-mediated iron acquisition remains elusive; however, an energized cytoplasmic membrane and the TonB-ExbB-ExbD energy-transducing complex provide the energy required for ligand uptake (Biswas et al., 1997). Accordingly, both holo and apotransferrin remain irreversibly bound to de-energized *N. gonorrhoeae* cells (Cornelissen et al., 1997; Stojiljkovic & Srinivasan, 1997). A conserved region located near the N-termini of TbpA and LbpA, termed the 'TonB-box', is postulated to mediate a conformation-dependent interaction with the energy-transducing protein TonB. As observed with the siderophore and vitamin B_{12} receptors, TbpA and LbpA are predicted to form high-conductance channels through which iron gains access to the periplasm.

5c. *Iron acquisition from haem*

In the bloodstream of animals, iron bound to haemoglobin is contained within erythrocytes, which play a critical role in the transport and exchange of oxygen throughout the body. Some bacterial pathogens are capable of scavenging iron from haem (a complex of Fe^{III} with porphyrin), haemoglobin, and haemoglobin-haptoglobin complexes.

Neiserria meningitidis and *Neiserria gonorrhoeae* contain Fur-regulated genes that encode for two cell surface receptors involved in acquiring iron from haem-containing host proteins (Stojiljkovic et al., 1995). Gene expression varies depending on the availability of haem and environmental conditions (Lewis et al., 1999). The first haem receptor consists of the outer membrane protein HpuB, and the surface-accessible lipoprotein HpuA (Lewis et al., 1997). This bipartite TonB-dependent receptor binds haem, haemoglobin, and haemoglobin-haptoglobin complexes (Lewis et al., 1997). *hpuA* shares little sequence homology with *tbpB* and *lbpB*, and in contrast to these lipoproteins is required for HpuB activity (Chen et al., 1998; Lewis et al., 1999). The second haem receptor is HmbR, a TonB-dependent outer membrane protein that binds haem, haemoglobin, and haemoglobin-haptoglobin complexes (Stojiljkovic et al., 1996). The expression of *hmbR* appears to be regulated by the cytoplasmic haem oxygenase *hemO* (Zhu et al., 2000). A third TonB-dependent haem uptake system is under phase variation control (Stojiljkovic et al., 1996). Phase variation provides an adaptive response to fluctuating supplies of haem during various phases of infection, and limits the exposure of cell surface haem receptors to host defence systems molecules. An additional TonB-independent haem uptake system (HemX) may also participate in haem acquisition.

The amino acid sequences of HpuB and HmbR share some regions of modest homology with the siderophore and vitamin B_{12} receptors of *E. coli*, and significant primary structure conservation with the transferrin and lactoferrin receptors, implying that these proteins may be functionally and structurally related. Analogous to the capture of iron bound to transferrin or lactoferrin, HmbR and HpuAB-mediated transport of haem follows the removal of the haem moiety from the carrier molecule. Although the precise mechanism by which this event is accomplished remains to be established, an energized cytoplasmic membrane and the TonB-ExbB-ExbD energy-transducing module are required for this process (Stojiljkovic & Srinivsan, 1997). Once in the cytoplasm, a cytoplasmic haem oxygenase enzymatically degrades the iron carrier. In the absence of this enzyme bacterial cells are unable to utilize haem, haemoglobin and haemoglobin-haptoglobin complexes as sources of iron (Zhu et al., 2000).

Alternative haem acquisition mechanisms have been observed with a number of gram-negative genera, including *Haemophilus influenzae*, *Pseudomonas aeruginosa* and

Serratia marcescens (Létoffé et al., 1994a; Cope et al., 1995). An ABC exporter comprising three envelope proteins secretes the *S. marcescens* 'haemophore' HasA (Létoffé et al., 1994b; Binet & Wandersman, 1996). The role of this extracellular protein is to capture free haem or acquire it from haemoglobin, transport the iron source to the TonB-dependent outer membrane receptor, HasR, and thus increase of efficiency of iron acquisition; HasR is capable of utilizing haem in the absence of HasA but not TonB (Ghigo et al., 1997; Létoffé et al., 1999). Although the crystallographic structure of HasA has been determined (Arnoux et al., 1999), the mechanism by which HasA extracts the haem group from haemoglobin, or the way HasR binds and removes haem from HasA remains to be determined. However, it is possible that HasA and HasR form a bipartite TonB-dependent receptor as observed with the two-component gonococcal and neiserrial transferrin, lactoferrin and haem receptors. The energy-transducing protein TonB may provide the necessary energy to remove haem from HasA (Létoffé et al., 1999).

5d. *Siderophore-mediated iron acquisition*

To colonize iron-restricted regions within host organisms and their local environments, gram-negative and gram-positive bacteria have developed extensive siderophore-mediated strategies to capture iron (reviewed by Braun et al., 1998). Under iron-limiting conditions, most bacteria secrete at least one low molecular weight iron-chelating siderophore. These water-soluble compounds can be arranged into three broad classes depending on their chemical structures (i) catechol-type (e.g. enterobactin); (ii) citrate-type (e.g. dicitrate, an α-carboxyhydroxylate-based siderophore); and (iii) hydroxamate-type, including aerobactin, coprogen, ferrichrome, and rhodoturulate. Of the approximately 200 known siderophores, most possess three bidentate iron-chelating groups that are derived from hydroxamate, catechols, oxazolines or other related functional groups (Neilands et al., 1987; Neilands, 1995). Although these agents display considerable structurally diversity, all form six coordinate octahedral complexes with Fe^{III} of extraordinary affinity.

Siderophores avidly scavenge Fe^{III} from the external medium or host proteins, and are subsequently bound by distinct receptors located within the bacterial cell envelope.

Siderophore-mediated iron uptake systems translocate siderophores across the outer membrane, against a concentration gradient, by an energy-dependent mechanism. *E. coli* has multiple Fur-regulated iron uptake operons; each composed of an outer membrane receptor, a periplasmic binding protein, one or two hydrophobic membrane proteins that span the cytoplasmic membrane, and an ATP-binding protein that is associated with the inner leaflet of the cytoplasmic membrane. That some bacteria express parallel iron acquisition systems, each specific for a single siderophore, underscores their biological significance. Despite the presence of several operons that target structurally diverse siderophores, *E. coli* only carries the genes for the synthesis of a single indigenous siderophore, enterobactin. Plasmid-encoded genes may provide an additional siderophore and its cognate outer membrane receptor (Valvano & Crosa, 1984). Microbes that do not secrete their own siderophores can utilize those produced by neighbouring bacteria and fungi. For example, the ferric hydroxamate uptake operon (the Fhu system) allows *E. coli* to utilize the fungal siderophore ferrichrome and other hydroxamates as an iron source. Similarly, although *N. menigitidis* does not synthesize any known siderophore, functional homologues of the ferric enterobactin and ferrichrome receptors of *E. coli* have been identified for this human pathogen (Carson et al., 1999; Klee et al., 2000).

5e. *Siderophore and vitamin B_{12} receptors*

Siderophore-mediated iron acquisition pathways are arranged such that iron-chelates are transported across the outer membrane, periplasm, and the cytoplasmic membrane. The proteins needed for each phase of the transport process are localized to specific compartments within the cell envelope and have defined functions (Figure 4). In *E. coli* K-12, the receptors for hydroxamate-type siderophores are (i) IutA, which transports aerobactin (Krone et al., 1985); (ii) FhuA, which transports ferrichrome and the structurally related antibiotic albomycin (Coulton et al., 1986); and (iii) FhuE, which transports coprogen and rhodoturulate (Sauer et al., 1990). The catechol-type siderophore receptors are (i) FepA, which transports ferric enterobactin (Lundrigan & Kadner, 1986); (ii) Cir, which transports dihydroxybenzoate and catechol-substituted

cephalosporin antibiotics (Curtis et al., 1985; Nau & Konisky, 1989); and (iii) Fiu, which transports dihydroxybenzoylserine, dihydroxybenzoate and catechol-substituted cephalosporins (Nau & Konisky, 1989; Tatsumi et al., 1995; Möllmann et al., 1998). The sole receptor for citrate-type siderophores is FecA (Pressler et al., 1988). In *E. coli*, this receptor mediates the uptake of ferric citrate across the outer membrane. The vitamin B_{12} uptake system is grouped with those for siderophores, as they share a similar organization of proteins and utilize an analogous mechanism of ligand transport. The vitamin B_{12} receptor in the outer membrane of *E. coli* is BtuB (Heller & Kadner, 1985).

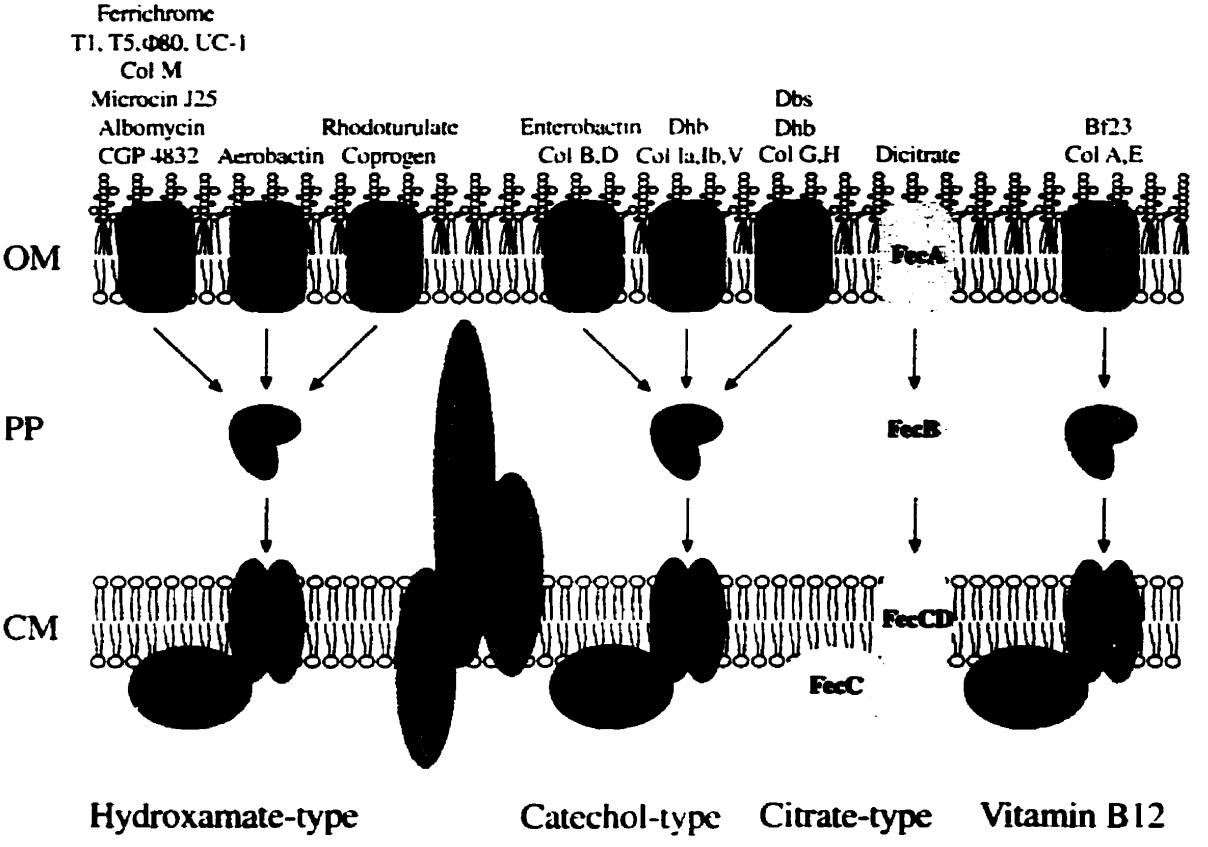

Figure 4. Selected TonB-dependent uptake systems of *E. coli*. Abbreviations: T1, bacteriophage T1; T5, bacteriophage T5; ϕ80, bacteriophage ϕ80, UC-1, bacteriophage UC-1; Bf23, bacteriophage Bf23; Col M, colicin M; CGP 4832, rifamycin CGP 4832; Col B, colicin B; Col D, colicin D; Dhb, dihydroxybenzoate; Col Ia, colicin Ia; Col Ib, colicin Ib; Col V, colicin V; Dhs, dihydroxybenzoylserine; Col A; colicin A; Col E, colicin E; OM, outer membrane; PP, periplasm; CM, cytoplasmic membrane.

6. Three-dimensional structure of FhuA and its complex with ferricrocin

6a. *General description of the structure*

The three-dimensional structures of FhuA and its complex with ferricrocin have been determined to 2.50 and 2.70 Å resolution, respectively (Ferguson et al., 1998b; Locher et al., 1998). The crystallographic structure shows that FhuA is a monomeric integral membrane protein that is organized into two domains, which fold independently (Figure 5, A and B; Braun et al., 1999). The C-terminal β-barrel domain (residues 161 to 714) is a 22-stranded antiparallel β-barrel (β1 through β22) that spans the outer membrane. The tilt of the β-strands relative to the barrel axis is approximately 45° and they range in length from eight to twenty-four residues (Figure 6). Many extracellular loops protrude beyond the lipid bilayer, such as L4, which extends 34 Å from the cell surface. Analogous to nonspecific and specific porins, β-strands that compose the barrel domain of FhuA are connected by longer extracellular loops (L1 through L11) and shorter periplasmic turns (T1 through T10). The elliptical-shaped β-barrel of FhuA represents the largest such structure observed to date. It is 69 Å in height and has an ellipsoidal cross-sectional diameter of 46 by 39 Å. The crystal structure of FepA shows a similar fold and molecular dimensions (Buchanan et al., 1999a). Extending from residue 681 to 690 from β21, is a β-bulge that protrudes outwards from the barrel surface of FhuA. This segment is highly conserved among all TonB-dependent receptors; however, its biological function remains to be established. FhuA also contains a pair of cystine bonds (Figure 6). The first disulphide-bridge, Cys318-Cys329, connects the adjacent segments of L4 and is readily surface accessible. The second, Cys692-Cys698, connects strands β21 and β22, and is positioned close to the extracellular rim of the β-barrel. These results are in accord with *in vivo* thiol-labelling experiments, which identified both disulphide-bridges and the limited accessibility of the C-terminal cystine bond (Bös & Braun, 1997; Bös et al., 1998). As observed with other integral outer membrane proteins, two aromatic girdles form a 25 Å hydrophobic zone on the membrane-embedded surface

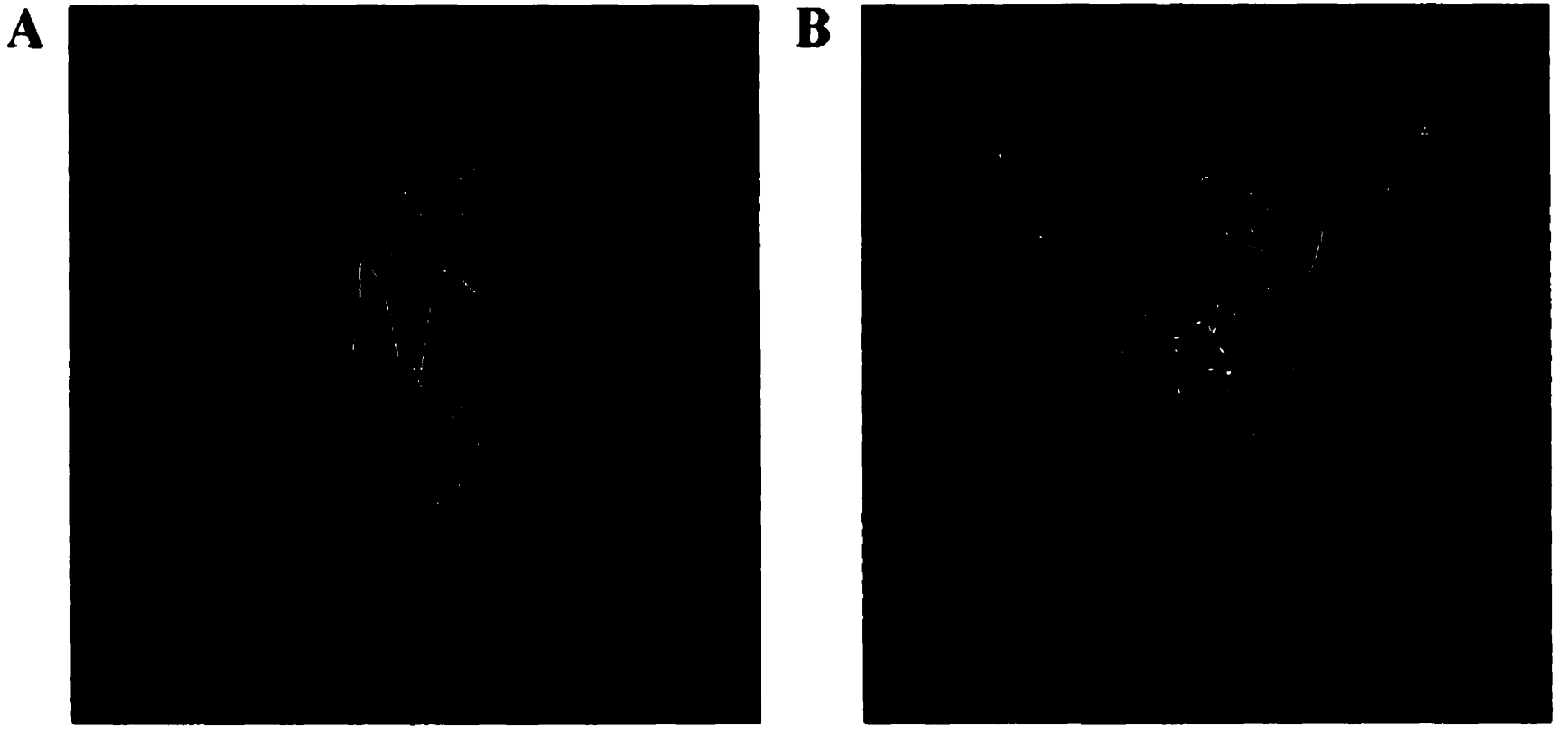

Figure 5. Ribbon representation of the crystallographic structure of FhuA in complex with ferricrocin. **A**: View parallel to the plane of the outer membrane. **B**: View from the extracellular medium. The barrel and cork domains of FhuA are coloured blue and yellow, respectively. The ferricrocin molecule is shown as a ball-and-stick model with carbon atoms black, nitrogen atoms blue, oxygen atoms red. The ferric iron atom is shown as a large red sphere. Apices A, B, and C are labelled.

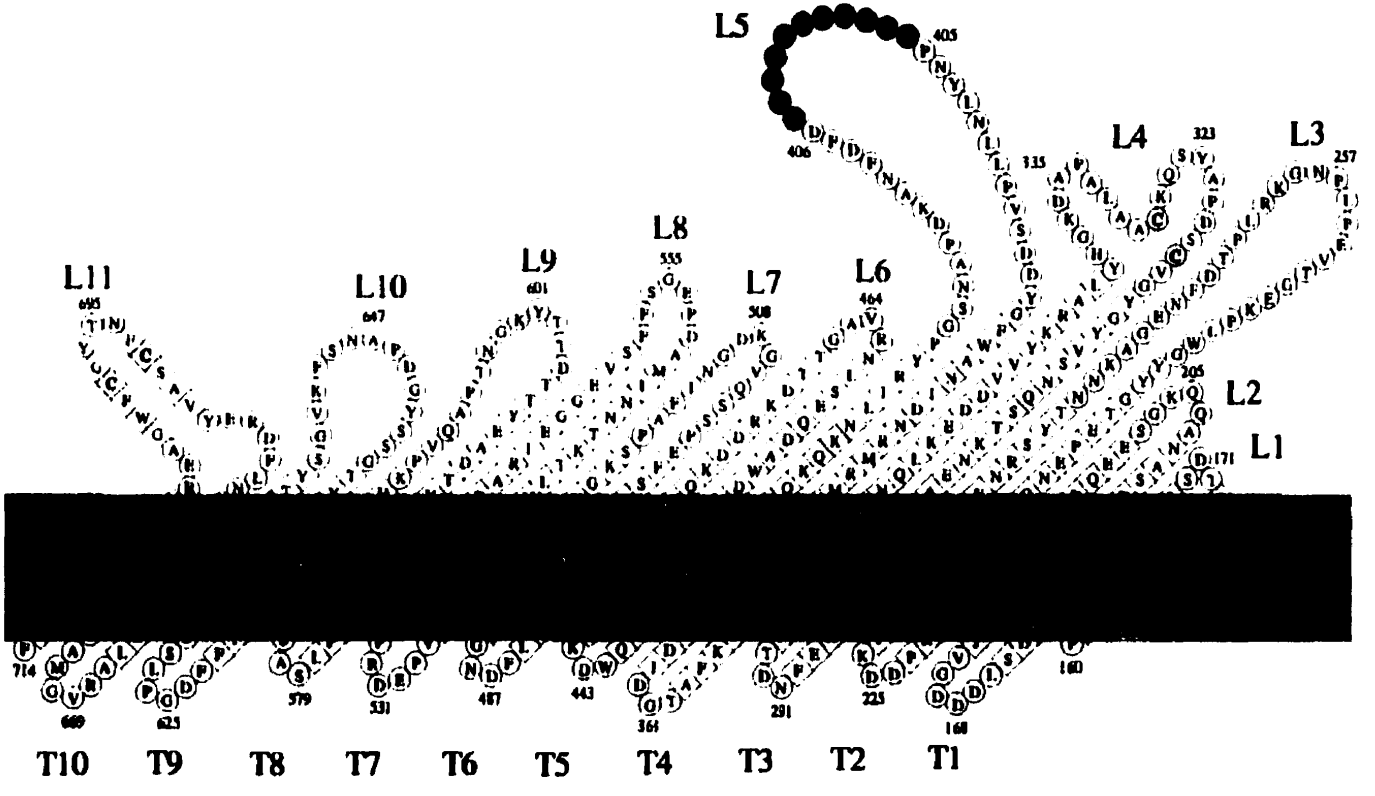

Figure 6. Secondary structure topology of the barrel domain of FhuA. The extracellular loops (L1 through L11) and the periplasmic turns (T1 through T10) are labelled. Squares indicate those side-chain residues that form inter-strand hydrogen bonds within the β-barrel; the remaining residues are displayed as circles. The blue shaded region represents the membrane-embedded portion of the receptor. The hexahistidine tag and five linker residues are coloured blue. Both disulphide-bridges are shown in yellow. FhuA is depicted, as it would be oriented within the outer membrane; extracellular loops and periplasmic turns are the top and bottom of the figure.

of FhuA. They are positioned to extend into the lipid bilayer, and delineate the interface between the hydrocarbon acyl chains and the phosphorylated glucosamine moieties of the LPS monolayer.

Positioned within the β-barrel of FhuA is the N-terminal 'cork' domain (residues 1 to 160). This domain is formed by a mixed four-stranded β-sheet with four interspersed α-helices and connecting segments. The first eighteen residues of the cork domain, including the TonB-box of FhuA (residues 7 to 11), are disordered in both the unliganded and liganded structures. Beginning with Glu19 of the liganded structure, a coil region extends into the first of four β-strands, βA, forming the periplasmic edge of the four-stranded β-sheet. After a pair of short helices, αB and αC, a coil region forms two apices, A and B, at Arg81 and Gln100, respectively. Apices A and B are located in the upper half of the barrel and contain side-chain residues directly involved in ligand binding. The polypeptide chain then leads into βB, forming the opposite edge of the β-sheet and positioned in the centre of the barrel. From there a coil region angles towards the upper barrel rim forming apex C at Tyr116, which forms hydrogen bonds with ferrichrome, then sharply downwards forming another short helix, αD, leading into strand βC in the lower region of the barrel. A short coil leads into the antiparallel β-strand, βD, which leads into the N-terminal end of the first β-strand of the barrel.

A three-dimensional alignment with all structures deposited in the Protein Data Bank indicates that the fold of the cork domain is unique. Although previous topology models of FhuA (Koebnik & Braun, 1993) and FepA (Armstrong & McIntosh, 1995) correctly predicted a large transmembrane β-barrel, only with the BtuB receptor was an N-terminal subdomain conceptually proposed (Lathrop et al., 1995). The plane of the four-stranded β-sheet is tilted by approximately 45° relative to the membrane normal, such that the direct passage of ligand across the outer membrane is occluded (Figure 7B). Accordingly, genetic excision of the cork domain (FhuAΔ5-160) facilitates the nonspecific passive diffusion of ferrichrome, antibiotics, and maltodextrins across the outer membrane (Braun et al., 1999). In the wild-type receptor, the presence of the cork domain within the β-barrel delineates a pair of pockets within FhuA. The larger extracellular pocket is restricted by β-strands, and apices A, B and C of the cork domain,

and is exposed to the external medium. The smaller periplasmic pocket is in contact with the periplasm.

6b. *The ligand-binding site*

Located within the extracellular pocket of FhuA is a single ferricrocin molecule. In its binding site, the siderophore is positioned ~20 Å above the external outer membrane interface. Residues from apices A, B, and C of the cork domain, and the β-strands of the barrel domain form direct hydrogen bonds with the ligand. Additional van der Waals contacts are formed with aromatic residues that line the interior walls of the β-strands and extracellular loops of the barrel. These side-chain residues may function to extract this and other ligands from the solvent by their low affinity for aromatic residues. This proposal is supported by the observation that the deletion mutant FhuAΔ5-160 is capable of capturing ferrichrome, albeit weakly, from the external medium (Braun et al., 1999); apices A, B and C are essential for high-affinity binding (K_D 0.1 μM; Locher & Rosenbusch, 1997). In accord with the composition of the ligand-binding site, deletion of residues 243 to 248 from L3 inhibits the binding of ferrichrome; although FhuAΔ243-248 still functions as a receptor for bacteriophages and colicin M (Killmann et al., 1998). Similarly, ferric enterobactin is likely extracted from the external environment and bound with high-affinity by an analogous series of interactions by its cognate receptor, FepA. The two 'sensor loops' of the N-terminal domain of FepA, and Arg286 from β5 and Arg316 from β6 of the barrel domain may be involved in ferric enterobactin binding (Newton et al., 1997; Buchanan et al., 1999a).

6c. *Ligand-induced allosteric transitions and transmembrane signalling*

Comparing the structure of FhuA to its complex with ferricrocin reveals two distinct conformations: unliganded and liganded. Within the barrel domain the α-carbon coordinates are essentially identical (root-mean-square deviation of 0.40 Å). However, in the ligand-binding site, an induced fit mechanism is observed. Specifically, in the unliganded conformation, Glu98, near apex B forms two hydrogen bonds with Ser504

and Gln505 from L7. The addition of ligand results in a 90° side-chain rotation and an approximately 1.5 Å α-carbon translation towards the barrel wall. The α-carbon of Gln100 near apex B undergoes an 1.8 Å vertical shift towards the ferricrocin molecule, accompanied by a 50° side-chain rotation; multiple hydrogen bonds are formed with the siderophore. All loops of the cork domain between apex A and the periplasmic pocket follow this vertical translation. The position of the four-stranded β-sheet and the loops of the cork domain near the putative channel-forming region between apex B and the periplasmic pocket remain fixed.

In the unliganded conformation, helix αA, which contains several hydrophobic residues, fits snugly into a complementary hydrophobic cavity formed by select side-chain residues from T8, T9, βA and helix αB. Upon the binding of ferricrocin, the upward translation of selected loops of the cork domain disrupts the interaction of this cavity with the hydrophobic face of helix αA, the switch helix, thereby promoting its destabilization. As a result of this helix-to-coil transition, all hydrogen bonds between residues of the switch helix and periplasmic turns T8 and T9 are lost. All residues N-terminal of Arg31 assume an extended conformation, bending away from the previous helix axis within the plane of the periplasmic pocket by ~180°. Furthermore, Ser20 positioned near Arg128 from βD in the unliganded conformation, is translated ~17 Å from its former α-carbon position in the liganded structure. Arg128, which is strictly conserved among all TonB-dependent receptors, forms extensive hydrogen bonds with residues of the cork domain in both structures. This residue, in conjunction with Asp40, stabilizes the association of the N-terminal coil away from the periplasmic opening of the putative channel-forming region in the liganded conformation. Previous genetic insertion studies have shown that insertion of a dipeptide into *fhuA* after residue Arg128 results in a complete loss of FhuA function (Carmel et al., 1990). Other dipeptide insertions after Ala59, Tyr82 and Pro135 led to diminished FhuA activities. These experiments affirm the importance of the topology of the cork domain. Given that TonB-dependent receptors must compete for a limited amount of energized TonB molecules, the unwinding of the switch helix and the associated altered protein surface, likely signals the ligand-loaded status of the receptor through the outer membrane (Kadner & Heller, 1995).

These crystallographic observations are in accord with previous functional and antibody recognition studies. It has been demonstrated that (i) ferrichrome binding to viable bacterial cells decreases the fluorescence of a surface-exposed cysteine residue (Bös et al., 1998); (ii) intrinsic tryptophan fluorescence measurements also show reduced levels of emitted fluorescence upon ferrichrome binding (Letellier et al., 1997); (iii) monoclonal antibodies that bind to sequences between residues 21 to 59 can presumably discriminate between the unliganded and liganded conformation of FhuA (Moeck et al., 1996); and (iv) incubation of purified FhuA with ferricrocin enhances complex formation between the receptor and TonB *in vivo* (Moeck et al., 1997). In light of the crystallographic structure of FhuA, these data may be reinterpreted as measurement of the movement of Trp22. This side-chain residue is located at the base of the switch helix, upon ligand binding it is translocated approximately 17 Å across the periplasmic pocket of the FhuA. The inability of bacteriophage T5 and microcin J25 to promote the formation of the cross-linked FhuA-TonB complex (Moeck et al., 1997), suggests that allosteric transitions induced by these ligands are distinct from those observed with ferricrocin.

7. Siderophore-induced gene transcription in *E. coli*

Metalloregulatory proteins control the transcription of genes involved in siderophore-mediated iron acquisition. However, under iron stress additional Fur-regulated gene transcription mechanisms that are responsive both to the intracellular iron concentration and the presence of certain siderophores in the external medium are induced. This method of gene regulation ensures an adaptive response to both the internal and external concentrations of iron (reviewed by Braun et al., 1998; Vasil & Ochsner, 1999).

In contrast to other siderophore-mediated iron acquisition systems of *E. coli*, under conditions of low iron and in the presence of ferric citrate, the rate of expression of genes involved in the active transport of this siderophore increase. The ferric citrate uptake system is composed of five genes, *fecABCDE* (Pressler et al., 1988). Analogous to other iron uptake pathways, a TonB-dependent receptor, FecA, is localized to the outer membrane. Once translocated across the outer membrane, the periplasmic binding

protein FecB binds the siderophore. An ABC transporter composed of two integral cytoplasmic membrane proteins, FecCD, together with the ATP-binding cassette FecE, actively pump ferric citrate into the cytoplasm upon the hydrolysis of ATP.

Different from other TonB-dependent receptors, FecA has two mutually exclusive functions. It facilitates both the uptake of ferric citrate, and is required to induce the transcription of the *fecABCDE* transport genes, but not the regulatory genes *fecIR* (Ochs et al., 1995; 1996). The uptake of ferric citrate and the induction of the signalling cascade are also dependent upon the chemiosmotic gradient of the cytoplasmic membrane as transduced by the TonB-ExbB-ExbD complex (Kim et al., 1997). The predicted transmembrane topology of FecA is a structural derivative of the characterized structures of FhuA (Ferguson et al., 1998b; Locher et al., 1998) and FepA (Buchanan et al., 1999a). It has been postulated that FecA possesses an N-terminal extension (Kim et al., 1997). The genetic excision of this segment (residues 14 to 68) abrogates induction; however, transport of ferric citrate across the outer membrane remains unaffected. Conversely, point mutations in *fecA* lead to constitutive induction of transcription and the loss of ferric citrate transport activity (Härle et al., 1995). The three-dimensional structure of the N-terminal extension of FecA will most likely be distinct from the equivalent domains of other TonB-dependent receptors from *E. coli*. The basic fold of the N and C-terminal domains may be similar to those observed with FhuA and FepA, their tertiary arrangement may also be maintained. Given the crystallographic disorder of the N-termini of FhuA and FepA, those residues that form the N-terminal extension of FecA will most likely form distinct globular domain that is placed in the periplasm. Moreover, the TonB-box of FecA (residues 81 to 84), which is required for both transport and induction activity, may not be located in a similar position as the TonB-boxes of FhuA and FepA.

Upon the binding of ferric citrate, FecA undergoes a conformational change that signals the occupancy of the receptor, which is presumably displayed in the periplasm by the N-terminal extension. A similar series of structural transitions as observed with the binding of hydroxamate-type siderophores and albomycin to FhuA, namely the unwinding of the switch helix, may also occur with FecA. However, in contrast to FhuA, the binding of ferric citrate to FecA initiates a signalling cascade. FecR is an integral

membrane regulatory protein that spans the cytoplasmic membrane. The transmembrane topology of FecR suggests a structural role for this molecule in the signal transduction pathway of the *fec* system (Ochs et al., 1995; Welz & Braun, 1998). In the absence of FecR, the binding of ferric citrate to FecA does not induce gene transcription (Ochs et al., 1995). Moreover, bacterial cells that express an N-terminal fragment of FecR constitutively transcribe the *fec* transport genes (Kim et al., 1997). Considering these observations it has been proposed that the binding of ferric citrate to FecA generates a signal that is transmitted across the cytoplasmic membrane by FecR. Paradoxically, FecR does not bind DNA. Thus, another regulatory protein is required to initiate transcription. This protein is FecI, a σ^{70}-type factor that responds to extracytoplasmic stimuli. When activated by FecR, FecI directs the binding of the RNA polymerase core enzyme to the promoter sequence upstream of *fecA* (Angerer et al., 1995). The formation of a binary complex between FecR and FecI has been demonstrated (Enz et al., 2000). Although these genes are not autoregulated, their expression is controlled by the Fur repressor (Ochs et al., 1996).

By consolidating the available genetic, biochemical and structural data, the following model for cell surface signalling can be constructed. The binding of ferric citrate to FecA induces a conformational change in the receptor, such that a signal indicating the liganded status of the receptor is transmitted from the cell surface into the periplasm by the N-terminal extension. A complex is subsequently formed between this segment of FecA and the C-terminal portion of FecR (Kim et al., 1997; Enz et al., 2000). The signal is subsequently transmitted into the cytoplasm, where FecI becomes activated. The FecI-RNA polymerase core enzyme complex then binds to the promoter sequence upstream of *fecA*, thereby initiating transcription of the *fec* transport genes.

8. Structure-function relationships of FhuA

8a. *Siderophore and vitamin B_{12} receptors form gated-channels*

The channel-forming ability of FhuA was first demonstrated by excising fragments from the *fhuA* gene (Killmann et al., 1993). When residues 322 to 355 are removed

(FhuAΔ322-355), a nonspecific channel is formed through which ligand passively diffuses at a rate proportional to the external ligand concentration. FhuAΔ322-355 incorporated into planar lipid bilayers forms permanently open ion-channels, with a single channel conductance three times larger than those observed with the porins. In contrast, wild-type FhuA does not form channels under identical experimental conditions. The segment that is critical for channel formation was later restricted to residues 335 to 355. The deletion mutant FhuAΔ335-355 supports TonB-independent growth, albeit at a lower growth rate than cells which express the wild-type receptor, and when incorporated in artificial bilayers forms stable channels of defined size and conductance (Killmann et al., 1996). Bacterial cells that express FhuAΔ322-355 or FhuAΔ335-355 become sensitive to sodium dodecyl sulphate and bacitracin. As expected, cells that express these deletion mutants or the mutant FhuAΔ5-160 are also capable of utilizing maltodextrins as a carbon source in the absence of maltoporin (Braun et al., 1999). These growth assays demonstrate that membrane-impermeable agents can readily traverse the outer membrane through channels formed by FhuA. Considering the structure of FhuA, residues 335 to 355 compose portions of L4 (residues 315 to 342) and strand β8 (residues 343 to 367) of the barrel domain. The structure suggests that specific connections formed between residues located on the inner barrel surface and apex C would be disrupted by deletion mutations in this region. As a result, certain coil segments of the cork domain may become more flexible, and thus facilitate transient opening of an aqueous diffusion channel. *In vivo*, the transport of siderophores and vitamin B_{12}, both of which require channel formation, consumes energy derived from the chemiosmotic gradient of the cytoplasmic membrane.

8b. *Binding sites for bacteriophages and colicin M*

FhuA functions as the primary receptor for four bacteriophages (T1, T5, ϕ80, and UC-1) and the bacterial toxin, colicin M. Sequences between residues 333 and 355 have been shown to be important for the binding of FhuA-specific bacteriophages. Cells that synthesize and export the mutants FhuAΔ322-355 or FhuAΔ335-355 to the outer membrane are resistant to cell killing by bacteriophages T1, T5 and ϕ80, and the import

of colicin M (Killmann et al., 1993; 1996). In contrast, those cells that expresses FhuAΔ322-333 or FhuAΔ322-336 remain fully sensitive to bacteriophages, suggesting that residues 335 to 355 from L4 participate in the binding of bacteriophages and colicin M. Competitive peptide mapping has shown that overlapping synthetic hexapeptides covering residues 316 to 356 reduced bacteriophage-mediated cell killing and the import of colicin M (Killmann et al., 1995). Considering that residues 335 to 355 comprise portions of L4 and strand β8, it is conceivable that FhuA-specific bacteriophages bind to the outer surface of the barrel domain above the external LPS monolayer. In the case of bacteriophage T5, the straight tail fibre protein pb5, mediates this interaction (Mondigler et al., 1995; 1996).

Primary structure comparisons of the FhuA proteins from *E. coli*, *P. agglomerans*, *S. paratyphi* strain B, and *S. typhimurium* further support the proposal that residues 335 to 355 are directly involved in bacteriophage binding (Killmann et al., 1998). The FhuA protein from *S. paratyphi* strain B shares significant homology with the equivalent segment of the FhuA protein from *E. coli*. When expressed in *E. coli*, the FhuA protein from *S. paratyphi* strain B confers full sensitivity to bacteriophages T1, T5, and ϕ80. When expressed in *E. coli*, the FhuA proteins from *S. typhimurium* and *P. agglomerans*, which do not have homologous 335 to 355 sequences, render the bacterium completely resistant to FhuA-specific bacteriophages. In contrast, cells that express the mutant FhuAΔ5-160 remain fully susceptible to the TonB-dependent bacteriophages T1 and ϕ80, and colicin M. Thus, the cork domain of FhuA is not required for the binding of bacteriophages or the import of colicin M (Braun et al., 1999).

When FhuA is incorporated into planar lipid bilayers, the binding of bacteriophage T5 to FhuA triggers a conformational change in the receptor such that a stable high-conductance channel opens (Bonhivers et al., 1996). This channel is electrophysiologically equivalent to the permanently open channels formed by FhuAΔ322-355, suggesting that these channels resemble those formed *in vivo* (Killmann et al., 1993; 1996). A structure composed of six copies of the pb2 protein, which is located at the distal end of the tail of bacteriophage T5, clearly traverses the bilayer as revealed by cryoelectron micrographs (Lambert et al., 1998). This unique channel-forming structure contracts following an interaction of the bacteriophage with FhuA, and

likely mediates the transfer of the DNA template across the outer and cytoplasmic membranes (Feucht et al., 1990; Guihard et al., 1992). Such a mechanism would eliminate the need for the cork domain to be completely removed from the barrel. Moreover, the ousting of the cork domain as a prerequisite for the transfer of viral DNA would require nearly 100 hydrogen bonds and other charge and van der Waals interactions to be simultaneously broken.

8c. *TonB-dependent import of group B colicins*

The formation of ion-permeable channels in target cell membranes is a widely used cytotoxic mechanism (reviewed by Gouaux, 1997; Lazdunski et al., 1998). Channel formation reduces the electrochemical gradient across plasma membrane. Such toxins include exotoxin A from *P. aeruginosa*, diphtheria toxin from *C. diphtheriae*, and the plasmid-encoded colicins that are synthesized by *E. coli*. The functional properties of channel-forming colicins are contained within a single polypeptide chain, and can be localized to three functional segments. The three-dimensional structure of colicin Ia revealed that the receptor-binding domain of this 'harpoon-shaped' molecule is separated from the N-terminal translocation and C-terminal catalytic domains (Wiener et al., 1997). Two exceptionally long α-helices of the receptor-binding domain enable colicin Ia to span the entire cell envelope.

For colicins to kill bacterial cells, they must first traverse the outer membrane. This is accomplished by co-opting nonspecific and specific porins or energy-dependent receptors, which inadvertently mediate toxin-host recognition. Channel-forming colicins can be separated into functionally related families depending on which uptake pathway and energetic requirement is used for entry into cells. Colicins that utilize active outer membrane receptors include (i) group A colicins (e.g. E1 and N), which exploit the TolA-TolQ-TolR complex (Webster, 1991); and (ii) group B colicins (e.g. Ia, Ib and B), which use the TonB-ExbB-ExbD energy-transducing module for their import. Accordingly, colicin-resistant *E. coli* strains have defects in their *tonB*, *tolA*, *exbB* and *exbD* genes. The group B colicin that is specifically imported by FhuA, colicin M, does not form channels; however, it does display unique activity that inhibits peptidoglycan and LPS

biosynthesis by interfering with the regeneration of an essential lipid carrier. An immunity protein can inhibit the activity of colicin M in the periplasm before the toxin reaches its target in the cytoplasmic membrane (Olschläger et al., 1991; Gross & Braun, 1996).

The receptor-binding domain of colicin Ia initially interacts with the outer membrane receptor Cir. It has been proposed that the transfer of colicins across the outer membrane may involve the unfolding of the toxin, in order to pass through the lumen of the gated-channels formed by outer membrane receptors or the permanently open channels of porins; however, this remains to be established experimentally. Given the restricted channel diameter of porins (7 by 11 Å) and the orientation of the constriction loop, and the secondary structure composition of colicins, it is implausible that the translocation and channel-forming domains of these agents pass through the porins (Jeanteur et al., 1994). Moreover, considering the three-dimensional structures of FhuA and FepA it is unlikely that the N-terminal domains of these TonB-dependent receptors are ousted as a requisite event for colicin import. More likely is the proposal that a conserved segment localized to the membrane-embedded surface of the β-barrel functions as a binding site.

It is interesting to speculate why group B colicins have TonB-boxes. For colicin Ia, residues 23 to 27 constitute the TonB-box. Mutations in the TonB-boxes of colicins abolish activity (Pilsl et al., 1993). This conserved segment is required for colicin translocation, suggesting that competitive displacement by the TonB-box of colicin Ia may be part of the colicin import mechanism as mediated by co-opted TonB-dependent receptors. However, other group B colicins exploit nonspecific and specific porins, which do not have TonB-boxes; demonstrating that competitive displacement is not a strictly conserved import mechanism. The formation of channels in the cytoplasmic membrane is accomplished by distinct membrane-associated conformations of the channel-forming domain. Positively charged surfaces on the C-terminal domain of colicin Ia interact favourably with negatively charged lipids of the cytoplasmic membrane, demonstrating that electrostatics drive initial docking (Elkins et al., 1997). Hydrophobic forces facilitate the spontaneous insertion of the channel-forming domain of colicin Ia into the cytoplasmic membrane. Following the membrane insertion event a 7 Å transmembrane waisted channel is formed, and potassium ions are released from the

cytoplasm. As a result, the cytoplasmic membrane is depolarized. Bacterial ATP-driven export pumps can partially compensate for the depolarization of the cytoplasmic membrane; however, a single channel rapidly depletes the cytoplasmic ATP pool (Guihard et al., 1993). Unless an immunity protein is encoded on the same plasmid or chromosomal region (Gross & Braun, 1996), the cell-killing potential of colicins is clearly illustrated in that only one toxin molecule is needed to kill a bacterial cell.

9. Energetics of ligand transport across the outer membrane

Different from transport across the cytoplasmic membrane, where primary or secondary energy-driven transporters utilize ion translocation or the hydrolysis of ATP for uptake, there is no available energy source in the outer membrane to drive the translocation of siderophores and vitamin B_{12} into the periplasm. Thus, gram-negative bacteria couple the chemiosmotic gradient of the cytoplasmic membrane with ligand transport across the outer membrane (Bradbeer, 1993). Transport across the cytoplasmic membrane is mediated by periplasmic binding protein-dependent ABC transporters, and is energized by the hydrolysis of ATP. The division of energetic requirements reflects the compartmentalization of the transport process. While the precise mechanism by which the proton motive force and ATP catalysis drive ligand uptake remains to be determined, it is known that the TonB-ExbB-ExbD complex plays a key role in the transfer of energy across the periplasm (reviewed by Kadner, 1990; Postle, 1990; 1993; Klebba et al., 1993; Braun, 1995; Braun et al., 1998; Moeck & Coulton, 1998).

9a. *Putative sites of interaction between TonB-dependent receptors and TonB*

All TonB-dependent receptors and group B colicins have one N-terminal segment of conserved primary structure, the 'TonB-box' (Schramm et al., 1987). The consensus seven residue TonB-box sequence is: acidic residue (Asp or Glu)-Thr-(hydrophobic residue)$_2$-Val-polar residue (Ser or Thr)-Ala (Kadner, 1990). A functional role has been assigned to the TonB-box. With the BtuB receptor, the introduction of a proline residue at position 8 or 10, or a glycine residue at position 10, abolishes TonB-dependent uptake

of vitamin B_{12} (Heller & Kadner, 1985). However, these and other point mutations do not impair the binding of vitamin B_{12}, the irreversible adsorption of the TonB-independent bacteriophage BF23, or the import of colicins E1 and E3 (Gudmundsdottir et al., 1989). By substituting an isoleucine residue at position 9 with a proline side-chain in FhuA, TonB-dependent uptake of ferrichrome is inhibited, whereas Ile9Thr and Ile9Ser substitutions have no effect (Schöffler & Braun, 1989). With the Cir receptor, replacing valine 8 with a glycine residue renders *E. coli* cells resistant to colicin Ia, without inhibiting the recognition and uptake of dihydroxybenzoate (Bell et al., 1990). A similar substitution uncouples TonB-dependent uptake as mediated by the FhuE receptor (Sauer et al., 1990).

Initial evidence that TonB may associate with the TonB-boxes of outer membrane receptors was provided by genetic suppresser mutation studies. Heller et al., (1988) isolated plasmid-encoded *tonB* mutants that partially restore TonB-dependent activity in *E. coli* strains expressing the BtuB mutants mentioned above. The mutation was revealed to be a single amino acid substitution (leucine, lysine or proline) at position 160 of TonB (Heller et al., 1988; Bell et al., 1990). Analogous *tonB* suppressor mutations have been characterized for TonB-box mutants of FhuA (Schöffler & Braun, 1989), Cir (Schöffler & Braun, 1989; Bell et al., 1990), and FhuE (Sauer et al., 1990). The ability of *tonB* suppressor mutants to partially restore activity may be explained if a segment of TonB at or near residue 160 physically interacts with TonB-dependent receptors (Bruske & Heller, 1993). Considering that seemingly invariant TonB-box residues can be mutated without affecting function, it is likely that it is the conformation rather than the primary structure of the TonB-box that is required for efficient energy-transduction. Accordingly, point mutations presumably distort the conformation of the TonB-box or adjacent regions of TonB-dependent receptors, such that specific protein-protein interactions with TonB are impaired.

The direct physical interaction of TonB with its cognate receptors was first demonstrated by cross-linking studies. When treated with formaldehyde, FepA embedded in the outer membrane of *E. coli* can be chemically cross-linked to TonB in the absence of ferric enterobactin (Skare et al., 1993). That a point mutation in the TonB-box of this receptor (Ile14Pro) prevents TonB-dependent ligand transport and chemical cross-

linking to TonB (Larsen et al., 1997), suggests that conformational changes in this region likely inhibit protein-protein interactions with TonB. Similar cross-linking studies have been carried out with the FhuA receptor in the presence and absence of ligand (Moeck et al., 1997). In the absence of ferrichrome, the FhuA-TonB complex could not be detected *in vivo*. The formation of the FhuA-TonB complex is dependent upon the binding of ferricrocin to FhuA. Other FhuA-specific ligands, bacteriophage ϕ80 and to a lesser extent colicin M, also enhance the formation of FhuA-TonB complexes *in vitro*. Cells that express certain *tonB* suppressor mutations are capable of restoring partial activity to TonB-box mutants and the formation of cross-linked complexes *in vivo* (Larsen et al., 1997). Following the solution of the crystal structures of FhuA and FepA, and the observation that the TonB-boxes of these proteins are localized in the periplasm, site-directed disulphide cross-linking was used to unequivocally demonstrate the existence of direct physical interactions between the TonB-boxes of receptors and TonB (Cadieux & Kadner, 1999). Cysteine residues introduced at successive positions within the TonB-box of BtuB, which also resides in the periplasm, form disulphide-bridges with a single cysteine residue inserted at or near to position 160 of TonB (Cadieux & Kadner, 1999; Merianos et al., 2000). Only those BtuB mutants with engineered cysteines in their TonB-boxes were capable of forming a complex with TonB. As observed with FepA and FhuA, the efficiency of cross-linking was increased in the presence of ligand. This study also suggests that interactions between TonB and TonB-dependent receptors probably occur by a parallel N-to-C-terminal arrangement of both proteins. Site-directed spin labelling and electron paramagnetic resonance assays indicate that the TonB-box of BtuB in the unliganded conformation may be localized to a helix that forms interactions with side-chain residues from the periplasmic turns of the barrel domain of the receptor (Merianos et al., 2000). The binding of vitamin B_{12} to BtuB induces a helix-to-coil transition, such that the TonB-box assumes an extended conformation.

9b. *The TonB-ExbB-ExbD complex and its role in energy-transduction*

Alignment of Enterobacteriaceae *tonB* sequences identifies three conserved domains that contribute in distinct ways to TonB's function as an energy-transducer (Traub et al.,

1993; Larsen et al., 1996). The N-terminus of TonB (residues 1 to 32) functions as an uncleaved export signal that anchors the protein in the cytoplasmic membrane (Postle & Skare, 1988). The remainder of the protein is localized in the periplasm (Roof et al., 1991). Although deletion of the signal anchor (residues 12 to 32) does not inhibit the formation of cross-linked FepA-TonB complexes *in vivo* (Larsen et al., 1994), this segment is required for energy-transduction (Karlsson et al., 1993a). The second domain of TonB (residues 63 to 102) is the proline-rich region, which contains a $(Glu\text{-}Pro)_n$-acetyl linker-$(Lys\text{-}Pro)_n$ repeat. This motif was predicted to have functional significance as synthetic peptides corresponding to this segment were shown by nuclear magnetic resonance to be capable of bridging the distance between the cytoplasmic and outer membranes (Evans et al., 1986a; Brewer et al., 1990). However, cells that express a deletion mutant of TonB (TonBΔ66-100) display near wild-type levels of TonB-dependent activity (Larsen et al., 1993). These results indicate that the proline-rich domain is not essential for TonB-dependent function, although its presence does enhance TonB's ability to span the periplasm. The third domain of TonB with predicted functional significance is the C-terminus of the protein (residues 102 to 239). This region, specifically residues 160 to 167, most likely mediates a conformation-dependent interaction with TonB-dependent receptors, as shown by cross-linking and *tonB* suppressor mutation studies. Deletion of the C-terminal domain prevents cross-linking to FepA and reduces TonB's association with the outer membrane (Letain & Postle, 1997). Residues 199 to 216 of the C-terminal domain are predicted to form an amphipathic α-helix (Larsen et al., 1993). Larsen et al., (1997) isolated bacterial strains with point mutations at position 215 of TonB. All substitutions at this location result in some level of TonB-dependent activity. However, the fact that only histidine, leucine, or phenylalanine side-chain residues confer near wild-type levels of activity suggest that tyrosine 215 does not physically interact with TonB-dependent receptors, but rather influences the conformation of distal sites of TonB. Additional genetic studies revealed that removing thirteen or fifteen C-terminal residues of TonB from *Enterobacter aerogenes* or *E. coli*, abrogates all TonB-dependent function, whereas excising the final eight residues only diminishes function (Anton & Heller, 1991; Bruske & Heller, 1993).

TonB's association with the cytoplasmic membrane, stability and function is dependent upon two additional membrane proteins with unusual transmembrane topologies, ExbB and ExbD. Different from TonB, the N-terminus of ExbB is localized in the periplasm (Eick-Helmerich & Braun, 1987; Kampfenkel & Braun, 1993). Two additional segments of this protein span the cytoplasmic membrane; the remainder resides in the cytoplasm (Karlsson et al., 1993b). Similar to TonB, ExbD is anchored in the cytoplasmic membrane by its N-terminus; the remainder of the protein is largely placed in the periplasm (Kampfenkel & Braun, 1992). In addition to forming TonB-ExbB and TonB-ExbD complexes (Fischer et al., 1989; Skare et al., 1993; Ahmer et al., 1995; Braun et al., 1996), both ExbB and ExbD form homomultimers in the absence or presence of TonB and TonB-dependent receptors (Higgs et al., 1998). These chemically cross-linked complexes indicate that ExbB and ExbD may form a heterohexameric complex *in vivo*. This membrane-embedded complex would span the cytoplasmic membrane twelve times, and presumably bind the TonB signal anchor (Letain & Postle, 1997). The ability of these proteins to (i) protect one another from proteolytic degradation (Fischer et al., 1989; Skare et al., 1993; Ahmer et al., 1995); (ii) copurify as a complex (Braun et al., 1996); and (iii) form chemically cross-linked complexes (Higgs et al., 1998), suggests that the respective transmembrane domains of these proteins form protein-protein interactions, and a ternary complex *in vivo*. Residues 12 to 32 of the signal anchor of TonB are postulated to assume an α-helical conformation, one face of the transmembrane helix may display four highly conserved residues, Ser16, His20, Leu27, and Ser31; the 'SHLS motif'. This region has been demonstrated to be involved in protein-protein interactions with ExbB. By replacing the signal anchor of TonB with the first transmembrane segment of the cytoplasmic membrane protein TetA, generates an inactive, yet properly exported chimera (Jaskula et al., 1994; Braun, 1989). This fusion protein can be cross-linked to FepA (Jaskula et al., 1994) but not to ExbB (Larsen et al., 1994), presumably because critical interactions between the signal anchor of TonB and the transmembrane portion of ExbB are abrogated. Furthermore, the deletion of a single valine residue at position 17 of TonB (TonBΔ17), inhibits the formation of chemically cross-linked ExbB-TonB complexes, in addition to dramatically reducing all TonB-dependent activities (Skare et al., 1993; Larsen et al., 1994). Additional signal

anchor point mutations (Ser16Leu and His20Tyr) generate functionally impaired TonB derivatives (Larsen et al., 1999). As observed elsewhere, ExbB suppressor mutations (Val35Glu, Val36Asp and Ala39Glu) are capable of partially restoring TonB-dependent activity mutant strains [TonBΔ17, TonB(Ser16Leu) and TonB (His20Tyr)], and the formation of cross-linked ExbB-TonB complexes (Larsen et al., 1999). Formaldehyde cross-linked complexes between TonB and ExbD have been detected using immunoblot analysis (Higgs et al., 1998). Whereas the signal anchor of TonB and the first transmembrane domain of ExbB mediate interactions between these proteins, specific regions of contact between TonB and ExbD remain to be established. However, substituting a single aspartate residue at position 25 of the transmembrane domain of ExbD with arginine, or replacing leucine at position 132 of the periplasmic domain with asparagine, inactivates ExbD (Braun et al., 1996). The single charged residue of the transmembrane domain of ExbD (Asp25) may interact with His 20 of the SHLS motif of TonB, and when altered, abrogate the conformation of TonB and TonB-dependent activity (Traub et al., 1993).

In the absence of ExbB and ExbD, bacterial cells are resistant to bacteriophage and colicin infection, and manifest a 90% reduction in all TonB-dependent activities (Skare et al., 1993; Ahmer et al., 1995). The residual level of TonB activity results from the presence of TolQ and TolR, which are functional analogues of the ExbB and ExbD proteins of *E. coli* (Braun, 1989; Eick-Helmerich & Braun, 1989; Braun & Herrmann, 1993; Kampfenkel & Braun, 1993). The TolA protein provides a similar function as TonB (Koebnik, 1993). Although the primary structures of TonB and TolA are not homologous, their predicted secondary structures, and ultimately their three-dimensional structures may be related (Braun & Herrmann, 1993). Analogous to TonB, the N-terminal domain of TolA anchors the protein to the cytoplasmic membrane. Indeed, replacing the signal anchor of TonB with the equivalent segment of TolA generates a functional TolQ-TolR-dependent chimera. A central elongated α-helical domain positions the C-terminal domain of TolA in close proximity to the outer membrane, in which it is embedded (Levengood et al., 1991). The crystal structure of the C-terminal domain of TolA in complex with the bacteriophage coat protein g3p (a protein involved in the infection process) has recently been determined (Click & Webster, 1997;

Riechman & Holliger, 1997; Lubkowski et al., 1999). The ordered C-terminal residues of TolA form a three-stranded antiparallel β-sheet that is flanked by four α-helices positioned on one side of the β-sheet. This region of TolA shares significant amino acid sequence homology with *tonB* homologues, suggesting that the C-terminal domain of TonB may assume a similar fold. This proposal is supported by the observations of Cadieux and Kadner (1999), who demonstrated that side-chain residues at positions 8, 10, and 12 of BtuB preferentially interact with cysteine residues introduced at or near position 160 of TonB.

9c. *Proposed mechanism for TonB-dependent energy-transduction*

By integrating the available biochemical, genetic and structural data, a model of TonB-dependent energy-transduction can be proposed. TonB, embedded within the cytoplasmic membrane is closely associated with the heterohexameric ExbB-ExbD complex. The binding of siderophores or vitamin B_{12} to the extracellular pocket of outer membrane receptors causes a TonB-independent conformational change that is propagated through the outer membrane, and is displayed by select periplasmic segments of the protein; the switch helix and periplasmic turns. The unwinding of the switch helix and the translocation of the TonB-box, or the conformation of the TonB-box itself, may signal the occupancy of the receptor. As TonB is present in lower concentrations compared to the TonB-dependent receptors in bacterial cells, outer membrane transporters must compete for energized TonB molecules (Kadner & Heller, 1995).

The transfer of chemiosmotic energy from the cytoplasmic membrane to the outer membrane by the TonB-ExbB-ExbD complex may occur by an allosteric mechanism. The proton motive force likely drives the transition of TonB from the 'uncharged' to the 'charged' conformation, and this in turn promotes its interaction with outer membrane receptors. The ExbB protein is directly involved in this cycle, by forming protein-protein interactions with the signal anchor of TonB (Larsen et al., 1999). The role of ExbD in this process remains poorly defined (Ahmer et al., 1995; Higgs et al., 1998; Larsen et al., 1999). It has also been postulated that ExbB might mediate additional protein-protein interactions between TonB and an, as yet, unidentified ion-translocator. This proposed

mechanism is similar to that observed with the archael rhodopsins, whose conformations and functional activities are responsive to light. The light-driven translocation of ions generates electrochemical potential, which is captured in the charged conformation of prokaryotic and eukaryotic seven-transmembrane α-helical proteins. Could a homologous proton translocator, tightly associated with the TonB-ExbB-ExbD complex, be required to harness the chemiosmotic energy of the cytoplasmic membrane and mediate energy-transduction to TonB? Although no such protein has been discovered, *in vivo* chemical cross-linking reveal complexes of TonB with two unidentified 41 kDa and 7 kDa proteins (Skare et al., 1993). The functions of these proteins remain to be determined, and they may be auxiliary components in the TonB-dependent energy transduction complex. Alternatively, the heterohexameric ExbB-ExbD complex may entirely constitute the proton translocation apparatus. This complex may couple the proton motive force to conformational changes in TonB and the active transport of siderophores and vitamin B_{12} across the outer membrane.

Following the unwinding of the switch helix and the transition to the liganded conformation charged TonB preferentially interacts with outer membrane receptors. However, a portion of the available TonB molecules may form complexes with liganded TonB-dependent receptors whose switch helices have not unwound, as observed with the FhuA-CGP 4832 complex (Ferguson et al., 2000c). This proposal is supported by (i) the observation that some TonB co-purifies with outer membrane receptors during cell fractionation (Letain & Postle, 1997); (ii) *in vitro*, the deletion mutant FhuAΔ21-128 forms chemically cross-linked complexes with TonB (Moeck et al., 1997); and (iii) bacterial cells that synthesize the deletion derivative FhuAΔ5-160, which does not have a TonB-box, also retain a diminished level of TonB-dependent activity (Braun et al., 1999). In either case, the C-terminal domain of TonB likely forms direct physical contacts with the TonB-box and other side-chain residues found within the periplasmic turns of the β-barrel domain of TonB-dependent receptors (Braun et al., 1999; Merianos et al., 2000). This physical association occurs independently of the energy state of TonB and the ExbB-ExbD complex (Letain & Postle, 1997), but is enhanced by the presence of ligand (Skare et al., 1993; Moeck et al., 1997; Cadieux & Kadner, 1999). Whether TonB is entirely released from the ExbB-ExbD complex to shuttle to the outer membrane remains

to be established. However, this proposed proton motive force responsive-mechanism is not novel. For example, the translocation of proteins across the cytoplasmic membrane is performed by the Sec system (Kadner, 1996). Analogous to the uptake of siderophores and vitamin B_{12}, protein translocation requires both the proton motive force and the hydrolysis of ATP. The SecA protein regulates this process by undergoing cyclical membrane insertion and release events. The proton motive force increases the efficiency of SecA release from the cytoplasmic membrane (Nishiyama et al., 1999), whereas insertion is dependent upon the binding and hydrolysis of ATP (Economou et al., 1995). Alternatively, TonB may remain permanently anchored within the cytoplasmic membrane and associated with the ExbB-ExbD complex.

Irrespective of the mechanism, upon forming a complex with outer membrane receptors TonB transduces its stored conformational energy to the receptor. This event triggers a conformational change in the receptor such that the ligand-binding site is disrupted and the binding affinity is reduced. Because Tyr244 and Trp246 from L3 remain fixed upon ligand binding, disruption of the binding site may be affected by a small shift of apices A, B and C towards the periplasm. Alternatively, the arrangement of aromatic side-chain residues that line the extracellular pocket, specifically those found on L4, may alter their conformations (Bös et al., 1998). The formation of a transient complex with charged TonB causes a high-conductance channel to open within TonB-dependent receptors. Subtle conformational changes of the loops of the cork domain between apex B and the periplasmic pocket of FhuA might constitute the structural basis for this event. The TonB-box presumably returns to its original position upon channel formation. When viewed along the barrel axis the extracellular pocket is connected to the periplasmic pocket in one segment of the barrel cross-section by a 10 Å aqueous channel, the 'putative channel-forming region'. Once released from their binding sites, ligands move into this region where they are confined, thereby assuring rapid and directed transport. Siderophores and vitamin B_{12} may subsequently diffuse into the periplasm by utilizing a series of strictly conserved side-chain residues that line the interior barrel wall of the putative channel-forming region from the ligand-binding site to the periplasmic pocket of FhuA. The arrangement of these residues might function as a series of low-affinity binding sites for the surface diffusion of ligand through TonB-dependent

receptors. Upon arrival in the periplasm these ligands are rapidly bound by specific high-affinity periplasmic binding proteins, and shuttled to distinct ABC transporters embedded within the cytoplasmic membrane.

Do the TonB-independent channels formed by outer membrane receptors upon the binding of bacteriophage T5 (Boulanger et al., 1996) or by the deletion mutants of FepA (Rutz et al., 1992), FhuA (Killmann et al., 1993; 1996) and BtuB (Lathrop et al., 1995), differ from those formed *in vivo*? Electron spin resonance spectroscopy revealed that during ligand transport, FepA assumes at least two TonB-dependent conformations (Liu et al., 1994; Jiang et al., 1997). These *in vivo* results demonstrate that the chemiosmotic energy from the cytoplasmic membrane as transduced by the TonB-ExbB-ExbD complex, is required to liberate bound siderophores or vitamin B_{12} from their respective binding sites. Once released these ligands are confined to putative-channel forming regions of TonB-dependent receptors, through which they pass. The proposal that these transporters simply function as 'gated-porins' (Murphy et al., 1990) ignores the fact that these proteins actively pump ligand across the outer membrane, thereby establishing a 1000-fold increase in the cytoplasmic ligand concentration relative to the external medium (Reynolds et al., 1980). The presence of high-affinity periplasmic binding proteins presumably ensure the rapid delivery of the ligand to cytoplasmic membrane-embedded ABC transporters, and thus, establish a significant concentration gradient. Furthermore, the rate of ligand transport by wild-type TonB-dependent receptors at low ligand concentrations is higher than observed with the deletion mutants of FhuA (Killmann et al., 1993). Regardless of the precise transport mechanism, the release of potential energy leaves TonB in the 'discharged' conformation, from which it either recovers or is proteolytically degraded. The ExbB and ExbD proteins appear to be essential for this cyclical process (Larsen et al., 1999).

10. Transport across the cytoplasmic membrane

10a. *ATP-binding cassette transport systems*

The ATP-binding cassette (ABC) proteins form a diverse group of highly conserved transport complexes that are found in prokaryotes and eukaryotes, which couple ATP binding and hydrolysis to a wide variety of physiological processes (reviewed by Boos & Lucht, 1996; Linton & Higgins, 1998; Nikaido & Hall, 1998). Many human ABC transporters are associated with disease (e.g. cystic fibrosis); bacterial ABC transporters are primarily involved in ligand translocation (import or export) across the cytoplasmic membrane. The generic ABC transporter consists of two transmembrane domains that form a channel through which ligand passes. The components of the permease may be homologous but nonidentical, and can be composed of one or two gene products. Each transmembrane domain is postulated to consist of five, six or eight transmembrane α-helices that are connected by periplasmic loops and cytoplasmic turns. Asymmetric protein-protein interactions between homodimeric, pseudoheterodimeric or heterodimeric transmembrane domains and their cognate periplasmic binding proteins have been observed. Ligand transport into the cytoplasm is catalyzed by the hydrolysis of ATP as mediated by two hydrophilic ATP-binding domains that are peripherally associated with the inner leaflet of the cytoplasmic membrane. Primary structure comparisons of periplasmic binding protein-dependent ABC importers reveal some regions of homology. A stretch of 200 conserved amino acid residues of the ATPase, including two ATP-binding 'Walker motifs', A and B, are required for ligand translocation and the hydrolysis of ATP (Walker et al., 1982; Higgins et al., 1985). The Walker A and B motifs are postulated to form the ATP-binding pocket. A signature termed the 'EAA loop' is located between the second and third transmembrane helices of the permease. This sequence is essential for energy-transduction and protein-protein interactions with the ATP-binding domains of the transporter. Accordingly, deletion or mutation of this functionally important sequence abrogates transport activity (Dassa & Hofnung, 1985; Higgins et al., 1986; Köster & Bohm, 1992; Saurin et al., 1994; Mourez et al., 1997).

Those ABC transporters involved in bacterial iron acquisition and vitamin B_{12} uptake require auxiliary components, including an outer membrane receptor and periplasmic binding protein. These proteins bind their cognate ligands with high-affinity and mediate their uptake into the periplasm and their presentation to the cytoplasmic membrane-embedded and ATP-binding domains of the importer. Different from most periplasmic binding protein-dependent transport systems, the affinity and ligand specificity of those ABC transporters involved in iron and vitamin B_{12} uptake is defined by the outer membrane receptor and not the periplasmic binding protein.

Gram-negative bacteria utilize three distinct mechanisms for transporting iron into the cytoplasm. The first is a periplasmic binding protein-independent mechanism, which modulates the high-affinity uptake of Fe^{II} into the cytoplasm. Both periplasmic binding protein-dependent pathways, couple the transport of ionic Fe^{III}, and Fe^{III} bound to haem and siderophores to the hydrolysis of ATP. Different from outer membrane receptors, periplasmic binding proteins display broad ligand specificity. They bind their cognate ligands with high-affinity (K_D ~1 μM), and thus provide unidirectional transport. These proteins have functionally distinct regions that participate in ligand binding and protein-protein interactions. Direct physical interactions between the periplasmic and cytoplasmic membrane-associated domains of ABC transporters have been demonstrated by protease protection assays, cross-linking studies, and competitive peptide mapping (Rohrbach et al., 1995b; Mademidis et al., 1997). Although these proteins share little primary structure homology, those with known crystallographic structures assume closely-related topologies; a monomeric protein composed of two similar globular lobes that are connected by a flexible hinge (Spurlino et al., 1991; Mowbray & Cole, 1992; Olah et al., 1993; Sharff et al., 1993; Flocco & Mowbray, 1994; Oh et al., 1994; Yao et al., 1994; Bruns et al., 1997; Clarke et al., 2000). The ligand-binding site, formed by noncontiguous regions of the polypeptide chain, is located in a cleft located between the lobes. The binding of ligand induces a conformational change in the carrier such that the protein assumes the liganded conformation (Sharff et al., 1993). However, periplasmic binding proteins can fluctuate between conformations in the absence of ligand (Flocco & Mowbray, 1994); ligand binding stabilizes the liganded conformation.

10b. *Transport of ionic Fe^{II}*

In an anaerobic environment Fe^{II} is moderately soluble and can passively diffuse across the outer membrane without the aid of siderophores. Some facultative anaerobic pathogens including *Bifidobacterium bifidum* (Bezkorovainy et al., 1987), *Legionella pneumophilia* (Johnson et al., 1991), *Streptococcus mutans* (Evans et al., 1986b), and *Saccharomyces cerevisae* (Dancis et al., 1992) actively reduce Fe^{III} to Fe^{II} with ferric reductases located at their cell surfaces. In *E. coli* and *S. typhimurium*, ionic Fe^{II} is transported with high-affinity across the cytoplasmic membrane by the Fur-regulated *feoABC* operon (Hantke, 1987; Kammler et al., 1993; Tsolis et al., 1996). *feoA* and *feoC* encode for two small proteins with unknown functions. FeoB is a cytoplasmic membrane-localized protein with an ATP-binding motif, suggesting that Fe^{II} uptake may be dependent upon the hydrolysis of ATP; however, this remains to be established experimentally. The magnesium transport system also contributes to the uptake of Fe^{II} (Hantke, 1997). The uptake of Fe^{II} under anaerobic conditions makes an important contribution to the iron supply of the bacterial cell compared to Fe^{III} uptake, and is thus a bacterial virulence factor under oxygen-deprived conditions in host organisms (Stojiljkovic & Hantke, 1992; Tsolis et al., 1996).

10c. *Transport of ionic Fe^{III}*

Gram-positive and gram-negative bacteria possess periplasmic binding protein-dependent ABC importers that translocate ionic Fe^{III} across the cytoplasmic membrane (Janulczyk et al., 1999). This active transport mechanism is utilized by a diverse array of bacterial pathogens (reviewed by Dugourd et al., 1999). Once translocated into the periplasm, Fe^{III} is complexed by a periplasmic Fe^{III}-binding protein. The three-dimensional structure of the periplasmic component of the *hitABC* iron import operon from *H. influenzae* has been determined (Adhikari et al., 1995; 1996; Bruns et al., 1997). Analogous to other periplasmic binding proteins, HitA is formed from two globular domains that are connected by a hinge. The topology of the molecule closely resembles the N-terminal lobe of transferrin. A high degree of primary structure conservation

suggests that this fold may be shared among other periplasmic Fe^{III}-binding proteins. Similar to other bacterial permeases, two fused transmembrane domains (HitB) span the cytoplasmic membrane, which bind Fe^{III}-loaded HitA. Translocation of Fe^{III} across the cytoplasmic membrane is catalyzed by the hydrolysis of ATP as mediated by the ATPase HitC, which is closely associated with the cytoplasmic face of the inner membrane. The HitBC ABC transporter may remove the Fe^{III} ion from HitA by a pH-mediated release mechanism, as postulated for disassociation of Fe^{III} from transferrin. However, these Fur-regulated operons are not homologous to the periplasmic binding protein-dependent siderophore-mediated iron uptake pathways. Moreover, the uptake of Fe^{III} also occurs independently of indigenous siderophores and the TonB-ExbB-ExbD complex (Zimmermann et al., 1989).

10d. *Transport of Fe^{III} bound to haem and siderophores*

Uptake systems that mediate the transport of Fe^{III} bound to haem and siderophores have been identified in a diverse array of gram-negative and gram-positive bacteria. In these systems, Fe^{III} is translocated across the cytoplasmic membrane by ABC transporters in its liganded form. Of the known ABC importers involved in siderophore-mediated iron uptake, the Fhu system has been studied extensively (reviewed by Braun et al., 1998).

The transport of hydroxamate-type siderophores into the periplasm is modulated by three TonB-dependent receptors: FhuA, FhuE and IutA. With FhuA, ligand is passed through the outer membrane by an aqueous channel formed by the receptor following a physical interaction with TonB and the subsequent transfer of energy. Once present in the periplasm, all ferric hydroxamates are transported across the cytoplasmic membrane by a single periplasmic binding protein-dependent transport system composed of the gene products of *fhuBCD* (Burkhardt & Braun, 1987; Coulton et al., 1987; Köster & Braun, 1989).

FhuD is a high-affinity periplasmic binding protein that binds a diverse array of hydroxamates including aerobactin, coprogen, ferrichrome, ferrioxamine B, schizokinen, rhodoturulate, and the antibiotic albomycin. When loaded with ligands that are uniquely

transported by the Fhu system, FhuD is protected against proteolytic cleavage, indicating a conformational transition (Köster & Braun, 1990a; Rohrbach et al., 1995a). Dissociation constants of these ferric hydroxamates have been estimated by the concentration-dependent decrease in the intrinsic fluorescence intensity of an affinity tagged FhuD protein (0.4 μM for aerobactin, 5.4 μM for albomycin, 0.3 μM for coprogen, and 1.0 μM for ferrichrome; Rohrbach et al., 1995b).

The three-dimensional structure of FhuD in complex with a ferrichrome analogue (gallichrome) has also been solved (Clarke et al., 2000). Analogous to other periplasmic binding proteins FhuD is a bilobate protein; an unusually long α-helix connects the lobes. Related Fe^{III}-binding proteins use a flexible β-strand as an interdomain linker (Bruns et al., 1997). The N-terminal lobe of FhuD is primarily formed by a twisted four-stranded parallel β-sheet; the C-terminal lobe consists of a four-stranded mixed β-sheet. A predominantly hydrophobic ligand-binding cleft is located between the lobes. As observed with the ligand-binding pocket of FhuA, multiple hydrophobic and hydrophilic interactions are formed with the siderophore. A single arginine residue forms multiple hydrogen bonds with carbonyl oxygen atoms of the iron-chelating portion of the siderophore. Additional aromatic side-chain residues contribute to high-affinity binding by forming van der Waals contacts with hydrophobic regions of the ligand (K_D 0.1 μM; Rohrbach et al., 1995b). In its binding site, approximately 50% of the siderophore remains surface-exposed when bound to FhuD. The composition and electrostatic potential of the ligand-binding site provides an explanation for the broad affinity of FhuD. Although the three-dimensional structure of FhuD in the absence of ligand remains to be determined, Clarke et al., (2000) suggest that the protein undergoes a conformational change upon the binding of ligand. The presence of an elongated α-helical hinge region likely restricts interlobar movements, suggesting that ligand-induced conformational changes may be far less dramatic or completely dissimilar to those described for related proteins. However, the α-helix that connects the N and C-terminal lobes of FhuD is kinked at one position, thereby creating two helical segments that could potentially permit limited rotation with respect to one another. A rigid-body rearrangement may plausibly facilitate high-affinity ligand binding to FhuD and the transition from the unliganded to the liganded conformation.

FhuD shuttles hydroxamate-type siderophores and albomycin across the periplasm, delivering them to the permease FhuB; a pseudoheterodimer composed of two homologous transmembrane domains that are connected by a short hydrophilic linker. Both domains are required for functional activity (Köster & Braun, 1990b). Accordingly, bacterial strains with *fhuB* mutations are unable to transport hydroxamates into the cytoplasm, and thereby accumulate radiolabelled ligand in the periplasm. Using primary structure homology between the transmembrane domains of other periplasmic binding protein-dependent ABC transport systems and genetic data, a topological model for FhuB has been proposed (Köster, 1991). In contrast to other integral cytoplasmic membrane proteins, each domain of FhuB is believed to be formed by ten transmembrane α-helices. Direct physical interaction between FhuD and FhuB has been shown with cross-linking and protease protection assays (Rohrbach et al., 1995a; 1995b). Unliganded FhuD was equally effective in protecting FhuB from enzymatic degradation compared to liganded FhuD. These results suggest that, in the absence of ligand, FhuD may fluctuate between conformations, both of which interact with FhuB, albeit with different specificities. Competitive peptide mapping using biotinylated synthetic peptides and a modified enzyme-linked immunosorbent assay have been used to identify possible sites of physical interaction between FhuB and FhuD (Mademidis et al., 1997). FhuB-derived peptides corresponding to one of five predicted periplasmic loops and a transmembrane segment including the EAA loop bound and inhibited ferrichrome transport.

The docking of liganded FhuD generates a signal that is transmitted into the cytoplasm by FhuB. The FhuC protein contains an ABC domain; two FhuC molecules form a homodimer that is closely associated with the inner face of the cytoplasmic membrane. The physical interaction of FhuB with FhuC has been demonstrated by immunoelectron microscopy (Schultz-Hauser et al., 1992). In accord with its function as an ATPase, mutating those FhuC residues that form the ATP-binding motif abrogates transport (Becker et al., 1990). At the current time, there is no crystallographic information for the transmembrane domain of any ABC transporter. However, electron microscopy data collected from the multidrug resistance P-glycoprotein, which is a member of the ABC superfamily, may provide a working structural model (Rosenberg et al., 1997). Analogous to bacterial ABC transporters (Nikaido & Hall, 1998), this protein

consists of four domains that are fused together. Both transmembrane domains consist of six membrane-spanning α-helices, which together are believed to form a channel through which ligand passes. Two ABC domains are tightly associated with the inner leaflet of the membrane, which couple ATP hydrolysis with ligand transport. The multidrug resistance P-glycoprotein forms a membrane-spanning hexagonal cylinder with a large central pore, approximately 50 Å in diameter, that is occluded presumably by hydrophilic loops at its cytoplasmic end. Two globular lobes, corresponding to the ABC domains, are closely associated with the cytosolic face of the cytoplasmic membrane and the transmembrane cylinder.

The crystallographic structure of an ATP-binding subunit of an ABC transporter from *S. typhimurium* has been recently determined (Hung et al., 1998). This molecule (HisP) assumes an 'L-shape' with two 'arms' (domain I and II). Both domains contain α and β-type secondary structure elements. The ATP-binding site, containing the nucleotide-binding motif, is located near the end of domain I. The current biochemical, biophysical, genetic and structural data demonstrate that HisP is accessible from both sides of the cytoplasmic membrane, and that domain II of HisP, embedded in the cytoplasmic membrane, is likely surrounded by HisQ and HisM. HisP-mediated ATP hydrolysis is catalyzed by the binding of liganded HisJ (a periplasmic binding protein) to the periplasmic-exposed loops of the transmembrane domain (HisQ and HisM). Following an interaction with liganded HisJ, HisQ and/or HisM may undergo conformational changes, that are presumably driven by an alteration in domain II of HisP; which is in direct physical contact with both HisQ and HisM. Such changes could induce ATP hydrolysis in domain I (Davidson et al., 1992; Hung et al., 1998). Alternatively, ATP hydrolysis may be driven by a conformational change within HisP itself. This could be accomplished by altering the orientation of domain I and II with respect to one another.

Assuming that FhuB and FhuC adopt similar three-dimensional structures as the multidrug resistance P-glycoprotein and HisP, the interaction with liganded FhuD may be mediated by the insertion of the elongated backbone α-helix of FhuD within an open pore formed by FhuB. This interaction would then generate a transmembrane signal and convert FhuD from the liganded to the unliganded conformation, possibly through direct interactions with FhuC. Direct protein-protein interactions and conformational changes

may also facilitate ligand release from FhuD. FhuC-catalyzed ATP hydrolysis subsequently induces FhuB to form a transmembrane channel through which the ligand passes into the cytoplasm.

Once in the cytoplasm, intracellular flavin reductases release the Fe^{III} ion from hydroxamate-type siderophores by enzymatic reduction (Fontecave et al., 1994). Whether this event occurs in the cytoplasm or within the cytoplasmic membrane, remains to be established. In contrast, the removal of iron from enterobactin requires an esterase (Brickman & McIntosh, 1992). In these studies, esterase cleavage of enterobactin increases the dissociation constant from 10^{-52} to 10^{-8} M. In the absence of a functional esterase, cells accumulate ferric enterobactin in the cytoplasm and remain iron starved.

11. References

Adhikari, P., Kirby, S.D., Nowalk, A.J., Veraldi, K.L., Schryvers, A.B., Mietzner, T.A. (1995). Biochemical characterization of a *Haemophilus influenzae* periplasmic iron transport operon. *J. Biol. Chem.* **270**:25142-25149.

Adhikari, P., Berish, S.A., Nowalk, A.J., Veraldi, K.L., Morse, S.A., Mietzner, T.A. (1996). The *fbpABC* locus of *Neisseria gonorrhoeae* functions in the periplasm-to-cytosol transport of iron. *J. Bacteriol.* **178**:2145-2149.

Ahmer, B.M.M., Thomas, M.G., Larsen, R.A., Postle, K. (1995). Characterization of the *exbBD* operon of *Escherichia coli* and the role of ExbB and ExbD in TonB function and stability. *J. Bacteriol.* **177**:4742-4747.

Anderson, B.F., Baker, H.M., Norris, G.E., Rice, D.W., Baker, E.N. (1989). Structure of human lactoferrin: Crystallographic structure analysis and refinement at 2.8 Å resolution. *J. Mol. Biol.* **209**:711-734.

Anderson, B.F., Baker, H.M., Norris, G.E., Rumball, S.V., Baker, E.N. (1990). Apolactoferrin structure demonstrates ligand-induced conformational change in transferrins. *Nature* **344**:784-787.

Anderson, J.A., Sparling, P.F., Cornelissen C.N. (1994). Gonococcal transferrin-binding proteins 2 facilitates but is not essential for transferrin utilization. *J. Bacteriol.* **176**:3162-3170.

Anderson, C., Bachmeyer, C., Tauber, H., Benz, R., Wang, J., Michel, V., Newton, S.M.C., Hofnung, M., Charbit, A. (1999). *In vivo* and *in vitro* studies of major surface loop deletion mutants of the *Escherichia coli* K-12 maltoporin: contribution to maltose and maltooligosaccharide transport and binding. *Mol. Microbiol.* **32**:851-867.

Andrews, N.C., Levy. J.E. (1998). Iron is hot: An update on the pathophysiology of hemochromatosis. *Blood* **92**:1845-1851.

Angerer, A., Enz, S., Ochs, M., Braun, V. (1995). Transcriptional regulation of ferric citrate transport in *Escherichia coli* K-12. FecI belongs to a new subfamily of σ^{70}-type factors that respond to extracytoplasmic stimuli. *Mol. Microbiol.* **18**:163-174.

Angyal, S.J., Odier, L., Tate, M.E. (1995). A simple synthesis of *cis*-inositol. *Carbohydrate Res.* **266**:143-146.

Anton, M., Heller, K.J. (1991). Functional analysis of a C-terminally altered TonB protein of *Escherichia coli*. *Gene* **105**:23-29.

Appelmelk, J., An, Y-Q., Geerts, M., Thijs, B.G., de Boer, H.A., MacLaren, D.M., de Graaff, J., Nuijens, J.H. (1994). Lactoferrin is a lipid A binding protein. *Infect. Immun.* **62**:2628-2632.

Armstrong, S.K., McIntosh, M.A. (1995). Epitope insertions define functional and topological features of the *Escherichia coli* ferric enterobactin receptor. *J. Biol. Chem.* **270**:2483-2488.

Arnoux, P., Haser, R., Izadi, N., Lecroisey, A., Delepierre, M., Wandersman, C., Czjzek, M. (1999). The crystal structure of HasA, a hemophore secreted by *Serratia marcescens*. *Nature Struct. Biol.* **6**:516-520.

Bailey, S., Evans, R.W., Garratt, R.C., Gorinsky, B., Hasnain, S., Horsburgh, C., Jhoti, H., Lindley, P.F., Mydrin, A., Sarra, R., *et al.* (1988). Molecular structure of serum transferrin at 3.3-Å resolution. *Biochemistry* **27**:5804-5812.

Bauer, K., Struyve, M., Bosch, D., Benz, R., Tommassen, J. (1989). One single lysine residue is responsible for the interaction between polyphosphates and the outer membrane porin PhoE of *Escherichia coli*. *J. Biol. Chem.* **264**:16393-16398.

Beamer, L.J., Carroll, S.F., Eisenberg, D. (1998). The BPI/LBP family of proteins: A structural analysis of conserved regions. *Prot. Science* **7**:906-914.

Becker, K., Köster, W., Braun, V. (1990). Iron (III) hydroxamate transport of *Escherichia coli* K12: single amino acid replacements at potential ATP-binding sites inactivate the FhuC protein. *Mol. Gen. Genet.* **223**:159-162.

Bell, P.E., Nau, C.D., Brown, J.T., Konisky, J., Kadner, R.J. (1990). Genetic suppression demonstrates interaction of TonB protein with outer membrane transport proteins in *Escherichia coli*. *J. Bacteriol.* **172**:3826-3829.

Bennett, M.J., Lebrón, J.A., Bjorkman, P.J. (2000). Crystal structure of the hereditary haemochromatosis protein HFE complexed with transferrin receptor. *Nature* **403**:46-53.

Benz, R. Schmid, A., Greetje, H., Vos-Scheperkeuter, H. (1987). Mechanism of sugar transport through sugar-specific LamB channel of *Escherichia coli* outer membranes. *J. Membr. Biol.* **100**:21-29.

Bezkorovainy, A., Soberg, L., Poch, M., Miller-Catchpole, R. (1987). Ferrous iron uptake by *Bifidobacterium bifidum* var. *pennsylvanicum*: the effect of metals and metabolic inhibitors. *Int. J. Biochem.* **19**:517-522.

Binet, R., Wandersman, C. (1996). Cloning of the *Serratia marcescens hasF* gene encoding the Has ABC exporter outer membrane component: a TolC analogue. *Mol. Microbiol.* **22**:265-273.

Biswas, G.D., Anderson, J.E., Sparling, P.F. (1997). Cloning and functional characterization of *Neisseria gonorrhoeae tonB*, *exbB* and *exbD* genes. *Mol. Microbiol.* **24**:169-179.

Bonhivers, M., Ghazi, A., Boulanger, P., Letellier, L. (1996). FhuA, a transporter of the *Escherichia coli* outer membrane, is converted into a channel upon binding of bacteriophage T5. *EMBO J.* **15**:1850-1856.

Bonnah, R.A., Schryvers, A.B. (1998). Preparation and characterization of *Neiserria menigitidis* mutants deficient in the production of the human lactoferrin-binding protein proteins LbpA and LbpB. *J. Bacteriol.* **180**:3080-3090.

Boos, W., Lucht, J.M. (1996). Periplasmic binding protein-dependent ABC transporters. In: *Escherichia coli* and *Salmonella*. Cellular and Molecular Biology. Neidhardt, F.C. (ed.), Washington, D.C., ASM Press, pp. 1175-1209.

Bös, C., Braun, V. (1997). Specific *in vivo* thiol-labeling of the FhuA outer membrane ferrichrome transport protein of *Escherichia coli* K-12: evidence for a disulfide bridge in the predicted gating loop. *FEMS Microbiol. Lett.* **153**:311-319.

Bös, C., Lorenzen, D., Braun, V. (1998). Specific *in vivo* labeling of cell surface-exposed protein loops: Reactive cysteines in the predicted gating loop mark a ferrichrome binding site and a ligand-induced conformational change of the *Escherichia coli* FhuA protein. *J. Bacteriol.* **180**:605-613.

Boulanger, J., Le Marie, M., Bonhivers, M., Dubois, S., Desmadril, M., Letellier, L. (1996). Purification and structural and functional characterisation of FhuA, a transporter of the *E. coli* outer membrane. *Biochemistry* **35**:14216-14224.

Bradbeer, C. (1993). The proton motive force drives outer membrane transport of cobalamin in *Escherichia coli*. *J. Bacteriol.* **175**:3146-3150.

Brandenburg, K., Seydel, U., Schromm, A.B., Loppnow, H., Koch, M.H.J., Rietschel, E.T. (1996). Conformation of lipid A, the endotoxic center of bacterial lipopolysaccharide. *J. Endotoxin Res.* **3**:173-178.

Braun, V., Günther, K., Hantke, K., Zimmermann, L. (1983). Intracellular activation of albomycin in *Escherichia coli* and *Salmonella typhimurium*. *J. Bacteriol.* **156**:308-315.

Braun, V. (1989). The structurally related *exbB* and *tolQ* genes are interchangeable in conferring *tonB*-dependent colicin, bacteriophage, and albomycin sensitivity. *J. Bacteriol.* **171**:6387-6390.

Braun, V, Herrmann, C. (1993). Evolutionary relationship of uptake systems for biopolymers in *Escherichia coli*: cross-complementation between the TonB-ExbB-ExbD and the TolA-TolQ-TolR proteins. *Mol. Microbiol.* **8**:261-268.

Braun, V. (1995). Energy-coupled transport and signal transduction through the gram-negative outer membrane via TonB-ExbB-ExbD-dependent receptor proteins. *FEMS Microbiol. Rev.* **16**:295-307.

Braun, V., Gaisser, S., Herrmann, C., Kampfenkel, K., Killmann, H., Traub, I. (1996). Energy-coupled transport across the outer membrane of *Escherichia coli*: ExbB binds ExbD and TonB in vitro, and leucine 132 in the periplasmic region and aspartate 25 in the transmembrane region are important for ExbD activity. *J. Bacteriol.* **178**:2836-2845.

Braun, V. (1997). Avoidance of iron toxicity through regulation of bacterial iron transport. *Biol. Chem.* **378**:779-786.

Braun, V., Hantke, K., Köster, W. (1998). Iron transport and storage in microorganisms, plants, and animals. In: Sigel, A., Sigel, H. (eds.), *Metal Ions in Biological Systems*, Marcel Dekker, New York, pp. 67-145.

Braun, M., Killmann, H., Braun, V. (1999). The β-barrel domain of FhuAΔ5-160 is sufficient for TonB-dependent FhuA activities of *Escherichia coli*. *Mol. Microbiol.* **33**:1037-1049.

Brewer, S., Tolley, M., Trayer, I.P., Barr, G.C., Dorman, C.J., Hannavy, K., Higgins, C.F., Evans, J.S., Levine, B.A., Wormald, M.R. (1990). Structure and function X-Pro dipeptide repeats in the TonB proteins of *Salmonella typhimurium* and *Escherichia coli*. *J. Mol. Biol.* **216**:883-895.

Briat, J-F. Iron assimilation and storage in prokaryotes. (1992). *J. Gen. Microbiol.* **138**:2475-2483.

Brickman, T.J., McIntosh, M.A. (1992). Overexpression and purification of ferric enterobactin esterase from *Escherichia coli*. Demonstration of enzymatic hydrolysis of enterobactin and its iron complex. *J. Biol. Chem.* **267**:12350-12355.

Bruns, C.M., Nowalk, A.J., Arvai, A.S., McTigue, M.A., Vaughan, K.G., Mietzner, T.A., McRee, D.E. (1997). Structure of the *Haemophilus influenzae* Fe^{3+}-binding protein reveals convergent evolution within a superfamily. *Nature Struct. Biol.* **4**:919-924.

Bruske, A.K., Heller, K.J. (1993). Molecular characterization of *the Enterobacter aerogenes tonB* gene: identification of a novel type of TonB box suppressor mutant. *J. Bacteriol.* **175**:6158-6168.

Buchanan, S.K., Smith, B.S., Venkatramani, L., Xia, D., Esser, L., Palnitkar, M., Chakraborty, R., van der Helm, D., Deisenhofer, J. (1999a). Crystal structure of the active outer membrane transporter FepA from *Escherichia coli*. *Nature Struct. Biol.* **6**:56-63.

Buchanan, S.K. (1999b). β-barrel proteins from bacterial outer membranes: structure, function, and refolding. *Curr. Opin. Struct. Biol.* **9**:455-461.

Burkhardt, R., Braun, V. (1987). Nucleotide sequence of the *fhuC* and *fhuD* genes involved in iron (III) hydroxamate transport: domains in FhuC homologous to ATP-binding proteins. *Mol. Gen. Genet.* **209**:49-55.

Cadieux, N., Kadner, R.J. (1999). Site-directed disulfide bonding reveals an interaction site between energy-coupling protein TonB and BtuB, the outer membrane cobalamin transporter. *Proc. Natl. Acad. Sci. USA* **96**:10673-10678.

Carmel, G., Hellstern, D., Henning, D., Coulton, J.W. (1990). Insertion mutagenesis of the gene encoding the ferrichrome-iron receptor of *Escherichia coli* K-12. *J. Bacteriol.* **172**:1861-1869.

Carson, S.D., Klebba, P.E., Newton, S.M., Sparling, P.F. (1999). Ferric enterobactin binding and utilization by *Neisseria gonorrhoeae*. *J. Bacteriol.* **181**:2895-2901.

Chaney, R.L., Brown, J.C., Tiffin, L.O. (1972). Obligatory reduction of ferric chelates in iron uptake by soybeans. *Plant Physiol.* **50**:208-213.

Chen, C.J., Elkins, C., Sparling, P.F. (1998). Phase variation of haemoglobin utilization in *Neisseria gonorrhoeae*. *Infect. Immun.* **66**:987-993.

Clarke, T.E., Ku, S-Y., Dougan, D.R., Vogel, H.J., Tari, L.W. (2000). The structure of the ferric siderophore binding protein FhuD complexed with gallichrome. *Nature Struct. Biol.* **7**:287-291.

Click, E.M., Webster, R.E. (1997). Filamentous phage infection: required interactions with the TolA protein. *J. Bacteriol.* **179**:6464-6471.

Cope, L.D., Yogev, R., Muller-Eberhard, U., Hansen, E.J. (1995). A gene cluster involved in the utilisation of both free heme and heme:hemopexin *by Haemophilus influenzae* type B. *J. Bacteriol.* **177**:2644-2653.

Cornelissen, C.N., Biswas, G.D., Tsai, J., Paruchuri, D.K., Thompson, S.A., Sparling, P.F. (1992). Gonococcal transferrin-binding protein 1 is required for transferrin utilization and is homologous to TonB-dependent outer membrane receptors. *J. Bacteriol.* **174**:5788-5797.

Cornelissen, C.N., Sparling, P.F. (1994). Iron piracy: acquisition of transferrin-bound iron by bacterial pathogens. *Mol. Microbiol.* **14**:843-851.

Cornelissen, C.N., Sparling, P.F. (1996). Binding and surface exposure characteristics of the gonococcal transferrin receptor are dependent on both transferrin-binding proteins. *J. Bacteriol.* **178**:1437-1444.

Cornelissen, C.N., Anderson, J.E., Sparling, P.F. (1997). Energy-dependent changes in the gonococcal transferrin receptor. *Mol. Microbiol.* **26**:25-35.

Coulton, J.W., Mason, P., Cameron, D.R., Carmel, G., Jean, R., Rode, H.N. (1986). Protein fusions of galactosidase to the ferrichrome-iron receptor of *Escherichia coli*. *J. Bacteriol.* **165**:181-192.

Coulton J.W., Mason, P., Allatt, D.D. (1987). *fhuC* and *fhuD* genes for iron (III)-ferrichrome transport into *Escherichia coli* K-12. *J. Bacteriol.* **169**:3844-3849.

Cowan, S.W., Schirmer, T., Rummel, G., Steiert, M., Ghosh, R., Pauptit, R.A., Jansonius, J.N., Rosenbusch, J. (1992). Crystal structures explain functional properties of two *E. coli* porins. *Nature* **358**:727-733.

Curtis, N.A., Eisenstadt, R.L., Turner, K.A., White, A.J. (1985). Porin-mediated cephalosporin resistance in *Escherichia coli* K-12. *J. Antimicrobial. Chemother.* **15**:642-644.

Dancis, A., Roman, D.G., Anderson, G.J., Hinnebusch, A.G., Klausner, R.D. (1992). Ferric reductase of *Saccharomyces cerevisiae*: molecular characterization, role of iron uptake, and transcriptional control by iron. *Proc. Natl. Acad. Sci. USA* **89**:3869-3873.

Dassa, E., Hofnung, M. (1985). Sequence of the *malG* gene in *E. coli* K-12: homologies between integral membrane components from binding protein-dependent transport systems. *EMBO J.* **4**:2287-2293.

Davidson, A.L., Shuman, H.A., Nikaido, H. (1992). Mechanism of maltose transport in *Escherichia coli*: Transmembrane signaling by periplasmic binding proteins. *Proc. Natl. Acad. Sci. USA* **89**:2360-2364.

Dekker, N. (2000). Outer-membrane phospholipiase A: known structure, unknown biological function. *Mol. Microbiol.* **35**:711-717.

Delcour, A.H. (1997). Function and modulation of bacterial porins: Insights from electrophysiology. *FEMS Microbiol. Lett.* **151**:115-123.

DE Lorenzo, V., Wee, S., Herrero, M., Neilands, J.B. (1987). Operator sequences of the aerobactin operon of plasmid ColV-K30 binding the ferric uptake regulation (*fur*) repressor. *J. Bacteriol.* **169**:2624-2630.

DE Lorenzo, V., Giovannini, F., Herrero, M., Neilands, J.B. (1988a). Metal iron regulation of gene expression. Fur repressor-operator interaction at the promoter region of the aerobactin system of pColV-K30. *J. Mol. Biol.* **203**:875-884.

DE Lorenzo, V., Herrero, M., Giovannini, F., Neilands, J.B. (1988b). Fur (ferric uptake regulation) protein and CAP (catabolite-activator protein) modulate transcription of the *fur* gene in *Escherichia coli*. *Eur. J. Biochem.* **173**:537-546.

Diederichs, K., Freigang, J., Umhau, S., Zeth, K., Breed, J. (1998). Prediction by a neural network of outer membrane β-strand protein topology. *Prot. Science* **7**:2413-2420.

Dijkstra, A.J., Keck, W. (1996). Peptidoglycan as a barrier to transenvelope transport. *J. Bacteriol.* **178**:5555-5562.

Ding, X., Zeng, H., Schiering, N., Murphy, J.R. (1996). Identification of the primary metal ion-activation sites of the diphtheria tox repressor by X-ray crystallography and site-directed mutational analysis. *Nature Struct. Biol.* **3**:382-387.

Duogourd, D., Martin, C., Rioux, C.R., Jacques, M., Harel, J. (1999). Characterization of a periplasmic ATP-binding cassette iron import system *of Brachyspira (Serpulina) hyodysenteriae*. *J. Bacteriol.* **181**:6948-6957.

Dutzler, R., Wang, Y-F., Rizkallah, P.J., Rosenbusch, J.P., Schirmer, T. (1995). Crystal structures of various maltooligosaccharides bound to maltoporin reveal a specific sugar translocation pathway. *Structure* **4**:127-134.

Dutzler, R., Rummel, G., Albertí, S., Hernández, A., Phale, P.S., Rosenbusch, J.P., Benedí, V.J., Schirmer, T. (1999). Crystal structure and functional characterization of OmpK36, the osmoporin of *Klebsiella pneumoniae*. *Structure* **7**:425-434.

Economou, A., Pogliano, J.A., Beckwith, J., Oliver, D.B., Wickner, W. (1995). SecA membrane cycling at SecYEG is driven by distinct ATP binding and hydrolysis events and is regulated by SecD and SecF. *Cell* **83**:1171-1181.

Eick-Helmerich, K., Hantke, K., Braun, V. (1987). Cloning and expression of the *exbB* gene of *Escherichia coli* K-12. *Mol. Gen. Genet.* **206**:246-251.

Eick-Helmerich, K., Braun, V. (1989). Import of biopolymers into *Escherichia coli*: nucleotide sequences of the *exbB* and *exbD* genes are homologous to those of the *tolQ* and *tolR* genes, respectively. *J. Bacteriol.* **171**:5117-5126.

Elass-Rouchard, E., Roseanu, A., Legrand, D., Trif, M., Salmon, V., Motas, C., Montreuil, J., Spik, G. (1995). Lactoferrin-LPS interactions: involvement of the 28-34 loop region of human lactoferrin in the high-affinity binding to *Escherichia coli* 055:B5 lipopolysaccharides. *Biochem. J.* **312**:839-845.

Elass-Rouchard, E., Legrand, D., Salmon, V., Roseanu, A., Trif, M., Tobias, P.S., Mazurier, J., Spik, G. (1998). Lactoferrin inhibits the endotoxin interaction with CD14 by competition with the lipopolysaccharide-binding protein. *Infect. Immun.* **66**:486-491.

Elkins, P., Bunker, A., Cramer, W.A., Stauffacher, C.V. (1997). A mechanism for toxin insertion into membrane is suggested by the crystal structure of the channel-forming domain of colicin E1. *Structure* **5**:443-458.

Enz, S., Mahren, S., Stroeher, U.H., Braun, V. (2000). Surface signaling in ferric citrate transport gene induction: Interaction of the FecA, FecR, and FecI regulatory proteins. *J. Bacteriol.* **182**:637-646.

Escolar, L., DE Lorenzo, V., Pérez-Martin, J. (1997). Metalloregulation *in vitro* of the aerobactin promoter of *Escherichia coli* by the Fur (ferric uptake regulation) protein. *Mol. Microbiol.* **26**:799-808.

Escolar, L., Pérez-Martín, J., DE Lorenzo, V. (1998). Binding of the Fur (ferric uptake regulator) repressor of *Escherichia coli* to arrays of the GATAAT sequence. *J. Mol. Biol.* **283**:537-547.

Escolar, L., Pérez-Martín, J., DE Lorenzo, V. (1999). Opeing the iron box: Transcriptional metalloregulation by the Fur protein. *J. Bacteriol.* **181**:6223-6229.

Evans, J.S., Levine, B.A., Trayer, I.P., Dorman, C.J., Higgins, C.F. (1986a). Sequence imposed structural constraints in the TonB protein of *Escherichia coli*. *FEBS Lett.* **208**:211-216.

Evans, S.L., Arcenaux, J.E.L., Byers, B.R., Martin, M.E., Aranha, N. (1986b). Ferrous iron transport in *Streptococcus mutans*. *J. Bacteriol.* **168**:1069-1099.

Farr, S.B., Kogoma, T. (1991). Oxidative stress responses in *Escherichia coli* and *Salmonella typhimurium*. *Microbiol. Rev.* **55**:561-585.

Feder, J.N., Penny, D.M., Irrinki, A., Lee, V.K., Lebrón, J.A., Watson, N., Tsuchihashi, Z., Sigal, E., Bjorkman, P.J., Schatzman, R.C. (1998). The hemochromatosis gene product complexes with the transferrin receptor and lowers its affinity for ligand binding. *Proc. Natl. Acad. Sci. USA* **95**:1472-1477.

Feucht, A., Schmid, A., Benz, R., Schwarz, H., Heller, K. (1990). Pore formation associated with the tail-tip protein pb2 of bacteriophage T5. *J. Biol. Chem.* **265**:18561-18567.

Ferguson, A.D., Breed, J., Diederichs, K., Welte, W., Coulton, J.W. (1998a). An internal affinity-tag for purification and crystallization of the siderophore receptor FhuA, integral outer membrane protein from *Escherichia coli* K-12. *Prot. Science* **7**:1636-1638.

Ferguson, A.D., Hofmann, E., Coulton, J.W., Diederichs, K., Welte, W. (1998b). Siderophore-mediated iron transport: Crystal structure of FhuA with bound lipopolysaccharide. *Science* **282**:2215-2220.

Ferguson, A.D., Welte, W., Hofmann, E., Lindner, B., Holst, O., Coulton, J.W., Diederichs, K. (2000a). A conserved structural motif for lipopolysaccharide recognition by procaryotic and eucaryotic proteins. *Structure* In press.

Ferguson, A.D., Braun, V., Fiedler, H-P., Coulton, J.W., Diederichs, K., Welte, W. (2000b). Crystal structure of the antibiotic albomycin in complex with the outer membrane transporter FhuA. *Prot. Science* In press.

Ferguson, A.D., Ködding, J., Coulton, J.W., Diederichs, K., Braun, V., Welte, W. (2000c). Crystal structure of a rifamycin derivative in complex with the active outer membrane transporter FhuA. To be submitted.

Ferguson, A.D., Hergetschweiler, K., Morgenstern, B., Welte, W., Breed, J. (2000d). *cis*-inositol: an additive to improve crystal quality. Submitted.

Ferguson, A.D., Boismenu, D., Coulton, J.W., Mamer, O.A. (2000e). Unpublished.

Fischer, E., Günther, K., Braun, V. (1989). Involvement of ExbB and TonB in transport across the outer membrane of *Escherichia coli*: phenotypic complementation of *exbB* mutants by overexpressed *tonB* and physical stabilization of TonB by ExbB. *J. Bacteriol.* **171**:5127-5134.

Flocco, M.M., Mowbray, S.L. (1994). The 1.9 angstrom X-ray structure of a closed unliganded form of the periplasmic glucose/galactose receptor from *Salmonella typhimurium*. *J. Biol. Chem.* **269**:8931-8936.

Fontecave, M., Coves, J., Pierre, J.L. (1994). Ferric reductases or flavin reductases? *Biometals* **7**:3-8.

Foulds, J., Barrett, C. (1973). Characterization of *Escherichia coli* mutants tolerant to bacteriocin JF246: Two new classes of tolerant mutants. *J. Bacteriol.* **116**:885-892.

Forst, D., Welte, W., Wacker, T., Diederichs, K. (1998). Structure of the sucrose-specific porin ScrY from *Salmonella typhimurium* and its complex with sucrose. *Nature Struct. Biol.* **5**:37-46.

Gazzano-Santoro, H., Mészáros, K., Birr, C., Carroll, S.F., Theofan, G., Horwitz, A.H., Lim, E., Aberle, S., Kasler, H., Parent, J.B. (1994). Competition between rBPI23, a

recombinant fragment of bactericidal permeability-increasing protein, and lipopolysaccharide (LPS)-binding protein for binding to LPS and Gram-negative bacteria. *Infect. Immun.* **62**:1185-1191.

Ghigo, J.M., Létoffé, S., Wandersman, C. (1997). A new type of hemophore-dependent hem acquisition system of *Serratia marcescens* reconstituted in *E. coli*. *J. Bacteriol.* **179**:3572-3579.

Gudmondsdottir, A., Bell, P.E., Lundrigan, M.D., Bradbeer, C., Kadner, R.J. (1989). Point mutations in a conserved region (TonB Box) of *Escherichia coli* outer membrane protein BtuB affect vitamin B_{12} transport. *J. Bacteriol.* **171**:6526-6533.

Guerinot, M.L. (1994). Microbial iron transport. *Ann. Rev. Microbiol.* **48**:743-772.

Guihard, G., Boulanger, P., Letellier, L. (1992). Involvement of T5 tail proteins and contacts sites between the outer and inner membrane of *Escherichia coli* in phage T5 DNA injection. *J. Biol. Chem.* **267**:3173-3178.

Guihard, G., Bénédetti, H., Besnard, M., Letellier, L. (1993). Phosphate efflux through the channels formed by colicins and phage T5 in *Escherichia coli* cells is responsible for the fall in cytoplasmic ATP. *J. Biol. Chem.* **268**:17775-17780.

Guihard, G., Boulanger, P., Benedetti, H., Lloubes, R., Besnard, M., Letellier, L. (1994). Colicin A and the Tol proteins involved in its translocation are preferentially located in the contact sites between the inner and outer membrane of *Escherichia coli* cells. *J. Biol. Chem.* **269**:5874-5880.

Gómez, J.A., Criado, M.T., Ferreirós, C.M. (1998). Cooperation between the components of the meningococcal transferrin receptor, TbpA and TbpB, in the uptake of transferrin iron by the 37-kDa ferric-binding protein (FbpA). *Res. Microbiol.* **149**:381-387.

Gouaux, E. (1997). The long and short of colicin action: the molecular basis of the biological activity of channel-forming colicins. *Structure* **5**:313-317.

Gray-Owen, S.D., Schyvers, A.B. (1996). Bacterial transferrin and lactoferrin receptors. *Trends Microbiol.* **4**:185-191.

Gross, P., Braun, V. (1996). Colicin M is inactivated during import by its immunity protein. *Mol. Gen Genet.* **251**:388-396.

Hancock, R.E.W., Braun, V. (1976). Nature of the energy requirement for the irreversible adsorption of bacteriophages T1 and ϕ80 to *Escherichia coli*. *J. Bacteriol.* **125**:409-415.

Hantke, K., Braun, V. (1978). Functional interaction of the *tonA/tonB* receptor system in *Escherichia coli*. *J. Bacteriol.* **125**:409-415.

Hantke, K. (1981). Regulation of ferric iron transport in *Escherichia coli* K12: isolation of a constitutive mutant. *Mol. Gen. Genet.* **182**:288-292.

Hantke, K. (1987). Ferrous iron transport mutants in *Escherichia coli* K-12. *FEMS Microbiol. Lett.* **44**:53-57.

Hantke, K. (1997). Ferrous iron uptake by a magnesium transport system is toxic for *Escherichia coli* and *Salmonella typhimurium*. *J. Bacteriol.* **179**:6201-6204.

Härle, C., Kim, I., Angerer, A., Braun, V. (1995). Signal transfer through three compartments: transcription initiation of the *Escherichia coli* ferric citrate transport system from the cell surface. *EMBO J.* **14**:1430-1438.

Hartmann, A., Fiedler, H-P., Braun, V. (1979). Uptake and conversion of the antibiotic albomycin by *Escherichia coli* K-12. *Eur. J. Biochem.* **99**:517-524.

Heller, K., Kadner, R.J. (1985). Nucleotide sequence of the gene for the vitamin B_{12} receptor protein in the outer membrane of *Escherichia coli*. *J. Bacteriol.* **161**:904-908.

Heller, K.J., Kadner, R.J., Gunther, K. (1988). Suppression of *btuB451* mutation by mutations in the *tonB* gene suggests a direct interaction between TonB and TonB-dependent receptor protein in the outer membrane of *Escherichia coli*. *Gene* **64**:147-153.

Hennecke, H. (1990). Regulation of bacterial gene expression by metal-protein complexes. *Mol. Microbiol.* **4**:1621-1628.

Hether, N.H., Olsen, R.A., Jackson, L.L. (1984). Chemical identification of iron reductants exuded by plant roots. *J. Plant Nutr.* **7**:667-676.

Higgins, C.F., Hiles, I.D., Whalley, K., Jamieson, D. (1985). Nucleotide binding by membrane components of bacterial periplasmic binding protein-dependent transport systems. *EMBO J.* **4**:1033-1040.

Higgins, C.F., Hiles, I.D., Salmond, G.P., Gill, D.R., Downie, J.A., Evans, I.J., Holland, I.B., Gray, L., Buckel, S.D., Bell, A.W., Hermodson, M.A. (1986). A family of related ATP-binding subunits coupled to many distinct biological processes in bacteria. *Nature* **323**:448-450.

Higgs, P.I., Myers, P.S., Postle, K. (1998). Interactions in the TonB-dependent energy transduction complex: ExbB and ExbD for homomultimers. *J. Bacteriol.* **180**:6031-6038.

Higuchi, K., Suzuki, K., Nakanishi, H., Yamaguchi, H., Nishizawa, N-K., Mori, S. (1999). Cloning of nicotianamine synthase genes, novel genes involved in the biosynthesis of phytosiderophores. *Plant Physiol.* **119**:471-479.

Hirota, Y., Suzuki, H., Nishimura, Y., Yasuda, S. (1977). On the process of cellular division in *E. coli* lacking a murein-lipoprotein. *Proc. Natl. Acad. Sci. USA* **74**:1417-1420.

Hirsch, A., Breed, J., Saxena, K., Richter, O.M., Ludwig, B., Diederichs, K., Welte, W. (1997). The structure of porin from *Paracoccus denitrificans* at 3.1 Å resolution. *FEBS Lett.* **404**:208-210.

Hobot, J.A., Carlemalm, E., Villiger, W., Kellenberger, R. (1984). Periplasmic gel: new concept resulting from the reinvestigation of bacterial cell envelope ultrastructure by new methods. *J. Bacteriol.* **160**:143-152.

Hoess, A., Watson, S., Siber, G.R., Liddington, R. (1993). Crystal structure of an endotoxin-neutralizing protein from the horseshoe crab, *Limulus* anti-LPS factor, at 1.5 Å resolution. *EMBO J.* **9**:3351-3356.

Hoffmann, J.A., Kaftatos, F.C., Janeway Jr., C.A., Ezekowitz, R.A.B. (1999). Phylogenetic perspectives in innate immunity. *Science* **284**:1313-1318.

Holst, O. (1999). Chemical structures of the core region of lipopolysaccharides. In: *Endotoxin in Health and Disease.* Brade, H., Morrison, D.C., Opal, S, Vogel, S. (eds.), Marcel Dekker Inc., New York, pp. 115-154.

Hung, L-W., Wang, I.W., Nikaido, K., Liu, P-Q., Ames, G.F-L., Kim, S-H. (1998). Crystal structure of the ATP-binding subunit of an ABC transporter. *Nature* **396**:703-707.

InSook, K., Stiefel, A., Plantör, S., Angerer, A., Braun, V. (1997). Transcription induction of the ferric citrate transport genes via the N-terminus of the FecA outer membrane protein, the Ton system and the electrochemical potential of the cytoplasmic membrane. *Mol. Microbiol.* **23**:333-344.

Iverson, T.M., Luna-Chavez, C., Cecchini, G., Rees, D.C. (1999). Structure of the *Escherichia coli* fumarate reductase respiratory complex. *Science* **284**:1961-1966.

Iwata, S., Ostermeier, C., Ludwig, B., Michel, H. (1995). Structure at 2.8 Å resolution of cytochrome *c* oxidase from *Paracoccus denitrificans*. *Nature* **376**:660-669.

Jancarik, J., Kim, S-H. (1991). Sparse matrix sampling: a screening method for crystallization of proteins. *J. Appl. Cryst.* **24**:409-411.

Janulczyk, R., Pallon, J., Björck, L. (1999). Identification and characterization of a *Streptococcus pyogenes* ABC transporter with multiple specificity for metal cations. *Mol. Microbiol.* **34**:596-606.

Jaskula, J.C., Letain, L.E., Roof, S.K., Skare, J.T., Postle, K. (1994). Role of the TonB amino acid terminus in energy transduction between membranes. *J. Bacteriol.* **176**:2326-2338.

Jeanteur, D., Schirmer, T., Fourel, D., Simonet, V., Rummel, G., Widmer, C., Rosenbusch, J.P., Pattus, F., Pagès, J.M. (1994). Structural and functional alterations of a colicin-resistant mutant of OmpF porin from *Escherichia coli*. *Proc. Natl. Acad. Sci. USA* **91**:10675-10679.

Jiang, X., Payne, M.A., Cao, Z., Foster, S.B., Feix, J.B., Newton, S.M.C., Klebba, P.E. (1997). Ligand-specific opening of a gated-porin channel in the outer membrane of living bacteria. *Science* **276**:1261-1264.

Johnson, W., Varner L., Poch, M., (1991). Acquisition of iron by *Legionella pneumophilia*: role of iron reductase. *Infect. Immun.* **59**:2376-2381.

Jordy, M., Anderson, C., Schulein, K., Ferenci, T., Benz, R. (1996). Rate constants of sugar transport through two LamB mutants of *Escherichia coli*: Comparison with wild-type maltoporin and LamB of *Salmonella typhimurium*. *J. Mol. Biol.* **259**:666-678.

Jurkevitch, E., Hadar, Y., Chen, Y., Libman, J., Shanzer, A. (1992). Iron uptake and molecular recognition in *Pseudomonas putida*: Receptor mapping with ferrichrome and its biomimetic analogs. *J. Bacteriol.* **174**:78-83.

Kadner, R.J. (1990). Vitamin B_{12} transport in *Escherichia coli*: energy coupling between membranes. *Mol. Microbiol.* **4**:2027-2033.

Kadner, R.J., Heller, K.J. (1995). Mutual inhibition of cobalamin and siderophore uptake systems suggests their competition for TonB function. *J. Bacteriol.* **177**:4829-4835.

Kadner, R.J. (1996). Cytoplasmic membrane. In: *Escherichia coli* and *Salmonella*. Cellular and Molecular Biology. Neidhardt, F.C. (ed.), Washington, D.C., ASM Press, pp. 58-87.

Kammler, K., Schön, C., Hantke, K. (1993). Characterization of the ferrous iron uptake system of *Escherichia coli*. *J. Bacteriol.* **175**:6212-6219.

Kampfenkel, K., Braun, V. (1992). Membrane topology of the *Escherichia coli* ExbD protein. *J. Bacteriol.* **174**:5485-5487.

Kampfenkel, K., Braun, V. (1993). Membrane topologies of the TolQ and TolR proteins of *Escherichia coli*: inactivation of TolQ by a missense mutation in the proposed first transmembrane segment. *J. Bacteriol.* **175**:4485-4491.

Karlsson, M., Hannavy, K., Higgins, C.F. (1993a). A sequence-specific function for the *N*-terminal signal-like sequence of the TonB protein. *Mol. Microbiol.* **8**:389-396.

Karlsson, M., Hannavy, K., Higgins, C.F. (1993b). ExbB acts as a chaperone-like protein to stabilize TonB in the cytoplasm. *Mol. Microbiol.* **8**:389-396.

Killmann, H., Benz, R., Braun, V. (1993). Conversion of the FhuA transport protein into a diffusion channel through the outer membrane of *Escherichia coli*. *EMBO J.* **12**:3007-3016.

Killmann, H., Videnov, G., Jung, G., Schwarz, H., Braun, V. (1995). Identification of receptor binding sites by competitive peptide mapping: phages T1, T5, and phi 80 and colicin M bind to the gating loop of FhuA. *J. Bacteriol.* **177**:694-698.

Killmann, H., Benz, R., Braun, V. (1996). Properties of the FhuA channel in the *Escherichia coli* outer membrane after deletion of FhuA portions within and outside the predicted gating loop. *J. Bacteriol.* **178**:6913-6920.

Killmann, H., Herrmann, C., Wolff, H., Braun, V. (1998). Identification of a new site for ferrichrome transport of *Escherichia coli*, *Salmonella paratyphi* B, *Salmonella typhimurium*, and *Pantoea agglomerans*. *J. Bacteriol.* **180**:3845-3852.

Kim, I., Stiefel, A., Plantör, S., Angerer, A., Braun, V. Transcription induction of the ferric citrate transport genes via the N-terminus of the FecA outer membrane protein, the Ton system and the electrochemical potential of the cytoplasmic membrane. (1997). *Mol. Microbiol.* **23**:333-344.

Klebba, P.E., Rutz, J.M., Liu, J., Murphy, C.K. (1993). Mechanisms of TonB-catalyzed iron transport through the enteric bacterial cell envelope. *J. Bioenerg. Biomemb.* **25**:603-611.

Klee, S.R. et al. (2000). Unpublished. GenBank Accession Code AJ3912778

Kleywegt, G. (1999). Recognition of spatial motifs in protein structures. *J. Mol. Biol.* **285**:1887-1897.

Kloczewiak, M., Black, K.M., Loiselle, P., Cavaillon, J.M., Wainwright, N., Warren, H.S. (1994). Synthetic peptides that mimic the binding site of horseshoe crab antilipopolysaccharide factor. *J. Infect. Dis.* **170**:1490-1497.

Koebnik, R. (1993). The molecular interaction between components of the TonB-ExbBD-dependent and of the TolQRA-dependent bacterial uptake systems. *Mol. Microbiol.* **9**:219.

Koebnik, R., Braun, V. (1993). Insertion derivatives containing segments of up to 16 amino acids identify surface- and periplasm-exposed regions of the FhuA outer membrane receptor of *Escherichia coli* K-12. *J. Bacteriol.* **175**:826-839.

Koebnik, R. (1995). Proposal for a peptidoglycan associating α-helical motif in the C-terminal regions of some bacterial cell-surface proteins. *Mol. Microbiol.* **16**:1269-1270.

Koebnik, R. (1999). Structural and functional roles of the surface-exposed loops of the barrel membrane protein OmpA from *Escherichia coli*. *J. Bacteriol.* **181**:3688-3694.

Korteland, J., Tommassen, J., Lugtenberg, B. (1982). PhoE protein pore of the outer membrane of *Escherichia coli* K12 is a particularly efficient channel for organic and inorganic phosphate. *Biochim. Biophys. Acta* **690**:282-289.

Köster, W., Braun, V. (1989). Iron-hydroxamate transport into *Escherichia coli* K12: localization of FhuD in the periplasm and of FhuB in the cytoplasmic membrane. *Mol. Gen. Genet.* **217**:233-239.

Köster, W., Braun, V. (1990a). Iron (III) hydroxamate transport into *Escherichia coli*. Substrate binding to the periplasmic FhuD protein. *J. Biol. Chem.* **265**:21407-21410.

Köster, W., Braun, V. (1990b). Iron (III) hydroxamate transport of *Escherichia coli*: restoration of iron supply by coexpression of the N- and C-terminal halves of the cytoplasmic membrane protein FhuB cloned on separate plasmids. *Mol. Gen. Genet.* **223**:379-384.

Köster, W. (1991). Iron (III) hydroxamate transport across the cytoplasmic membrane of *Escherichia coli*. *Biol. Met.* **4**:23-32.

Köster, W, Bohm, B. (1992). Point mutations in two conserved glycine residues within the integral membrane protein FhuB affect iron (III) hydroxamate transport. *Mol. Gen. Genet.* **232**:399-407.

Kreusch, A., Schulz, G.E. (1994). Refined structure of the porin from *Rhodopseudomonas blastica*. Comparison with the porin from *Rhodobacter capsulatus*. *J. Mol. Biol.* **243**:891-905.

Krone, W.J.A., Stegehuis, F., Koningstein, G., van Doorn, C., Roosendaal, B., de Graaf, F.K., Oudega, B. (1985). Characerization of the pColV-K30 encoded cloacin DF13/aerobactin outer membrane receptor protein of *Escherichia coli*: isolation and purification of the protein and analysis of its nucleotide sequence and primary structure. *FEMS Microbiol. Lett.* **26**:153-161.

Kuhn, H-M., Meier-Dieter, U., Mayer, H. (1998). ECA, the enterobacterial common antigen. *FEMS Microbiol. Rev.* **54**:195-222.

Lambert, O., Plançon, L., Rigaud, J.L., Letellier, L. (1998). Protein-mediated DNA transfer into liposomes. *Mol. Microbiol.* **30**:761-765.

Lamping, N., Hoess, A., Yu, B., Park, T.C., Kirschning, C-J., Pfeil, D., Reuter, D., Wright, S.D., Herrmann, Schumann, R.R. (1996). Effects of site-directed mutagenesis of basic residues (Arg94, Lys95, Lys99) of lipopolysaccharide (LPS)-binding protein on binding and transfer of LPS and subsequent immune cell activation. *J. Immunol.* **157**:4648-4656.

Lancaster, C.R.D., Kröger, A., Auer, M., Michel, H. (2000). Structure of fumarate reductase from *Wolinella succinogenes* at 2.2 Å resolution. *Nature* **402**:377-385.

Larsen, R.A., Wood, G.E., Postle, K. (1993). The conserved proline-rich motif is not essential for energy transduction by *Escherichia coli* TonB protein. *Mol. Microbiol.* **10**:943-953.

Larsen, R.A., Thomas, M.G., Wood, G.E., Postle, K. (1994). Partial suppression of an *Escherichia coli* TonB transmembrane domain mutation (ΔV17) by a missense mutation in ExbB. *Mol. Microbiol.* **13**:627-640.

Larsen, R.A., Mysers, P.S., Skare, J.T., Seachord, C.L., Darveau, R.P., Postle, K. (1996). Identification of TonB homologs in the family *Enterobacteriaceae* and evidence for conservation of TonB-dependent energy transduction complexes. *J. Bacteriol.* **178**:1363-1373.

Larsen, R.A., Foster-Hartnett, D., McIntosh, MA., Postle, K. (1997). Regions *of Escherichia coli* TonB and FepA proteins essential for *in vivo* physical interactions. *J. Bacteriol.* **179**:3213-3221.

Larsen, R.A., Thomas, M.G., Postle, K. (1999). Protonmotive force, ExbB and ligand-bound FepA drive conformational changes in TonB. *Mol. Microbiol.* **31**:1809-1824.

Lathrop, J.T., Wei B.Y., Touchie, G.A., Kadner, R.J. (1995). Sequences of the *Escherichia coli* BtuB protein essential for its insertion and function in the outer membrane. *J. Bacteriol.* **177**:6810-6819.

Lawrence, C.M., Ray, S., Babyonyshev, M., Galluser, R., Borhani, Harrison, S.C. (1999). Crystal structure of the ectodomain of human transferrin receptor. *Science* **286**:779-782.

Lazdunski, C.J. (1995). Colicin import and pore formation: a system for studying protein transport across membranes? *Mol. Microbiol.* **16**:1059-1066.

Lazdunski, C.J., Bouveret, E., Rigal, A., Journet, L., Lloubès, Bénédetti, H. (1998). Colicin import into *Escherichia coli* cells. *J. Bacteriol.* **180**:4993-5002.

Lebrón, J.A., Bennett, M., Vaughn, D.E., Chirino, A.J., Snow, P.M., Mintier, G.A., Feder, J.N., Bjorkman, P.J. (1998). Crystal structure of hemochromatosis protein HFE and characterization of its interactions with transferrin receptor. *Cell* **93**:111-123.

Lebrón, J.A., West, A.P., Bjorkman, P.J. (1999). The hemochromatosis protein HFE competes with transferrin for binding to the transferrin receptor. *J. Mol. Biol.* **294**:239-245.

Legrain, M., Jacobs, E., Irvin, S.W., Schyvers, A.B., Quentin-Millet, M.J. (1993). Molecular cloning and characterization of *Neiserria menigitidis* genes encoding the transferrin binding proteins Tbp1 and Tbp2. *Gene* **130**:73-80.

Letain, T.E., Postle, K. (1997). TonB protein appears to transduce energy by shuttling between the cytoplasmic membrane and the outer membrane in gram-negative bacteria. *Mol. Microbiol.* **24**:271-283.

Letellier, L., Locher, K.P., Plançon, L., Rosenbusch, J.P. (1997). Modeling ligand-gated receptor activity. FhuA-mediated ferrichrome efflux from lipid vesicles is triggered by phage T5. *J. Biol. Chem.* **272**:1448-1451.

Létoffé, S., Ghigo, J.M., Wandersman, C. (1994a). Iron acquisition from heme anf hemoglobin by *Serratia marcescens* extracellular protein. *Proc. Natl. Acad. Sci. USA* **91**:9876-9880.

Létoffé, S., Ghigo, J.M., Wandersman, C. (1994b). Secretion of the *Serratia marcescens* HasA protein by an ABC transporter. *J. Bacteriol.* **176**:5372-5377.

Létoffé, S., Nato, F., Goldberg, M.E., Wandersman, C. (1999). Interactions of HasA, a bacterial haemophore, with haemoglobin and with its outer membrane receptor HasR. *Mol. Microbiol.* **33**:546-555.

Levengood, S.K., Beyer, W.F. Jr., Webster, R.E. (1991). TolA: a membrane protein involved in colicin uptake contains an extended helical region. *Proc. Natl. Acad. Sci. USA* **88**:5939-5943.

Lewis, L.A., Gray, E., Wang, Y.P., Roe, B.A., Dyer, D.W. (1997). Molecular characterization of *hpuAB*, the haemoglobin-haptoglobin utilization operon of *Neiserria meningitidis*. *Mol. Microbiol.* **23**:737-749.

Lewis, L.A., Gipson, M., Hartman, K., Ownbey, T., Vaughn, J., Dyer, D.W. (1999). Phase variation of HpuAB and HmbR, two distinct haemoglobin receptors of *Neiserria meningitidis* DNM2. *Mol. Microbiol.* **32**:977-989.

Linton, K.J., Higgins, C.F. (1998). The *Escherichia coli* ATP-binding cassette (ABC) proteins. *Mol. Microbiol.* **28**:5-13.

Lissolo, L., Maitre-Wilmotte, G., Dumas, P., Mignon, M., Danve, B., Quentin-Millet, M.J. (1995). Evaluation of transferrin-binding proteins 2 within the transferrin-binding protein complex as a potential antigen for future meningococcal vaccines. *Infect. Immun.* **63**:884-890.

Little, R.G., Kelner, D.N., Lim, E., Burke, D.J., Conlon, P.J. (1994). Functional domains of recombinant bactericidal/permeability increasing protein (rBPI23). *J. Biol. Chem.* **269**:1865-1872.

Litwin, C.M., Calderwood, S.B. (1993). Role of iron in regulation of virulence genes. *Clin. Microbiol. Rev.* **6**:137-149.

Liu, J., Rutz, J.M., Feix, J.B., Klebba, P.E. (1993). Permeability properties of a large gated channel within the ferric enterobactin receptor, FepA. *Proc. Natl. Acad. Sci. USA* **90**:10653-10657.

Liu, J., Rutz, J.M., Klebba, P.E., Feix, J.B. (1994). A site-directed spin-labeling study of ligand-induced conformational change in the ferric enterobactin receptor, FepA. *Biochemistry* **33**:13274-13283.

Locher, K.P., Rosenbusch, J.P. (1997). Oligomeric states and siderophore binding of the ligand-gated FhuA protein that forms channels across *Escherichia coli* outer membranes. *Eur. J. Biochem.* **247**:770-775.

Locher, K.P., Rees, B., Koebnik, R., Mitschler, A., Moulinier, L., Rosenbusch, R., Moras, D. (1998). Transmembrane signaling across the ligand-gated FhuA receptor: Crystal structures of free and ferrichrome-bound states reveal allosteric changes. *Cell* **95**:771-778.

Lubkowski, J., Hennecke, F., Plückthun, A., Wlodawer, A. (1999). Filamentous phage infection: crystal structure of g3p in complex with its coreceptor, the C-terminal domain of TolA. *Structure* **7**:711-722.

Lundrigan, M.L., Kadner, R.J. (1986). Nucleotide sequence of the gene for the ferrienterochelin receptor FepA in *Escherichia coli*. *J. Biol. Chem.* **261**:10797-10801.

MacGillivray, R.T.A., Moore, S.A., Chen, J., Anderson, B.F., Baker, H., Luo, Y.G., Bewley, M., Smith, C.A., Murphy, M.E., Mason, A.B., Woodworth, R.C., Brayer, G.D., Baker, E.N. (1998). Two high-resolution crystal structures of the recombinant N-lobe of human transferrin reveal a structural change implicated in iron release. *Biochemistry* **37**:7919-7928.

Mademidis, A., Killmann, H., Kraas, W., Flechsler, I., Jung, G., Braun, V. (1997). ATP-dependent ferric hydroxamate transport system in *Escherichia coli*: periplasmic FhuD interacts with a periplasmic and with a transmembrane/cytoplasmic region of the integral membrane protein FhuB, as revealed by competitive peptide mapping. *Mol. Microbiol.* **26**:1109-1123.

Mazarin, V., Rokbi, B., Quentin-Millet, M.J. (1995). Diversity of the transferrin binding protein Tbp2 of *Neiserria menigitidis*. *Gene* **158**:145-146.

Medzhitov, R., Janeway Jr., C.A. (1997). Innate Immunity: The virtues of a nonclonal

system of recognition. *Cell* **91**:295-298.

Merianos, H.J., Cadieux, N., Lin, C.H., Kadner, R.J., Cafiso, D.S. (2000). Substrate-induced exposure of an energy-coupling motif of a membrane transporter. *Nature Struct. Biol.* **7**:205-209.

Miller, M.J., Malouin, F. (1993). Microbial iron chelators as drug delivery agents: The rational design and synthesis of siderophore-drug conjugates. *Acc. Chem. Res.* **26**:241-249.

Miller, M.J., Malouin, F., Dolence, E.K., Gasparski, C.M., Ghosh, M., Guzzo, P.R., Lotz B.T., McKee, J.A., Minnick, A.A., Teng, M. (1993). Iron transport-mediated drug delivery. In: Bentley, P.H., Ponsford, R. (eds.), *Recent Advances in the Chemistry of Anti-infective Agents*. Cambridge, UK, The Royal Society of Chemistry, pp 135-159.

Moeck, G.S., Fazly Bazzaz, B.S., Gras, M.F., Ravi, T.S., Ratcliffe, M.J.H., Coulton, J.W. (1994). Genetic insertion and exposure of a reporter epitope in the ferrichrome-iron receptor of *Escherichia coli* K-12. *J. Bacteriol.* **176**:4250-4259.

Moeck, G.S., Ratcliffe, M.J.H., Coulton, J.W. (1995). Topological analysis of the *Escherichia coli* ferrichrome-iron receptor by using monoclonal antibodies. *J. Bacteriol.* **177**:6118-6125.

Moeck, G.S., Tawa, P., Xiang, H., Ismail, A.A., Turnbull, J.L., Coulton, J.W. (1996). Ligand-induced conformational change in the ferrichrome-iron receptor *of Escherichia coli* K-12. *Mol. Microbiol.* **22**:459-471.

Moeck, G.S., Coulton, J.W., Postle, K. (1997). Cell envelope signaling in *Escherichia coli*. Ligand binding to the ferrichrome-iron receptor FhuA promotes interaction with the energy-transducing protein TonB. *J. Biol. Chem.* **272**:28391-28397.

Moeck, G.S., Coulton, J.W. (1998). TonB-dependent iron acquisition: mechanisms of siderophore-mediated active transport. *Mol. Microbiol.* **28**:675-681.

Möllmann, U., Ghosh, A., Dolence, E.K., Dolence, J.A., Ghosh, M., Miller, M.J., Reissbrodt, R. (1998). Selective growth promotion and growth inhibition of gram-negative and gram-positive bacteria by synthetic siderophore- β-lactam conjugates. *BioMetals* **11**:1-12.

Mondigler, M., Vögele, R.T., Heller, K.J. (1995). Overproduced and purified receptor binding protein pb5 of bacteriophage T5 binds to the T5 receptor protein FhuA. *FEMS Lett.* **130**:293-300.

Mondigler, M., Holz, T., Heller, K.J. (1996). Identification of the receptor-binding regions of pb5 proteins of bacteriophage T5 and BF23. *Virology* **219**:19-28.

Morona, R., Klose, M., Henning, U. (1984). *Escherichia coli* K12 outer membrane protein (OmpA) as a bacteriophage receptor: analysis of mutant genes expressing altered proteins. *J. Bacteriol.* **159**:570-578.

Morona, R., Krämer, C., Henning, U. (1985). Bacteriophage receptor area of outer membrane protein OmpA of *Escherichia coli* K-12. *J. Bacteriol.* **164**:539-543.

Mourez, M., Hofnung, M., Dassa, E. (1997). Subunit interactions in ABC transporters: a conserved sequence in hydrophobic membrane proteins of periplasmic permeases defines an important site of interactions with the ATPase subunits. *EMBO J.* **16**:3066-3077.

Mowbray, S.L., Cole, L.B. (1992). 1.7 Å X-ray structure of the periplasmic ribose receptor from *Escherichia coli*. *J. Mol. Biol.* **225**:155-175.

Murphy, C.K., Kalve, V.I., Klebba, P.E. (1990). Surface topology of the *Escherichia coli* K-12 ferric enterobactin receptor. *J. Bacteriol.* **172**:2736-2746.

Nau, C.D., Konisky, J. (1989). Evolutionary relationship between the TonB-dependent outer membrane transport proteins: nucleotide and amino acid sequences of the *Escherichia coli* colicin I receptor gene. *J. Bacteriol.* **171**:1041-1047.

Neilands, J.B., Konopka, K., Schwyn, B., Coy, M., Francis, R.T., Paw, B.H., Bagg, A. (1987). Comparitive biochemistry of microbial iron assimilation. In: Winklemann, G., van der Helm, D., Neilands, J.B. (eds.), *Iron Transport in Microbes, Plants and Animals*. VCH Press, Weinheim, pp. 3-33.

Neilands, J.B. (1995). Siderophores: structure and function of microbial iron transport compounds. *J. Biol. Chem.* **270**:26723-26726.

Newton, S.H.C., Allen, J.S., Cao, Z., Qi, Z., Jiang, X., Sprencel, C., Igo, J.D., Foster, S.B., Payne, M.A., Klebba, P.E. (1997). Double mutagenesis of a positive charge cluster in the ligand-binding site of the ferric enterobactin receptor, FepA. *Proc. Natl. Acad. Sci. USA* **94**:4560-4565.

Nikaido, H., Bavoil, P., Hirota, Y. (1977). Outer membrane of gram-negative bacteria. Transmembrane diffusion rates in lipoprotein-deficient mutants of *Escherichia coli*. *J. Bacteriol.* **132**:1045-1047.

Nikaido, H., Vaara, M. (1985). Molecular basis of bacterial outer membrane permeability. *Microbiol. Rev.* **49**:1-32.

Nikaido, H. (1996). Outer membrane. In: *Escherichia coli* and *Salmonella*. Cellular and Molecular Biology. Neidhardt, F.C. (ed.), Washington, D.C., ASM Press, pp. 29-47.

Nikaido, H., Hall, J.A. (1998). Overview of bacterial ABC transporters. *Meth. Enzymol.* **292**:3-21.

Nishiyama, K-I., Fukuda, A., Morita, K., Tokuda, H. (1999). Membrane deinsertion of SecA underlying proton motive force-dependent stimulation of protein translocation. *EMBO J.* **18**:1049-1058.

Ochs, M., Veitinger, S., Kim, I., Welz, D., Angerer, A., Braun, V. (1995). Regulation of citrate-dependent iron transport of *Escherichia coli*: FecR is required for transcription activation by FecI. *Mol. Microbiol.* **15**:119-132.

Ochs, M., Angerer, A., Enz, S., Braun, V. (1996). Surface signaling in transcriptional regulation of the ferric citrate transport system of *Escherichia coli*: mutational analysis of the alternative sigma factor supports its essential role in *fec* transport gene transcription. *Mol. Gen. Genet.* **250**:455-465.

Odell, E.W., Sarra, R., Foxworthy, M., Chapple, D.S., Evans, R.W. (1996). Antibacterial activity of peptides homologous to a loop region in human lactoferrin. *FEBS Lett.* **382**:175-178.

Oh, B-H., Kang, C-H., De Bondt, H., Kim, S-H., Nikaido, K., Joshi, A.K., Ames, G.F-L. (1994). The bacterial periplasmic histidine-binding protein. Structure/function analysis of the ligand-binding site and comparison with related proteins. *J. Biol. Chem.* **269**:4135-4143.

Olah, G.A., Trakhanov, S., Trewhella, J., Quiocho, F.A. (1993). Leucine/isoleucine/valine-binding protein contracts upon binding of ligand. *J. Biol. Chem.* **268**:16241-16247.

Oliver, D.B. (1996). Periplasm. In: *Escherichia coli* and *Salmonella*. Cellular and Molecular Biology. Neidhardt, F.C. (ed.), Washington, D.C., ASM Press, pp. 88-103.

Olschläger, T., Turba, A., Braun, V. (1991). Binding of the immunity protein inactivates colicin M. *Mol. Microbiol.* **5**:1105-1111.

Park, J.T. (1996). The murein sacculus. In: *Escherichia coli* and *Salmonella*. Cellular and Molecular Biology. Neidhardt, F.C. (ed.), Washington, D.C., ASM Press, pp. 48-57.

Pautsch, A., Schulz, G.E. (1998). Structure of the outer membrane protein A transmembrane domain. *Nature Struct. Biol.* **5**:1013-1017.

Pettersson, A., Prinz, T., Umar, A., van der Blezen, J., Tommassen, J. (1998). Molecular characterization of LbpB, the second lactoferrin-binding protein of *Neiserria menigitidis*. *Mol. Microbiol.* **27**:599-610.

Phale, P.S., Schirmer, T., Prilipov, A., Lou, K.L., Hardmeyer, A., Rosenbusch, J.P. (1997). Voltage gating of *Escherichia coli* porin channels: Role of the constriction loop. *Proc. Natl. Acad. Sci. USA* **94**:6741-6745.

Pilsl, H., Glaser, C., Gross, P., Killmann, H., Olschläger, T., Braun, V. (1993). Domains of colicin M involved in uptake and activity. *Mol. Gen. Genet.* **240**:103-112.

Plançon, L., Chami, M., Letellier, L. (1997). Reconstitution of FhuA, an *Escherichia coli* outer membrane protein, into liposomes. Binding of phage T5 to FhuA triggers the transfer of DNA into the proteoliposomes. *J. Biol. Chem.* **272**:16868-16872.

Postle, K., Skare, J.T. (1988). *Escherichia coli* TonB protein is exported from the cytoplasm without proteolytic cleavage of its amino terminus. *J. Biol. Chem.* **263**:11000-11007.

Postle, K. (1990). TonB and the gram-negative dilemma. *Mol. Microbiol.* **4**:2019-2025.

Postle, K. (1993). TonB protein and energy transduction between membranes. *J. Bioenerg. Biomemb.* **25**:591-601.

Pressler, U., Staudenmaier, H., Zimmermann, L., Braun, V. (1988). Genetics of the iron dicitrate transport system of *Escherichia coli*. *J. Bacteriol.* **170**:2716-2724.

Prinz, T., Meyer, M., Pettersson, A., Tommassen, J. (1999). Structural characterization of the lactoferrin receptor from *Neisseria meningitidis*. *J. Bacteriol.* **181**:4417-4419.

Przybylski, M., Glocker, M.O., Nestel, U., Schnaible, V., Bluggel, M., Diederichs, K., Weckesser, J., Schad, M., Schmid, A., Welte, W., Benz, R. (1996). X-ray crystallographic and mass spectrometric structure determination and functional

characterization of succinylated porin from *Rhodobacter capsulatus*: Implications for ion selectivity and single-channel conductance. *Prot. Science* **5**:1477-1189.

Pugsley, A.P., Zimmerman, W., Wehrli, W. (1987). Highly efficient uptake of a rifamycin derivative via the FhuA-TonB-dependent uptake route in *Escherichia coli*. *J. Gen. Microbiol.* **133**:3505-3511.

Qiu, X., Verlinde, C.L.M.J., Zhang, S., Schmitt, M.P., Holmes, R.K., Hol, W.G.J. (1995). Three-dimensional structure of the diphtheria toxin repressor in complex with divalent cation co-repressors. *Structure* **3**:87-100.

Qiu, X., Pohl, E., Holmes, R.K., Hol, W.G.J. (1996). High-resolution structure of the diphtheria toxin repressor complexed with cobalt and manganese reveals an SH3-like third domain and suggests a possible role of phosphate as corepressor. *Biochemistry* **35**:12292-12302.

Raetz, C.R.H. (1996). Bacterial lipopolysaccharides: a remarkable family of bioactive macroamphiphiles. In: *Escherichia coli* and *Salmonella*, Cellular and Molecular Biology. Neidhardt, F.C. (ed.), Washington, D.C., ASM Press, pp. 1035-1063.

Retzer, M.D., Yu, R-H., Zhang, Y., Gonzalez, G.C., Schryvers, A.B. (1998). Discrimination between the apo and iron-loaded forms of transferrin by transferrin binding protein B and its N-terminal subfragment. *Microb. Pathog.* **25**:175-180.

Retzer, M.D., Yu, R-H., Schryvers, A.B. (1999). Identification of sequences in human transferrin that bind to the bacterial receptor protein, transferrin-binding protein B. *Mol. Microbiol.* **32**:111-121.

Reynolds, P.R., Mottur, G.P., Bradbeer, C. (1980). Transport of vitamin B_{12} in *Escherichia coli*. Some observations on the role of the gene products of *btuC* and *tonB*. *J. Biol. Chem.* **255**:4313-4319.

Rick, P.D., Silver, R.P. (1996). Enterobacterial common antigen and capsular polysaccharides. In: *Escherichia coli* and *Salmonella*. Cellular and Molecular Biology. Neidhardt, F.C. (ed.), Washington, D.C., ASM Press, pp. 104-122.

Riechmann, L., Holliger, P. (1997). The C-terminal domain of TolA is the coreceptor for filamentous phage infection of *E. coli*. *Cell* **90**:351-360.

Ried, C., Wahl, C., Miethke, T., Wellnhofer, G., Landgraf, C., Schneider-Mergener, J., Hoess, A. (1996). High affinity endotoxin-binding and neutralizing peptides based on

the crystals structure of recombinant *Limulus* anti-lipopolysaccharide factor. *J. Biol. Chem.* **271**:28120-28127.

Rohrbach, M.R., Paul, S., Köster, W. (1995a). *In vivo* reconstitution of an active siderophore transport system by a binding protein lacking a signal sequence. *Mol. Gen. Genet.* **248**:33-42.

Rohrbach, M.R., Braun, V., Köster, W. (1995b). Ferrichrome transport in *Escherichia coli* K-12: Altered substrate specificity of mutated periplasmic FhuD and interaction of FhuD with the integral membrane protein FhuB. *J. Bacteriol.* **177**:7186-7193.

Römheld, V., Müller, C., Marschner, H. (1984). Localization of capacity of proton pumps in roots of intact sunflower plants. *Plant Physiol.* **76**:603-606.

Römheld, V., Marschner, H. (1986a). Mobilization of iron in the rhizosphere of different plant species. *Adv. Plant. Nutr.* **2**:155-204.

Römheld, V., Marschner, H. (1986b). Evidence for a specific uptake system for iron phytosiderophores in roots and grasses. *Plant Physiol.* **80**:175-180.

Römheld, V. (1987). Different strategies for iron acquisition in higher plants. *Physiol. Plantarum* **70**:231-234.

Roof, S.K., Allard, J.D., Bertrand, K.P., Postle, K. (1991). Analysis of *Escherichia coli* TonB membrane topology by use of PhoA fusions. *J. Bacteriol.* **173**:5554-5557.

Rosenberg, M.F., Callaghan, Ford, R.C., Higgins, C.F. (1997). Structure of the multidrug resistance P-glycoprotein to 2.5 nm resolution determined by electron microscopy and image analysis. *J. Biol. Chem.* **272**:10685-10694.

Rutz, J.M., Liu, J., Lyons, J.A., Goranson, J., Armstrong, S.K., McIntosh, M.A., Feix, J.B., Klebba, P.E. (1992). Formation of a gated channel by a ligand-specific transport protein in the bacterial outer membrane. *Science* **258**:471-475.

Sauer, M., Hantke, K., Braun, V. (1990). Sequence of the *fhuE* outer-membrane receptor gene of *Escherichia coli* K12 and properties of mutants. *Mol. Microbiol.* **4**:427-437.

Saurin, W., Köster, W., Dassa, E. (1994). Bacterial binding protein-dependent permeases: characterization of distinctive signatures for functionally related integral cytoplasmic membrane proteins. *Mol. Microbiol.* **12**:993-1004.

Schäffer, S., Hantke, K., Braun, V. (1985). Nucleotide sequence of the iron regulatory gene *fur*. *Mol. Gen. Genet.* **200**:110-113.

Scharff, A.J., Rodseth, L.E., Quiocho, F. (1993). Refined 1.8-Å structure reveals the mode of binding of β-cyclodextrin to the maltodextrin binding protein. *Biochemistry* **32**:10553-10559.

Schiering, N., Tao, X., Zeng, H., Murphy, J.R., Petsko, G.A., Ringe, D. (1995). Structures of the apo- and the metal ion-activated forms of the diphtheria *tox* repressor from *Corynebacterium diphtheriae*. *Proc. Natl. Acad. Sci. USA* **92**:9843-9850.

Schirmer, T., Keller, T.A., Wang, Y.F., Rosenbusch, J. (1995). Structural basis for sugar translocation through maltoporin channels at 3.1 Å resolution. *Science* **267**:512-514.

Schmitt, M.P., Holmes, R.K. (1993). Analysis of diphtheria toxin repressor-operator interactions and characterization of a mutant suppressor with decreased binding activity for divalent metals. *Mol. Microbiol.* **9**:173-181.

Schöffler, H., Braun, V. (1989). Transport across the outer membrane of *E. coli* K-12 via the FhuA receptor is regulated by the TonB protein in the cytoplasmic membrane. *Mol. Gen. Genet.* **217**:378-383.

Schramm, E., Mende, J., Braun, V., Kamp, R.M. (1987). Nucleotide sequence of the colicin B activity gene *cba*: consensus pentapeptide among TonB-dependent colicins and receptors. *J. Bacteriol.* **169**:3350-3357.

Schryvers, A.B., Morris, L.J. (1988). Identification and characterization of the transferrin receptor from *Neiserria menigitidis*. *Mol. Microbiol.* **2**:281-288.

Schryvers, A.B., Stojiljkovic, I. (1999). Iron acquisition systems in the pathogenic *Neisseria*. *Mol. Microbiol.* **32**:1117-1123.

Schultz-Hauser, G., Köster, W., Schwarz, H., Braun, V. (1992). Iron (III) hydroxamate transport in *Escherichia coli* K-12: FhuB-mediated membrane association of the FhuC protein and negative complementation of *fhuC* mutants. *J. Bacteriol.* **174**:2305-2311.

Sehn, A.P., Meier, B. (1994). Regulation of an *in vivo* metal-exchangeable superoxide dismutase from *Propionibacterium shermanii* exhibiting activity with different metal cofactors. *Biochem. J.* **304**:803-808.

Sen, K., Hellman, J., Nikaido, H. (1988). Porin channels in intact cells of *Escherichia coli* are not affected by Donnan potentials across the outer membrane. *J. Biol. Chem.* **263**:1182-1187.

Skare, J.T., Ahmer, B.M.M., Seachord, C.L., Darveau, R.P., Postle, K. (1993). Energy transduction between membranes-TonB, a cytoplasmic membrane protein, can be chemically cross-linked *in vivo* to the outer membrane receptor FepA. *J. Biol. Chem.* **272**:16302-16308.

Smith, B.S., Kobe, B., Kurumbail, R., Buchanan, S.K., Venkatramani, L., van der Helm, D., Deisenhofer, J. (1998). Crystallization and preliminary X-ray analysis of ferric enterobactin receptor FepA, an integral membrane protein from *Escherichia coli*. *Acta Cryst. D* **54**:697-699.

Snijder, H.J., Ubarretxena-Belandia, I., Blaauw, M., Kalk, K.H., Verheij, H.M., Egmond, M.R., Dekker, N., Dijkstra, B.W. (1999). Structural evidence for dimerization-regulated activation of an integral membrane phospholipase. *Nature* **401**:717-721.

Sonntag, I., Schwarz, H., Yirota, Y., Henning, U. (1978). Cell envelope and shape of *Escherichia coli*: Multiple mutants missing the outer membrane lipoprotein and other major outer membrane proteins. *J. Bacteriol.* **136**:280-285.

Spurlino, J.C., Lu, G-Y., Quiocho, F. (1991). The 2.3-Å resolution structure of the maltose- or maltodextrin-binding protein, a primary receptor of bacterial active transport and chemotaxis. *J. Biol. Chem.* **266**:5202-5219.

Stock, D., Leslie, A.G.W., Walker, J.E. (1999). Molecular architecture of the rotary motor in ATP synthase. *Science* **286**:1700-1705.

Stojiljkovic, I., Hantke, K. (1992). Haemin uptake system of *Yersinia enterocolitica*: similarities with other TonB-dependent systems in Gram-negative bacteria. *EMBO J.* **11**:4359-4367.

Stojiljkovic, I., Hwa, V., de Saint Martin, L., O'Gaora, P., Nassif, X., Heffron, F., So, M. (1995). The *Neiserria meningitidis* haemoglobin receptor: its role in iron utilization and virulence. *Mol. Microbiol.* **15**:531-541.

Stojiljkovic, I., Hantke, K. (1995). Functional domains of the *Escherichia coli* ferric uptake regulator protein (Fur). *Mol. Gen. Genet.* **247**:199-205.

Stojiljkovic, I., Larson, J., Hwa, V., Anic, S., So, M. (1996). HmbR outer membrane proteins of pathogenic *Neisseriae*: iron-regulated, hemoglobin binding proteins with high degree of primary structure conservation. *J. Bacteriol.* **178**:3341-3352.

Stojiljkovic, I., Srinivasan, N. (1997). *Neiserria menigitidis tonB*, *exbB*, and *exbD* genes: Ton-dependent utilization of protein-bound iron in *Neisseriae*. *J. Bacteriol.* **179**:805-812.

Tanaka, S., Nakamura, T., Morita, T., Iwanaga, S. (1982). *Limulus* anti-LPS factor: an anticoagulant which inhibits the endotoxin-mediated activation of *Limulus* coagulation system. *Biochem. Biophy. Res. Commun.* **105**:17-723 (1982).

Tao, X., Murphy, J.R. (1992). Binding of the metalloregulatory protein DtxR to the diphtheria *tox* operator requires a divalent heavy metal and protects the palidromic sequence from DNase I digestion. *J. Biol. Chem.* **267**:121761-21764.

Tao, X., Schiering, N., Zeng, H., Ringe, D., Murphy, J.R. (1994). Iron, DtxR, and the regulation of diphtheria toxin expression. *Mol. Microbiol.* **14**:191-197.

Tatsumi, Y., Maejima, T., Mitsuhashi, S. (1995). Mechanism of *tonB*-dependent transport of KP-736, a 1,5-dihydroxy-4-pyridone-substituted cephalopsorin, into *Escherichia coli* K-12 cells. *Antimicrob. Agents Chemo.* **39**:613-619.

Taylor, A.H., Heavner, G., Nedelman, M., Sherris, D., Brunt, E., Knight, D., Ghrayeb, J. (1995). Lipopolysaccharide (LPS) neutralizing peptides reveal a lipid A binding site of LPS binding protein. *J. Biol. Chem.* **270**:17934-17938.

Traub, I., Gaisser, S., Braun, V. (1993). Activity domains of the TonB protein. *Mol. Microbiol.* **8**:409-423.

Tsolis, R.M., Bäumler, A.J., Heffron, F., Stojiljkovic, I. (1996). Contribution of TonB- and Feo-mediated iron uptake to growth of *Salmonella typhimurium* in the mouse. *Infect. Immun.* **64**:4549-4556.

Ubarretxena-Belandia, I., Boots, J.W.P., Verheij, H.M., Dekker, N. (1998). Role of the cofactor calcium in the activation of outer membrane phospholipase A. *Biochemistry* **37**:16011-16018.

Ulmke, C., Kreth, J., Lengeler, J.W., Welte, W., Schmid, K. (1999). Site-directed mutagensis of loop L3 of sucrose porin ScrY leads to changes in substrate selectivity. *J. Bacteriol.* **181**:1920-1923.

Valvano, M.A., Crosa, J.H. (1984). Aerobactin iron transport genes commonly encoded by certain ColV plasmids occur in the chromosome of a human invasive strains of *Escherichia coli* K1. *Infect. Immun.* **46**:159-167.

Valvano, M.A., Silver, R.P., Crosa, J.H. (1986). Occurrence of chromosome- or plasmid-mediated aerobactin iron transport systems and hemolysin production among clonal groups of human invasive strains of *Escherichia coli* K1. *Infect. Immun.* **52**:192-199.

Van Berkel, P.H.C., Geerts, M.E.J., van Veen, H.A., Mericskay, M., de Boer, H.A., Nuijens, J.H. (1997). N-terminal stretch Arg2, Arg3, Arg4 and Arg5 of human lactoferrin is essential for binding to heparin, bacterial lipopolysaccharide, human lysozyme and DNA. *Biochem. J.* **328**:145-151.

Vasil, M.L., Ochsner, U.A. (1999). The response of *Pseudomonas aeruginosa* to iron: genetics, biochemistry and virulence. *Mol. Microbiol.* **34**:399-413.

Vogt, J., Schulz, G.E. (1999). The structure of the outer membrane protein OmpX from *Escherichia coli* reveals possible mechanisms of virulence. *Structure* **7**:1301-1309.

Walker, J.E., Saraste, M., Runswick, M.J., Gay, N.J. (1982). Distantly related sequences in the α- and β-subunits of ATP synthase, myosin, kinases and other ATP-requiring enzymes and a common nucleotide binding fold. *EMBO J.* **8**:945-951.

Watanabe, M., Rosenbusch, J.P., Schirmer, T., Karplus, M. (1997). Computer simulations of the OmpF porin from the outer membrane of *Escherichia coli*. *Biophys. J.* **72**:2094-2102.

Warren, H.S., *et al.*, Novitsky, T.J. (1992). Binding and neutralization of endotoxin by *Limulus* antilipopolysaccharide factor. *Infect. Immun.* **60**:2506-2513.

Webster, R.E. (1991). The *tol* gene products and the import of macromolecules into *Escherichia coli*. *Mol. Microbiol.* **5**:1005-1011.

Wehrli, W., Zimmermann, W., Kump, W, Tosch W., Vischer, W., Zak, O. (1987). CGP 4832, a semisynthetic rifamycin derivative highly active against some Gram-negative bacteria. *J. Antibiotics* **40**:1733-1739.

Weiss, M.S., Abele, U., Weckesser, J., Welte, W., Schiltz, E., Schulz, G.E. (1991). Molecular architecture and electrostatic properties of a bacterial porin. *Science* **254**:1627-1630.

Welte, W., Nestel, U., Wacker, T., Diederichs, K. (1995). Structure and function of the porin channel. *Kidney Int.* **48**:930-940.

Welz, D., Braun, V. (1998). Ferric citrate transport of *Escherichia coli*: Functional regions of the FecR transmembrane regulatory protein. *J. Bacteriol.* **180**:2387-2394.

White, A., Ding, X., vanderSpek, J.C., Murphy, J.R., Ringe, D. (1998). Structure of the metal-ion-activated diphtheria toxin repressor/*tox* operator complex. *Nature* **394**:502-506.

Whitfield, C., Valvano, M.A. (1993). Biosynthesis and expression of cell-surface polysaccharides in gram-negative bacteria. *Adv. Microb. Physiol.* **35**:135-246.

Wiener, M., Freymann, D., Ghosh, P., Stroud, R.M. (1997). Crystal structure of colicin Ia. *Nature* **385**:461-464.

Wright, G.C., Weiss, J., Kim, K.S., Verheij, H., Elsbach, P. (1990). Bacterial phospholipid hydrolysis enhances the destruction of *Escherichia coli* ingested by rabbit neutrophils. *J. Clin. Invest.* **85**:1925-1935.

Yao, N., Trakhanov, S., Quiocho, F. (1994). Refined 1.89-Å structure of the histidine-binding protein complexed with histidine and its relationship with many other active transport/chemosensory proteins. *Biochemistry* **33**:4769-4779.

Zähringer, U., Lindner, B., Rietschel, E.T. (1999). *Endotoxin in Health and Disease.* (Brade, H., Morrison, D.C., Opal, S., Vogel, S. (eds.), Marcel Dekker Inc., New York, pp. 93-114.

Zhu, W., Hunt, D.J., Richardson, A.R., Stojiljkovic, I. (2000). Use of heme compounds as iron sources by pathogenic Neisseriae requires the product of the *hemO* gene. *J. Bacteriol.* **182**:439-447.

Zimmermann, L., Angerer, A., Braun, V. (1989). Mechanistically novel iron (III) transport system in *Serratia marcescens*. *J. Bacteriol.* **171**:238-243.

Preface to chapter two

This chapter describes the purification, crystallization, and preliminary X-ray diffraction analysis of the ferric hydroxamate uptake receptor, FhuA, from *Escherichia coli* K-12. To obtain FhuA in quantities sufficient for crystallization, a hexahistidine tag was inserted into the *fhuA* gene at various surface-exposed locations. An efficient method for the purification of recombinant FhuA using immobilized-metal affinity chromatography under native conditions was established. This procedure yields copious amounts of homogeneous, monodisperse protein, and has broad applicability to the purification of other affinity tagged outer membrane proteins. Sparse matrix screening conducted with seven chimeric FhuA proteins, solublized with numerous primary detergents, identified a variety of crystal growth conditions. Following optimization of crystal growth parameters, one of these FhuA proteins formed well-ordered crystals. X-ray diffraction data collected from these crystals revealed outermost reflections to 3.0 Å resolution. The development of a concise protocol for the isolation of pure protein, the optimal placement of the affinity tag, and the identification of a compatible primary detergent, were essential components in the determination of the three-dimensional structure of FhuA.

An internal affinity-tag for purification and crystallization of the siderophore receptor FhuA, an integral outer membrane protein from *Escherichia coli* K-12

Andrew D. Ferguson[1,2], Jason Breed[2], Kay Diederichs[2], Wolfram Welte[2], James W. Coulton[1]

1 Department of Microbiology and Immunology, McGill University, 3775 University Street, Montreal, Quebec, Canada H3A 2B4

2 Fakultät für Biologie, Universität Konstanz, M656, D-78457 Konstanz, Germany

Abstract

FhuA (M_r 78,992, 714 amino acids), siderophore receptor for ferrichrome-iron in the outer membrane of *Escherichia coli*, was affinity tagged, rapidly purified, and crystallized. To obtain FhuA in quantities sufficient for crystallization, a hexahistidine tag was genetically inserted into the *fhuA* gene after amino acid 405, which resides in a known surface-exposed loop. Recombinant FhuA protein was overexpressed in an *E. coli* strain that is devoid of several major porins and using metal-chelate chromatography was purified in large amounts to homogeneity. FhuA crystals were grown using the hanging drop vapor diffusion technique and were suitable for X-ray diffraction analysis. On a rotating anode X-ray source, diffraction was observed to 3.0 Å resolution. The crystals belong to space group $P6_1$ or $P6_5$ with unit cell dimensions of $a = b = 174$ Å, $c = 88$ Å ($\alpha = \beta = 90°$, $\gamma = 120°$).

Abbreviations: PEG, polyethylene glycol; C_{10}DAO, N,N-dimethyldecylamine-N-oxide; C_{12}DAO, N,N-dimethyldodecylamine-N-oxide; SDS-PAGE, sodium dodecyl sulfate polyacrylamide gel electrophoresis.

Key words: FhuA; TonB-dependent receptor; outer membrane; siderophore; protein crystals; X-ray crystallography; membrane protein; crystallization

Introduction

Biological membranes serve to partition the cell interior from the external milieu, and they play a critical role in maintaining cell integrity and cell function. The cell envelope of gram-negative bacteria consists of three distinct layers: the surface-located outer membrane, the periplasm in which the peptidoglycan layer is found, and the cytoplasmic membrane. Bacteria have a variety of transport systems available for the import of essential nutrients through these cell envelope layers (reviewed by Nikaido & Saier, 1992). The outer membrane acts as a permeability barrier for the cell. It also functions as a molecular sieve, excluding deleterious substances and permitting passive diffusion of small solutes through porins into the periplasm (Nikaido, 1996).

Some compounds essential for bacterial growth are found at exceedingly low concentrations; iron is one such nutrient. To scavenge ferric iron from their environment, bacteria synthesize and secrete iron-chelating substances called siderophores of molecular mass 700 - 1000 Da. Nonspecific porin channels from *Escherichia coli* have an apparent molecular mass exclusion limit of 600 Da and, therefore, do not function in the import of these complexes. Hence, bacteria have evolved high-affinity iron transport mechanisms, distinct from porin-mediated diffusion, and these mechanisms require proteins in the outer membrane, the periplasm, and the cytoplasmic membrane. Outer membrane-localized receptors bind their cognate ferric siderophore with high affinity and in *E. coli*, the outer membrane receptor for ferric hydroxamate uptake is FhuA, 714 amino acids, M_r 78,992 (Coulton et al., 1986). In addition to binding ferrichrome-iron, FhuA also acts as receptor for four bacteriophages (T1, T5, ϕ80, and UC-1), colicin M, and the antibiotics albomycin and microcin J25. Binding of ferrichrome-iron to FhuA induces localized conformational changes (Moeck et al., 1996; Bös et al., 1998). Such structural alterations signal the ligand-bound status of the receptor and, therefore, the requirement for TonB-dependent energy transduction (Moeck et al., 1997). The cytoplasmic membrane-localized TonB-ExbB-ExbD complex transduces energy from the proton motive force to FhuA (Braun, 1997; reviewed by Moeck & Coulton, 1998). Once transferred to the periplasm, chelated iron is translocated into the cytoplasm through a cytoplasmic membrane-localized ATP-dependent mechanism (Mademidis et al., 1997).

Crystallographic analyses of nonspecific porins (Weiss et al., 1991; Cowan et al., 1992) and of specific outer membrane channels (Schirmer et al., 1995; Forst et al., 1998) show a conserved β-barrel structure consisting of 16 or 18 amphiphilic transmembrane β-strands. Outer membrane receptors are energy-dependent, ligand-specific gated porin channels (Rutz et al., 1992; Jiang et al., 1997) and, therefore, may share this β-barrel structure. One of the outer membrane receptors in *E. coli* is the receptor for ferric enterobactin FepA, a protein that was crystallized by Jalal and van der Helm (1989). FepA was predicted to form a β-barrel containing 29 transmembrane β-strands (Murphy et al., 1990). Removal of a large centrally located ligand-binding domain converted the protein into an open diffusion pore (Liu et al., 1993). In contrast, the topological organization of FhuA was modeled as 32 transmembrane β-strands (Koebnik & Braun, 1993). This model is further supported by a neural network designed for topology predictions of outer membrane proteins and available at http://structbio.biologie.uni-konstanz.de/~kay/om_topo_predict.html (Diederichs et al., 1998). FhuA can be induced to form a channel by the electrochemical potential of the cytoplasmic membrane via the TonB-ExbB-ExbD complex (Postle, 1993) and by the binding of the bacteriophage T5 (Bonhivers et al., 1996; Plançon et al., 1997). Ligand binding sites on FhuA have been deduced by competitive peptide mapping (Killmann et al., 1995) and by in vivo thiol-labeling of surface-exposed cysteines (Bös & Braun, 1997; Bös et al., 1998). There is a surface-exposed region termed the gating loop, excision of which, converts the energy-dependent receptor into an aqueous nonspecific diffusion channel (Killmann et al., 1993).

Results and discussion

To study structure-function relationships of FhuA, we designed an overexpression and purification protocol, both of which are prerequisites for crystallization trials and ultimately for structural analysis by X-ray crystallography. For proteins possessing an affinity tag of six consecutive histidine residues, the hexahistidine-tag, a highly selective purification strategy utilizes metal-chelate matrices (Arnold & Haymore, 1991). We previously identified amino acid 405 of FhuA to be surface exposed by flow cytometry (Moeck et al., 1994; 1995). We reasoned that because this residue is surface exposed, the

splicing of an affinity tag into this position would generate a recombinant FhuA protein amenable to affinity purification using metal-chelate chromatography. Accordingly, synthetic double stranded oligonucleotides encoding for a hexahistidine tag were spliced into the *fhuA* gene at codon 405. To assess the fidelity of cloning, DNA sequencing across the splice sites confirmed the plasmid (pHX405). Plasmid pHX405 was transformed into the *E. coli* strain AW740 [*ΔompF zcb*:Tn*10 ΔompC fhuA*31], which lacks the major outer membrane proteins OmpC and OmpF. The recombinant protein was strongly expressed with respect to ferrichrome-iron transport and its sensitivity to four lytic viruses. Our conclusion is that insertion of an affinity tag at amino acid 405 does not interfere with the functions of FhuA.

The *E. coli* K-12 strain AW740 harbouring the plasmid pHX405 was grown as previously described (Moeck et al., 1996). Outer membrane vesicles were isolated by Tris-HCl / lysozyme / EDTA (Hantke, 1981) and treated with 1.0 % C_{12}DAO. Solubilized protein extract was dialyzed against 2 L of 50 mM Tris-HCl (pH 8.0), 250 mM NaCl, 0.10 % C_{12}DAO, 5 mM imidazole buffer, and loaded onto a Ni^{2+}-NTA superflow column (QIAGEN, Ontario, Canada) coupled to an automated BioLogic high-resolution protein purification system (Bio-Rad Laboratories, Ontario, Canada). No FhuA was observed in the flow through, indicating efficient and selective binding of the hexahistidine tagged protein to metal-chelate resin. A linear gradient of imidazole (5 to 500 mM) was established over five column volumes, and a single symmetrical peak containing purified FhuA eluted at an imidazole concentration of approximately 200 mM. To remove omnipresent lipids from purified FhuA, protein-containing fractions were pooled, dialyzed against 1 L of 50 mM ammonium acetate (pH 8.0), 250 mM NaCl, 0.10 % C_{12}DAO, 10 mM imidazole buffer, and loaded onto a Ni^{2+}-charged POROS 20 MC (PerSeptive Biosystems, Massachusetts, USA) column. When a linear gradient of imidazole up to 250 mM was applied over five column volumes, the major protein-containing peak eluted at an imidazole concentration of approximately 100 mM. SDS-PAGE analysis of purified FhuA and silver staining of 1,000 ng amounts showed a single band and an apparent absence of micellar lipopolysaccharide. Measurements of dynamic light scattering (Protein Solutions, Virginia, USA) showed purified FhuA preparations to

be monodisperse. From 6 L of cell culture harvested at A_{600} = 1.80, the yield of protein was approximately 50 mg.

Detergent exchange of purified protein was performed by chromatography on Source-Q resin (Pharmacia-LKB, Uppsala, Sweden), thereby replacing C_{12}DAO with C_{10}DAO. Bound protein was washed extensively with 50 mM ammonium acetate, pH 8.0, and 0.50 % C_{10}DAO buffer and then eluted in the same buffer with a gradient of NaCl up to 1 M. Salt was removed by dialysis of pooled fractions against 10 mM ammonium acetate (pH 8.0), and 0.50 % C_{10}DAO. FhuA was concentrated to 10-20 mg/mL by ultrafiltration (Centricon 30, Amicon, Massachusetts, USA), and dialyzed for three days against 100 mL of 10 mM ammonium acetate (pH 8.0) and 0.80 % C_{10}DAO.

Initial sparse matrix screening was performed using commercially available screening kits (Hampton Research, California, USA). Using 1.0 % C_{10}DAO as the primary detergent and protein concentrations in the range of 10-20 mg/mL, small hexagonal crystals formed over a 14-day period. The hanging drop vapor diffusion technique (McPherson, 1982) was used to optimize crystal growth at 18°C. By mixing 5 µL of protein with an equal volume of 13-16 % PEG 6,000, 100 mM sodium cacodylate (pH 6.4) and equilibrated with 1 mL of the reservoir solution, well-diffracting crystals of FhuA were obtained. Crystals grew in seven days to a final size of 750 x 750 x 300 µm.

FhuA crystals together with a column of mother liquor were mounted in glass capillaries. X-ray diffraction data were collected at room temperature using a STOE imaging plate detector. From a rotating anode generator operated at 40 kV and 100 mA, monochromatic CuKα (λ = 1.5418 Å) radiation was used to collect still photographs and native data sets. Reflections could be measured to 3.0 Å (Figure 1). Reflection intensity did not diminish during data collection, indicating limited crystal damage as the result of exposure to X-rays. Data reduction, space group assignment, and unit cell parameters were determined using the DENZO data processing software package (Otwinowski & Minor, 1997). FhuA crystals exhibited the symmetry of the primitive hexagonal lattice. Measured intensities and native Pattersons are consistent with the space groups $P6_1$ or $P6_5$, with refined unit cell parameters of $a = b = 173.5$ Å, $c = 88.1$ Å, and $\alpha = \beta = 90°$, $\gamma = 120°$. Given the molecular weight of FhuA (M_r 79,852) and assuming 1 molecule per asymmetric unit, the Matthews coefficient was calculated to be 4.82 Å^3/Da, with a

solvent content of 74.3 %. These data are in the range of calculated values for other membrane proteins. We now search for heavy atom derivatives to be used for multiple isomorphous replacement and solution of the crystal structure.

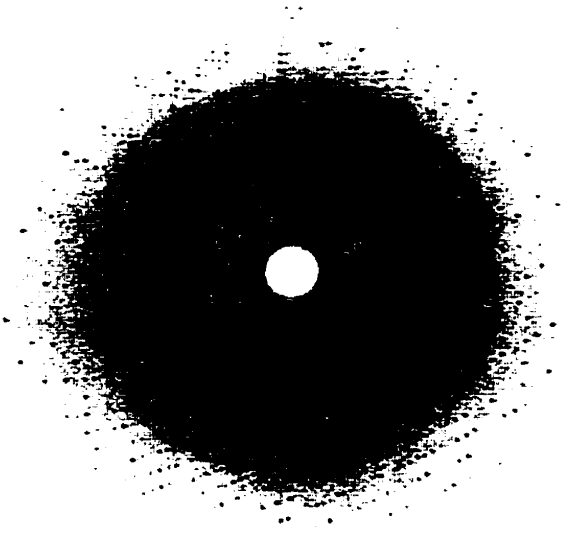

Figure 1. Still photograph of a FhuA crystal on a STOE image plate / rotating anode generator combination. The crystal-to-image plate distance is 159 mm. The detector edge corresponds to 3.0 Å resolution.

Acknowledgements

This work was supported by the Medical Research Council, Canada (MT-14133 to JWC), and by the Deutsche Forschungsgemeinschaft (to WW). Collaborative Research Grant 960082 for international travel was awarded to JWC and WW under the NATO Scientific Exchange Program. ADF is the recipient of a Deutscher Akademischer Austauschdienst Annual Grant for Study and Research. JB is an EMBO fellow (ALTF 751-1995). We thank Eckhard Hofmann for assistance with data collection, and Joannis Telioridis and Christine Peinelt for help with crystallization trials.

References

Arnold FH, Haymore BL. 1991. Engineering metal-binding proteins: Purification to protein folding. *Science 252*: 1796-1797.

Bonhivers M, Ghazi A, Boulanger P, Letellier L. 1996. FhuA, a transporter of the *Escherichia coli* outer membrane, is converted into a channel upon binding of bacteriophage T5. *EMBO J 15*: 1850-1856.

Bös C, Braun V. 1997. Specific *in vivo* thiol labeling of the FhuA outer membrane ferrichrome transport protein of *Escherichia coli* K-12: evidence for a disulfide bridge in the predicted gating loop. *FEMS Microbiol Lett 153*: 311-319.

Bös C, Lorenzen D, Braun V. 1998. Specific *in vivo* labeling of cell surface-exposed protein loops: Reactive cysteines in the predicted gating loop mark a ferrichrome binding site and a ligand-induced conformational change of the *Escherichia coli* FhuA protein. *J Bacteriol 180*: 605-613.

Braun V. 1997. Avoidance of iron toxicity through regulation of bacterial iron transport. *Biol Chem 378*: 779-786.

Coulton JW, Mason P, Cameron DR, Carmel G, Jean R, Rode HN. 1986. Protein fusions of β-galactosidase to the ferrichrome-iron receptor of *Escherichia coli* K-12. *J Bacteriol 165*: 181-192.

Cowan SW, Schirmer T, Rummel G, Steiert M, Ghosh R, Pauptit RA, Jansonius JN, Rosenbusch JP. 1992. Crystal structures explain functional properties of two *E. coli* porins. *Nature 358*: 727-733.

Diederichs K, Freigang J, Umhau S, Zeth K, Breed J. 1998. Prediction by a neural network of outer membrane β-strand protein topology. *Protein Sci 7*: 2413-2420.

Forst D, Welte W, Wacker T, Diederichs K. 1998. Structure of the sucrose-specific porin ScrY from *Salmonella typhimurium* and its complex with sucrose. *Nature Struct Biol 5*: 37-46.

Hantke K. 1981. Regulation of ferric iron transport in *Escherichia coli* K-12: isolation of a constitutive mutant. *Mol Gen Genet 182*: 288-292.

Jalal MAF, van der Helm D. 1989. Purification and crystallization of ferric enterobactin receptor protein, FepA, from the outer membranes of *Escherichia coli* UT5600/pBB2. *FEBS Lett 243*: 366-370.

Jiang X, Payne MA, Cao Z, Foster SB, Feix JB, Newton SMC, Klebba, PE. 1997. Ligand-specific opening of a gated porin channel in the outer membrane of living bacteria. *Science 276*: 1261-1264.

Killmann H, Benz R, Braun V. 1993. Conversion of the FhuA transport protein into a diffusion channel through the outer membrane of *Escherichia coli*. *EMBO J 12*: 3007-3016.

Killmann H, Videnov G, Jung G, Schwarz H, Braun V. 1995. Identification of receptor binding sites by competitive peptide mapping: Phages T1, T5, and ϕ80 and colicin M bind to the gating loop of FhuA. *J Bacteriol 177*: 694-698.

Koebnik R, Braun V. 1993. Insertion derivatives containing segments of up to 16 amino acids identify surface- and periplasm-exposed regions of the FhuA outer membrane receptor of *Escherichia coli* K-12. *J Bacteriol 175*: 826-839.

Liu J, Rutz JM, Feix JB, Klebba PE. 1993. Permeability properties of a large gated channel within the ferric enterobactin receptor, FepA. *Proc Natl Acad Sci USA 90*: 10653-10657.

Mademidis A, Killmann H, Kraas W, Flescher I, Jung G, Braun V. 1997. ATP-dependent ferric hydroxamate transport system in *Escherichia coli*: periplasmic FhuD interacts with a periplasmic and with a transmembrane/cytoplasmic region by competitive peptide mapping. *Mol Microbiol 26*: 1109-1123.

McPherson A. 1982. In: *Preparation and analysis of protein crystals*. New York, NY: Wiley & Sons Inc.

Moeck GS, Fazly Bazzaz BS, Gras MF, Ravi TS, Ratcliffe MJH, Coulton JW. 1994. Genetic insertion and exposure of a reporter epitope in the ferrichrome-iron receptor of *Escherichia coli* K-12. *J Bacteriol 176*: 4250-4259.

Moeck GS, Coulton JW. 1998. TonB-dependent iron acquisition: mechanisms of siderophore-mediated active transport. *Mol Microbiol 28*: 675-681.

Moeck GS, Coulton JW, Postle K. 1997. Cell envelope signaling in *Escherichia coli*. Ligand binding to the ferrichrome-iron receptor FhuA promotes interaction with the energy-transducing protein TonB. *J Biol Chem 272*: 28391-28397.

Moeck GS, Ratcliffe MJH, Coulton JW. 1995. Topological analysis of the *Escherichia coli* ferrichrome-iron receptor by using monoclonal antibodies. *J Bacteriol 177*: 6118-6125.

Moeck GS, Tawa P, Xiang H, Ismail AA, Turnbull JL, Coulton JW. 1996. Ligand-induced conformational change in the ferrichrome-iron receptor of *Escherichia coli* K-12. *Mol Microbiol 22*: 459-471.

Murphy CK, Kalve VI, Klebba PE. 1990. Surface topology of the *Escherichia coli* K-12 ferric enterobactin receptor. *J Bacteriol 172*: 2736-2746.

Nikaido H. 1996. Outer membrane. In: *Escherichia coli* and *Salmonella. Cellular and Molecular Biology*. Washington, DC: ASM Press. pp. 29-47.

Nikaido H, Saier MH. 1992. Transport proteins in bacteria: common themes in their design. *Science 258*: 936-942.

Otwinowski Z, Minor W. 1997. The HKL suite of programs. *Meth Enzymol 276*: 307-326.

Plançon L, Chami M, Letellier L. 1997. Reconstitution of FhuA, an *Escherichia coli* outer membrane protein, into liposomes. *J Biol Chem 272*: 16868-18872.

Postle K. 1993. TonB protein and energy transduction between membranes. *J. Bioenerg Biomembr 25*: 591-601.

Rutz JM, Liu J, Lyons JA, Goranson J, Armstrong SK, McIntosh MA, Feix JB, Klebba PE. 1992. Formation of a gated channel by a ligand-specific transport protein in the bacterial outer membrane. *Science 258*: 471-475.

Schirmer T, Keller TA, Wang YF, Rosenbusch JP. 1995. Structural basis for sugar translocation through maltoporin channels at 3.1 Å resolution. *Science 267*: 512-514.

Weiss MS, Abele U, Weckesser J, Welte W, Schiltz E, Schulz GE. 1991. Molecular architecture and electrostatic properties of a bacterial porin. *Science 254*: 1627-1630.

Preface to chapter three

The previous chapter described the identification of conditions for the growth of well-ordered crystals of FhuA. The focus of this chapter is a detergent-based additive termed *cis*-inositol: an amphipathic hexose sugar with a unilateral distribution of axial or equatorial hydroxyl groups. The use of chemical additives as agents to improve the quality of protein crystals is well established. By including *cis*-inositol in the crystallization buffer, crystal growth kinetics are altered such that, larger more regular FhuA crystals are obtained. Conversely, other detergent-based additives, including secondary detergents and small amphiphiles, had no effect. The resulting *cis*-inositol-mediated increase in crystal volume allowed X-ray diffraction data to be collected from FhuA crystals to a higher resolution than previously possible. While the precise mechanism by which *cis*-inositol influences crystal growth remains to be established, it may function as a 'molecular plaster': covering small apolar patches on solvent-exposed protein surfaces, increasing protein solubility and reducing nonspecific aggregation, thereby leading to the growth of higher quality protein crystals.

cis-inositol: an additive to improve crystal quality

Andrew D. Ferguson[ab], Kaspar Hergetschweiler[c], Bernd Morgenstern[c], Wolfram Welte[a], Jason Breed[a]

a Fakultät für Biologie, Universität Konstanz, M656, D-78457 Konstanz, Germany

b Department of Microbiology and Immunology, McGill University, 3775 University Street, Montreal, Quebec, Canada H3A 2B4

c Anorganische Chemie, Universität des Saarlandes, Postfach 151150, D-66041 Saarbrücken, Germany

Synopsis

cis-inositol has been utilised as a crystal growth additive for the crystallisation of both water-soluble and membrane proteins. Improvements in crystal quality have been observed and characterised.

Abstract

cis-inositol, an amphipathic cyclic hexitol with an unilateral distribution of axial or equatorial hydroxyl groups, improves crystal quality by increasing protein solubility. Applying *cis*-inositol as a crystal growth additive, large single crystals of hen egg white lysozyme were obtained from growth conditions that previously yielded clusters of small crystals. Furthermore, the observed diffraction limit of crystals of FhuA, a bacterial integral outer membrane protein, was extended from 2.7 to 2.5 Å resolution when *cis*-inositol was included in the crystallisation buffer.

Introduction

The growth of well-ordered crystals, as measured by their diffraction properties, is often the primary obstacle in the structural characterisation of proteins. As technologies for the sequencing of genes, protein expression and purification, and the crystallographic determination of protein structure become more automated, efficient crystallisation techniques will become increasingly more important. Many strategies (reviewed by McPherson, 1998) including extended post-crystallisation soaking (Fu *et al.*, 1999); crystal cryo-annealing (Harp *et al.*, 1998); manipulation of vapour diffusion kinetics (Chayen, 1997; Luft & DeTitta, 1997); and the inclusion of compatible solutes (cosmotropes) and cryoprotectants in the crystallisation buffer have been demonstrated to improve the stability and/or quality of a wide-range of protein crystals (Xiao & Gamblin, 1996; Jeruzalmi & Steitz, 1997; Sousa, 1997). The most common method used to improve crystal quality is the use of additives - compounds with specific properties at fixed, usually low, concentrations. Previous studies have shown a variety of substances, including neutral detergents (McPherson *et al.*, 1986) and non-detergent sulfobetaines (Vuillard *et al.*, 1996), to be useful in the crystallisation of both water-soluble and membrane proteins. Additional detergent-based additives termed small amphiphiles, have also been shown to have a positive effect on the internal crystal order of membrane proteins (Michel, 1983; Timmins *et al.*, 1991; Smith *et al.*, 1998). Biophysical investigations of their mode of action revealed that these substances intercalate into the detergent belt surrounding the hydrophobic surfaces of membrane proteins, thereby affecting detergent micelle size and packing (Timmins *et al.*, 1991; 1994).

cis-inositol is an amphipathic cyclic hexitol with an unilateral distribution of axial or equatorial hydroxyl groups which gives the compound its amphiphilic character (Angyal *et al.*, 1995). We have characterised the usefulness of this molecule as a crystal growth additive using a water-soluble and an integral membrane protein. Hen egg white (HEW) lysozyme is the standard model system for the study of protein crystallisation and thus was also used as a model water-soluble protein in this investigation. The protein FhuA, an integral outer membrane receptor from *E. coli* K-12 (Ferguson *et al.*, 1998*a*; 1998*b*) was used as the representative membrane protein. The addition of *cis*-inositol to the

crystallisation buffer leads to improvements in crystal quality and increased protein solubility for both proteins.

Materials and methods

Protein purification and materials

HEW lysozyme was purchased from Sigma and used without further purification. Reagents used in the crystallisation of HEW lysozyme were purchased from Sigma and were of the highest available grade. FhuA was expressed and purified as previously described (Ferguson *et al.*, 1998a; 1998b). *cis*-inositol was synthesised as previously reported (Angyal *et al.*, 1995). Chemicals used in the crystallisation of FhuA including N,N-dimethyldecylamine-N-oxide (DDAO), sodium cacodylate, polyethylene glycol (PEG) monomethyl ether (MME) 2000 and PEG 200 were purchased from Fluka and Merck.

Solubility, crystallisation and data collection

Protein solubility experiments were conducted using the vapour diffusion technique at 18°C. With HEW lysozyme, 10 µl sitting drops containing 20 mg ml^{-1} of protein, 100 mM sodium acetate (pH 4.6) and sodium chloride (NaCl) were equilibrated against a 500 µl reservoir. In the case of FhuA, 6.5 mg ml^{-1} of protein was suspended in 6 µl hanging drops of 0.8 % DDAO, 10 mM ammonium acetate, 100 mM sodium cacodylate (pH 6.4), 20 % glycerol, 3 % PEG 200, and PEG 2,000 MME. The drops were equilibrated against 1 ml of reservoir solution [100 mM sodium cacodylate (pH 6.4), 20 % glycerol, 3 % PEG 200, and PEG 2,000 MME]. For both proteins, the initial precipitant concentrations [(0.3 to 0.6 M NaCl) and (8 to 14 % PEG 2,000 MME)] were set at 50 % of that found in the reservoir.

Crystallisation experiments to assess crystal quality were also carried out using the hanging drop vapour-diffusion technique at 18°C. HEW lysozyme crystals were grown from drops consisting of equal volumes (4.5 µl) of protein [50 mg ml^{-1} HEW lysozyme in 10 mM sodium acetate (pH 4.6)] and reservoir solution [0.5 M NaCl and 10 mM sodium acetate (pH 4.6)] suspended over a 500 µl reservoir. Crystals of FhuA were grown from

drops that contained 4.5 µl of protein [6.5 mg ml^{-1} of FhuA in 0.8 % DDAO and 10 mM ammonium acetate (pH 8.0)] and 4.5 µl of reservoir solution [11 % PEG 2000 MME, 0.1 M sodium cacodylate (pH 6.4), 20 % glycerol, and 3 % PEG 200]. The drops were suspended over 1 ml of reservoir solution. For both preparations either 1 µl of *cis*-inositol (10 % w/v) or 1 µl of sterile water was included in twenty-four test and control drops produced under identical conditions. All drops were monitored every six hours for the first twenty-four hours following their initial set up and then every twenty-four hours for a period of seven days. All FhuA crystals grown in the absence and presence of *cis*-inositol were flash-frozen in liquid nitrogen. Diffraction data was collected from these crystals at 100 K using synchrotron radiation [European Radiation Synchrotron Facility (Grenoble, France), and Max Lab-II (Lund, Sweden)].

Results

Assessment of crystal quality

HEW lysozyme crystals were observed in all control and test drops. However, significant differences between the groups were observed (Fig. 1, A and B). HEW lysozyme crystals were observed in the control drops within six hours compared to twelve hours for the test drops. The mean number of crystals observed per drop obtained after seven days were lower in those drops containing 1 % *cis*-inositol (1.8 ± 1.0) *versus* (4.7 ± 1.7) for the control drops. In addition, the mean crystal volume also increased in the additive-containing drops (0.0627 ± 0.0077 mm^3) compared to those drops with water only (0.0422 ± 0.0112 mm^3). Clusters and showers of small crystals that were often observed in the absence of *cis*-inositol did not occur in any of the drops containing this additive.

Representative FhuA crystals grown with and without *cis*-inositol are shown in Fig. 1, C and D, respectively. The irregular leaf-like crystals obtained in the absence of *cis*-inositol reach their maximum size (100 x 100 x 30 µm) within twenty-four hours. These crystal growth conditions could not be further optimised for crystal morphology, number and volume. Crystals grown in the presence of 1 % *cis*-inositol attained their maximum size (350 x 350 x 200 µm) within five days. These crystals exhibited a more regular

hexagonal crystal appearance, with well-defined crystal edges and faces. The resulting increase in crystal volume resulted in improved diffraction properties. Specifically, the maximum resolution limit of diffraction data collected from flash-frozen FhuA crystals was extended from 2.7 to 2.5 Å resolution (Ferguson *et al.*, 1998b). However, no clear improvements in the crystallographic statistics as judged by Wilson Plot analysis and crystal mosaicity were identified by comparison of data sets collected from test and control crystals.

Protein solubility

For both HEW lysozyme and FhuA, higher concentrations of precipitant (NaCl and PEG 2,000 MME) were required to obtain crystals in the presence of *cis*-inositol than in its absence (Table 1). For HEW lysozyme, the presence of 3 % of this additive in the drop doubled the concentration of NaCl required to initiate crystal growth. For FhuA, the presence of 1 or 2 % *cis*-inositol significantly increased the required PEG 2,000 MME concentrations (Table 1) for crystallisation.

Discussion

Proteins either precipitate or crystallise from aqueous solution under conditions of reduced solubility, induced by the presence of high concentrations of precipitants. Solubility is the result of many complex protein-solvent and protein-protein interactions that are affected by a diverse range of environmental parameters. One important contribution to protein solubility is the nature of the solvent-exposed protein surface. Apolar protein surface patches form unfavourable interactions with solvent molecules and strong hydrophobic interactions with one another when dehydrated by precipitant, which favours aggregation over crystallisation. In addition, these surface patches reduce protein solubility such that poorly defined solubility limits and a decreased nucleation barrier may give rise to microcrystals or microcrystalline precipitant. Indeed, exchanging surface-exposed hydrophobic residues for polar residues has lead to improvements in crystal quality in a number of cases (Pautsch *et al.*, 1999).

cis-inositol may modulate crystal growth by increasing the viscosity of the hanging drop and thus slowing crystallisation kinetics. To test this proposal crystallisation experiments of HEW lysozyme and FhuA were conducted using glucose, assuming that glucose and *cis*-inositol have similar effects on drop viscosity. The crystals obtained were similar to those of the water control experiments with crystal clusters and occasional crystal showers being observed with HEW lysozyme and irregular leaf-like crystals of FhuA (data not shown). However, a small decrease in mean crystal number and a small increase in mean crystal volume in comparison to the water control experiments were observed with HEW lysozyme. With membrane proteins, *cis*-inositol may function as a classical small amphiphile and function by altering the size and packing arrangement of detergent micelles within the growing crystal. Crystallisation experiments conducted with FhuA and the small amphiphiles dimethylhexylamine-N-oxide and heptane-1,2,3-triol (high-melting-point isomer), failed to show any positive effect on mean crystal number and volume, although modest improvements in crystal morphology were observed (data not shown).

Substances that cover hydrophobic surfaces to form a more uniform hydrophilic protein surface might also be expected to have beneficial effects on protein solubility and crystallisation, as observed with the neutral detergent β-octylglucoside (McPherson *et al.*, 1986). We therefore propose that *cis*-inositol may function as a 'molecular plaster' that covers small hydrophobic patches on the protein surface with its hydrophobic face while presenting its hydrophilic face to the aqueous medium. Thus, the entropic cost of displacing bound water molecules is reduced and the effective hydrophilic surface of the protein is increased, thereby increasing protein solubility. This mechanism is probably dependent upon weak binding of *cis*-inositol to particular sites located on surface-exposed portions of the protein. Considering the weakness and transience of such interactions, it is unlikely that electron density corresponding to individual *cis*-inositol molecules could be identified. This proposal is in accord with the observation that, following an extensive search of the FhuA data, no electron density could be unambiguously assigned to any *cis*-inositol molecule. In the light of the successful elucidation of membrane protein - detergent interfaces by neutron diffraction (Penel *et*

al., 1998) it may be possible that *cis*-inositol - FhuA interactions might be characterised using this technique.

In these experiments, *cis*-inositol proved effective as an additive for improved crystal properties (increased mean crystal size, improved crystal morphology, reduced crystal clustering, extended resolution limit) and increased protein solubility. These data were obtained from water-soluble and membrane proteins using representatives of the two most commonly used types of precipitant (PEG and high ionic strength). Although the positive effects of *cis*-inositol on protein solubility and crystallisation are clear for HEW lysozyme and FhuA, the question whether or not this additive will prove beneficial for the crystallisation of other proteins remains to be determined. The general applicability of this compound as a crystal growth additive will be established by its wider application within the community of protein crystallographers and crystal growers.

Table 1. Minimum concentrations of precipitant required for crystal formation in the presence and absence of *cis*-inositol.

	Lysozyme	**FhuA**
***cis*-inositol (w/v)**	**NaCl**	**PEG 2,000 MME**
0 %	0.3 M	8 %
1 %	0.4 M	10 %
2 %	0.5 M	11 %
3 %	0.6 M	14 %

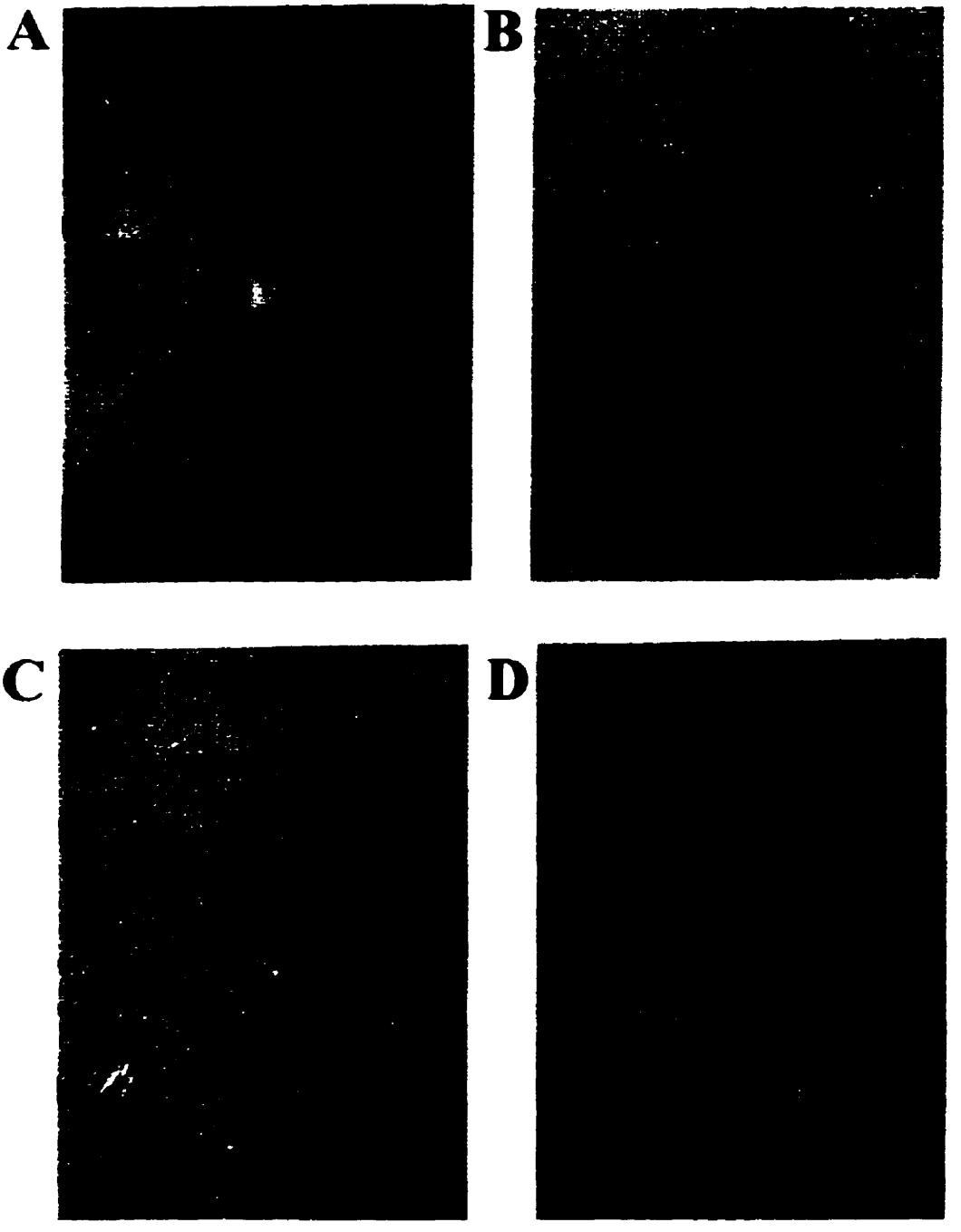

Figure 1. Representative protein crystals. **(A)** HEW lysozyme crystals grown in the absence and **(B)** presence of 1 % *cis*-inositol. **(C)** FhuA crystals grown in the absence and **(D)** presence of 1 % *cis*-inositol.

Acknowledgements

We gratefully acknowledge A. Svensson at Max-Lab II, and A. Thompson at the ERSF for their assistance and generous support during data collection. This work was supported by the Deutsche Forschungsgemeinschaft and the project 'Biologically Composed Materials and Systems (BKMS)' of the Ministerium für Bildung, Kultur und Wissenschaft des Saarlandes. A.D.F. is the recipient of a Deutscher Akademischer Austauschdienst Grant for Study and Research and a Medical Research Council of Canada Doctoral Research Award.

References

Angyal, S.J., Odier, L. & Tate, M.E. (1995). *Carbohydr. Res.* **266**, 143-146.

Chayen, N.E. (1997). *J. Appl. Cryst.* **30**, 198-202.

Ferguson, A.D., Breed, J., Diederichs, K., Welte, W. & Coulton, J.W. (1998*a*). *Prot. Sci.* **7**, 1636-1638.

Ferguson, A.D., Hofmann, E., Coulton, J.W., Diederichs, K. & Welte, W. (1998*b*). *Science* **282**, 2215-2220.

Fu, Z-Q., Du Bois, G.C., Song, S.P., Harrison, R.W. & Weber, I.T. (1999). *Acta Cryst. D* **55**, 5-7.

Garman, E.F. & Schneider, T.R. (1997). *J. Appl. Cryst.* **30**, 211-237.

Harp, J.M., Timm, D.E. & Bunick, G.J. (1998). *Acta Cryst. D* **54**, 622-628.

Jeruzalmi, D. & Steitz, T.A. (1997). *J. Mol. Biol.* **274**, 748-756.

Luft, J.R. & DeTitta, G.T. (1997). *Meth. Enzymol.* **276**, 110-130.

McPherson, A., Koszelak, S., Axelrod, H., Day, J., Robinson, L., McGrath, M., Williams, R. & Cascio, D. (1986). *J. Cryst. Growth* **76**, 547-553.

McPherson, A. (1998). *Crystallization of Biological Macromolecules*. Cold Spring Harbor Laboratory Press.

Michel, H. (1983). *Trends Biochem. Sci.* **8**, 56-59.

Penel, S., Pebay-Peyroula, E., Rosenbusch, J., Rummel, G., Schirmer, T. & Timmins, P.A. (1998). *Biochemie* **80**, 543-551.

Smith, B., Kobe, B., Kurumbail, R., Buchanan, S., Venkatramani, L., van der Helm, D. & Deisenhofer, J. (1998). *Acta Cryst D* **54**, 697-699.

Sousa, R. (1997). *Meth. Enzymol.* **276**, 131-143.

Timmins, P.A., Hauk, J., Wacker, T. & Welte, W. (1991). *FEBS Letts.* **280**, 115-120.

Timmins, P.A., Pebay-Peyroula, E. & Welte, W. (1994). *Biophys. Chem.* **53**, 27-36.

Vuillard, L., Baalbaki, B., Lehmann, M., Nørager, S., Legrand, P. & Roth, M. (1996). *J. Cryst. Growth* **168**, 150-154.

Xiao, B. & Gamblin, S.J. (1996). *J. Cryst. Growth* **168**, 244-247.

Preface to chapter four

The identification and optimization of crystallization parameters for the growth of well-ordered FhuA crystals culminated with this study. The focus of this chapter is the solution of the three-dimensional structure of FhuA in two conformations, with and without ferricrocin, at resolutions of 2.7 Å and 2.5 Å, respectively. One method of crystallographic phase determination is multiwavelength anomalous dispersion phasing, a technique dependent upon the measurement of the anomalous signal of intrinsic scatterers, such as selenium. Protein crystals can be specifically labelled with anomalous scatterers using pre-translational or post-translational techniques. Pre-translational labelling exploits the inability of bacterial methionyl tRNA synthetase to distinguish between selenomethionine and methionine during translation. A methionine-requiring *E. coli* K-12 strain expressing the hexahistidine tagged FhuA protein was grown in the presence of selenomethionine. The resulting selenomethionine derivative of FhuA was purified under reducing conditions, and crystallized using established crystal growth parameters. X-ray diffraction data were collected, experimental phases determined and molecular models for unliganded FhuA and its liganded complex established. FhuA is a β-barrel composed of 22 antiparallel β-strands. Located within the β-barrel is a structurally distinct domain, the 'cork', which consists of a four-stranded β-sheet and four short α-helices. Upon binding of the siderophore, conformational changes are propagated from the extracellular pocket to the periplasmic pocket of FhuA, a transmembrane signal indicating the liganded status of the receptor. Structural analysis combined with sequence homologies and mutagenesis data were used to propose a structure-based mechanism for TonB-dependent siderophore-mediated iron acquisition. These results are significant because they represent the first crystallographic structure of this unique class of active outer membrane transporters, the TonB-dependent receptors. Furthermore, the FhuA structure forced reconsideration of all previous structural and functional models for TonB-dependent receptors, and provided novel insights into the active transport mechanisms of the bacterial outer membrane.

Siderophore-mediated iron transport: Crystal structure of FhuA with bound lipopolysaccharide

Andrew D. Ferguson*†, Eckhard Hofmann†, James W. Coulton*, Kay Diederichs†, Wolfram Welte†

* Department of Microbiology and Immunology, McGill University, 3775 University Street, Montreal, Quebec, Canada H3A 2B4

† Fakultät für Biologie, Universität Konstanz, M656, D-78457 Konstanz, Germany

Abstract

FhuA, receptor for ferrichrome-iron in *Escherichia coli*, is a member of a family of integral outer membrane proteins, which, together with the energy transducing protein TonB, mediate active transport of ferric siderophores across the outer membrane of Gram-negative bacteria. The three-dimensional structure of FhuA is presented here in two conformations: with and without ferrichrome-iron at resolutions of 2.7 and 2.5 angstroms, respectively. FhuA is a β-barrel composed of 22 antiparallel β-strands. In contrast to the typical trimeric arrangement found in porins, FhuA is monomeric. Located within the β-barrel is a structurally distinct domain, the "cork", which mainly consists of a four-stranded β-sheet and four short α-helices. A single lipopolysaccharide molecule is noncovalently associated with the membrane-embedded region of the protein. Upon binding of ferrichrome-iron, conformational changes are transduced to the periplasmic pocket of FhuA, signaling the ligand-loaded status of the receptor. Sequence homologies and mutagenesis data are used to propose a structural mechanism for TonB-dependent siderophore-mediated transport across the outer membrane.

Introduction

Iron is universally required for all living cells. However, in aerobic environments, iron is found as highly insoluble ferric hydroxide complexes, which are forms that severely limits the bioavailability of iron (*1*). To acquire iron, microorganisms synthesize and secrete siderophores, compounds that chelate ferric iron and thereby form soluble iron complexes. In Gram-negative bacteria, all essential ions and nutrients are transported across the cell envelope in discrete steps. Transport across the cytoplasmic membrane is an energy-dependent high-affinity process, whereas transport across the outer membrane is primarily mediated by passive diffusion through nonspecific or substrate-specific porins (*2*). Because siderophore-iron complexes are found at exceedingly low concentrations in the external media, their rate of passive diffusion across the outer membrane is insufficient for supporting requirements of cellular growth. Therefore, a class of high-affinity siderophore receptors exists within the outer membrane. They bind specific iron-siderophores and promote their active transport into the periplasm, exploiting the electrochemical potential of the cytoplasmic membrane that is transduced to the outer membrane by the TonB-ExbB-ExbD complex. All TonB-dependent receptors possess a short sequence of residues at the NH_2-terminus, which is termed the TonB box (*1,3*). It has been proposed that this region functions as a mediator of the physical interaction between TonB and TonB-dependent receptors. TonB spans the periplasmic space and physically interacts with siderophore receptors, resulting in energy transduction by a mechanism that is common to all TonB-dependent receptors (*3*).

FhuA in the outer membrane of *Escherichia coli* (*4*) is the receptor for ferrichrome-iron. In addition to binding ferrichrome-iron, FhuA also functions as the primary receptor for the structurally related antibiotic albomycin, for several bacteriophages (T1, T5, UC-1, and ϕ80), for the peptide antibiotic microcin 25, and for the bacterial toxin colicin M. Because the deletion of a surface-located linear sequence converted FhuA from an energy-dependent receptor into a general diffusion channel, it was concluded that FhuA (*5*) and other TonB-dependent receptors (*6*) act as ligand-specific gated porins. When wild-type FhuA was incorporated into an artificial lipid bilayer, it did not form channels. However, the addition of bacteriophage T5 resulted in the formation of stable,

high-conductance ion channels, which were electrically similar but not identical to those observed with channel-forming mutants of FhuA (*7*).

Results and discussion

General description

The X-ray structure (Table 1) of FhuA is composed of a COOH-terminal β-barrel domain (residues 161 to 723) and an NH_2-terminal cork domain (residues 1 to 160), which fills the barrel interior (Fig. 1, A and B). According to a search through a database of protein structures (*8*), the fold of the cork domain has not been observed. In contrast to the typical trimeric arrangement found in porins, FhuA is monomeric. The barrel is formed by 22 antiparallel transmembrane β-strands (β1 through β22). Loops connect adjacent strands; there are short periplasmic turns (T1 through T10) and longer surface-located loops (L1 through L11) (Fig. 1A). The FhuA barrel is larger than any barrel formed by the porins - it is 69 Å in height and has an elliptical cross-section of 46 by 39 Å (Fig. 1, A and B). In common with other membrane proteins, two girdles of aromatic residues mark the boundary of an apolar cylindrical zone on the barrel surface (Fig. 1A). They are positioned to extend into the lipid bilayer and delineate the border between the lipid hydrocarbon chains and the polar head groups. The distance (34 Å) from the upper aromatic girdle to the apex of L4 and the distance to the apices of other surface-located loops of FhuA are significantly larger compared to the equivalent distance in the known crystallographic structures of porins (Fig. 1A). This feature may facilitate the use of these loops for the attachment of FhuA-specific bacteriophages. Porins, which have much shorter surface-located loops, also function as receptors for bacteriophages (*2*).

The single lipopolysaccharide (LPS) molecule that is noncovalently associated with the membrane-embedded outer surface of FhuA exhibits the expected chemical structure for *E. coli* K-12 LPS (*9*). Specifically, lipid A is composed of two linked phosphorylated glucosamines and six fatty acid chains, the inner core possesses two octose and two heptose residues, and the outer core contains three hexose residues. The LPS molecule is positioned such that the glucosamine moieties are placed slightly above the upper aromatic girdle. Five of the six alkyl chains are closely apposed with the barrel surface

and are parallel to the barrel axis, as expected for the chains of the external LPS monolayer (Fig. 1A) (*10*).

The cork domain, consisting mainly of a mixed four-stranded β-sheet (βA through βD), extends from the periplasm to the ferrichrome-iron binding site (Fig. 1A). The electron density permits tracing of the cork domain beginning at Glu^{19}. The cork domain is arranged in the barrel with the β-sheet plane inclined by ~45° to the membrane normal, so that it sterically occludes most of the cross-section of the barrel (Fig. 1, A and B). The presence of the cork domain suggests that the direct passage of ferrichrome-iron and small molecules through FhuA is not possible. This agrees with the finding that FhuA that has been reconstituted into planar lipid bilayers shows no channel conductance (*5, 7*). The cork domain is connected to the barrel wall by extensive hydrogen bonding. The number of hydrogen bonds observed in the FhuA-ferrichrome-iron complex is slightly reduced in comparison with FhuA in the absence of ligand. Given the large buried surface area (5,000 $Å^2$) between the inner barrel wall and the cork domain, we consider it unlikely that the entire cork domain detaches for ferrichrome-iron transport, for channel formation, or as a result of an interaction with TonB.

The cork domain delineates a pair of pockets within FhuA. The larger external pocket is open to the external environment and is restricted by barrel strands, surface-located loops, and cork domain apices A, B, and C (Fig. 1, A and B). The boundaries of the smaller periplasmic pocket are the barrel, cork domain loops, and the four-stranded β-sheet (Fig. 1A).

The ferrichrome-iron binding site and the external pocket

Located in the external pocket of the FhuA-ferrichrome-iron complex is a single ferrichrome-iron molecule. The binding site for ferrichrome-iron is situated slightly above the external outer membrane interface (Fig. 1, A and B). Residues from apices A, B, and C of the cork domain and the barrel domain make direct hydrogen bonds or are in van der Waals contact with ferrichrome-iron atoms (Fig. 2). These residues are strongly conserved as assigned by sequence alignment of ferrichrome-iron receptors from *E. coli*, *Pantoea agglomerans*, *Salmonella paratyphi* strain B, and *Salmonella typhimurium* (*11, 12*). Moreover, two water molecules have been identified in the binding site for

ferrichrome-iron and may mediate the formation of additional hydrogen bonds between the ligand and FhuA (Fig. 3). Thus, the ferrichrome-iron binding site is coated with a tailored and complementary pattern of residues that tightly bind the ligand (K_D, 0.2 μM) (*1,13*). The deletion of residues 236 to 248 from L3 resulted in the loss of ferrichrome-iron uptake (*12*), a result in accord with the composition of the binding site. Although none of the residues within L4 (residues 318 to 339) contribute directly to the high-affinity binding of ferrichrome-iron, the conformation of this loop is critical for targeting of the ligand to its binding site (Fig. 1, A and B) (*14*). The inner walls of the external pocket, surface-located loops, and barrel strands from the ferrichrome-iron binding site to the external opening are lined by numerous aromatic residues (*15*). Ferrichrome-iron interacts favourably with aromatic residues, because it can be extracted from fungal extracts with benzoyl alcohol (*16*). Hydroxamate-type siderophores such as ferrichrome are uncharged at physiological pH and are not inherently hydrophobic. We propose that the interaction of aromatic residues with ferrichrome-iron involves electrostatic interactions between the quadropole moment of the π electron system (*17*) and the dipoles of surface-located peptide bonds. Accordingly, the aromatic residues lining the inner walls of the external pocket function to extract ferrichrome-iron from the external medium; those found in the ferrichrome-iron binding site contribute to the high-affinity binding of ferrichrome-iron.

Ferrichrome-iron induced conformational changes and transmembrane signaling

Comparing the structure of FhuA to its complex with ferrichrome-iron reveals two distinct conformations: the ligand-free and ligand-loaded conformation. In the barrel domain, the coordinates of the backbone atoms of FhuA and its complex with ferrichrome-iron are very similar (root mean square deviation, 0.42 Å), except for minor differences in the periplasmic turns T8 and T9 (Fig. 4). Key differences between the structures are localized in the cork domain. In the ferrichrome-iron binding site, an induced fit mechanism is observed. Apex B (residues 98 to 100) is translated 1.7 Å upward toward ferrichrome-iron, resulting in the formation of multiple hydrogen bonds with the ligand. All loops of the cork domain between apex A and the periplasmic pocket

follow this translation. The four-stranded β-sheet and the loops of the cork domain situated below apex C and the periplasmic pocket remain stationary (Fig. 4).

As a dramatic exception to the otherwise overall conservation of FhuA's secondary structure upon ferrichrome-iron binding, a helix [termed the switch helix (residues 24 to 29)] that is located in the periplasmic pocket in the ligand-free conformation is completely unwound in the FhuA-ferrichrome-iron complex (Figs. 4 and 5B). The switch helix contains a number of inherently hydrophobic residues, and in the ligand-free conformation, it fits into a complementary hydrophobic pocket that is formed by select residues from T8, T9, and βA. Upon ferrichrome-iron binding, the upward translation of selected loops of the cork domain disrupts the interaction of this pocket with the hydrophobic face of the switch helix, thus promoting its destabilization. The stabilization of helices in short peptides due to interactions with hydrophobic side chains has been observed and theoretically discussed (*18*). All residues from Arg^{31} to the NH_2-terminal (Glu^{19}) assume an extended conformation, bending ~180° in the opposite direction of the former helix axis. Glu^{19} is placed near Arg^{128} from βD, in the center of the periplasmic pocket, 17.3 Å away from its former α-carbon position (Figs. 4 and 5B) (*19*). All residues from Glu^{19} to the NH_2-terminus, including the TonB box (residues 7 to 11), are disordered in both the FhuA and the FhuA-ferrichrome-iron structures. As a result of this helix-coil transition, Trp^{22} occludes the periplasmic end of the putative channel-forming region, and the location of the TonB box in the ligand-bound conformation is changed (Fig. 5B) (*20*).

These observed allosteric transitions are in agreement with previous antibody recognition studies. All monoclonal antibodies that were bound to sequences between residues 21 to 59 discriminated between ligand-free and ligand-loaded FhuA (*21*). The incubation of purified FhuA with ferrichrome-iron, colicin M, and (to a lesser extent) ϕ80 increased the relative amount of the FhuA-TonB complex that was cross-linked as compared to the amount of FhuA-TonB complex that was cross-linked in the absence of ligand (*22*). The ability of these TonB-dependent FhuA-specific ligands to promote the physical interaction between FhuA and TonB suggests that allosteric transitions observed in the cork domain of the FhuA-ferrichrome-iron complex may be similar (notably, the unwinding of the switch helix). The unwinding of the switch helix is a clear

periplasmically disposed conformational change, which signals the ligand-loaded status of the receptor and therefore the need for TonB-dependent energy transduction. Considering that siderophore receptors must compete for a limited amount of TonB (*23*), efficient signal transduction across the cell envelope to indicate the occupancy of the receptor is essential for the physiology of the bacterial cell (*24*).

A mechanism of ferrichrome-iron transport

A model for the transport of siderophores by TonB-dependent receptors is necessarily subject to constraints imposed by structural data, studies of ligand binding, phenotypes of genetic mutants, and residue conservation among different FhuAs. We propose the following basic model. After the initial physical interaction between ferrichrome-iron and the surface-located loops of FhuA, the ligand is partitioned from the external medium into the external pocket by its affinity for aromatic residues. It is then bound with high affinity by an induced fit mechanism, resulting in an allosteric transition. Subsequent transport of ferrichrome-iron to the periplasm is dependent upon the disruption of the binding site. We propose that formation of the FhuA-TonB complex and the subsequent energy transduction induces a further allosteric transition to reduce the stability of the ferrichrome-iron binding site. A disruption of the induced fit binding mechanism may be effected by a small shift of apices A, B, and C toward the periplasm as a consequence of energy being transduced by TonB.

When viewed along the barrel axis, the external pocket is connected to the periplasmic pocket in one segment of the barrel cross section by a narrow water-filled channel. We designate this segment as the putative channel-forming region (Fig. 5A). Located directly below apex B is a short coil containing the strongly conserved residues Leu^{106}, Asn^{107}, and Gly^{108} (*12*). Subtle conformational changes of this and other loops of the cork domain between apex B and the periplasmic pocket of FhuA would suffice to allow the permeation of ferrichrome-iron through the putative channel-forming region (Figs. 4 and 5A). We therefore propose that, following the formation of the FhuA-TonB complex, a channel opens in this region by the rearrangement of loops of the cork domain.

Among TonB-dependent receptors, there are few regions of strict sequence conservation. However, sequence alignments of FhuA proteins identify a series of strongly conserved residues (*25*) that are positioned on the inner barrel wall of the putative channel-forming region. These residues coat an extended inner barrel surface from the ferrichrome-iron binding site to the periplasmic pocket of FhuA (Fig. 5A). The arrangement of these residues may function as a series of low-affinity binding sites for the surface diffusion of ferrichrome-iron through FhuA. The weak adsorption of ferrichrome-iron to the inner barrel wall could mediate both the rapid diffusion (*26*) of the ligand inside the putative channel-forming region and, by its binding, confinement to this region.

This proposal is supported by previous studies involving channel forming deletion mutants of FhuA. The excision of some surface-located linear sequences from TonB-dependent siderophore receptors resulted in the formation of nonspecific open diffusion channels. Specifically, deletion of residues 322 to 355 (residues from β7, L4, and β8) and 335 to 355 (residues from L4 and β8) from FhuA abolished TonB-dependent ferrichrome-iron transport while permitting the nonspecific diffusion of ferrichrome-iron, sodium dodecyl sulfate, and maltodextrins across the outer membrane (*5,27,28*). Small fluctuations in the conductance patterns of channel-forming FhuAs were observed; they were different from those of porins and possibly resulted from changes in the cross-sectional diameter of the channel. The binding of bacteriophage T5 to FhuA induced similar channels (*7*). Considering the structure, the removal of residues 340 to 355 from β8 would disrupt critical connections between the barrel wall and apex C of the cork domain, resulting in a higher degree of conformational flexibility of the coil segments around apices B and C and of more remote regions of the cork domain. The result may be the transient opening and closing of an aqueous channel (Fig. 5A). The location and structure of the channel may be similar to that formed in vivo by the FhuA-TonB complex. This suggestion is supported by planar lipid bilayer experiments involving the FhuA-bacteriophage T5 complex. The addition of ferrichrome-iron to either chamber of the bilayer apparatus resulted in a reduction in channel conductance; ferrichrome-iron may have bound to a distorted binding site (*7*).

We postulate that ferrichrome-iron is liberated from its high-affinity binding site and diffuses to the periplasm through a channel similar in structure and size to that induced by the binding of bacteriophage T5. This surface diffusion model resembles that postulated for the permeation of sugars through the glycoporins (*29*). When ferrichrome-iron reaches the periplasmic pocket of FhuA, it is bound by the high-affinity periplasmic binding protein FhuD (K_D, 0.1 μM) (*1,30*), thereby ensuring unidirectional transport across the cell envelope (*31*). We further postulate that other TonB-dependent siderophore receptors undergo similar ligand-induced allosteric transitions, transport their cognate siderophore through channels by surface diffusion, and therefore utilize a common siderophore-mediated iron transport mechanism.

This proposed mechanism suggests an explanation for the evolution of high-affinity receptors for different siderophore-iron complexes by Gram-negative bacteria. Only the external aromatic pocket and the high-affinity binding site must be tailored to different ligands. Ligand-induced allosteric transitions and transport are common mechanistic features and essentially receptor independent. The inherent flexibility of this design is advantageous in adapting siderophore receptors such as FhuA for the fungal siderophore ferrichrome (which is an obvious advantage, given variations in iron supply for bacteria). Moreover, the correlation between bacterial virulence in vivo and the expression of high-affinity TonB-dependent iron acquisition systems, including receptors for transferrin, lactoferrin, heme, and ferric siderophores (*1,32*), indicates adaptations that allow bacteria to survive in the interstitial spaces and the bloodstream of host organisms. The high affinity and specificity of TonB-dependent siderophore receptors make them ideal targets for the design of novel antibacterial agents such as siderophore-antibiotic conjugates (*33*). The principle relies on the specific recognition of the outer membrane receptor by the siderophore moiety, thereby ensuring transport of the conjugate through the receptor and into the periplasm of the bacterial cell.

Table 1. Crystallographic data. FhuA and SeMet-FhuA were purified by immobilized ligand affinity chromatography using 0.05 % dimethyldodecylamine-*N*-oxide and exchanged into 0.8 % dimethyldecylamine-*N*-oxide (*35*). For SeMet-FhuA, 2.5 mM reduced glutathione was added to all buffers. Crystals of FhuA and SeMet-FhuA were grown using the hanging drop vapor diffusion technique by mixing 5 µl of protein at 6.5 mg/ml with an equal volume of reservoir solution [0.1 M sodium cacodylate (pH 6.4), 11 % polyethylene glycol (PEG), 2,000 monmethyl ether (MME), 20 % glycerol, 3 % PEG 200, 0.8 % dimethyldecylamine-*N*-oxide, and 1 % *cis*-inositol] (*36*). FhuA and SeMet-FhuA in complex with ferrichrome-iron (Fc) were crystallized under similar conditions. All crystals grew within 7 days to a final size of 350 by 350 by 350 μm^3 at 18°C. They belonged to the primitive hexagonal space group $P6_1$ ($a = b = 171.4$ Å; $c = 85.7$ Å), with one molecule per asymmetric unit, a Matthews coefficient of 4.82 $Å^3$/dalton, and a solvent content of 74.3 %. Native data were collected at 100 K from flash-frozen crystals of FhuA and SeMet-FhuA complexed with Fc to resolutions of 2.5 Å and 2.7 Å, respectively. MAD data were collected from a SeMet-FhuA-Fc complex crystal to a resolution of 3.05 Å, allowing the structure to be solved. For details of structure solution and refinement, see (*37*). Parentheses denote the highest shell. Phasing power is the mean value of heavy-atom structure factor amplitude divided by lack of closure. $R_{sym} = \Sigma_{hkl} \Sigma_i | I_{hkl} - \{I_{hkl}\} | / \Sigma_{hkl} \Sigma_i I_{hkl}$, where $\{I_{hkl}\}$ is the average of symmetry-related I_{hkl}.

			MAD		
Diffraction data	FhuA	SeMet-FhuA-Fc complex	Remote	Point of inflection	Peak
Wavelength (Å)	1.051	1.051	0.8876	0.9782	0.9779
Resolution (Å)	2.45 (2.45-2.50)	2.70 (2.70-2.80)	3.05 (3.05-3.10)	3.05 (3.05-3.10)	3.05 (3.05-3.10)
Unique reflections	53,749 (2,931)	39,633 (4,038)	26,521 (1,268)	27,448 (1,282)	27,233 (1,268)
Completeness (%)	99.3 (92.2)	98.9 (98.0)	96.6 (99.3)	99.5 (98.9)	98.8 (97.8)
Redundancy	6.4 (3.1)	5.9 (3.7)	8.4 (6.8)	6.4 (2.8)	5.2 (2.3)
R_{sym} (%)	7.8 (33.4)	7.9 (40.6)	14.6 (67.8)	11.0 (46.8)	11.4 (42.0)
Phasing power (acentric)					
Dispersive	-	-	2.27	0	1.85
Anomalous	-	-	1.43	1.45	1.75
Figure of merit			-	0.45	-

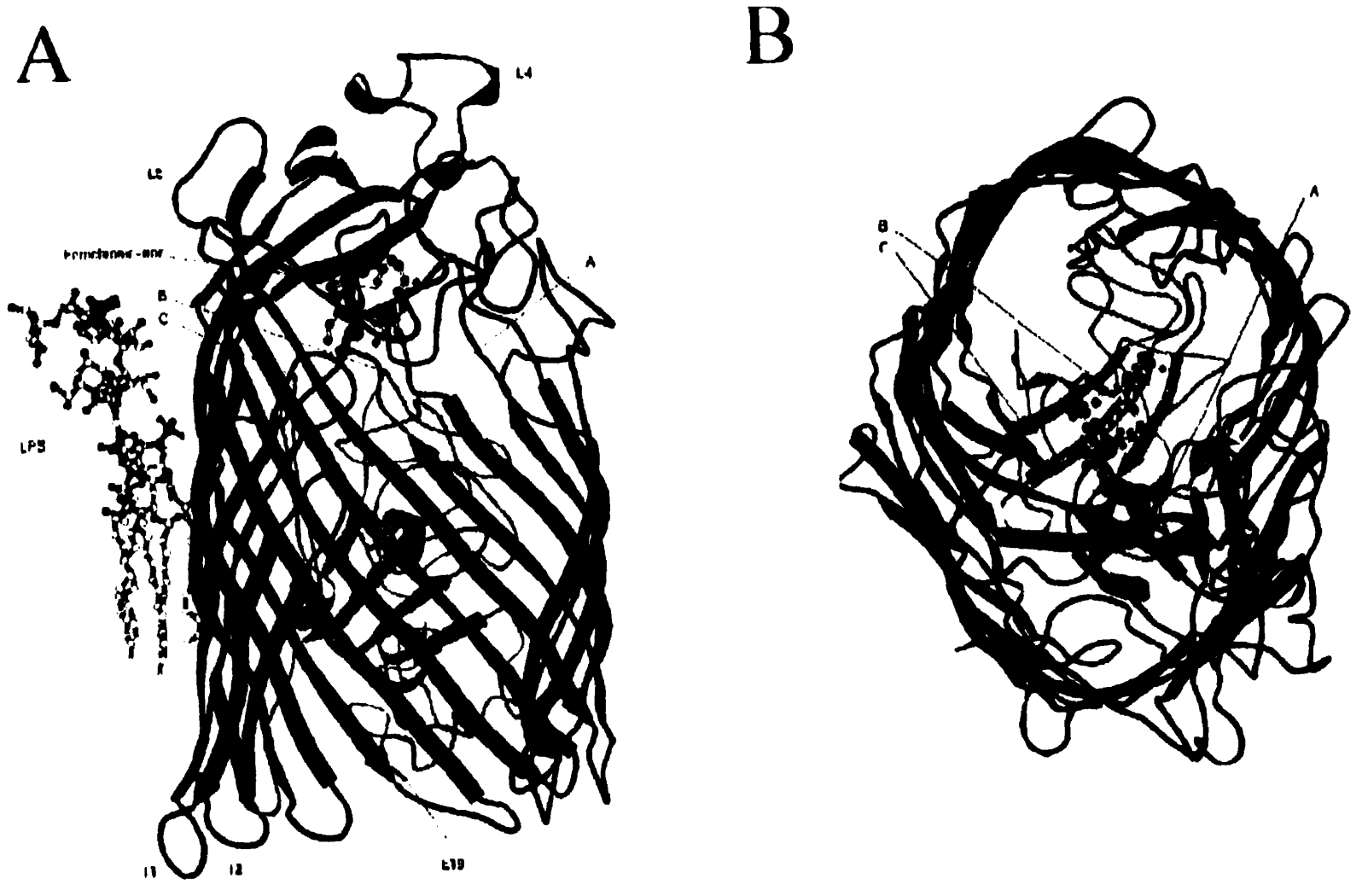
A
B
C
LPS
A
B
C
A

Figure 1. The FhuA-ferrichrome-iron complex and a single LPS molecule noncovalently associated with its membrane-embedded surface. **(A)** FhuA in ribbon representation. The barrel is colored blue, and residues 621 to 723 have been removed to allow an unobstructed view of the cork domain, which is shown in yellow. The LPS and ferrichrome-iron molecules are represented as ball-and-stick models, with the iron atom indicated as a large red sphere. Small red spheres are oxygen atoms, small white spheres are carbon atoms in the LPS molecule, small blue spheres are nitrogen atoms, small pink spheres are phosphorus atoms, and small black spheres are carbon atoms in the ferrichrome-iron molecule. FhuA is oriented as it would be found in the outer membrane; surface-located loops face the external environment (top), and periplasmic turns face the periplasm (bottom). Apices A (Arg^{81}), B (Gln^{100}), and C (Tyr^{116}); βA through βD of the cork domain; surface-located loops [L4 (residues 318 to 339) and L5 (residues 402 to 428)]; periplasmic turns [T1 (residues 184 to 189) and T2 (residues 222 to 226)]; and Glu^{19} are labeled. The positions of the upper and lower aromatic girdles are indicated with dashed lines. The spaces above and below the cork domain are the external and periplasmic pockets, respectively. **(B)** FhuA as viewed from the external environment along the barrel axis. The barrel is colored blue, and the cork domain is shown in yellow. Ferrichrome-iron is represented as a ball-and-stick model, with the iron atom indicated as a large red sphere. In Fig. 1B and in Fig. 5, A and B, small red spheres are oxygen atoms, small blue spheres are nitrogen atoms, and small black spheres are carbon atoms. Apices A, B, and C are labeled (*34,38*).

Figure 2. Stereoview of the ferrichrome-iron binding site in ribbon representation. The ferrichrome-iron molecule is represented as a green ball-and-stick model, with the iron atom indicated as a red sphere. Small red spheres are oxygen atoms, small blue spheres are nitrogen atoms, and small black spheres are carbon atoms of select side-chain residues of FhuA, and small gray spheres are carbon atoms of the ferrichrome-iron molecule. The cork domain is shown in yellow; barrel strands and loops are shown in blue. Side-chains residues (Arg^{81} from apex A, Gln^{100} from apex B, Phe^{115} and Tyr^{116} from apex C, Tyr^{244} and Trp^{246} from L3, Tyr^{313} and Tyr^{315} from β7, Phe^{391} from β9, and Phe^{702} from β21) within 4.5 Å of ferrichrome-atoms are labeled and shown in gray.

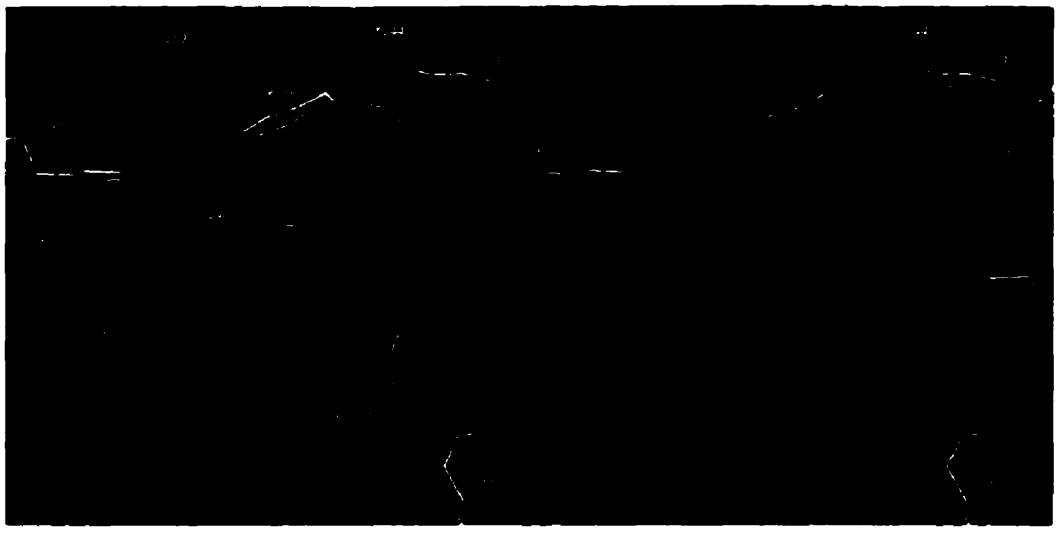

Figure 3. Representative section of the electron density map. Stereoview of the final $3F_{obs}$ -$2F_{calc}$ electron density map (blue) at a resolution of 2.7 Å resolution is contoured at 1.5 σ, showing the ferrichrome-iron binding site, including water molecules. The ferrichrome-iron molecule is shown in yellow, and the iron atom is indicated as a large red sphere. Select side-chain residues (Glu^{98}, Gly^{99} and Gln^{100} from apex B; Tyr^{116} from apex C; Tyr^{244} and Trp^{246} from L3; Phe^{313} from β7; Phe^{391} from β9; and Phe^{702} from β21) and the two water molecules (Wat151 and Wat154) found in the binding site are labeled (*34*) and colored white and red, respectively.

Figure 4. Conformational changes induced upon ferrichrome-iron binding. Superposition of the α-carbon coordinates of FhuA and its complex with ferrichrome-iron illustrating the ligand-induced conformational changes observed in the cork domain. The cork domains of FhuA and its complex with ferrichrome-iron are shown in purple and yellow, respectively. The barrel strands (shown in blue) are represented as thin lines for clarity of the cork domain. Apices A, B, and C, and Glu^{19} are labeled (*34*).

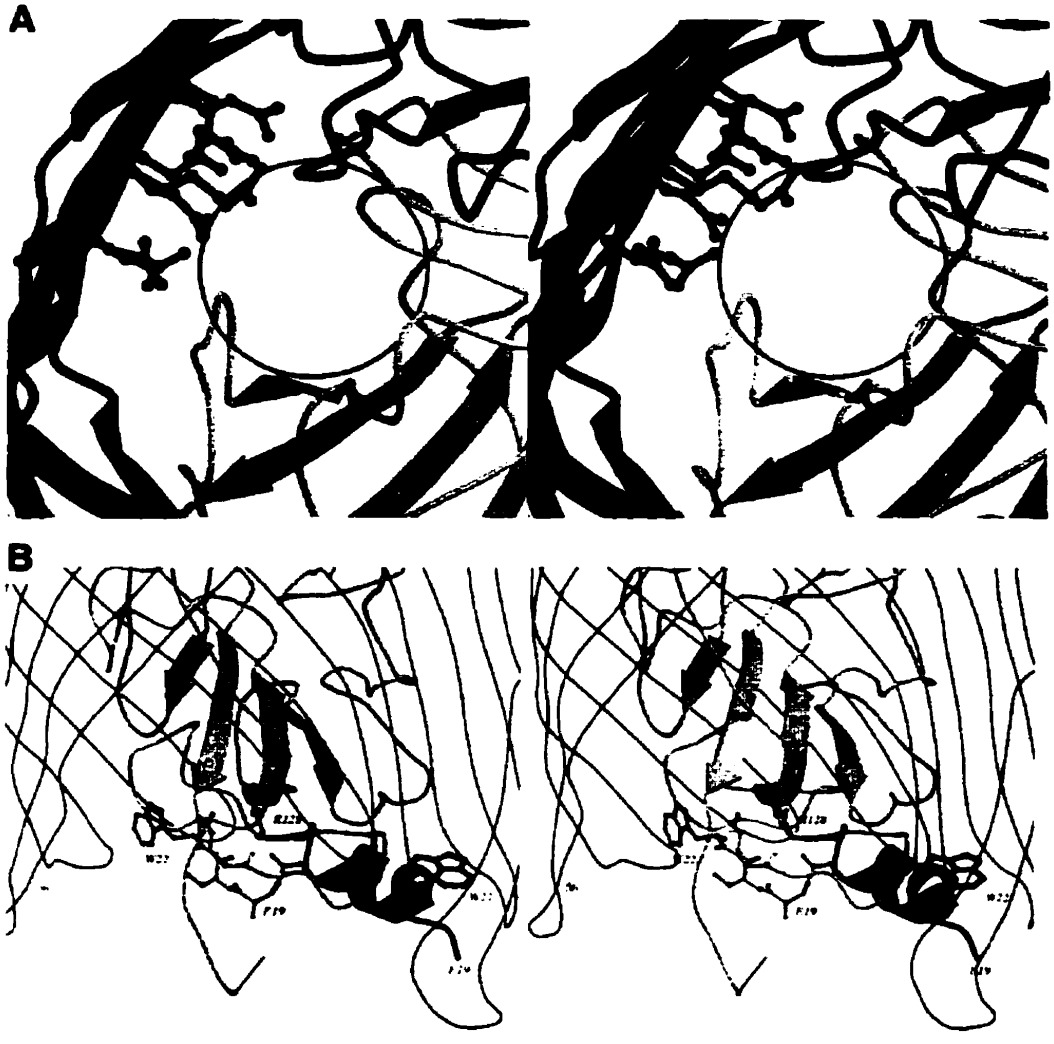
A
B

Figure 5. The putative channel-forming region with bound ferrichrome-iron complexes. **(A)** Stereoview of the putative channel-forming region in ribbon representation as viewed from the external environment along the barrel axis. This is an enlargement of the upper left portion of Fig. 1B. The barrel is colored blue, and the cork domain is shown in yellow. The putative channel-forming region is indicated by a circle (diameter, 10 Å). Strictly conserved side-chain residues (Arg^{297} and Asn^{299} from β7; Asp^{358}, Gln^{360} and Asp^{379} from β9; Asn^{436}, Gln^{438} and Gln^{440} from β10) that are thought to be involved in the surface diffusion of ferrichrome-iron through the putative channel-forming region are shown in green. **(B)** Stereoview illustrating the unwinding of the switch helix as a result of an allosteric transition that was induced upon ferrichrome-iron binding. The barrel strands (shown in blue) are represented as thin lines for clarity. Cork domain strands βA through βD, Glu^{19}, Trp^{22}, and Arg^{128} are labeled. The switch helix in the ligand-free conformations and the coil in the ligand-loaded conformations are shown in purple and yellow, respectively.

References and notes

1. V. Braun, K. Hantke, W. Köster, in *Metal Ions in Biological Systems*, A. Sigel and H. Sigel, Eds. (Marcel Decker, New York, 1998), pp. 67-145.
2. W. Welte *et al.*, in *Proceedings of the NATO Advanced Workshop: New Methods for the Study of Molecular Aggregates*, K. Standing and W. Ens, Eds. (Kluwer Academic, Boston, 1998), pp. 239-276; W. Welte, U. Nestel, T. Wacker, K. Diederichs, *Kidney Int.* **48**, 930 (1995).
3. K. Postle, *Mol. Microbiol.* **4**, 2019 (1993); T.E. Letain and K. Postle, *ibid.* **24**, 271 (1997).
4. J.W. Coulton *et al.*, *J. Bacteriol.* **165**, 181 (1986).
5. H. Killmann, R. Benz, V. Braun, *EMBO. J.* **12**, 3007 (1993).
6. J.M. Rutz *et al.*, *Science* **258**, 471 (1992).
7. M. Bonhivers *et al.*, *EMBO. J.* **15**, 1850 (1996).
8. L. Holm and C. Sander, *J. Mol. Biol.* **233**, 123 (1993); K. Diederichs, *Prot. Struct. Funct. Genet.* **23**, 187 (1995).
9. C.R.H. Raetz, in *Escherichia coli* and *Salmonella Cellular and Molecular Biology*, F.C. Neidhardt, Ed., (American Society for Microbiology Press, Washington, DC, 1996), pp. 1035-1071.
10. Crystallization of FhuA is dependent upon the presence of stoichiometric amounts of LPS. If LPS is completely removed from FhuA protein preparations or if an excess of LPS is present in such preparations, the growth of FhuA crystals is inhibited. We propose that LPS remained bound to FhuA throughout the steps of purification and crystallization and that it did not adsorb to FhuA during isolation. Because it is known that LPS is localized to the outer leaflet of the outer membrane, the location of bound LPS marks its position relative to the upper aromatic girdle of FhuA and to the outer membrane.
11. Strongly conserved residues found in the ferrichrome-iron binding site are Arg^{81} from apex A, Gly^{99} and Gln^{100} from apex B, Phe^{115} and Tyr^{116} from apex C, Tyr^{244} and Trp^{246} from L3, Tyr^{313} and Tyr^{315} from β7, Phe^{391} from β9, and Phe^{702} from β21.
12. H. Killmann *et al.*, *J. Bacteriol.* **180**, 3845 (1998).

13. The binding site possesses a higher affinity for ferrichrome-iron than for apoferrichrome [P. Boulanger *et al.*, *Biochemistry* **35**, 14216 (1996)]. In the ligand-loaded structure Tyr^{244} comes in close contact with the iron atom of ferrichrome-iron molecule. This observation may explain the decreased affinity for apoferrichrome.
14. A single amino acid deletion ΔAsp^{348} [H. Killmann and V. Braun, *J. Bacteriol.* **174**, 3479 (1992)], inhibited ferrichrome-iron binding and transport activity of FhuA.
15. Residues lining the external aromatic pocket are Tyr^{325} from L4, Tyr^{342} from β8, Tyr^{393} from β9, Phe^{566} and Phe^{567} from L8, Tyr^{610} from L9, Tyr^{705} from L11, and Phe^{708} from β22.
16. J.B. Neilands, *J. Am. Chem. Soc.* **74**, 4846 (1952).
17. D.A. Dougherty, *Science* **271**, 163 (1996).
18. D. Butcher, M.D. Bruch, G.R. Moie, *Pept. Biopoly.* **35**, 109 (1995); A.-S. Yang and B. Honig, *J. Mol. Biol.* **252**, 351-365 (1995).
19. Insertion of a dipeptide into the *fhuA* gene after residue Arg^{128} results in a complete loss of all FhuA function [G. Carmel *et al.*, *J. Bacteriol.* **172**, 1861 (1990)].
20. The tryptophan emission spectra were measured for FhuA and the FhuA-ferrichrome-iron complex [K. Locher and J. Rosenbusch, *Eur. J. Biochem.* **247**, 779 (1997)]. The tryptophan fluorescence was shown to decrease upon the addition of ferrichrome-iron suggesting a change in accessibility.
21. G.S. Moeck *et al.*, *Mol. Microbiol.* **22**, 459 (1996).
22. G.S. Moeck, J.W. Coulton, K. Postle, *J. Biol. Chem.* **272**, 28391 (1997).
23. P.E. Klebba *et al.*, *J. Bioener. Biomemb.* **25**, 603 (1993); R.J. Kadner and K.J. Heller, *J. Bacteriol.* **177**, 4829 (1995).
24. G.S. Moeck and J.W. Coulton, *Mol. Microbiol.* **28**, 675 (1998).
25. Strictly conserved side-chain residues thought to be involved in the surface diffusion of ferrichrome-iron through the putative channel-forming region may be Arg^{297} and Asn^{299} from β7, Asp^{358}, Gln^{360} and Asp^{379} from β9, Asn^{436}, Gln^{438} and Gln^{440} from β10.
26. G. Adam and M. Delbrück, in *Structural Chemistry & Molecular Biology*, A. Rich and N. Davidson, Eds. (Freeman, San Francisco, 1968), pp. 198-215.
27. H. Killmann, R. Benz, V. Braun, *J. Bacteriol.* **178**, 6913 (1996).

28. Strand β7 is composed of residues 294 to 317, L4 is composed of residues 318 to 339, and strand β8 is composed of residues 340 to 366.

29. T. Schirmer *et al.*, *Science* **267**, 512 (1995); D. Forst *et al.*, *Nature Struct. Biol.* **5**, 37 (1998).

30. A. Mademidis *et al.*, *Mol. Microbiol.* **26**, 1109 (1997).

31. A more complicated mechanism could avoid the possible loss of ferrichrome-iron into the external medium after formation of the FhuA-TonB complex by steric blockage of the surface-located pocket. However, the TonB-dependent binding and uptake of the FhuA-specific toxin colicin M through FhuA would require that the putative channel-forming region remain open from the external environment to the periplasm for an extended period of time and therefore would contradict such a mechanism [C.J. Lazdunski *et al.*, *J. Bacteriol.* **180**, 4993 (1998); R.M. Stroud *et al.*, *Curr. Opin. Struct. Biol.* **8**, 525 (1998)].

32. M.L. Guerinot, *Annu. Rev. Microbiol.* **48**, 743 (1994).

33. A. Ghosh *et al.*, *Chem. Biol.* **3**, 1011 (1996).

34. Single-letter abbreviations for the amino acid residues are as follows: A, Ala; C, Cys; D, Asp; E, Glu; F, Phe; G, Gly; H, His; I, Ile; K, Lys; L, Leu; M, Met; N, Asn; P, Pro; Q, Gln; R, Arg; S, Ser; T, Thr; V, Val; W, Trp; and Y, Tyr.

35. Because FhuA is difficult to purify to homogeneity in large amounts, one prerequisite for crystallization and subsequent structural analysis by X-ray crystallography was the development of an overexpression system and efficient protocols for the rapid purification of FhuA [A.D. Ferguson *et al.*, *Protein Sci.* **7**, 1636 (1998)]. A recombinant FhuA was constructed by splicing a hexahistidine tag plus three additional residues (SHHHHHHGS) at a previously identified surface-located location [G.S. Moeck *et al.*, *J. Bacteriol.* **176**, 4250 (1994)], amino acid 405. Functional assays confirmed (21) that the protein FhuA405.H_6 (native FhuA) is fully active as bacteriophage receptor and for TonB-dependent ferrichrome-iron transport at levels comparable to wild type. To generate selenomethionyl-labeled FhuA (SeMet-FhuA), plasmid pHX405 was transformed into the *met*$^-$ auxotrophic *E. coli* strain DL41 and grown as recommended [S. Doublié, *Meth. Enz.* **276**, 523 (1997)].

36. S.J. Angyal, L. Odier, M.E. Tate, *Carbohydrate Res.* **266**, 143 (1995).

37. Phase information was derived from multiple anomalous dispersion (MAD) [W.A. Hendrickson, *Science* **254**, 51 (1991)] data that were measured at three wavelengths that correspond to the point of inflection, the peak of the selenium absorption profile, and a remote point. All data were reduced and processed using the XDS software package [W. Kabsch, *J. Appl. Cryst.* **21**, 916 (1988)]. The 10 selenium sites were located with SOLVE [T.C. Terwilliger and J. Berendzen, *Acta. Cryst.* **D53**, 571 (1997)], and MAD phases were obtained with SOLVE and SHARP [E. de La Fortelle and G. Bricogone, *Meth. Enz.* **276**, 472 (1997)]. Initial phases, which were calculated to a resolution of 3.05 Å, were improved by solvent flattening with the program DM [K. Cowtan, *Acta. Cryst.* **D50**, 760 (1994)]. The resulting electron density maps were of sufficient quality to build a model with the program O [T.A. Jones *et al.*, *Acta. Cryst.* **A47**, 110 (1991)] and unambiguously place a ferrichrome-iron molecule and an LPS molecule. The model was refined with the programs X-PLOR 3.1 (Yale University, New Haven, CT, 1992) and CNS [A.T. Brünger *et al.*, *Acta Cryst.* **D54**, 905 (1998)] and was used to solve the structure of FhuA to 2.5 Å resolution by difference Fourier techniques. Standard protocols for simulated annealing and minimization as implemented in CNS were used for refinement. Individual restrained *B*-factor refinement was justified as judged by a substantial drop in R_{free} [A.T. Brünger, *Nature* **355**, 472 (1992)]. The current FhuA model contains residues 19 to 723, 1 LPS, and 99 water molecules. The average *B*-factors for main-chain and side-chain atoms and the LPS molecule are 65 Å^2, 67 Å^2, and 78 Å^2, respectively. The FhuA model was used in the refinement of the FhuA-ferrichrome-iron complex to 2.7 Å resolution. The current model for the FhuA-ferrichrome-iron complex contains residues 19 to 723, 1 LPS, 1 ferrichrome-iron, and 52 water molecules. The average *B*-factors for main-chain and side-chain atoms, the LPS, and ferrichrome-iron molecules are 63 Å^2, 66 Å^2, 75 Å^2, and 49 Å^2, respectively. Refinement is not complete for both structures. For the FhuA model, the R_{cryst} is 24.2 % (48,359 reflections), and the R_{free} is 28.3 % (2,309 reflections); for the FhuA-ferrichrome-iron complex, the R_{cryst} is 23.2 % (37,362 reflections), and the R_{free} is 28.1 % (1,532 reflections). All residues lie in allowed regions of the Ramachrandran plot, and all residues that are explicitly mentioned in the text reside in good electron density.

Protein Data Bank accession codes are 2fcp and 1fcp for FhuA and the FhuA-ferrichrome-iron complex, respectively.

38. All figures were prepared using the programs MOLSCRIPT [P. Kraulis, *J. Appl. Cryst.* **24**, 946 (1991)] and Raster-3D [E.A. Merrit and D.J. Bacon, *Meth. Enz.* **277**, 505 (1997)], except for Fig. 3, which was prepared using the program O.

39. We gratefully acknowledge A. Svensson, MAX-lab II and A. Thompson, European Radiation Synchrotron Facility for their assistance and generous support during data collection; E.A. Meighen for providing *E. coli* strain DL41; P.A. Karplus for critical reading of the manuscript; J. Wang for genetic constructs; V. Braun and H. Killmann for bacterial strains and discussions; A. Patel for his assistance with protein purification; J. Breed for crystallization trials and critical reading of the manuscript; D.M. Allan and J.A. Kashul for editing; K. Hegetschweiler for providing *cis*-inositol; and B. Herrmann, A. Hirsch, C. Peinelt, O. Seth and J. Telioriclis, who made important contributions to the early phase of this project. This work was supported by the Deutsche Forschungsgemeinschaft (W.W.); by the Medical Research Council, Canada (grant MT-14133 to J.W.C.); and by NATO International Collaborative Research Grant 960082. A.D.F. is the recipient of a Deutscher Akademischer Austauschdienst Grant for Study and Research.

Preface to chapter five

One unexpected feature of the solution of the crystallographic structure of FhuA was the identification of an ordered LPS molecule noncovalently associated with the membrane-embedded surface of the receptor. Examination of FhuA-LPS contacts revealed that eight positively charged side-chain residues interact electrostatically with the negatively charged components of the lipoglycan. To determine if a similar arrangement of side-chain residues were also found on the surfaces of other proteins, a structure-based search algorithm was utilized. With this method, a conserved four-residue LPS-binding motif that is present among known LPS-binding proteins of prokaryotic and eukaryotic origin was identified. In addition to establishing the first crystallographic structures of LPS and the precise placement of an outer membrane protein within the outer membrane, this data supports the proposal that a conserved mode of pattern recognition by LPS-binding proteins is involved in the innate immune response. The LPS-binding motif may readily be used both to map LPS-binding sites on proteins and to model their complexes with LPS. Such models may facilitate the rational design of proteins with modified LPS-binding properties.

A conserved structural motif for lipopolysaccharide recognition by procaryotic and eucaryotic proteins

Andrew D. Ferguson[1,2], Wolfram Welte[1], Eckhard Hofmann[1], Buko Lindner[3], Otto Holst[3], James W. Coulton[2], Kay Diederichs[1]

1 Fakultät für Biologie, Universität Konstanz, M656, D-78457 Konstanz, Germany

2 Department of Microbiology and Immunology, McGill University, 3775 University Street, Montreal, Quebec, Canada H3A 2B4

3 Forschungszentrum Borstel, Zentrum für Medizin und Biowissenschaften, Parkallee 1-45, D-23845 Borstel, Germany

Key words: innate immune response; lipopolysaccharide; septic shock; structural motif; TonB-dependent receptor; siderophore-mediated iron acquisition

Abstract

Background: Lipopolysaccharide (LPS), a lipoglycan from the outer membrane of gram-negative bacteria, is an immunomodulatory molecule that stimulates the innate immune response. High amounts of LPS cause excessive release of inflammatory mediators and are responsible for the septic shock syndrome. The interaction of LPS with its cognate binding proteins has not yet been structurally elucidated.

Results: The X-ray crystallographic structure of LPS in complex with the integral outer membrane protein FhuA from *Escherichia coli* K-12 is reported. It is in accord with mass spectroscopic and nuclear magnetic resonance data. Eight positively charged residues of FhuA provide hydrogen bonding or electrostatic interactions with LPS. Three-dimensional arrangements similar to these residues were searched on all structurally known proteins with a fast template-matching algorithm, and a subset of four residues was identified which is common to known LPS-binding proteins.

Conclusion: These four residues, three of which form specific interactions with lipid A, appear to provide the structural basis of pattern recognition in the innate immune response. Their arrangement can serve to identify LPS-binding sites on proteins known to interact with LPS, and could serve as a template for molecular modeling of a LPS scavenger designed to reduce the septic shock syndrome.

Introduction

Lipopolysaccharide (LPS or endotoxin), a complex lipoglycan found exclusively in the outer membrane of gram-negative bacteria [1-3], is a potent activator of the innate (nonclonal) immune system [4,5]. Low doses of LPS stimulate macrophages and neutrophils to produce cytokines and inflammatory mediators, thereby providing resistance to bacterial infections. High doses of LPS cause excessive release of inflammatory mediators and may lead to septic shock, a medical condition that is responsible for an estimated 200,000 deaths per year in the United States alone. Although some proteins have been identified as targets of LPS activity, detailed atomic interactions between the cognate residues on those targets and specific sites of LPS are unknown.

The objectives of our studies were to establish by X-ray crystallography the three-dimensional structure of LPS, to integrate LPS into the current model of the molecular architecture of the bacterial outer membrane, and to identify characteristic patterns of protein-LPS interactions that derive from the crystal structure of a complex of LPS with an outer membrane protein. Our target protein is FhuA, ferric hydroxamate uptake receptor on the surface of *Escherichia coli*. FhuA belongs to a family of proteins that mediates the active transport of siderophores including ferrichrome into gram-negative bacteria [6]. We recently solved [7] the crystal structure of FhuAs that were isolated from two strains of *E. coli* K-12: strain AW740 (2.5 Å resolution) and strain DL41 (2.7 Å). FhuA consists of a C-terminal β-barrel formed by 22 antiparallel transmembrane β-strands and an N-terminal cork that fills the barrel interior. During the course of model building and structural refinement, we observed additional electron density proximal to the membrane-embedded region of the barrel. This electron density was modeled as a single LPS molecule, tentatively using the most abundant *E. coli* LPS Ra-chemotype [8].

LPS is composed of three covalently linked domains, which are differentiated by their genetic organization, biosynthetic pathways, chemical structures and biological features [8]. These domains are lipid A, a mostly invariant glycolipid that acts as an amphiphilic anchor in the outer membrane (Figure 1); the core, a variable non-repeating heterooligosaccharide; and O-antigen, an immunogenic highly variable repeating

polysaccharide which extends into the external medium. The chemical composition and conformation of lipid A are determinants of its endotoxic activity [9]. The gram-negative bacterium *E. coli* K-12 has defects in the gene cluster responsible for the biosynthesis of O-antigen; strains AW740 and DL41 therefore synthesize a truncated or 'rough' form of LPS consisting of lipid A and the core only, whereas wild-type *E. coli* expresses the complete or 'smooth' form.

This paper details the molecular conformation of LPS and its interactions with surface residues of FhuA in the FhuA-LPS complex as obtained by compositional data, mass spectrometric analyses, and crystallographic refinement, and reports a mode of protein-LPS interaction which appears to be shared by known LPS-binding proteins.

Results and discussion

Given the lack of detailed chemical information about the LPS molecules in our FhuA-LPS complexes and the limited resolution of our electron density maps, we conducted a complete chemical analysis of LPS extracted from the outer membrane of *E. coli* strains AW740 and DL41 and of LPS derived from purified FhuA-LPS preparations. This information was used to model the ambiguous regions of the LPS molecules in our crystal structures. Our compositional and detailed mass spectrometric analyses of LPS from outer membrane extracts of both bacterial strains and from protein preparations used for crystallization (Figure 1) lead to complete crystallographic models of the LPS molecules (Figure 2).

Structural refinements of the two FhuA-LPS complexes provide improved crystallographic R-factors compared to those reported in [7], and good matches to the electron density maps (Figure 2c). For the FhuA-AW740-LPS complex, it was possible to complete the atomic model by including eight crystallographically visible glycerol and three detergent molecules. The temperature factors of all parts of the atomic models are at a high level; in both complex structures, average atomic B-factors are around 66Å^2 for the protein and lipid A, 70Å^2 for the inner core and 96Å^2 for the outer core of LPS. Detergent, glycerol (in the FhuA-AW740-LPS complex) and water molecules show average B-factors around 90Å^2, 90Å^2 and 60Å^2, respectively. Ferricrocin (in the FhuA-

DL41-LPS-ferricrocin complex), at a temperature factor around 50Å^2, is bound in the cork domain, which, together with parts of the β-strands, is the most rigid part of the complexes (at average B-factors slightly less than 50Å^2). Despite the high average B-factors, the models reside in good electron density, with the exception of a few surface-exposed side chains at some of the outer loops.

In the crystallographic structure, the LPS molecule is closely associated with the FhuA barrel, burying an accessible surface area of 1,800 Å^2. Numerous van der Waals contacts with hydrophobic side chains of FhuA fix all acyl chains of the bound LPS molecule, except for the 3-hydroxymyristate, in a highly ordered conformation, approximately parallel to the barrel axis (Figure 2a). In common with all outer membrane proteins studied so far, FhuA has two girdles of aromatic residues that are 25 Å apart, extending into the lipid bilayer and marking the boundary of a cylindrical zone of hydrophobic residues on the barrel surface. These girdles were proposed to delineate the interface between the membrane lipids and the polar head groups of LPS. Indeed, we find the amide and ester bonds linking the acyl chains to the glucosamine disaccharide being situated slightly above the upper aromatic belt. In both FhuA-LPS complexes, the line connecting the O1 and O4'-phosphate moieties of lipid A is perpendicular to the barrel axis and thus parallel to the plane of the outer membrane. The outer core bends away from the barrel axis and is in contact neither with the barrel nor with the surface-exposed loops of FhuA (Figure 2b). The bend may be induced by a crystal contact between a phosphorylated heptose group of the inner core and the hexahistidine tag of a symmetry-related FhuA molecule.

Our findings are in general agreement with current models of the architecture of the outer membrane [10]. The outer leaflet of the outer membrane is the LPS monolayer, which contributes to the integrity of the gram-negative cell envelope. Absence of O-antigen does not alter the integrity of the outer membrane [11] nor does absence of the outer core or the non-phosphorylated heptose residues of the inner core. Bacterial mutants with defects in the synthesis or incorporation of the phosphorylated heptose of the inner core (deep rough mutants) display hypersensitivity to lipophilic solutes. The phosphorylated heptose moieties of the inner core thus play an important role in stabilization of this part of the membrane.

In the outer membrane of *E. coli*, electrostatic repulsions between adjacent, negatively charged LPS molecules are neutralized by divalent cations. Removal of these cations from the outer membrane with chelating agents destabilizes the LPS monolayer by disrupting specific intermolecular LPS-LPS contacts [10]. The specific interaction of phosphates with positively charged groups on FhuA can serve as a model for the LPS-LPS interaction as promoted by divalent cations in the outer membrane. Our finding of an alignment of the diglucosamine phosphate moieties in the plane of the outer membrane is contrary to results based on small-angle X-ray scattering and molecular modeling [12]. The arrangement that we find offers an alternative mode of interaction between neighboring LPS molecules, predicting in-plane cross-linking of divalent cations and diglucosamine phosphates.

The innate immune response elicited against gram-negative bacteria is not triggered by the intact outer membrane, but by recognition of single LPS molecules, and involves specialized binding proteins and receptors [4,5]. Given the atomic details of the interaction between FhuA and LPS, it was our goal to identify the arrangement of residues that are conserved among LPS-binding proteins.

In the FhuA-LPS complex, eleven charged residues interact with the negatively charged phosphates of the inner core and the diglucosamine backbone of lipid A (Table 1 and Figure 2). These residues are responsible for the tight binding of LPS to FhuA, and we hypothesized that they constitute a conserved motif in LPS-binding proteins. They involve short discontinuous segments found on β-strands 7 through 11. Most of the favorable interactions are contributed by a cluster of eight positively charged residues on the surface of the barrel which interact by hydrogen bonding at distances around 3Å, or electrostatically (Lys306 and Arg424) at longer distances. The electrostatic Coulomb potential of the latter residues might appear to provide little contribution to the overall binding enthalpy, however, it falls off at only 1/r, and their presence may be important for charge compensation in the binding site.

Using a conventional sequence-based search with the template of all or subsets of the LPS-interacting residues on FhuA, we did not identify similar LPS-binding motifs in sequence databases. Furthermore, no other structures of protein-LPS complexes are available for comparison with the FhuA-LPS complex. Therefore we designed and

utilized a structure-based search strategy to identify in the Protein Data Bank (PDB) residue subsets that are structurally similar to those of FhuA's LPS-binding residues.

Any sequence- or structure-based search strategy must find a compromise between high specificity (which avoids false positive matches), and high sensitivity (which avoids false negatives). The objective is to produce a high number of true matches on a low background of false positives. The "proper" subset of residues detects those proteins that are known to interact specifically with LPS, but avoids matches with proteins that do not interact *in vivo* with LPS. Proteins with an LPS-binding motif similar to that on FhuA are expected to yield r.m.s. deviations below 1.5 Å for those residues that form a common LPS-binding motif. This value corresponds to an average bond distance between atoms and thus ensures that chemically equivalent atoms of superimposed motifs occupy equivalent positions in space.

Using all subsets consisting of five, six, seven, or the complete set of eight residues as search templates, no structural homologues with r.m.s. deviations <1.5 Å were identified in the PDB. Searches conducted with three-residue subsets detected a high number of non-specific matches at r.m.s. deviations <1.5 Å. All except one of the four-residue subsets detected a small number of matches in the PDB. That exception is the four-residue search template of FhuA residues Lys 306, Lys 351, Arg 382 and Lys 428, which identified a much larger group of matches at low r.m.s. deviations. Three of these four residues form strong hydrogen bonds with the phosphates of lipid A (Table 1 and Figure 3). We therefore denote these four FhuA residues as the LPS-binding motif. Indeed, lipid A, the most conserved component of LPS, has a specific stereochemistry due to multiple asymmetric carbon atoms, and has been implicated in recognition by high-affinity LPS-binding proteins [8].

Our structural search of the PDB using this LPS-binding motif identified membrane-associated proteins, bacterial toxins, colicins, and ribonucleotide-binding proteins. Among the proteins identified by using this subset of four residues are all those proteins in the PDB that are known to bind LPS specifically and that mediate the LPS-induced immune response (Table 2). In all cases, the proposed LPS-binding sites found on these proteins are consistent with functional and mutational data. All residues of the LPS-binding sites are surface-exposed and docking of LPS to these proteins is possible

without steric clashes. The four-residue subset thus represents an LPS-binding motif, which is remarkably conserved in proteins of procaryotic and eucaryotic origin.

Our data support the proposal [4,5] that a conserved mode of LPS recognition by LPS-binding proteins is involved in the innate immune response. A consequence of this mechanism is that increased bacterial virulence *in vivo* should result from LPS modifications, as has been observed [13]. While the structural scaffold of the four-residue motif, which we identify, appears to be necessary for LPS binding, our findings do not currently allow us to investigate the individual roles of the four residues. Their respective importance, as well as the contribution of other residues in the individual binding sites of FhuA and other LPS-binding proteins, remains to be established by site-directed mutagenesis. For those structurally known proteins identified by our search, as well as for new crystallographic structures, the four-residue LPS-binding motif of FhuA may readily be used both to map the LPS-binding site, and to model a complex with LPS. Such models may facilitate the rational design of proteins with modified LPS-binding properties.

Biological implications

Lipopolysaccharide is the major component of the outer membrane of gram-negative bacteria; as such, it is an important activator of the innate immune response. Its three-dimensional structure, alone or in complex with a protein, has hitherto not been elucidated in atomic detail. This work describes the crystallographic structure of its complex with FhuA, a ferric hydroxamate uptake receptor on the surface of *Escherichia coli*. The lipid A portion of LPS, which is its most invariant part, interacts specifically with positively charged residues on the outer surface of the β-barrel of FhuA.

A search through the database of known protein structures, using subsets of those residues identified in the LPS binding site of FhuA, identifies four residues whose arrangement on the surface of known LPS-binding proteins is conserved. These residues appear to be the crucial elements of pattern recognition in the innate immune response. The following applications of this knowledge are feasible. Known LPS-binding proteins may be altered for their binding properties: they could be engineered for higher or lower

LPS-binding affinity. Recombinant proteins that compete with naturally occurring LPS-binding proteins and that lack immunostimulatory activities will be advantageous in the treatment of bacterial sepsis. Novel bactericidal proteins or peptides may be designed [14] to intercalate into the outer membrane by their binding to lipid A. Such binding would increase the permeability of the outer membrane and compromise its protective effect, and thereby kill bacterial cells.

Materials and methods

Nuclear magnetic resonance

Compositional analysis of LPS extracted from the outer membranes of *E. coli* strains (AW740 and DL41), performed according to published methods [15], identified constituents and their approximate molar ratios: Gal (1.0/1.0), Glc (2.6/2.5), GlcN (1.9/1.9), Hep (3.1/2.9), Kdo (2.0/1.9), rhamnose (trace amounts/0.3), phosphate (4.4/5.6) and 2-aminoethanol (0.2/0.6). The relatively low Hep content is most likely due to the phosphate substitutions linked to the Hep residues, which further stabilize their glycosidic linkages. The GlcN content demonstrated that there are no additional GlcN substitutions at the non-reducing terminus of the core.

Mass spectrometry

Matrix-assisted laser desorption ionization mass spectrometry including post source decay analysis were performed with the two-stage reflectron time-of-flight mass analyzer Bruker-Reflex III (Details of the applied methods are described in [16]). Spectra from membrane-extracted AW740-LPS and DL41-LPS displayed the expected heterogeneity for *E. coli* K-12 LPS (data not shown). A series of molecular ions differing in their phosphate and 2-aminoethyl phosphate substitutions were identified as various combinations of Kdo, Hep, hexose (Gal and Glc) and lipid A residues. The most abundant core oligosaccharide in both LPS extracts consists of two Kdo residues, four Hep residues, and four hexose residues and up to four phosphate residues in nonstoichiometric amounts. In contrast to AW740-LPS, DL41-LPS showed further heterogeneity arising from additional 2-aminoethyl phosphate groups.

X-ray crystallography

The structure of the FhuA-AW740-LPS complex was solved and initially refined at 2.50 Å resolution [7]. Following additional rounds of model building using the program O [17] and structural refinement with CNS [18], the final model now contains residues 19 to 725, 1 LPS, 3 detergent (dimethyldecylamine-N-oxide, DDAO), 8 glycerol and 244 water molecules (R_{cryst} 22.1% and R_{free} 27.1%). This structure was used in the refinement of FhuA-DL41-LPS-ferricrocin complex at 2.70 Å resolution. The final model contains

residues 19 to 725, 1 LPS, 1 ferricrocin and 152 water molecules (R_{cryst} 23.1% and R_{free} 27.6%). Due to the lower resolution, glycerol or detergent molecules were not included in the model. The main differences between these models, compared to those previously reported [7], are in the two LPS molecules, and the modeling of detergent and glycerol molecules in the case of the FhuA-AW740-LPS crystals. Throughout this article we use the residue numbering of the wild-type FhuA sequence. The coordinates submitted to the PDB (1qff, FhuA-DL41-LPS and 1qfg, FhuA-AW740-LPS-ferricrocin) differ in their numbering due to the insertion of eleven residues of the affinity tag after Pro405 (the sequence in this region has been corrected with respect to that given in [7]).

Structural searches

After constructing a database from the PDB (status on January 25th, 1999) the program SPASM [19] was employed to superimpose subsets of LPS-binding residues (eight positively charged residues; see Table 1) upon all deposited crystallographic protein structures. The side chains of all residues were truncated at the Cγ atom because the side chain conformation of those residues that compose the LPS-binding motif were expected to differ beyond the Cγ in the LPS-bound and the LPS-free form. SPASM uses a fast search procedure based on differences between atomic positions. Neither chain directionality nor gap size constraints were imposed, and only Lys/Arg substitutions were permitted. The eight-residue set, and all seven-residue (8 combinations), six-residue (28 combinations), five-residue (56 combinations), four-residue (70 combinations), and three-residue (56 combinations) subsets were systematically assessed. This procedure mimics the properties of a sequence-based search which permits insertions and deletions with respect to a given sequence motif.

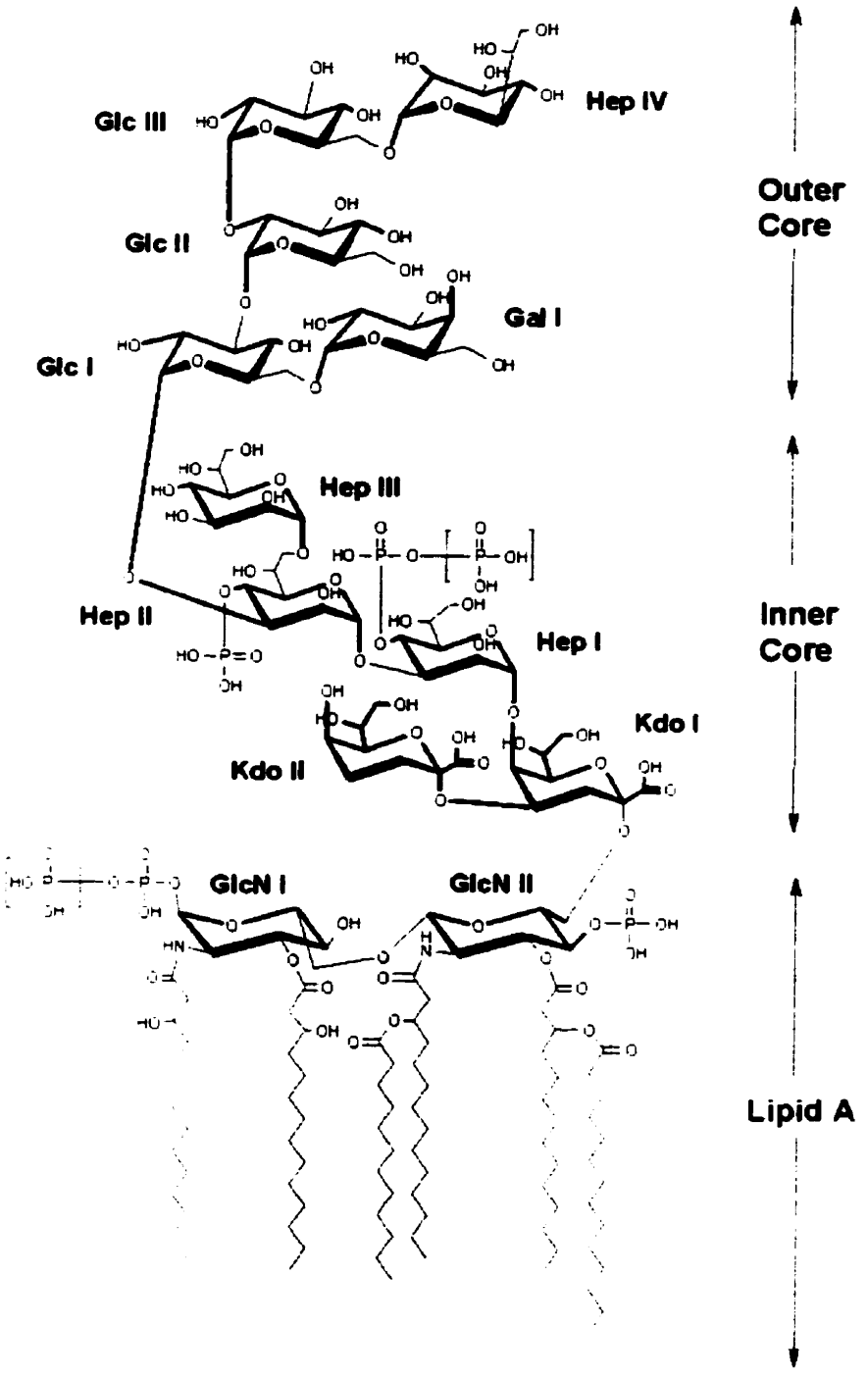
Glc III
Hep IV
Glc II
Gal I
Glc I
Hep III
Hep II
Hep I
Kdo I
Kdo II
GlcN I
GlcN II
Outer Core
Inner Core
Lipid A

Fig. 1. Chemical structure of *E. coli* K-12 LPS from strains AW740 and DL41 showing its three domains and their constituents. Enterobacterial lipid A is a phosphorylated 2-amino-2-deoxy-D-glucose (glucosamine) disaccharide. The two linked glucosamines (GlcN I and GlcN II) are bisphosphorylated at the O1-position of GlcN I and monophosphorylated at the O4'-position of GlcN II. The secondary phosphate position of the O1-diphosphate is not fully occupied (indicated with brackets). The glucosamine disaccharide is acylated (from left to right) at the 2- and 3-positions of GlcN I with 3-hydroxymyristatic [14:0 (3-OH)] acid, and at the 2'- and 3'-positions of GlcN II with 14:0[3-*O* (C12:0)] and 14:0[3-*O* (C14:0)], respectively. The 3-hydroxymyristate residue is partially disordered in both complexes and could not be modeled beyond the fourth carbon atom. The inner core comprises two 3-deoxy-D-*manno*-oct-2-ulopyranosonic acid residues (Kdo I and Kdo II), three L-*glycero*-D-*manno*-heptopyranose residues (Hep I, Hep II and Hep III) and phosphate residues. In AW740-LPS, Hep I is bisphosphorylated whereas in DL41-LPS, a 2-aminoethyl phosphate group is present. Hep II is monophosphorylated in both structures. The outer core of both LPS molecules consists of hexose moieties, including D-galactose (Gal), D-glucose (Glc) and a disordered fourth heptose residue (Hep IV). Although Hep III, Hep IV and Glc III were chemically identified in both complexes, they could not be modeled. This figure was prepared with ISIS Draw.

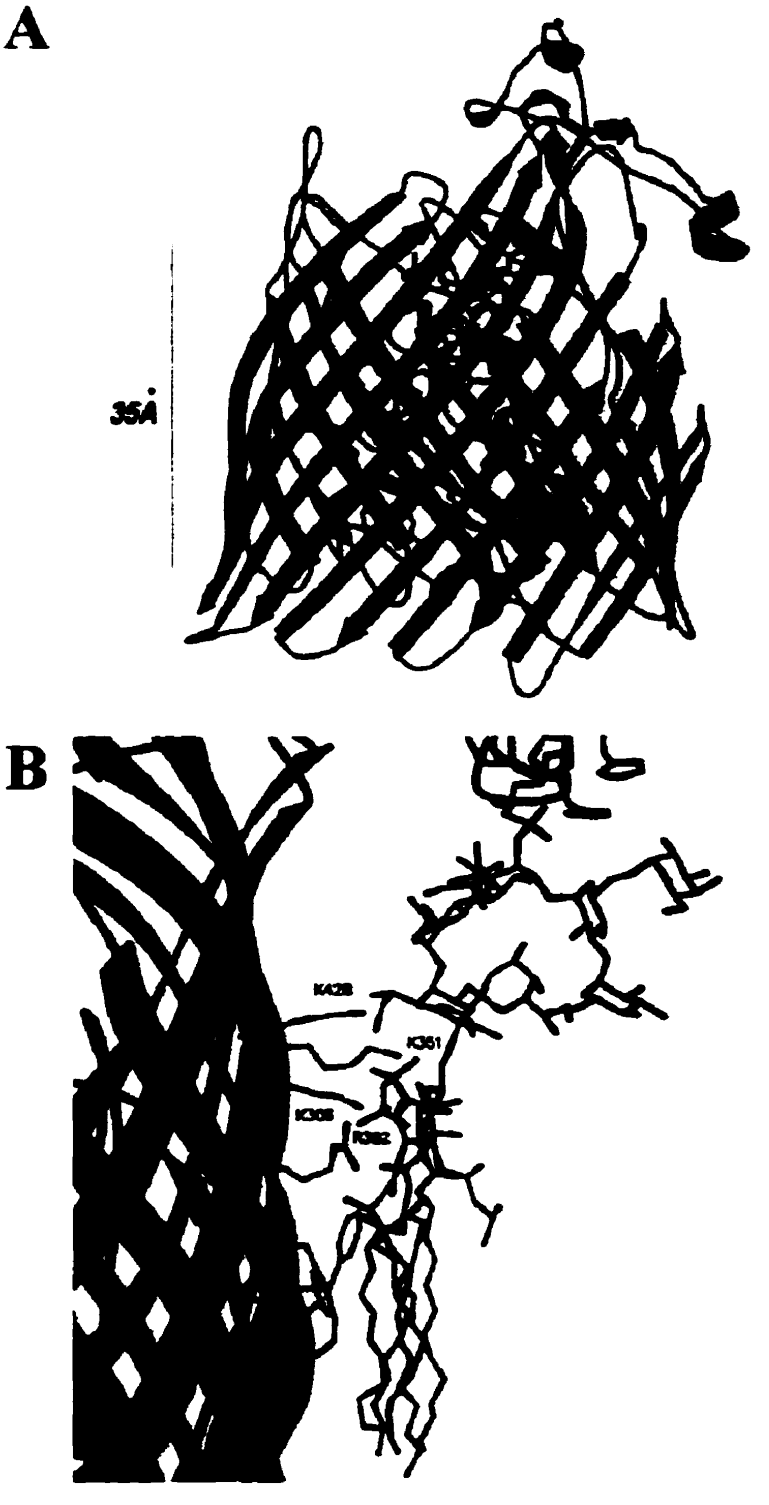
A
35Å
B

C

Fig. 2. Crystal structure of the FhuA-LPS complex. **(a)** The FhuA-AW740-LPS complex in ribbon representation shows the placement of the LPS molecule in relation to the outer barrel surface of FhuA. The view is perpendicular to the barrel axis. **(b)** Close-up view perpendicular to the barrel axis. Selected side chain residues of the upper aromatic girdle and those that composed the LPS-binding motif (with labels) are colored yellow. The AW740-LPS molecule is represented as a stick model with oxygen atoms red, nitrogen atoms blue, phosphorous atoms green, and carbon atoms gray. The His-tag of a symmetry-related FhuA molecule (pink) forms a crystal contact with the phosphates of the inner core of LPS. **(c)** Electron density (obtained with a simulated-annealing omit calculation) at 2.1σ around lipid A of the FhuA-AW740-LPS complex. The view is the same as in a). In all panels, the barrel surface of FhuA is colored blue. This figure and Fig. 3 were prepared using MOLSCRIPT [20] and Raster-3D [21].

Fig. 3. Stereoview of the FhuA LPS-binding site, perpendicular to the barrel axis. Selected FhuA side chain residues that form specific and non-specific van der Waals contacts with the LPS molecule are colored in yellow. The outer barrel surface of FhuA is shown in blue. Those residues that compose the conserved LPS-binding motif are marked with an asterisk. The AW740-LPS molecule is shown as a stick model with oxygen atoms red, nitrogen atoms blue, phosphorous atoms green, and carbon atoms gray.

Table 1. Specific FhuA-LPS interactions. Listed are the residues and atoms on FhuA, their location on the β-strands of FhuA, distance and type of interaction. Twelve additional side chain residues form non-specific van der Waals contacts with LPS atoms (not shown). Residues that form the conserved LPS-binding motif are marked with an asterisk.

Residue-Atom	Location	Distance	Type of Interaction
Glu 304-OE1	β7	2.6 Å	Hydrogen bond with the O3 atom of the 4'-phosphate
Glu 304-OE2		3.3 Å	Hydrogen bond with the O3 atom of the 4'-phosphate
Lys 306-NZ*	β7	6.5 Å	Electrostatic interactions with the 4'-phosphate
Lys 351-NZ*	β8	2.6 Å	Hydrogen bond with the O4 atom of the 4'-phosphate
Arg 382-NE*	β9	3.7 Å	Hydrogen bond with the O2-carbonyl atom of the 2-hydroxymyristate residue
Arg 382-NH1*		3.0 Å	Hydrogen bond with the O2-carbonyl atom of the 3'-myristate residue
Arg 382-NH2*		3.3 Å	Hydrogen bond with the O5 atom of GlcN I
Arg 384-NE	β9	3.1 Å	Hydrogen bond with the O7 atom of Kdo I
Arg 384-NH1		3.0 Å	Hydrogen bond with the O2 atom of the 1-diphosphate
Arg 384-NH2		2.9 Å	Hydrogen bond with the O1B atom of Kdo II
Asp 386-OD2	β9	2.8 Å	Hydrogen bond with the O7 atom of Kdo I
Asn 388-OD1	β9	3.5 Å	Hydrogen bond with the O6 atom of Hep III
Arg 424-NH1	β10	6.4 Å	Electrostatic interactions with the O2 atom of Hep I
Lys 428-NZ*	β10	3.1 Å	Hydrogen bond with the O2 atom of the 1-diphosphate
Lys 430-NZ	β10	2.6 Å	Hydrogen bond with the O7 atom of the 1-diphosphate
Arg 463-NH1	β11	2.8 Å	Hydrogen bond with the O6 atom of Hep I
Arg 463-NH2		2.8 Å	Hydrogen bond with the O5 atom of Hep I

Table 2. LPS-binding proteins and their LPS-binding residues identified by a structural search of the PDB. r.m.s.d. denotes the root-mean-square deviation after superposition with equivalent residues in the LPS-binding motif of FhuA (bold).

Protein	PDB Code		Superimposed Residues				r.m.s.d.
			Lys 306	**Lys 351**	**Arg 382**	**Lys 428**	
BPI*	1bp1		Lys 42	Arg 48	Lys 92	Lys 99	0.88 Å
Lactoferrin†	1bx1	NH_2-terminal lobe	Arg 24	Arg 27	Arg 2	Arg 4	1.47 Å
		COOH-terminal lobe	Lys 359	Arg 356	Lys 633	Lys 637	1.25 Å
Lysozyme‡	1jkc	Human	Arg 113	Arg 107	Lys 97	Arg 21	1.38 Å
	135l	C-type	Lys 96	Lys 97	Arg 61	Lys 73	1.45 Å
	1hhl	G-type	Arg 14	Lys 13	Lys 125	Arg 121	1.43 Å
	145l	V-type	Arg 148	Lys 147	Arg 137	Lys 135	1.07 Å
LALF§	-		Arg 41	Arg 40	Lys 64	Lys 47	1.43 Å

* The bactericidal/permeability-increasing (BPI) protein [21-25] produced by polymorphonuclear neutrophils and targeted against endocytosed bacteria, has a functional role in LPS-binding and LPS detoxification. The crystallographic structure of BPI consists of two similar, extended domains. The four BPI residues are located at the distal tip of the N-terminal domain and a functional role in LPS-binding and LPS detoxification has been assigned to these highly conserved residues. Peptides derived from residues 17 to 45 and residues 65 to 99 of BPI inhibit the LPS-induced inflammatory response.

† Lactoferrin [26-30], an iron binding glycoprotein found at mucosal surfaces and in biological fluids, is released from neutrophil granules during the LPS-induced inflammatory response. The crystallographic structure of human lactoferrin is composed of two related globular lobes. Two spatially distinct putative LPS-binding sites have been identified for lactoferrin: residues 2 to 4 in combination with residues 28 to 34 form the N-terminal high-affinity LPS binding site. A second low-affinity LPS binding site is present in the C-terminal lobe. Synthetic peptides containing residues 28 to 34 of lactoferrin are bactericidal against gram-negative bacteria.

‡ Lysozyme [31,32], a cationic protein found in leukocyte polymorphonuclear granules reduces the immunostimulatory activities of LPS. Detailed information about specific LPS-lysozyme interactions is not available. The crystallographic structures of several different lysozyme types have been solved: human lysozyme, hen egg-white lysoyzme (C-type [33]), goose egg-white lysozyme (G-type, [34]), and bacteriophage T4 lysozyme (V-type, [35]). Although these proteins share a common fold, sequence comparisons between lysozyme types reveal no significant similarity.

§ The *Limulus* antibacterial and anti-LPS factor (LALF) [36-38] inhibits the LPS-induced coagulation cascade by binding LPS and neutralizing its endotoxic effects. The crystallographic structure of LALF contains a cluster of positively charged residues found on an amphipathic loop and on the adjacent residues of the basic face of LALF. Some of these residues have been previously proposed, but not demonstrated to be involved in LPS-binding. Synthetic cyclic peptides derived from residues 36 to 45 of LALF have been shown to bind and inhibit the LPS-induced immune response.

Acknowledgements

We gratefully acknowledge H. Brade for Western blots and for providing anti-*E. coli* K-12 antibodies; A. Hoess for providing LALF coordinates; H. Lüthje and A. Müller for technical assistance; D.M. Allan, M.A. Arbing, M.G. Baines, M. Cygler and D. Malo for reading the manuscript; and M. Kastowsky for ISIS draw files. This work was supported by the Deutsche Forschungsgemeinschaft (W.W.), by the Medical Research Council, Canada (J.W.C.) and by a NATO International Collaborative Research Grant. A.D.F. is recipient of a Deutscher Akademischer Austauschdienst Grant for Study and Research and a Medical Research Council of Canada Doctoral Research Award.

References

1. Mamat, U., Seydel, U., Grimmecke, D., Holst, O. & Rietschel, E.T. (1999). *Comprehensive Natural Products Chemistry.* (Pinto, M. ed), pp. 179-239, Elsevier Science, Amsterdam.
2. Holst, O. (1999). *Endotoxin in Health and Disease.* (Brade, H., Morrison, D.C., Opal, S. & Vogel, S. eds), pp. 115-154, Marcel Dekker Inc., New York.
3. Zähringer, U., Lindner, B. & Rietschel, E.T. (1999). *Endotoxin in Health and Disease.* (Brade, H., Morrison, D.C., Opal, S. & Vogel, S. eds), pp. 93-114, Marcel Dekker Inc., New York.
4. Medzhitov, R. & C. A. Janeway Jr., C.A. (1997). Innate Immunity: The virtues of a nonclonal system of recognition. *Cell* **91**, 295-298.
5. Hoffmann, J.A., Kaftatos, F.C., Janeway Jr., C.A. & Ezekowitz, R.A.B. (1999). Phylogenetic perspectives in innate immunity. *Science* **284**, 1313-1318.
6. Moeck, G.S. & Coulton, J.W. (1998). TonB-dependent iron acquisition: mechanisms of siderophore-mediated active transport. *Mol. Microbiol.* **28**, 675-681.
7. Ferguson, A.D., Hofmann, E., Coulton, J.W., Diederichs, K. & Welte, W. (1998). Siderophore-mediated iron transport: Crystal structure of FhuA with bound lipopolysaccharide. *Science* **282**, 2215-2220.
8. Raetz, C.R.H. (1996). *Escherichia coli* and *Salmonella*, Cellular and Molecular Biology. (Neidhardt, F.C. ed), pp. 1035-1063, American Society for Microbiology Press, Washington, DC.
9. Brandenburg, K., *et al.*, & Rietschel, E.T. (1996). Conformation of lipid A, the endotoxic center of bacterial lipopolysaccharide. *J. Endotoxin Res.* **3**, 173-178.
10. Nikaido, H. (1996). *Escherichia coli* and *Salmonella*, Cellular and Molecular Biology. (Neidhardt, F.C. ed), pp. 29-47, American Society for Microbiology Press, Washington, DC.
11. Cygler, M., Rose D.R. & Bundle, D.R. (1991). Recognition of a cell-surface oligosaccharide of pathogenic *Salmonella* by an antibody Fab fragment. *Science* **253**, 442-445.
12. Kastowsky, M., Sabisch, A., Gutberlet, T. & Bradaczek, H. (1991). Molecular

modelling of bacterial deep rough mutant lipopolysaccharide of *Escherichia coli*. *Eur. J. Biochem.* **197**, 707-716.

13. Guo, L., *et al.*, & Miller, S.I. (1998). Lipid A acylation and bacterial resistance against vertebrate antimicrobial peptides. *Cell* **95**, 189-198.
14. Hwang, P.M. & Vogel, H.J. (1998). Structure-function relationships of antimicrobial peptides. *Biochem. Cell Biol.* **76**, 235-246.
15. Kaca, W., de Jongh-Leuveninick, J., Zähringer, U., Rietschel, E.T., Brade, H., Verhoef, J., Sinnwell, V. (1988). Isolation and chemical analysis of 7-*O*-(2-amino-2-deoxy-alpha-D-glucopyranosyl)-L-*glycero*-D-*manno*-heptose. *Carbohydrate Res.* **179**, 289-299.
16. Lindner, B. (1999). *Methods in Molecular Biology: Bacterial Toxins*. (Holst, O. ed), Humana Press Inc., In press.
17. Jones, T.A., Zou, J.Y., Cowan, S.W. & Kjeldgaard, G. (1991). Improved methods for building protein models in electron density maps and the location of errors in these models. *Acta Cryst. A* **47**, 110-119.
18. Brünger, A.T., & Warren, G.L. (1998). Crystallography & NMR system: A new software suite for macromolecular structure determination. *Acta Cryst. D* **54**,905-921.
19. Kleywegt, G. (1999). Recognition of spatial motifs in protein structures. *J. Mol. Biol.* **285**, 1887-1897.
20. Kraulis, P. (1991). MOLSCRIPT: a program to produce both detailed and schematic plots of protein structures. *J. Appl. Crystallogr.* **24**, 946-950.
21. Merrit, E.A. & Bacon, D.J. (1997). Raster3D photorealistic molecular graphics. *Methods Enzymol.* **277**, 505-524.
22. Little, R.G., Kelner, D.N., Lim, E., Burke, D.J. & Conlon, P.J. (1994). Functional domains of recombinant bactericidal/permeability increasing protein (rBPI23). *J. Biol. Chem.* **269**, 1865-1872.
23. Beamer, L.J., Carroll, S.F. & Eisenberg, D. (1998). The BPI/LBP family of proteins: A structural analysis of conserved regions. *Prot. Sci.* **7**, 906-914.
24. Taylor, A.H., *et al.*, Ghrayeb, J. (1995). Lipopolysaccharide (LPS) neutralizing peptides reveal a lipid A binding site of LPS binding protein. *J. Biol. Chem.* **270**, 17934-17938.

25. Lamping, N., *et al.*, & Schumann, R.R. (1996). Effects of site-directed mutagenesis of basic residues (Arg94, Lys95, Lys99) of lipopolysaccharide (LPS)-binding protein on binding and transfer of LPS and subsequent immune cell activation. *J. Immunol.* **157**, 4648-4656.

26. Appelmelk, J., *et al.*, & Nuijens, J.H. (1994). Lactoferrin is a lipid A binding protein. *Infect. Immun.* **62**, 2628-2632.

27. Anderson, B.F., Baker, H.M., Norris, G.E., Rice, D.W. & Baker, E.N. (1989). Structure of human lactoferrin: Crystallographic structure analysis and refinement at 2.8 Å resolution. *J. Mol. Biol.* **209**, 711-734.

28. Van Berkel, P.H.C., *et al.*, & Nuijens, J.H. (1997). N-terminal stretch Arg2, Arg3, Arg4 and Arg5 of human lactoferrin is essential for binding to heparin, bacterial lipopolysaccharide, human lysozyme and DNA. *Biochem. J.* **328**, 145-151.

29. Elass-Rochard, E., *et al.*, & Spik, G. (1998). Lactoferrin inhibits the endotoxin interaction with CD14 by competition with the lipopolysaccharide-binding protein. *Infect. Immun.* **66**, 486-491.

30. Odell, E.W., Sarra, R., Foxworthy, M., Chapple, D.S. & Evans, R.W. (1996). Antibacterial activity of peptides homologous to a loop region in human lactoferrin. *FEBS Lett.* **382**, 175-178.

31. Brandenburg, K., Koch, M.H.J. & Seydel, U. Biophysical characterisation of lysozyme binding to LPS Re and lipid A. *Eur. J. Biochem.* **258**, 686-695 (1998).

32. Artymiuk, P.J. & Blake, C.C.F. (1981). Refinement of human lysozyme at 1.5 Å resolution. Analysis of nonbonded and hydrogen-bond interactions. *J. Mol. Biol.* **152**, 733-762.

33. Blake, C.C.F., *et al.*, Sarma, V.R. (1965). Structure of hen egg-white lysozyme. *Nature* **206**, 757-761.

34. Grütter, M.G., Weaver, L.H. & Matthews, B.W. (1983). Goose lysozyme structure: an evolutionary link between hen and bacteriophage lysozymes? *Nature* **303**, 828-831.

35. Matthews, B.W. & Remington, S.J. (1974). The three-dimensional structure of the lysozyme from bacteriophage T4. *Proc. Natl. Acad. Sci. USA* **71**, 4178-4182.

36. Warren, H.S., *et al.*, & Novitsky, T.J. (1992). Binding and neutralization of endotoxin

by *Limulus* antilipopolysaccharide factor. *Infect. Immun.* **60**, 2506-2513.

37. Hoess, A., Watson, S., Siber, G.R. & Liddington, R. (1993). Crystal structure of an endotoxin-neutralizing protein from the horseshoe crab, *Limulus* anti-LPS factor, at 1.5 Å resolution. *EMBO J.* **12**, 3351-3356.
38. Ried, C., *et al.*, & Hoess, A. (1996). High affinity endotoxin-binding and neutralizing peptides based on the crystals structure of recombinant *Limulus* anti-lipopolysaccharide factor. *J. Biol. Chem.* **271**, 28120-28127.

Preface to chapter six

An expansion of these structural studies was the determination of the crystallographic structures of additional liganded complexes of FhuA. This chapter describes the three-dimensional structure of FhuA in complex with the antibiotic albomycin and the siderophore phenylferricrocin at resolutions of 3.10 Å and 2.95 Å, respectively. Characteristic side-chain residues form the binding sites for albomycin and phenylferricrocin, and binding of these ligands to FhuA induces conformational changes identical to those previously observed for ferricrocin. One method of drug delivery, in which potent antimicrobial agents covalently linked to iron-chelating siderophores are actively transported across the gram-negative outer membrane, involves the design and application of siderophore-antibiotic conjugates as antimicrobial agents. In addition to probing the plasticity and accessibility of the ligand-binding site of FhuA, these results establish a structural platform for the rational design of hydroxamate-type siderophore-antibiotic conjugates. By combining compatible iron-chelating siderophores, peptide linkers and antibiotic groups, a large variety of novel antibiotics may be chemically synthesized, and potentially used to combat infections by bacteria that have acquired multidrug resistance.

Crystal structure of the antibiotic albomycin in complex with the outer membrane transporter FhuA

Andrew D. Ferguson[1,2], Volkmar Braun[3], Hans-Peter Fiedler[4], James W. Coulton[1], Kay Diederichs[2], Wolfram Welte[2]

1 Fakultät für Biologie, Universität Konstanz, M656, D-78457 Konstanz, Germany

2 Department of Microbiology and Immunology, McGill University, 3775 University Street, Montreal, Quebec, Canada H3A 2B4

3 Lehrstuhl Mikrobiologie/Membranphysiologie, Universität Tübingen, Auf der Morgenstelle 28, D-72076 Tübingen, Germany

4 Lehrstuhl Mikrobiologie / Biotechnologie, Universität Tübingen, Auf der Morgenstelle 28, D-72076 Tübingen, Germany

Abstract

One alternative method for drug delivery involves the use of siderophore-antibiotic conjugates. These compounds represent a specific means by which potent antimicrobial agents, covalently linked to iron-chelating siderophores, can be actively transported across the outer membrane of gram-negative bacteria. These 'Trojan Horse' antibiotics may prove useful as an efficient means to combat multidrug resistant bacterial infections. Here we present the crystallographic structures of the natural siderophore-antibiotic conjugate albomycin and the siderophore phenylferricrocin, in complex with the active outer membrane transporter FhuA from *Escherichia coli*. To our knowledge, this represents the first structure of an antibiotic bound to its cognate transporter. Albomycins are broad-host range antibiotics that consist of a hydroxamate-type iron-chelating siderophore, and an antibiotically active, thioribosyl pyrimidine moiety. As observed with other hydroxamate-type siderophores, the three-dimensional structure of albomycin reveals identical coordination geometry surrounding the ferric iron atom. Unexpectedly, this antibiotic assumes two conformational isomers in the binding site of FhuA, an extended and a compact form. The structural information derived from this study provides novel insights into the diverse array of antibiotic moieties that can be linked to the distal portion of iron-chelating siderophores, and offers a structural platform for the rational design of hydroxamate-type siderophore-antibiotic conjugates.

Key words: FhuA; antibiotic; albomycin; siderophore-antibiotic conjugate; TonB-dependent outer membrane transporter; rational drug design

Introduction

Bacterial virulence is often related to an organism's ability to compete for essential nutrients (Martinez, 1990). The virtual insolubility of ferric iron under oxygen-rich conditions severely restricts bacterial growth. To satisfy their iron requirement most bacteria have evolved a diverse series of high-affinity iron acquisition systems that are dependent upon the synthesis and/or uptake of low molecular weight iron-chelators termed siderophores (Neilands, 1995; Braun et al. 1998). Transporters bind these iron-chelates with high-affinity and mediate their uptake across the outer membrane of gram-negative bacteria with an energy-dependent mechanism of transport. The energy required to translocate these compounds is derived from the proton motive force of the cytoplasmic membrane as transduced by the TonB-ExbB-ExbD complex (Braun, 1995).

The diverse range of siderophores that are transported by TonB-dependent transport systems can be exploited to develop novel strategies for drug delivery. The concept that siderophore analogues, termed siderophore-antibiotic conjugates, can be actively transported across the bacterial cell envelope is well-established (Roosenberg et al. 2000). Albomycins are 'natural' iron-chelating siderophores of fungal origin that display broad-spectrum bactericidal activity against both gram-positive and gram-negative bacteria (Knüsel & Zimmermann, 1975). The following bacterial strains are sensitive to albomycin: *E. coli*, *Staphylococcus aureus* and other Staphylococci, *Bacillus subtilis*, *Klebsiella pneumoniae*, *Streptococcus pneumoniae*, *Salmonella species*, *Bordetella pertussis*, and *Spirochaeta* spp. In contrast, *Listeria*, *Mycobacterium tuberculosis*, and *Bacillus mycoides* are albomycin-resistant (Nüesch & Knüsel, 1967). The exquisite inhibitory activity of albomycins (minimal inhibitory concentration of 0.005 μg/mL, compared to 0.1 μg/mL for ampicillin; Pugsley et al. 1987) depends upon their ability to utilize the ferric hydroxamate uptake system for their uptake across both the outer and cytoplasmic membranes. FhuA actively transports albomycin, a structural analogue of the fungal siderophore ferrichrome, across the outer membrane of *E. coli*. Once translocated into the periplasm, the antibiotic is bound by the periplasmic binding protein FhuD (Rohrbach et al. 1995), shuttled to an ABC transporter embedded within the cytoplasmic membrane (FhuBC), and actively transported into the cytoplasm (Schultz-

Hauser et al. 1992). Bacterial mutants with *fhuBCD* deletions are unable to transport albomycin across the cell envelope, and thus, are resistant to its antimicrobial effects (Kadner et al. 1980).

Similar to ferrichrome and its structural analogues, ferricrocin and phenylferricrocin, the iron-chelating component of albomycin is a tri-δ-*N*-hydroxy-δ-*N*-acetyl-L-ornithine peptide. Covalently linked to the iron-binding component of albomycin, by a short amino acetyl linker, is a thioribosyl pyrimidine antibiotic group (Hartmann et al. 1979). The chemical structures (Benz et al. 1982) and the thioribosyl pyrimidine substituent conformations in aqueous solution (Benz et al. 1984) of three albomycin subtypes (δ_1, δ_2, and ε) synthesized by *Streptomyces* strain WS116 have been determined. Substitution of the thioribosyl moiety with a ribosyl analogue abolishes the antimicrobial activity of δ_1-albomycin (Paulsen et al. 1987). In *E. coli*, enzymatic cleavage of the antibiotic group from the iron-chelating portion of albomycin is accomplished by peptidase N. Bacterial mutants devoid of peptidase N activity are albomycin-resistant, indicating that peptidase-mediated cleavage is essential for albomycin to exert its bactericidal activity (Braun et al. 1983). While the transport and activation pathways of albomycin are known, the intracellular target remains to be determined. The absence of albomycin-resistant target site mutants suggests that albomycin interferes with critical bacterial cell functions or has multiple intracellular targets.

Results and discussion

We have determined the three-dimensional structures of FhuA in complex with phenylferricrocin and albomycin at 2.95 Å and 3.10 Å resolution, respectively (Fig. 1 and Table 1). The structures of unliganded FhuA and FhuA in complex with ferricrocin (Ferguson et al. 1998a) and ferrichrome (Locher et al. 1998) are also available. These crystallographic structures show that FhuA is organized into two domains (Fig. 2A). The elliptical-shaped β-barrel domain is formed by 22 antiparallel transmembrane β-strands. The cork domain, consisting of a mixed four-stranded β-sheet and a series of short α-helices, fills the barrel interior. The presence of the cork domain delineates a pair of pockets within FhuA. The larger extracellular pocket is open to the external medium

while the smaller periplasmic pocket is in contact with the periplasm. The interior walls of the extracellular pocket, extracellular loops and strands of the barrel domain are lined with aromatic residues (Fig. 2B). Hydroxamate-type siderophores such as phenylferricrocin and albomycin, are polar but uncharged at physiological pH, and are not inherently hydrophobic. The aromatic side chain residues that line the inner walls of the extracellular pocket may function to extract the siderophore from the external medium.

Located within the extracellular pocket of FhuA, above the external outer membrane interface, is a single ligand molecule (Fig. 2A and 2B). The iron-chelating components of phenylferricrocin and albomycin are bound to FhuA in the same orientation and by the same side chain residues (Fig. 2B) as previously observed with ferricrocin (Ferguson et al. 1998a) and ferrichrome (Locher et al. 1998). Residues from the extracellular pocket, apices A (Arg81), B (Gln100) and C (Tyr116) of the cork domain and from the barrel domain, form hydrogen bonds or van der Waals contacts with the phenylferricrocin (Fig. 3A, 4A, and Table 2) or albomycin molecule (Fig. 3B, 3C, 4B, and Table 3).

Due to inherent flexibility of the amino acetyl linker connecting the iron-chelating moiety of albomycin to the thioribosyl pyrimidine substituent, two albomycin conformations, an extended and a compact conformational isomer, have been identified in the binding site of FhuA. These transport-active albomycin conformations may only represent a small portion of a larger set of conformations that exist in aqueous solution. The extended conformational isomer extends upward into the extracellular loops of FhuA, while the compact conformational isomer fills part of the lower portion of the extracellular pocket. Side chain residues from the extracellular pocket, extracellular loops, and strands of the barrel domain form numerous hydrogen bonds and van der Waals contacts with both conformational isomers (Fig. 3B, 3C, 4B and Table 3). In accord with the composition of the ligand-binding sites, deletion of residues 236 to 248 (Killmann et al. 1998) or insertion of a tetrapeptide after residue 241 (Koebnik & Braun, 1993) inhibits ferrichrome and albomycin transport. Furthermore, preincubation of ferricrocin with bacterial cells expressing the wild-type receptor inhibits cell killing by albomycin (Pugsley et al. 1987). These liganded complexes of FhuA provide a structural

explanation for the competitive binding of albomycin and ferricrocin to the binding site of the transporter.

Structural alignment of the α-carbon coordinates of FhuA and its liganded complexes reveals near perfect superposition (root-mean-square deviation of 0.25 Å) of the barrel domains. However, two distinct conformations, unliganded and liganded, are observed in the cork domain. Upon ligand binding to FhuA an upward translation (1 - 2 Å) of apices A and B, and other residues of the cork domain is observed. This movement is propagated to the periplasmic pocket of FhuA, promoting the unwinding of an amino proximal α-helix designated the switch helix (Ferguson et al. 1998a, Locher et al., 1998). The structures of FhuA complexed with ferrichrome, ferricrocin, phenylferricrocin and albomycin are virtually identical with regard to the protein and the bound iron-chelating component of the ligand. This conservation of the allosteric transition suggests that all liganded complexes promote FhuA's interaction with TonB, which is presumably mediated by the TonB-box of the transporter (Moeck & Coulton, 1998).

Early investigations into the application of siderophore-antibiotic conjugates as antimicrobial agents were provided by Zähner et al. (1977). In this study, a series of ferricrocin and ferroxamine B-based siderophore-antibiotic conjugates were synthesized, and their antimicrobial activities assessed. These early studies have been amplified by the synthesis of a large variety of hydroxamate and catechol-type siderophore-antibiotic conjugates. Many of these compounds display strong antimicrobial activity, and are actively transported across the outer membrane by TonB-dependent receptors (Diarra et al. 1996; Ghosh et al. 1996). However, the loss of specific outer membrane transporters may facilitate the development of resistance to certain classes of structurally related siderophore-antibiotic conjugates (Brochu et al. 1992; Minnick et al. 1992; Diarra et al. 1996). Developing siderophore-antibiotics conjugates that target more than one TonB-dependent receptor, which function both as transporters and bacterial virulence factors (Roosenberg et al. 2000) could minimize resistance to these agents. Moreover, spontaneous *tonB* mutations would severely restrict bacterial growth *in vivo*, as all TonB-dependent activity would be disrupted.

Siderophore-antibiotic conjugates consist of three parts: an iron-chelating siderophore, a peptide linker, and an antibiotic group. The principle requirement in the

design of these compounds is that the siderophore must be recognized, and thereby transported across the outer membrane. The available liganded complexes provide the structural basis for ligand recognition by FhuA. Most hydrogen bonds and van der Waals contacts are formed between the iron-chelating component of the siderophore and characteristic side chain residues from apices A, B, and C of the cork domain, and the extracellular loops and strands of the barrel domain. The structural composition of the binding site surrounding the iron-chelating component of the siderophore is spatially restrictive, demonstrating that recognition of hydroxamate-type siderophore analogues by FhuA is based primarily on the conformation of the iron-chelating component. It has been shown that chemical or conformational alteration of this portion of the siderophore abrogates receptor-specific recognition (Jurkevitch et al. 1992). The remaining portions of the siderophore are bound less tightly, with few apparent constraints on the chemical structure, conformation or the spatial requirements of the linker or the antibiotic substituent. Furthermore, the size of the extracellular pocket of FhuA has the potential to accommodate larger siderophore-antibiotic conjugates.

The tolerant constraints imposed upon the binding of hydroxamate-type siderophore analogues may also apply to ligand transport. The precise transport mechanism has not been elucidated. However, according to our proposal (Ferguson et al. 1998a), formation of the FhuA-TonB complex induces conformational changes in the cork domain, which disrupt the high-affinity ligand-binding site, and thus promote the release of the ligand from its binding site. This event is followed or accompanied by the formation of a channel located between the inner barrel wall and the cork domain termed the putative channel-forming segment. These tolerant binding constraints are in accord with this proposed transport mechanism (Ferguson et al. 1998a). Moreover, the fact that active transport is mediated by FhuA and the FhuBC complex, suggests that both transporters may recognize the iron-chelating component of hydroxamate-type siderophores and their analogues. In conclusion, these results provide a structural basis for the design of hydroxamate-type siderophore-antibiotic conjugates. Using rational modular design, a large variety of designer antibiotics may be chemically synthesized by combining compatible iron-chelating siderophores, peptide linkers, and potent antibiotic groups. By

utilizing specific siderophore receptors for their transport across the cell envelope antimicrobial agents of this type may selectively target and ultimately kill bacteria.

Materials and methods

Protein expression, purification and crystallization

A recombinant FhuA protein was constructed by inserting a hexahistidine tag plus five additional linker residues (SSHHHHHHGSS) into the *fhuA* gene after residue 405 (Moeck et al. 1994; 1996). FhuA was expressed and purified as previously described (Ferguson et al. 1998a; 1998b). δ_2-albomycin (albomycin) was purified from *Streptomyces griseus* strain TÜ 6 as previously described (Fiedler et al. 1985). FhuA was co-crystallized with albomycin and phenylferricrocin and one LPS molecule using a final ligand concentration of 0.3 mM. Crystals of FhuA were grown using the hanging drop vapor diffusion technique by mixing equal volumes (5 µL) of FhuA [10 mg/mL, 0.80% N,N-dimethyldecylamine-N-oxide and 10 mM ammonium acetate (pH 8.0)] and reservoir solution [12% polyethylene glycol (PEG) 2,000 monomethyl ether, 0.1 M sodium cacodylate (pH 6.4), 20% glycerol, 3% PEG 200, and 1% *cis*-inositol]. Crystals grew within seven days to a final size of 200 by 200 by 200 μm^3 at 18°C. All crystals were mounted in cryo-loops and flash frozen by direct immersion in liquid nitrogen.

Crystallographic data collection, structure determination and refinement

All X-ray diffraction data were collected at 100 K using a cryo-stream apparatus with synchrotron radiation at beam line I711, Max Lab-II (Table 1). X-ray diffraction data were processed and reduced using the program XDS (Kabsch, 1988). Initial phases for both liganded FhuA-complexes were calculated using the FhuA-ferricrocin coordinates (1qff.pdb) as an initial model. Structural models for both FhuA-ligand complexes were built into an experimental electron density map using the program O (Jones et al. 1991). Both models were refined with the program CNS using molecular dynamics and the maximum likelihood target (Brünger et al. 1998). Following rounds of model building and structural refinement the final models contain residues 19 to 714, one lipopolysaccharide molecule, one ligand molecule (albomycin or phenylferricrocin), and 332 and 299 water molecules for the FhuA-albomycin and FhuA-phenylferricrocin models, respectively. The lipopolysaccharide molecule is noncovalently bound to the

membrane-embedded surface of FhuA, and forms electrostatic and van der Waals contacts with side chain residues from β7 through β11.

Figures

All color figures were prepared using MOLSCRIPT (Kraulis, 1991) and Raster3D (Merrit & Bacon, 1997). Fig. 4 was prepared with the program ISIS Draw.

Protein Data Bank accession codes

Both sets of crystallographic coordinates have been deposited in the Protein Data Bank with the following accession codes: 1qkc (FhuA in complex with albomycin) and 1qjq (FhuA in complex with phenylferricrocin).

Table 1. Crystallographic data

Data collection and reduction		
Space group	$P6_1$	$P6_1$
Unit cell *a* (Å)	172.10	171.90
b (Å)	172.10	171.90
c (Å)	87.65	87.55
Number of molecules per asymmetric unit	1	1
Number of measured reflections	231,385	197,612
Number of unique reflections	31,400	38,021
Completeness (%)	94.8 (82.0)	94.9 (94.3)
Resolution (Å)	2.95	3.10
R_{sym} (%)	6.4 (22.0)	13.9 (34.9)
R_{meas} (%)	6.8 (25.8)	15.0 (40.2)
$R_{merge\text{-}F}$ (%)	6.5 (29.1)	15.3 (36.1)
I/σ	19.6 (3.8)	6.16 (2.2)
Structural refinement		
R_{cryst} (%)	22.5	22.2
R_{free} (%)	27.8	28.3
Root mean square deviation		
Bond lengths (Å)	0.008	0.020
Bond angles (°)	1.8	2.3
Dihedral angles (°)	26.2	25.8
Improper angles (°)	0.88	2.82

All X-ray diffraction data were collected at Max-Lab II beam line I711 (Lund, Sweden) at a temperature of 100 K using a wavelength of 1.051 Å. Brackets indicate the highest resolution shell.

Table 2. FhuA-phenylferricrocin interactions

Residue-Atom	Location	Distance	Type of Interaction
Arg 81-NH1	Apex A	2.8 Å	Hydrogen bond with the O8 atom
Arg 81-NH2	Apex A	2.7 Å	Hydrogen bond with O3 atom
Tyr 87-CE2	Coil region of the cork domain	3.9 Å	van der Waals contact with C35 atom
Gly 99-N	Apex B	3.6 Å	Electrostatic interactions with O17 atom
Gln 100-CG	Apex B	3.1 Å	van der Waals contact with C37 atom
Phe 115-CD1	Apex C	3.9 Å	van der Waals contact with the C27 atom
Tyr 116-OH	Apex C	2.8 Å	Hydrogen bond with O10 atom
Tyr 244-OH	L3	2.7 Å	Hydrogen bond with O6 atom
Trp 246-NE1	L3	3.1 Å	Hydrogen bond with O3 atom
Tyr 313-CZ	β7	3.5 Å	van der Waals contact with C25 atom
Tyr 315-OH	L4	3.2 Å	Hydrogen bond with O1 atom
Phe 391-CE2	β9	3.5 Å	van der Waals contact with O4 atom
Phe 693-CE1	L11	3.8 Å	van der Waals contact with C34 atom

Listed are the residue-atom, location, distance, and type of interaction formed between all FhuA side chain residues within 4 Å of phenylferricrocin atoms. See Fig. 2A for further details of the hydrogen bonding pattern and electrostatic interactions between FhuA and phenylferricrocin.

Table 3. FhuA-albomycin interactions

Residue-Atom	Location	Distance	Type of Interaction
Arg 81-NH1*†	Apex A	3.0 Å	Hydrogen bond with the O5 atom
Arg 81-NH2*†	Apex A	3.1 Å	Hydrogen bond with O1 atom
Gly 99-O*†	Apex B	3.7 Å	van der Waals contact with C13 atom
Gln 100-O*†	Apex B	3.7 Å	van der Waals contact with C18 atom
Phe 115-CZ*	Apex C	3.7 Å	van der Waals contact with the O17 atom
Tyr 116-OH*†	Apex C	3.0 Å	Hydrogen bond with N3 atom
Tyr 244-OH*†	L3	2.9 Å	Hydrogen bond with O3 atom
Trp 246-NE1*†	L3	3.5 Å	Hydrogen bond with O1 atom
Tyr 313-OH*†	β7	3.5 Å	van der Waals contact with C9 atom
Tyr 315-OH†	L4	3.1 Å	Hydrogen bond with the O12 atom
Lys 344-NZ†	β9	3.7 Å	Electrostatic interactions with the O12 atom
Phe 391-CG*	β9	3.0 Å	van der Waals contact with O18 atom
Phe 391-CD2†	β9	3.9 Å	van der Waals contact with C12 atom
Tyr 393-CD1*	L5	3.2 Å	van der Waals contact with O12 atom
Tyr 393-CD1†	L5	3.5 Å	van der Waals contact with O12 atom
Tyr 423-OH*	β10	3.7 Å	Electrostatic interactions with O15 atom
Gln 505-OE1*	L7	2.7 Å	Hydrogen bond with O16 atom
Gln 505-NE2*	L7	3.0 Å	Hydrogen bond with N10 atom
Phe 557-O†	β15	2.8 Å	Hydrogen bond with N11 atom
Phe 558-CE1†	β15	3.0 Å	van der Waals contact with N10 atom
Phe 693-CE2*†	L11	3.5 Å	van der Waals contact with C20 atom

Listed are the residue-atom, location, distance, and type of interaction formed between all FhuA side chain residues within 4 Å of albomycin atoms. Those interactions that are specific to the compact albomycin conformational isomer are marked with an asterisk (*); those that are specific for the extended albomycin conformational isomer are denoted with a dagger (†). See Fig. 2B for further details of the hydrogen bonding pattern and electrostatic interactions between FhuA and albomycin.

Figure 1. Representative electron density section of the FhuA-albomycin complex. Stereoview of the final $3F_{obs}$ - $2F_{calc}$ electron density map contoured at 2σ (orange) and 1 σ (green) at a resolution of 3.10 Å showing the albomycin-binding site. Both conformational isomers of the albomycin molecule are presented. The extended conformational isomer is shown with carbon atoms white, oxygen atoms red, nitrogen atoms blue, and sulfur atoms yellow. The thioribosyl pyrimidine group of the compact conformational isomer is colored purple. The ferric iron atom is shown as a large red sphere.

A

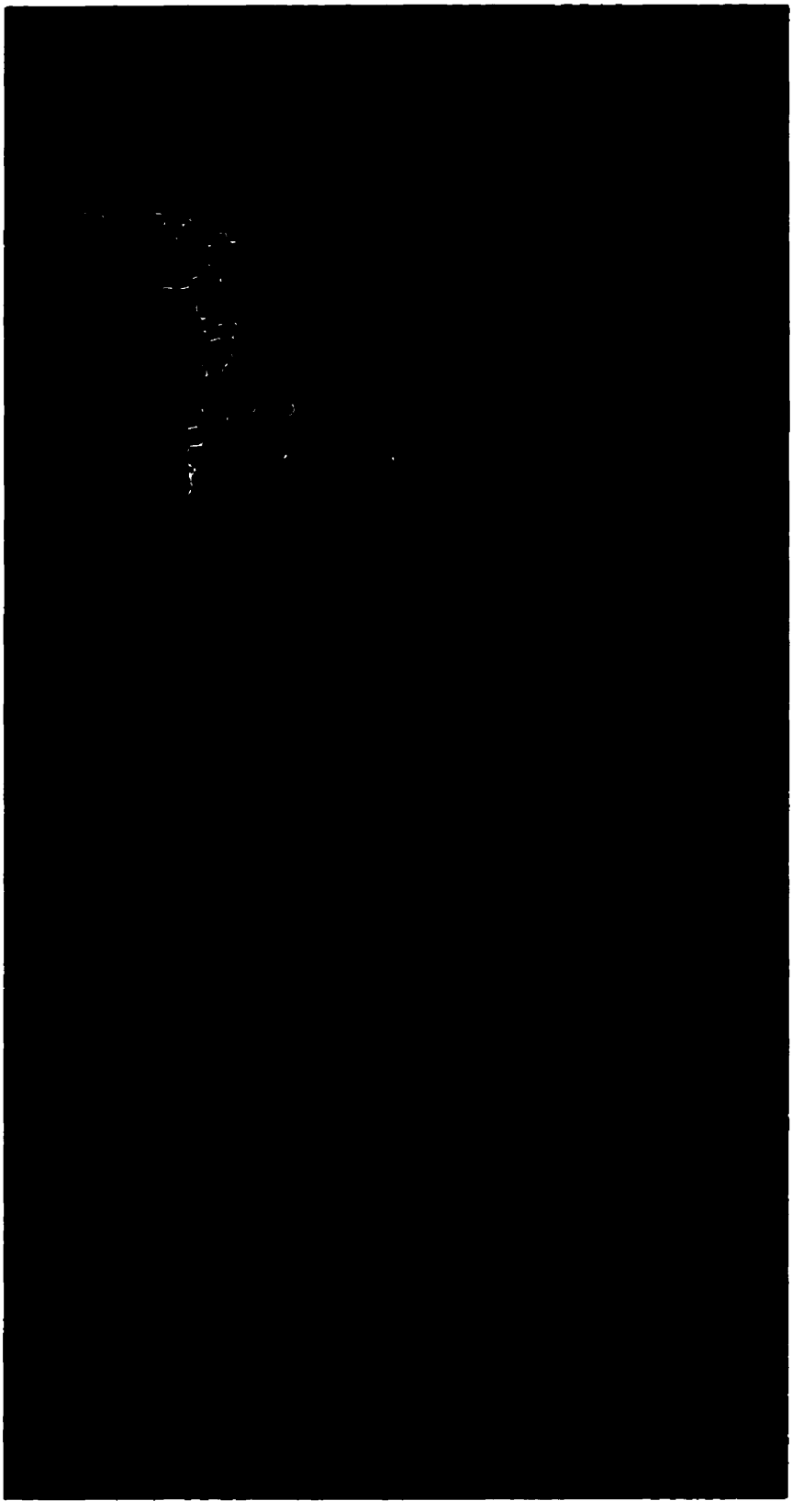

B

Figure 2. The FhuA-albomycin-lipopolysaccharide complex. **A**: General description of the complex. The view is perpendicular to the barrel axis. Those strands, which form the front of the barrel domain, have been removed to provide an unobstructed view of the cork domain. **B**: The external aromatic cavity of the complex as viewed from the external environment. Those side chain residues (Tyr 244, Trp 246, Tyr 275, Tyr 313, Tyr 315, Tyr 325, Tyr 345, Trp 379, Phe 391, Phe 410, Phe 412, Tyr 423, Phe 513, Phe 558, Tyr 595, Tyr 601, Phe 650, Phe 693, Tyr 696 and Phe 699), which compose the external aromatic cavity are colored green. In both panels, the barrel domain and the cork domain are colored blue and yellow, respectively. The extended albomycin conformational isomer and the lipopolysaccharide molecule are shown as a bond model with carbon atoms white, sulfur atoms yellow, oxygen atoms red, and nitrogen atoms blue. The ferric iron atom is shown as a large red sphere.

A

Figure 3. The FhuA-ligand binding site. **A**: The FhuA-phenylferricrocin binding site. **B**: The FhuA-albomycin binding site (extended conformational isomer). **C**: The FhuA-albomycin binding site (compact conformational isomer). In each panel, all FhuA residues that form direct hydrogen bonds or van der Waals contacts with ligand (phenylferricrocin or albomycin) atoms are labeled and colored green. The ligands are shown as bond models with carbon atoms white, sulfur atoms yellow, oxygen atoms red, and nitrogen atoms blue. In both panels, the ferric iron atom is shown as a large red sphere. In panels, B and C, Lys 344 from β8 and Tyr 423 from β10 are not shown to ensure an unobstructed view of albomycin.

B

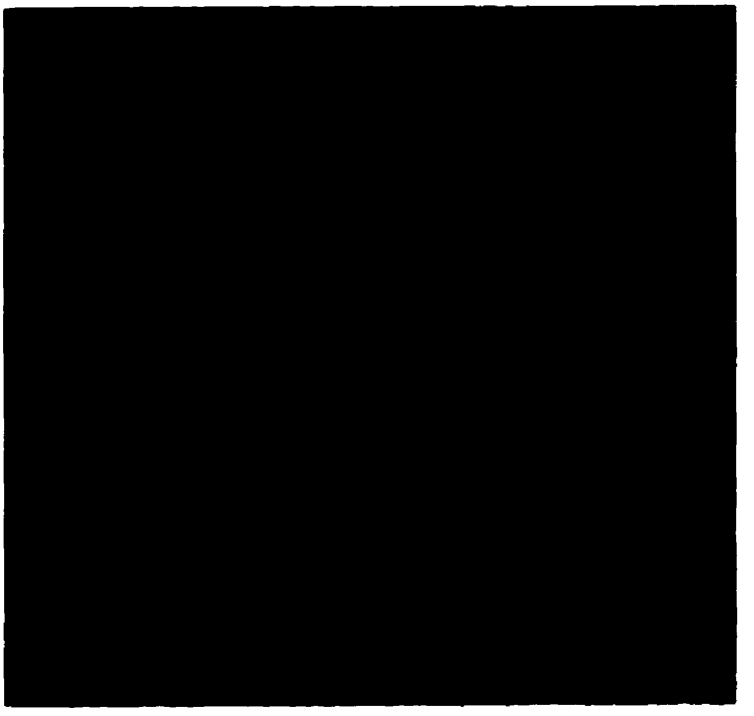

C

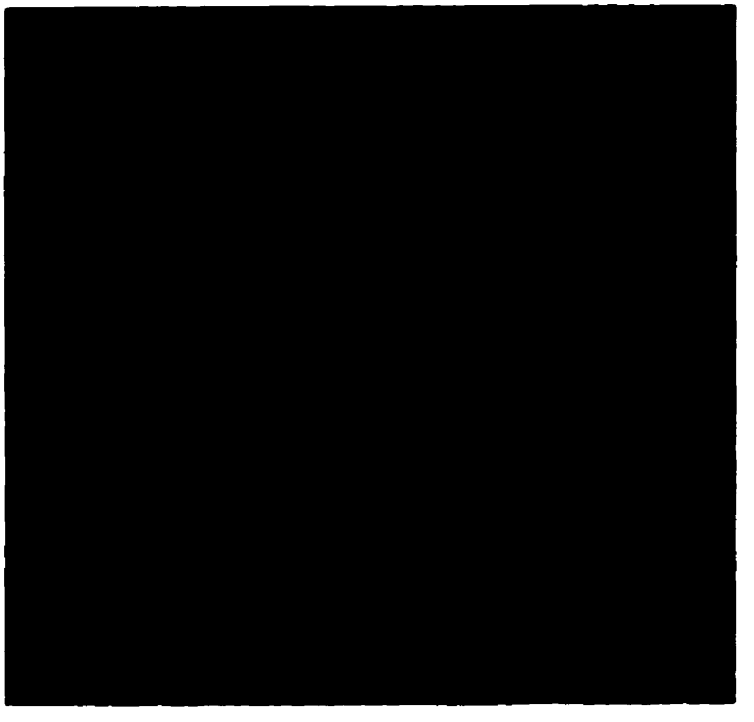

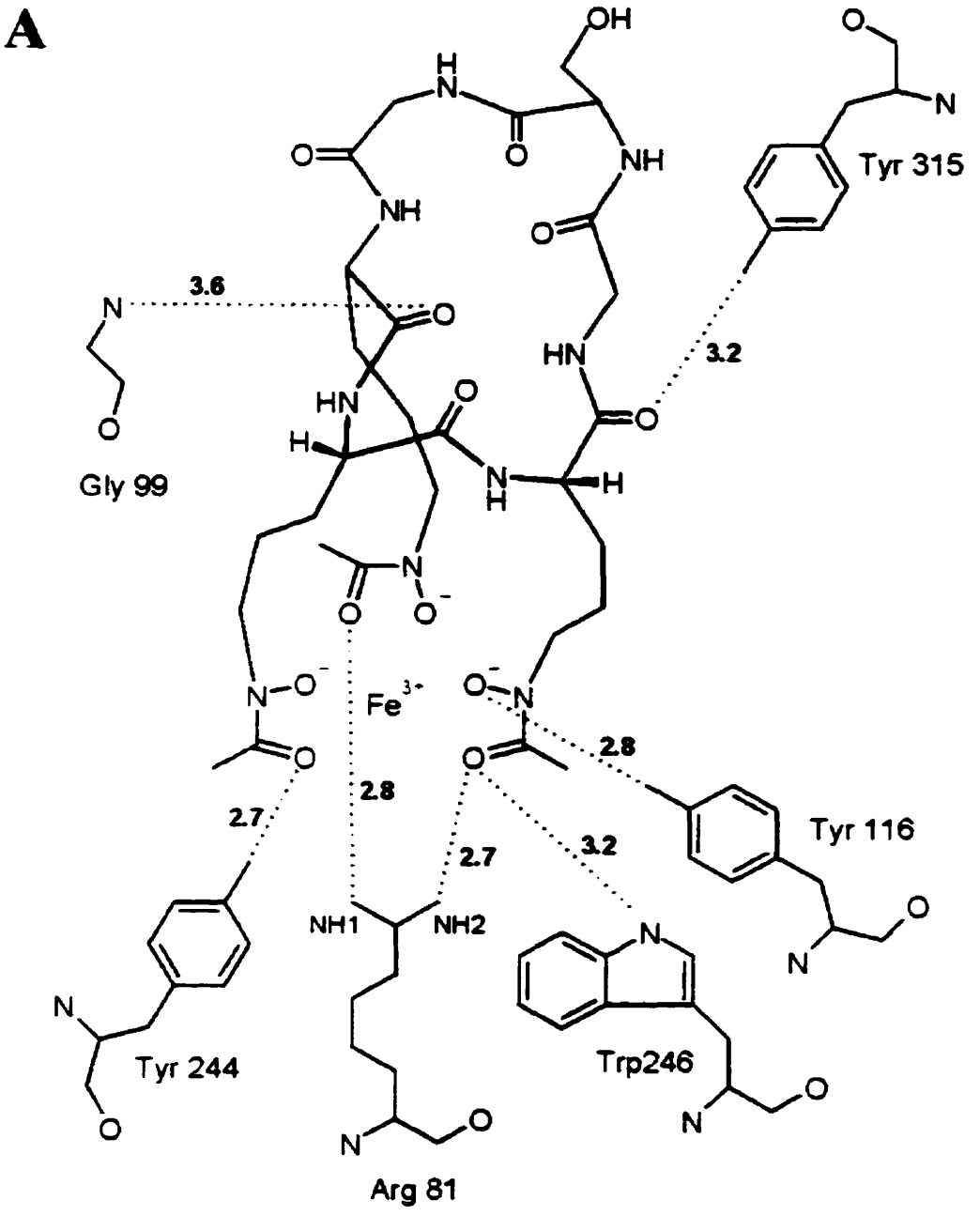

Figure 4. Schematic comparison of the hydrogen bonding pattern and electrostatic interactions of **A:** phenylferricrocin and **B:** albomycin (extended conformational isomer) with FhuA side chain residues in the ligand-binding site. The chemical structures of phenylferricrocin and albomycin are shown with hydrogen bonds and charge interactions indicated as dotted lines (distances are given in Å). See Table 2 (phenylferricrocin) and Table 3 (albomycin) for additional van der Waals contacts.

B

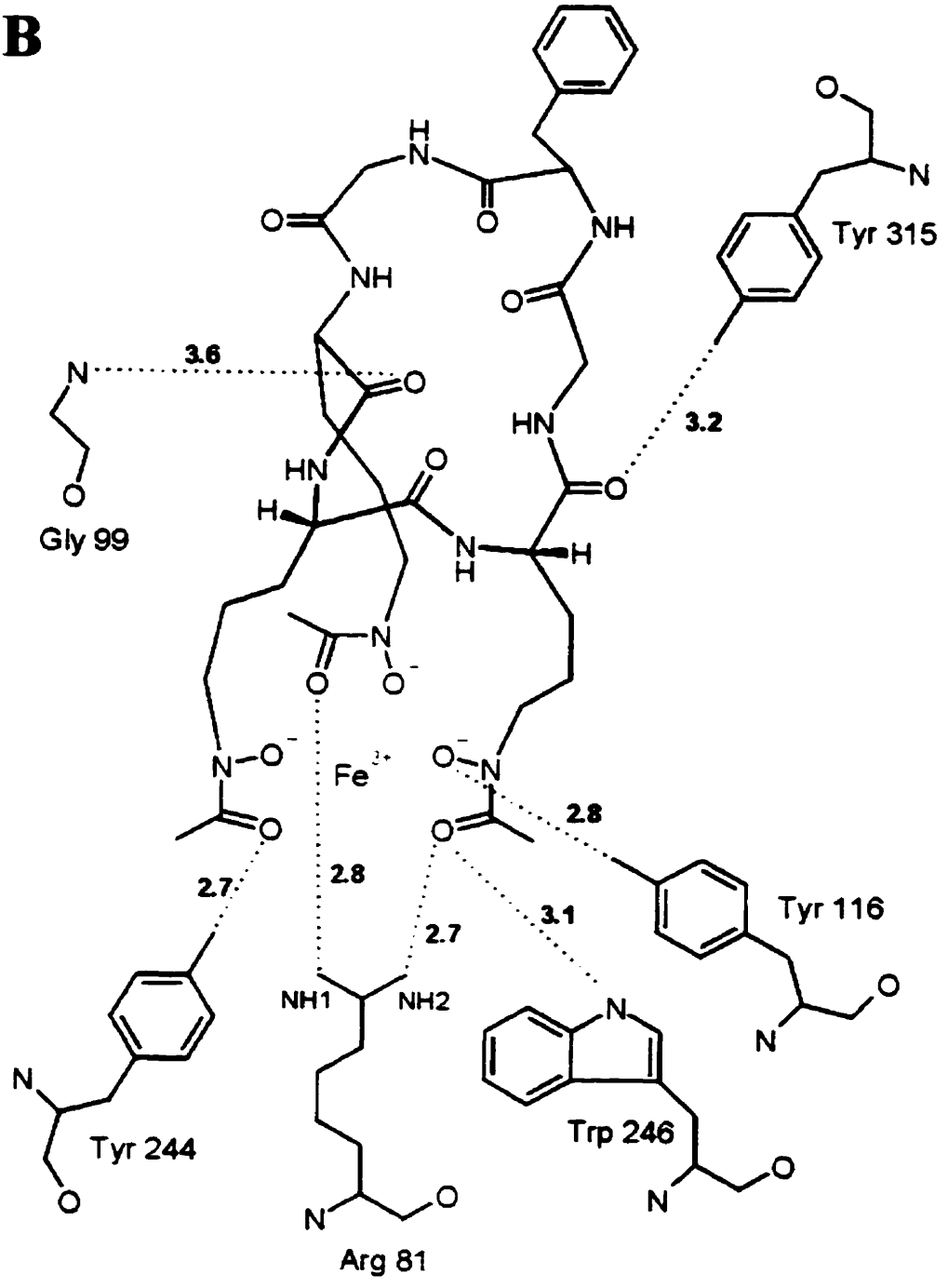
Gly 99
3.6
Tyr 315
3.2
Fe3+
2.8
2.7
2.8
2.7
3.1
2.8
Tyr 116
Tyr 244
NH1
NH2
Trp 246
Arg 81

C

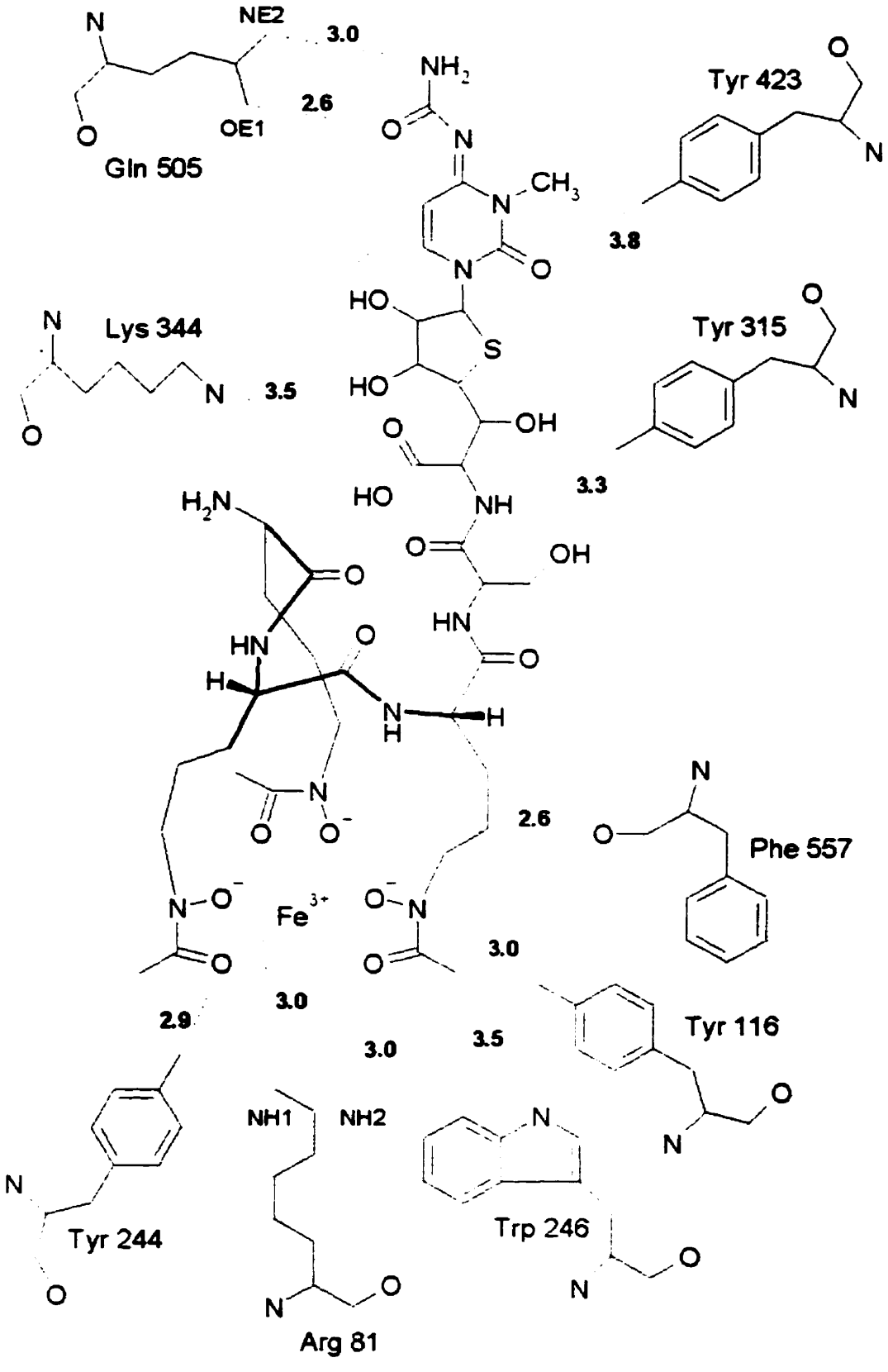
NE2
3.0
2.6
OE1
Gln 505
Tyr 423
3.8
Lys 344
3.5
Tyr 315
3.3
2.6
Phe 557
3.0
3.0
2.9
3.0
3.5
Tyr 116
NH1
NH2
Tyr 244
Trp 246
Arg 81

Acknowledgements

We gratefully acknowledge A. Svensson at Max-Lab II (beam line I711) for his assistance during data collection and J. Ködding for figure preparation. This work is supported by the Deutsche Forschungsgemeinschaft (to VB and WW), and by the Medical Research Council of Canada (to JWC). ADF is the recipient of a Deutscher Akademischer Austauschdienst Grant for Study and Research and a Medical Research Council of Canada Doctoral Research Award.

References

Benz G, Schröder T, Kurz J, Wünsche C, Karl W, Steffens G, Pfitzner J, Schmidt D. 1982. Konstitution der Desferriform der Albomycine δ_1, δ_2, ε. *Angew Chem Suppl* 1322-1335.

Benz G, Born L, Brieden M, Grosser R, Kurz J, Paulsen H, Sinnwell V, Weber B. 1984. Absolute Konfiguration der Desferriform der Albomycine. *Liebigs Ann Chem*:1408-1423.

Braun V, Günther K, Hantke K, Zimmermann L. 1983. Intracellular activation of albomycin in *Escherichia coli* and *Salmonella typhimurium*. *J Bacteriol 156*:308-315.

Braun V. 1995. Energy-coupled transport and signal transduction through the gram-negative outer membrane via TonB-ExbB-ExbD-dependent receptor proteins. *FEMS Microbiol Rev 16*:295-307.

Braun V, Hantke K, Köster W. 1998. Iron transport and storage in microorganisms, plants, and animals. In: Siegel A, Siegel H. eds. *Metal Ions in Biological Systems*. New York, NY: Marcel Dekker. pp 67-145.

Brochu A, Brochu N, Nicas T, Parr Jr TR, Minnick Jr AA, Dolence EK, McKee JA, Miller MJ, Lavoie MC, Malouin F. 1992. Modes of action and inhibitory activities of new siderophore-β-lactam conjugates that use specific iron uptake pathways for entry into bacteria. *Antimicrobial Agents Chemother 36*:2166-2175.

Brünger AT, Adams PD, Clore GM, DeLano WL, Gros P, Grosse-Kunstleve RW, Jiang J-S Kuszewski J, Nilges M, Pannu NS, Read RJ, Rice LM, Simonson T, Warren GL. 1998. Crystallography & NMR system: A new software suite for macromolecular structure determination. *Acta Cryst D 54*:905-921.

Diarra MS, Lavoie MC, Jacques M, Darwish I, Dolence EK, Dolence JA, Ghosh A, Ghosh M, Miller MJ, Malouin F. 1996. Species selectivity of new siderophore-drug conjugates that use specific iron uptake for entry into bacteria. *Antimicrobial Agents Chemother 40*:2610-2617.

Ferguson AD, Hofmann E, Coulton JW, Diederichs K, Welte W. 1998a. Siderophore-mediated iron transport: Crystal structure of FhuA with bound lipopolysaccharide. *Science 282*:2215-2220.

Ferguson AD, Breed J, Diederichs K, Welte W, Coulton JW. 1998b. An internal affinity-tag for purification and crystallization of the siderophore receptor FhuA, integral outer membrane protein from *Escherichia coli* K-12. *Prot Sci 7*:1636-1638.

Fiedler H-P, Walz F, Döhle A, Zähner H. 1985. Albomycin: Studies on fermentation, isolation and quantitative determination. *Appl Microbiol Biotechnol 21*:341-347.

Ghosh A, Ghosh M, Niu C, Malouin F, Moellmann U, Miller MJ. 1996. Iron transport-mediated drug delivery using mixed-ligand siderophore-β-lactam conjugates. *Chem Biol 3*:1011-1019.

Hartmann A, Fiedler H-P, Braun V. 1979. Uptake and conversion of the antibiotic albomycin by *Escherichia coli* K-12. *Eur J Biochem 99*:517-524.

Jones TA, Zou JY, Cowan SW, Kjeldgaard M. 1991. Improved methods for building protein models in electron density maps and the location of errors in these models. *Acta Cryst A 47*:110-119.

Jurkevitch E, Hadar Y, Chen Y, Libman J, Shanzer A. 1992. Iron uptake and molecular recognition in *Pseudomonas putida*: Receptor mapping with ferrichrome and its biomimetic analogs. *J Bacteriol 174*:78-83.

Kabsch W. 1988. Evaluation of single crystal X-ray diffraction data from a position sensitive detector. *J Appl Crystallogr 21*:916-924.

Kadner RJ, Heller K, Coulton JW, Braun V. 1980. Genetic control of hydroxamate-mediated iron uptake in *Escherichia coli*. *J Bacteriol 143*:256-264.

Killmann H, Herrmann C, Wolff H, Braun V. 1998. Identification of a new site for ferrichrome transport by comparison of the FhuA proteins of *Escherichia coli*, *Salmonella paratyphi* B, *Salmonella typhimurium* and *Pantoea agglomerans*. *J Bacteriol 180*:3845-3852.

Knüsel F, Zimmermann W. 1975. Sideromycins. In: Corcoran JW, Hahn FE. eds. *Antibiotics III. Mechanisms of Action of Antimicrobial and Antitumor Agents*. Heidelberg: Springer Verlag. pp 653-667.

Koebnik R, Braun V. 1993. Insertion derivatives containing segments of up to 16 amino acids identify surface- and periplasm-exposed regions of the FhuA outer membrane receptor of *Escherichia coli* K-12. *J Bacteriol 175*:826-839.

Kraulis PJ. 1991. MOLSCRIPT: a program to produce both detailed and schematic plots of protein structures. *J Appl Crystallogr 24*:946-950.

Locher KP, Rees B, Koebnik R, Mitschler A, Moulinier L, Rosenbusch J, Moras D. 1998. Transmembrane signaling across the ligand-gated FhuA receptor: Crystal structures of free and ferrichrome-bound states reveal allosteric changes. *Cell 95*:771-778.

Martinez JL, Delgado-Iribarren A, Baquero F. 1990. Mechanisms of iron acquisition and bacterial virulence. *FEMS Microbiol Rev 75*:45-56.

Merrit EA, Bacon DJ. 1997. Raster3D photorealistic molecular graphics. *Methods Enzymol 277*:505-524.

Miller MJ, Malouin F, Dolence EK, Gasparski CM, Ghosh M, Guzzo PR, Lotz BT, McKee JA, Minnick AA, Teng M. 1993. Iron transport-mediated drug delivery. In: Bentley PH, Ponsford R. eds. *Recent Advances in the Chemistry of Anti-infective Agents*. Cambridge, UK: The Royal Society of Chemistry. pp 135-159.

Minnick AA, McKee JA, Dolence EK, Miller MJ. 1992. Iron transport-mediated antibacterial activity of and development of resistance to hydroxamate and catechol siderophore-carbacephalosporin conjugates. *Antimicrobial Agents Chemother 36*:840-850.

Moeck GS, Fazly-Bazzaz BS, Gras MF, Ravi TS, Ratcliffe MJH, Coulton JW. 1994. Genetic insertion and exposure of a reporter epitope in the ferrichrome-iron receptor of *Escherichia coli* K-12. *J Bacteriol 176*:4250-4259.

Moeck GS, Tawa P, Xiang H, Ismail AA, Turnbull JL, Coulton JW. 1996. Ligand-induced conformational change in the ferrichrome-iron receptor of *Escherichia coli* K-12. *Mol Microbiol 22*:459-471.

Moeck GS, Coulton JW. 1998. TonB-dependent iron acquisition: mechanisms of siderophore-mediated active transport. *Mol Microbiol 128*:675-681.

Neilands JB. 1995. Siderophores: structure and function of microbial iron transport compounds. *J Biol Chem 270*:26723-26726.

Nüesch J, Knüsel F. 1967. Sideromycines. In: Gottlieb P, Shaw PD. eds. *Antibiotics I, Mechanisms of Action*. Berlin: Springer-Verlag, pp 449-541.

Paulsen H, Brieden M, Benz G. 1987. Synthese des Sauerstofanalogs der Desferriform von δ_1-Albomycine. *Liebigs Ann Chem 565*-575.

Pugsley AP, Zimmerman W, Wehrli W. 1987. Highly efficient uptake of a rifamycin derivative via the FhuA-TonB-dependent uptake route in *Escherichia coli*. *J Gen Microbiol 133*:3505-3511.

Rohrbach MR, Braun V, Köster W. 1995. Ferrichrome transport in *Escherichia coli* K-12: altered substrate specificity of mutated periplasmic FhuD and interactions of FhuD with the integral membrane protein FhuB. *J Bacteriol 177*:7186-7193.

Roosenberg JM, Lin Y-M, Lu Y, Miller MJ. 2000. Studies and syntheses of siderophores, microbial iron chelators, and analogs as potential drug delivery agents. *Curr Med Chem 7*:159-197.

Schultz-Hauser G, Köster W, Schwarz H, Braun V. 1992. Iron (III) hydroxamate transport in *Escherichia coli* K-12: FhuB-mediated membrane association of the FhuC protein and negative complementation of *fhuC* mutants. *J Bacteriol 174*:2305-2311.

Zähner H, Diddens H, Keller-Schierlein W, Nägeli H-U. 1977. Some experiments with semisynthetic sideromycins. *Jap J Antibioti Suppl 30*:201-206.

Preface to chapter seven

The focus of the previous chapter was the crystallographic structure of FhuA in complex with albomycin, and how this structural information might be plausibly used for the rational design of siderophore-antibiotic conjugates. This chapter describes the determination of the three-dimensional structure of FhuA in complex with a second, chemically unrelated antibiotic, the rifamycin derivative CGP 4832 at a resolution of 2.90 Å. FhuA-mediated transport of this antibiotic across the outer membrane of *E. coli* requires energy as transduced by the TonB protein. Comparing the chemical structures of hydroxamate-type siderophores and albomycin to rifamycin CGP 4832 reveals no structural similarities. However, structural superposition of those side-chain residues involved in ligand binding delineates a spatially distinct rifamycin CGP 4832-binding site within the extracellular pocket of the transporter. Binding of rifamycin CGP 4832 to FhuA induces distinct conformational changes in the cork domain; however, the switch helix does not unwind. This unexpected structural observation was confirmed by intrinsic tryptophan fluorescence measurements and antibody recognition assays. This data provides novel insights into the physical association of the energy-transducing protein TonB with TonB-dependent receptors, and strongly suggests that the β-barrel of FhuA forms interactions with TonB.

Crystal structure of a rifamycin derivative in complex with the active outer membrane transporter FhuA

Andrew D. Ferguson[1,2], Jiri Ködding[1], Georg Walker[3], James W. Coulton[2], Kay Diederichs[1], Volkmar Braun[3], Wolfram Welte[1]

1 Fakultät für Biologie, Universität Konstanz, M656, D-78457 Konstanz, Germany

2 Department of Microbiology and Immunology, McGill University, 3775 University Street, Montreal, Quebec, Canada H3A 2B4

3 Lehrstuhl Mikrobiologie / Membranphysiologie, Universität Tübingen, Auf der Morgenstelle 28, D-72076 Tübingen, Germany

Abstract

Gram-negative bacterial resistance to antimicrobial agents is modulated by the barrier properties and transport functions of the cell envelope. The TonB-dependent transporter FhuA mediates the active transport of the semi-synthetic rifamycin derivative CGP 4832 across the outer membrane of *Escherichia coli*. Here we present the crystallographic structure of FhuA in complex with rifamycin CGP 4832 at 2.90 Å resolution. Transport of radiolabeled [$^{55}Fe^{3+}$]-ferrichrome is inhibited by rifamycin CGP 4832, which selectively competes for binding to FhuA. Similar to hydroxamate-type siderophores and the antibiotic albomycin, binding of rifamycin CGP 4832 to FhuA induces conformational changes in the cork domain. However, this antibiotic does not promote the unwinding of the switch helix. This conformational transition was proposed to signal the liganded status of FhuA, and was thought to be an essential prerequisite for TonB-dependent energy-transduction. To confirm this intriguing structural data, intrinsic tryptophan fluorescence measurements and experiments using monoclonal antibodies sensitive to the secondary structure of the switch helix were conducted. The results are consistent with the observed three-dimensional structure of the FhuA-CGP 4832 complex. To further probe the structural requirements for TonB-dependent transport of ferrichrome and rifamycin CGP 4832, a series of bacterial mutants were assessed. Those with characterized point mutations in the TonB-box, a known site of interaction between TonB and TonB-dependent receptors, were equally impaired in their ability to transport ferrichrome or rifamycin CGP 4832, indicating conserved structural requirements. Bacterial mutants with uncharacterized mutations were more strongly affected in their sensitivity to rifamycin CGP 4832 compared to other FhuA-specific ligands, demonstrating the presence of unique structural features for rifamycin CGP 4832 transport, and thereby the functional significance of the rifamycin CGP 4832-binding site.

Introduction

Transport of antimicrobial agents across the outer membrane of gram-negative bacteria is modulated by a series of transport proteins and mechanisms. Nonspecific and specific porins transport small hydrophilic solutes, including ions and sugars, into the periplasm by passive diffusion. The structural architecture of bacterial porins with their apparent exclusion limit of 600 Da and the electrostatic arrangement of charged side-chain residues lining the channel contribute to the exclusion of antibiotics from the cell interior (Welte *et al.* 1995). Large solutes, such as iron-siderophore complexes, utilize active, TonB-dependent receptors for their uptake. Bacterial mutants with decreased expression of porins and high-affinity receptors display increased resistance to antibiotics (Jaffé *et al.* 1983; Curtis *et al.* 1985; Medeiros *et al.* 1987; Nikaido and Rosenberg, 1990). In the outer membrane of *Escherichia coli*, FhuA functions as the cognate receptor for the siderophore ferrichrome (Moeck and Coulton, 1998). In addition to binding ferrichrome with high-affinity, FhuA also functions as the primary receptor for the siderophore-antibiotic conjugate albomycin, several bacteriophages (T1, T5, ϕ80, and UC-1), the cyclic peptide antibiotic microcin J25, and the bacterial toxin, colicin M. Analogous to porins, FhuA can be induced to form an aqueous diffusion channel. However, the observed channel is electrically different from the permanently open channels observed with porins (Bonhivers *et al.* 1996).

A wide variety of clinically useful antibiotics are available for the treatment of bacterial infections. Those chemotherapeutic agents that selectively target nucleotide synthesis include rifamycins (rifampicin and rifabutin), which inhibit the enzymatic activity of DNA-dependent RNA polymerase (Chopra, 1999). Unfortunately, the nonspecific permeation of rifamycin through porins is limited due to the relative large size (Mr 823 Da) and inherent hydrophobicity of this drug (Vaara et al. 1990). CGP 4832 is a semi-synthetic rifamycin derivative (Mr 935 Da) that exhibits an approximate 400-fold decrease in minimal inhibitory concentration (MIC) against certain gram-negative bacteria, and has similar bactericidal properties compared to rifamycin (Pugsley *et al.* 1987; Wehrli *et al.* 1987). Pugsley *et al.* (1987) demonstrated that the increased antibiotic activity of CGP 4832 compared to rifamycin results from the ability of this

antibiotic to utilize the high-affinity transporter FhuA for its uptake across the outer membrane.

We have determined the three-dimensional structure of FhuA in complex with rifamycin CGP 4832 at 2.90 Å resolution (Fig. 1 and Table 1). The structure of the FhuA-CGP 4832 complex is similar to, yet distinct from all other recently determined FhuA-ligand complexes (Ferguson *et al.* 1998a; Locher *et al.* 1998; Ferguson *et al.* 2000).

Results and discussion

General description and the rifamycin CGP 4832-binding site

FhuA is composed of two domains. The elliptical-shaped barrel is formed by 22 antiparallel transmembrane β-strands that are connected by longer extracellular loops and shorter periplasmic turns. The cork domain, consisting of a mixed four-stranded β-sheet and a series of short α-helices, fills the barrel interior. The presence of the cork domain inside the β-barrel delineates a pair of pockets within the transporter: the extracellular and periplasmic pockets. Located within the extracellular pocket, approximately 20 Å above the external outer membrane interface is a single rifamycin CGP 4832 molecule (Fig. 2). Side-chain residues from apices B and C of the cork domain, and the barrel domain form hydrogen bonds, charge interactions or van der Waals contacts with rifamycin CGP 4832 atoms (Fig. 3, A, B, and C).

Previous structure-function studies conducted by Pugsley *et al.* (1987) demonstrated that the morpholino and the N-methyl-3-piperidyl-acetoxyacetyl groups are required for rifamycin CGP 4832 to exert its antibiotic activity (Fig. 3C). Analysis of FhuA-CGP 4832 interactions reveal that both moieties form multiple hydrogen bonds, charge interactions or van der Waals contacts with FhuA side-chain residues (Fig. 3C and Table 2). Replacement of the morpholino group with a methyl-piperidyl-iminomethyl substituent abolishes the bactericidal activity of rifamycin CGP 4832. Removing this chemical group would disrupt a critical hydrogen bond formed between the antibiotic and Tyr 116 from apex C; abrogating the high-affinity binding. Collectively, these results provide a structure-based explanation for the reduced antibiotic sensitivity of rifamycin

against *E. coli* (MIC of 4.0 μg/mL) compared to rifamycin CGP 4832 (MIC of 0.02 μg/mL), and are in accord with the composition of the rifamycin CGP 4832-binding site.

Structural comparison of the ligand-binding sites of FhuA

Comparing the structures of hydroxamate-type siderophores and albomycin to the chemically unrelated antibiotic rifamycin CGP 4832 reveals no structural similarities (Fig. 3, A, B, and C). However, comparison of those side-chain residues that compose the binding sites for these ligands identifies a series of characteristic residues that are involved in ligand binding (Table 3). The iron-chelating moiety of FhuA-specific hydroxamate-type ligands is a tri-δ-*N*-hydroxy-δ-*N*-acyl-L-ornithine peptide. This component of the siderophore forms multiple highly conserved interactions with side-chain residues from apices A, B, and C from the cork domain, and residues from the β-strands and extracellular loops of the barrel domain (Fig. 3, A and 3B). Additional contacts between the tri-peptide component of the siderophore [Gly-Gly-Gly (ferrichrome), Gly-Ser-Gly (ferricrocin) or Gly-Phe-Gly (phenylferricrocin)], and the amino acetyl thioribosyl pyrimidine moiety of albomycin, and side-chain residues of the extracellular pocket are also observed. In the rifamycin CGP 4832-binding site a similar pattern of interactions are observed (Fig. 4 and Table 2). However, there is one notable exception, Arg 81 from apex A does not interact with the rifamycin CGP 4832 molecule. This residue in the binding sites for hydroxamate-type ligands forms multiple hydrogen bonds with the iron-chelating component of the siderophore. In the FhuA-CGP 4832 complex, Arg 81 is placed 4.6 Å away from the nearest rifamycin CGP 4832 atom, and thus, only forms weak charge interactions with the antibiotic.

Rifamycin CGP 4832 competes with hydroxamate-type ligands for binding to the ligand-binding site

Rifamycin CGP 4832 competes with hydroxamate-type FhuA-specific ligands for binding to the ligand-binding site of FhuA. The antagonistic effects of this antibiotic have been previously determined (Pugsley *et al.* 1987). Transport inhibition assays using 10 μg/mL and 30 μg/mL of rifamycin CGP 4832 results in a 50% or 75% decrease in the rate of [$^{55}Fe^{3+}$]-ferrichrome transport (Fig. 5). In contrast to albomycin, rifamycin CGP

4832 transport is a FhuBCD-independent process (Kadner *et al.* 1980; Pugsley *et al.* 1987). These results are in accord with the similarities in composition of the FhuA ligand-binding sites (Table 3), and demonstrate that hydroxamate-type ligands are preferentially bound and transported by FhuA.

Rifamycin CGP 4832-resistant mutants

Bacterial mutants resistant to both rifamycin CGP 4832 and albomycin have been previously described (Pugsley *et al.* 1987). We have isolated and characterized fifty-eight rifamycin CGP 4832-resistant mutants in this study. Forty-six of the fifty-eight rifamycin CGP 4832-resistant mutants contained deletions or point mutations in the *fhuA* gene as judged by a resistance to bacteriophage T5-mediated cell killing or the absence of detectable amounts of FhuA in the outer membrane (Fig. 6; mutant P8). Four of the remaining mutants likely contained mutations in the *tonB* gene as they showed insensitivity to all TonB-dependent functions (data not shown). One rifamycin CGP 4832-resistant mutant (mutant 25; Table 4 and Fig. 6) displayed rifamycin-resistance and sensitivity to all other ligands tested. This mutant was the only presumed rifamycin-target site mutant isolated in this study. The final seven rifamycin CGP 4832-resistant mutants displayed a mixed phenotype (Table 4). Partially rifamycin CGP 4832-sensitive mutants can be either resistant or sensitive to albomycin and / or colicin M. Although these mutants synthesize and export a FhuA protein to the outer membrane (Fig. 6) they contain mutations that affect select FhuA functions. We assume these mutations to be small deletions or point mutations as larger deletions would affect multiple FhuA functions. Mutant 48 was devoid of all FhuA-related activities, except for a partial sensitivity to bacteriophages T5 and ϕ80 (Table 4). This mutant may synthesize residual amounts of FhuA (below the detection limit of SDS-PAGE) that were sufficient to facilitate limited infection by bacteriophages T5 and ϕ80 (Fig. 6, lane 7). Rifamycin CGP 4832 appears well suited to isolate *fhuA* genes with point mutations or small deletions. In contrast, bacteriophages T5 and ϕ80 isolate more than 99% *fhuA* genes with deletion mutants, while albomycin identifies mutants with defects in the *fhuABCD* and *pepN* genes (Hartmann *et al.* 1979; Braun *et al.* 1983).

Ligand-induced allosteric transitions

Structural superposition of the α-carbon coordinates of unliganded FhuA upon those of the liganded FhuA complexes reveals near perfect superposition of the barrel domains (root-mean-square deviation of 0.25 Å). However, comparing the α-carbon coordinates of the cork domain identifies three distinct cork domain conformations: unliganded, the hydroxamate-type liganded conformation, and the rifamycin CGP 4832-loaded conformation.

As a consequence of the distance of rifamycin CGP 4832 from Arg 81, different ligand-induced allosteric transitions from those detailed for other liganded complexes are observed in the FhuA-CGP 4832 complex (Ferguson *et al.* 1998a; Locher *et al.* 1998; Ferguson *et al.* 2000). In the hydroxamate-type ligand-binding site an induced fit mechanism is observed: residues 80 to 82 of apex A and 98 to 100 of apex B move upward (0.7 - 2.0 Å) toward the siderophore. In the rifamycin CGP 4832-binding site, only residues 97 to 100 from apex B move upward (0.5 - 1.5 Å) to interact with the antibiotic (Table 2). All other cork domain residues remain stationary.

In the hydroxamate-type liganded FhuA complexes, the upward translation of apex A is asymmetrically propagated to all cork domain loops between apex A and the periplasmic pocket of FhuA (Ferguson *et al.* 1998a; Locher *et al.* 1998; Ferguson *et al.* 2000). The upward movement of apex A and other loops of the cork domain alters the chemical environment of the hydrophobic pocket in which the NH_2-terminal switch helix resides; thereby promoting its unwinding. As a result all residues NH_2-terminal of Arg 31 assume an extended conformation within the periplasmic pocket. However, in the FhuA-CGP 4832 complex apex A remains fixed, no upward movement of cork domain loops is induced, and therefore, the switch helix remains wound.

It has been shown previously that ferrichrome binding to viable bacterial cells quenched the emitted fluorescence of a surface-exposed fluorescein-labeled Cys residue (Bös *et al.* 1998). Intrinsic tryptophan fluorescence measurements of FhuA have also shown a decrease in fluorescence upon binding of ferrichrome to purified protein (Locher and Rosenbusch, 1998). The decrease in tryptophan fluorescence and antibody accessibility upon ferrichrome binding to FhuA (Moeck *et al.* 1997) can be re-interpreted as measurement of the unwinding of the switch helix. More specifically, Trp 22 located

at the base of the switch helix, is translocated ~17 Å across the periplasmic pocket of the FhuA upon the binding of hydroxamate-type ligands (Ferguson *et al.* 1998a; Locher *et al.* 1998; Ferguson *et al.* 2000).

In order to confirm the validity of our unexpected crystallographic observations intrinsic tryptophan fluorescence measurements and monoclonal antibody binding studies (data not shown) with rifamycin CGP 4832 were conducted. A slight decrease in the intrinsic tryptophan fluorescence is induced upon binding of rifamycin CGP 4832 or desferriferrichrome to FhuA (Fig. 7A). In contrast, addition of ferrichrome produced a similar quenching of the emitted tryptophan fluorescence of FhuA (Fig. 7A), as previously reported (Locher and Rosenbusch, 1998). In both experiments the concentrations of the FhuA and tryptophan solutions were approximately equal [1.1 μM of FhuA (~79 kDa with nine Trp residues) was considered equivalent to 10 μM Trp]. Unexpectedly, the addition of ferrichrome to the tryptophan solution also decreased in the emitted fluorescence (Fig. 7B). However, the magnitude of the tryptophan fluorescence quenching was not equivalent to that observed with FhuA. The addition of rifamycin CGP 4832 or desferriferrichrome does not display a significant fluorescence quenching of the tryptophan solution (Fig. 7B).

FhuA-TonB interactions

We find it intriguing that rifamycin CGP 4832 transport across the outer membrane of *E. coli* as mediated by FhuA is a TonB-dependent process. The unwinding of the switch helix, a transmembrane signal transduced from the ligand-binding site to the periplasmic pocket of FhuA, was presumed to be a prerequisite for TonB-dependent energy transduction. In contrast to FhuA-specific siderophores and albomycin, the binding of rifamycin CGP 4832 to FhuA does not promote the unwinding of the switch helix.

To further examine the structural requirements for the TonB-dependent transport of rifamycin CGP 4832 through FhuA, and potential sites of interaction between FhuA and TonB, the rifamycin CGP 4832 sensitivity of a series of characterized bacterial mutants were assessed. All bacterial TonB-dependent receptors share a short conserved sequence of periplasmic residues, termed the TonB-box (FhuA residues 8 to 11). To create mutant bacterial strains devoid of TonB-dependent ferrichrome transport activity, plasmids

containing *fhuA* genes with point mutations in the TonB-box (Schöffler and Braun, 1989), were used to transform *E. coli* strain UL3 (see Material and Methods). When transformed with plasmids encoding Ile9Pro or Val11Asp mutant FhuA proteins, growth inhibition zones were observed at 33.3 µg/mL and 100 µg/mL of CGP 4832, compared to a wild-type sensitivity of 0.41 µg/mL. The rifamycin CGP 4832 sensitivity of the former mutant is equivalent to the wild-type rifampicin sensitivity of this strain; rifampicin passively diffuses across the outer membrane independently of FhuA. These results support previously described growth promotion data (Schöffler and Braun, 1989). This study shows that bacterial strains that express the Val11Asp mutant FhuA protein are unable to transport ferrichrome, compared to those that express the Ile9Pro mutant, which maintain residual TonB-dependent ferrichrome transport activity.

Materials and methods

Isolation and characterization of rifamycin CGP 4832-resistant mutants

Aliquots (20 μL of 0.1 μg/μL CGP 4832) were spotted onto TY nutrient agar plates [10 g/L tryptone (pH 7.0), 5 g/L yeast extract, 5 g/L NaCl, and 1.5% agar] seeded with 0.20 mL of 10^8 *E. coli* AB2847 *aroB malT thi tsx* cells. Rifamycin CPG 4832-resistant colonies were isolated, and streaked onto nutrient agar plates containing bacteriophage T5 (titer of 2.0 x 10^7 plaque-forming units in 50 μL), bacteriophage ϕ80 (2.0 x 10^7 plaque-forming units in 50 μL), colicin B (dilution titer of 10^3), colicin M (dilution titer of 10^3) or albomycin (dilution titer of 10^3). Growth promotion assays were performed using NBD nutrient agar plates [8 g/L nutrient broth (pH 7.0), 5 g/L NaCl, and 0.2 mM 2,2'-dipyridyl and 1.5% bactoagar] supplemented with 4 μM ferrichrome and 4 μM coprogen. Cell killing inhibition assays with rifamycin CGP 4832 were conducted by establishing a three-fold dilution series, ranging from 100 μg to 0.41 μg of CGP 4832, by placing 3 mL of TY soft agar layer supplemented with 10 μM ferrichrome onto TY nutrient agar plates. Inhibition of bacteriophage T5 infection by rifamycin CGP 4832 was tested using *E. coli* strain BR158, a *tonB* mutant of *E. coli* AB2847 that is unable to actively transport this antibiotic across the outer membrane.

Transport inhibition assays using rifamycin CGP 4832

E. coli AB2847 cells were grown overnight on TY nutrient agar plates. *E. coli* strain AB2847 has a mutation in the *aroB* gene. This gene is required for synthesis of the only siderophore produced by this strain, enterobactin. If appropriate precursors are not provided, this *E. coli* strain will transport exogenously added siderophores. Colonies were suspended in 0.5 mL of M9 minimal media salts (Miller, 1972) supplemented with 0.4% glucose, and grown to an optical density of 0.55 at 578 nm. 8.8 μL of 10 mM nitrilotriacetate was added to 0.35 mL of cell suspension. Following a two minute incubation period, 3.5 μL aliquots of rifamycin CGP 4832 (1.0, 3.0, and 10.0 mg/mL dissolved in 50% methanol) were added to the cell culture. Three minutes later transport was initiated by the addition of a mixture of 2.35 μM radiolabeled [$^{55}Fe^{3+}$]-ferrichrome and 5 μM desferriferrichrome. The cell suspension was shaken and 50 μL samples were

withdrawn after one and four minute intervals thereafter, for a total of twenty-one minutes. The samples were subsequently filtered, washed twice with 5 mL of 0.1 M LiCl, dried, and the [$^{55}Fe^{3+}$]-isotope signal measured with a liquid scintillation counter at 37°C. *E. coli* strain UL3 does not synthesize a wild-type FhuA protein, and has no polar effect on the expression of the *fhuCDB* genes, which are located downstream of the *fhuA* gene.

Protein expression, purification, and intrinsic tryptophan fluorescence measurements

A recombinant FhuA protein was constructed by inserting a hexahistidine-tag plus five additional linker residues (SSHHHHHHGSS) into the *fhuA* gene after residue 405 (Moeck *et al.* 1994; 1996). FhuA was expressed and purified as previously described (Ferguson *et al.* 1998a; 1998b). The intrinsic tryptophan fluorescence of FhuA and its complexes with rifamycin CGP 4832, ferrichrome or desferriferrichrome [solublized in 6 mM KH_2PO_4 (pH 7.0), 0.15 M NaCl, and 0.06% N,N-dimethyldodecylamine-N-oxide] were measured using protein and tryptophan concentrations of 1.10 μM and 10.0 μM, respectively. All data were collected at 20°C with a Fluoromax-2 spectrophotometer (Jobin Yvon-Spex Instruments S.A. Inc.) and processed using the GRAMS/386 software package. A single excitation wavelength, 280 nm, was used for all fluorescence measurements. Two emission wavelengths were collected at 335 nm and 355 nm, corresponding to the fluorescence maximums of FhuA and tryptophan, respectively.

Crystallization, data collection, structure determination and refinement of the FhuA-CGP 4832 complex

FhuA was co-crystallized with rifamycin CGP 4832 using the hanging drop vapor diffusion technique by mixing equal volumes (5 μL) of FhuA [10 mg/mL, 0.80% N,N-dimethyldecylamine-N-oxide (DDAO), 10 mM ammonium acetate (pH 8.0), 1% *cis*-inositol, and 1 mM rifamycin CGP 4832] and reservoir solution [12% polyethylene glycol (PEG) 2,000 monomethyl ether, 0.1 M sodium cacodylate (pH 6.4), 20% glycerol, and 3% PEG 200]. R. Naef (see acknowledgements) generously provided rifamycin CGP 4832. FhuA-CGP 4832 co-crystals grew within seven days to a final size of 300 by 300 by 220 μm at 18°C. All crystals were mounted in cryo-loops and flash frozen by direct

immersion into liquid nitrogen. All diffraction data were collected at 100 K using a cryo-stream apparatus with synchrotron radiation at the X-ray diffraction beam line at ELETTRA (Table 1). X-ray diffraction data were processed and reduced using the program XDS (Kabsch, 1988). Initial phases for the FhuA-CGP 4832 complex were calculated using the FhuA coordinates (1qfg.pdb) as an initial model. A model for the FhuA-CGP 4832 complex was built into an experimental electron density map with the program O (Jones *et al.* 1991). The model was refined with the program CNS, using molecular dynamics and the maximum likelihood target features (Brünger *et al.* 1998). Following rounds of model building and structural refinement the final model contains residues 19 to 714, one lipopolysaccharide molecule, one rifamycin CGP 4832 molecule, one DDAO molecule, and 178 ordered water molecules.

Figures

All color figures were prepared using MOLSCRIPT (Kraulis, 1991) and Raster3D (Merrit and Bacon, 1997). Fig. 1 and Fig. 2 were prepared using O (Jones *et al.* 1991) and ISIS Draw, respectively.

Protein Data Bank accession code

The crystallographic coordinates have been deposited in the Protein Data Bank with the following accession code: (FhuA-CGP 4832 complex).

Table 1. Crystallographic data. All diffraction data were collected at the X-ray diffraction beam line at ELETTRA (Trieste, Italy) at a constant temperature of 100 K using a wavelength of 1.000 Å. Brackets indicate the highest resolution shell.

Data collection and reduction	
Space group	$P6_1$
Unit cell *a* (Å)	172.82
b (Å)	172.82
c (Å)	87.91
Number of molecules per asymmetric unit	1
Number of measured reflections	161,168
Number of unique reflections	33,363
Completeness (%)	99.9 (99.8)
Resolution (Å)	2.90
R (%)	6.2 (29.8)
R_{meas} (%)	7.0 (33.5)
$R_{merge\text{-}F}$ (%)	7.2 (24.6)
I/σ	17.2 (4.2)
Structural refinement	
R_{cryst} (%)	23.3
R_{free} (%)	27.5
Root mean square deviation	
Bond lengths (Å)	0.008
Bond angles (°)	1.5
Dihedral angles (°)	25.9
Improper angles (°)	0.9

Table 2. FhuA-CGP 4832 interactions. Listed are the residue-atoms, location, distance, and type of interaction formed between all FhuA side-chain residues within 4 Å of rifamycin CGP 4832 atoms. See Fig. 2A for structural details of the hydrogen bonding pattern and charge interactions between side-chain residues and rifamycin CGP 4832.

[redacted]			
Glu 98-OE2	Apex B	3.7 Å	Charge interactions with O8 carbonyl atom of the N-methyl-3-piperidyl-acetoxyacetyl group
Glu 98-O	Apex B	3.8 Å	Charge interactions with O20 carbonyl atom of the N-methyl-3-piperidyl-acetoxyacetyl group
Gly 99-NH	Apex B	3.7 Å	Charge interactions with O20 carbonyl atom
Gln 100-OE1	Apex B	3.5 Å	van der Waals contact with the C5 methyl group
Ser 101-OG	Apex B	3.5 Å	Hydrogen bond with O20 carbonyl atom
Phe 115-O	Apex C	3.0 Å	van der Waals contact with C55 atom of the piperidyl group
Tyr 116-OH	Apex C	3.2 Å	Hydrogen bond with O18 atom of the morpholino group
Tyr 244-OH	L3	3.9 Å	Charge interactions with N6 atom
Trp 246-CZ2	L3	3.6 Å	van der Waals contact with the aromatic ring system (distance given is for the O17 atom)
Tyr 313-OH	β7	3.6 Å	Charge interactions with N4 atom
Tyr 315-OH	L4	2.8 Å	Hydrogen bond with O1 carbonyl atom of the aromatic ring system
Lys 344-CD	β8	3.4 Å	van der Waals contact with C24 methyl group
Phe 391-CE2	β9	3.0 Å	van der Waals contact with O18 atom of the morpholino group and the C31 and C32 methyl groups
Gly 392-O	β9	3.2 Å	van der Waals contact with C24 methyl group
Tyr 423-OH	β10	3.3 Å	van der Waals contact with the C31 and C32 methyl groups
Gln 505-NE2	L7	3.0 Å	Hydrogen bond with the O8 carbonyl atom of the N-methyl-3-piperidyl-acetoxyacetyl group
Phe 693-CE1	L11	3.5 Å	van der Waals contact with the aromatic ring system (distance given is for C40 atom)
Tyr 696-OH	L11	3.0 Å	Hydrogen bond with O2 hydroxyl atom

Table 3. All side-chain residues of the ligand-binding site that form interactions with FhuA-specific ligands. Listed are all side-chain residues within 4 Å of ligand atoms [ferricrocin; phenylferricrocin; albomycin, extended (*) and compact conformation (†); or rifamycin CGP 4832].

Side-chain residues	Ferricrocin	Phenylferricrocin	Albomycin*	Albomycin†	CGP 4832
Arg 81 from apex A	+	+	+	+	-
Tyr 87 from a cork domain loop	-	+	-	-	-
Glu 98 near apex B	-	-	-	-	+
Gly 99 near apex B	+	+	+	+	+
Gln 100 from apex B	+	+	+	+	+
Ser 101 from a cork domain loop	-	-	-	-	+
Phe 115 near apex C	-	+	-	+	+
Tyr 116 from apex C	+	+	+	+	+
Tyr 244 from L3	+	+	+	+	+
Trp 246 from L3	+	+	+	+	+
Tyr 313 from β7	+	+	+	+	+
Tyr 315 from L4	+	+	+	-	+
Lys 344 from β8	-	-	+	-	+
Phe 391 from β9	+	+	+	+	+
Gly 392 from β9	-	-	-	-	+
Tyr 393 from L5	-	-	+	+	-
Tyr 423 from β10	-	-	-	+	+
Gln 505 from L7	-	-	-	+	+
Phe 557 from L8	-	-	+	-	-
Phe 558 from L8	-	-	+	-	-
Phe 693 from L11	+	+	+	+	+
Tyr 696 from L11	-	-	-	-	+

Table 4. Partial sensitivity of *fhuA* mutants of *E. coli* strain AB2847. All mutants are colicin B-sensitive and grow on nutrient agar plates supplemented with coprogen, and therefore do not possess mutations in the *tonB* gene. Growth on coprogen also excludes bacterial mutants with mutations in the *fhuBCD* genes, as they are required for coprogen transport. Abbreviations: T5, bacteriophage T5; ϕ80, bacteriophage ϕ80; R, resistant; S, sensitive; ***R*** or ***S***, partial resistance or partial sensitivity; +, growth promotion by ferrichrome or the presence of a FhuA protein band on a SDS-PAGE gel as shown in Fig. 6 - no growth promotion or the absence of a FhuA protein band on a SDS-PAGE gel as shown on Fig. 6.

5	***R***	S	R	-	S	S	R	+
10	***R***	S	R	-	S	S	S	+
15	***R***	S	S	+	S	S	S	+
19	R	S	R	-	R	R	R	-
25	R	R	S	+	S	S	S	+
48	R	S	R	-	***S***	***S***	R	-
55	***R***	S	S	+	S	S	S	+
60	R	S	S	+	S	S	S	+
84	***R***	S	S	+	S	S	S	+

Figure 1. Representative section of the electron density of the FhuA-CGP 4832 complex. Stereoview of the final $3F_{obs}$ - $2F_{calc}$ electron map (green) at a resolution of 2.90 Å is contoured at 1.2 σ, showing the rifamycin CGP 4832-binding site. The rifamycin CGP 4832 molecule and select side-chain residues are shown with carbon atoms yellow, oxygen atoms red, and nitrogen atoms blue.

Figure 2. The FhuA-CGP 4832 complex. The view is perpendicular to the barrel axis. The β-strands that comprise the front of the barrel domain have been rendered transparent to provide an unobstructed view of the cork domain. The barrel domain and the cork domain are colored blue and yellow, respectively. Rifamycin CGP 4832 is shown as a bond model with carbon atoms white, oxygen atoms red, and nitrogen atoms blue.

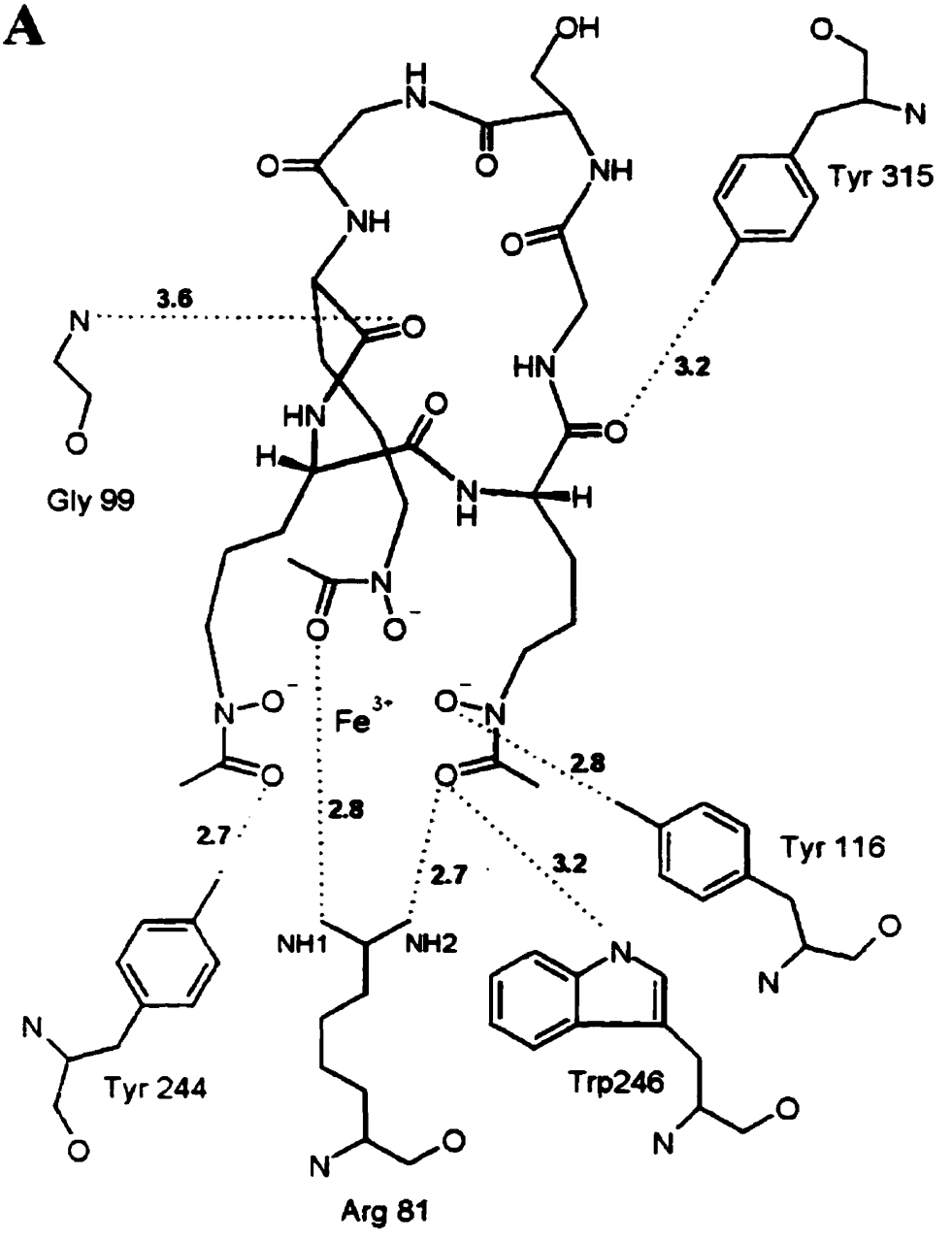

Figure 3. Schematic comparison of the hydrogen bonding pattern and charge interactions of (**A**) ferricrocin, (**B**) albomycin, and (**C**) rifamycin CGP 4832 with side-chain residues of the FhuA ligand-binding site. The chemical structures of ferricrocin, albomycin, and rifamycin CGP 4832 are shown with hydrogen bonds and charge interactions with side-chain residues as dotted lines (distances are given in Å). See Table 2 for details of additional van der Waals contacts between side-chain residues and rifamycin CGP 4832.

B

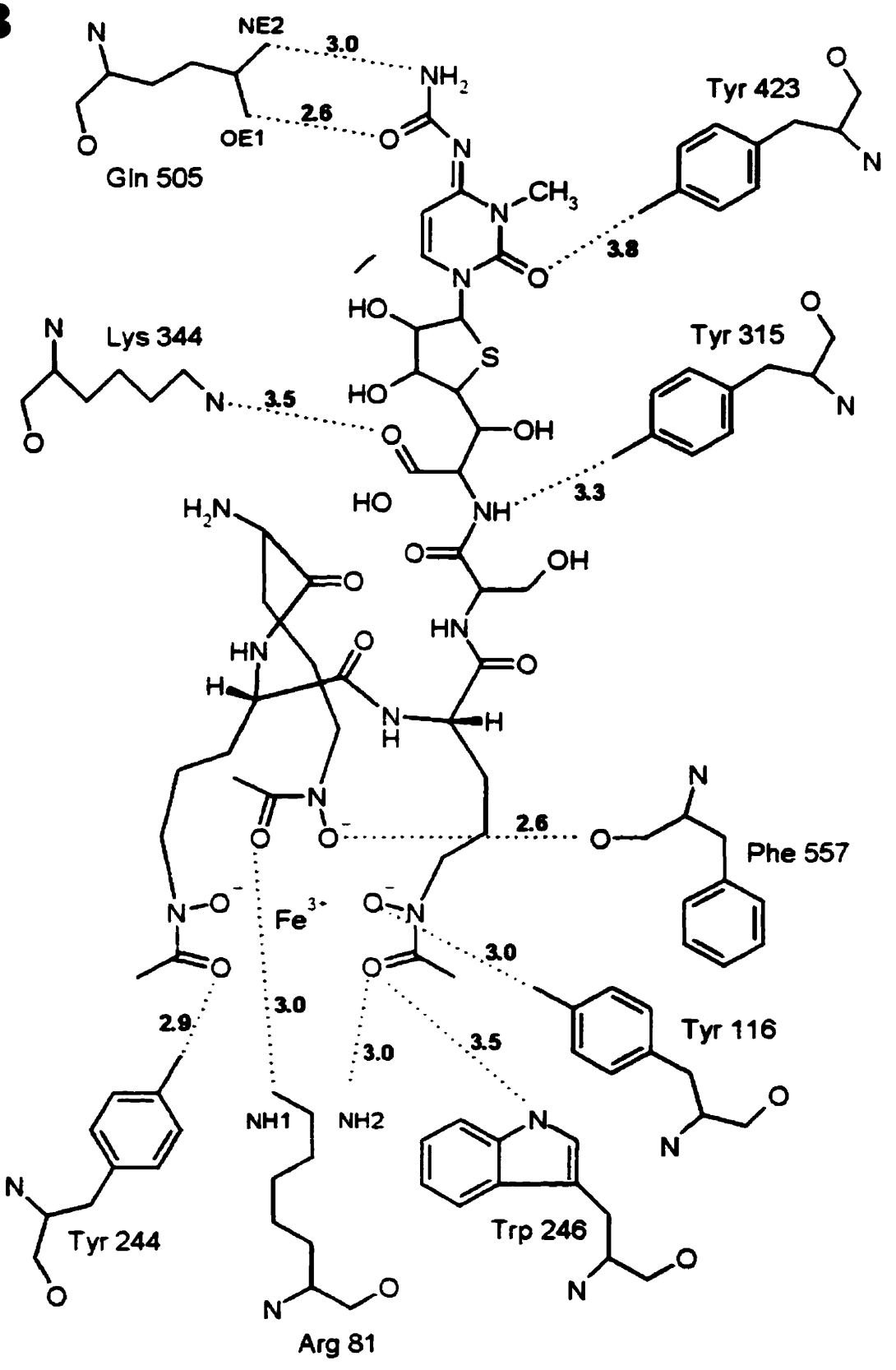
NE2
3.0
NH2
2.6
OE1
Gln 505
Tyr 423
CH3
3.8
Lys 344
3.5
Tyr 315
HO
S
OH
3.3
H2N
NH
OH
HN
HN
H
N
H
2.6
Phe 557
Fe3+
3.0
2.9
3.0
3.0
3.5
Tyr 116
NH1
NH2
Tyr 244
Trp 246
Arg 81

C

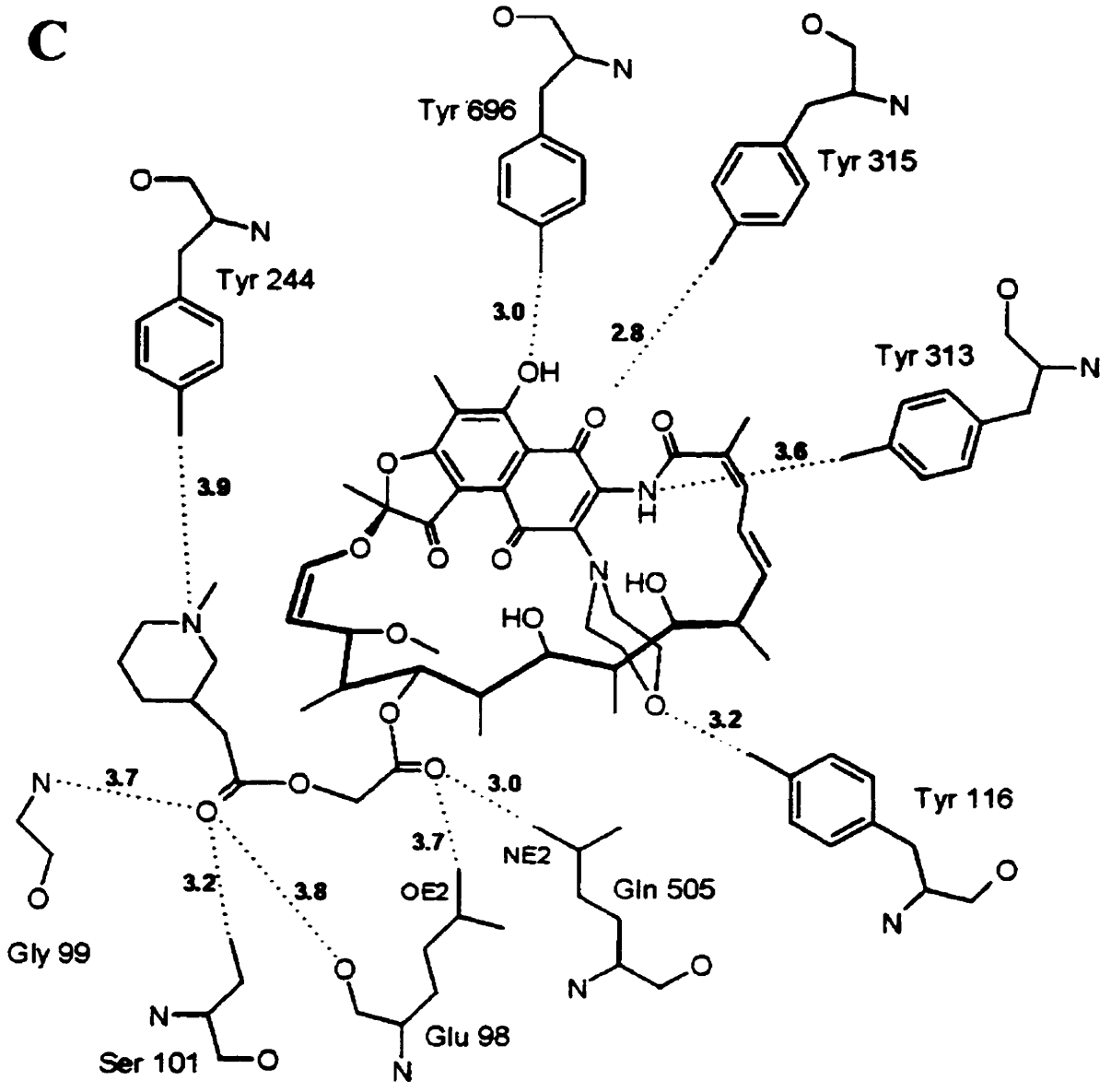
Tyr 696
Tyr 315
Tyr 244
Tyr 313
Tyr 116
Gly 99
Ser 101
Glu 98
Gln 505
3.0
2.8
3.9
3.6
3.2
3.7
3.0
3.7
3.2
3.8
OH
HO
HO
NE2
OE2

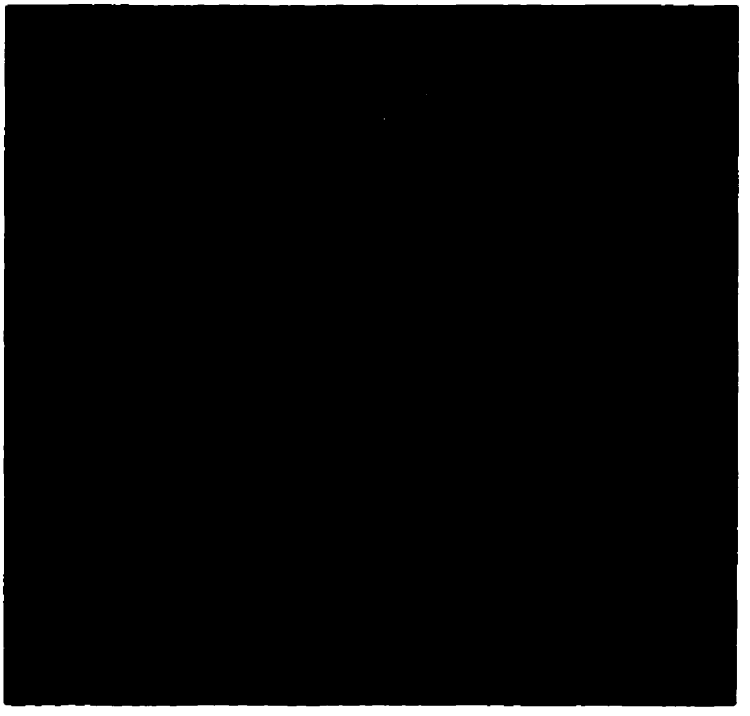

Figure 4. The FhuA CGP 4832-binding site. Those side-chain residues that form hydrogen bonds or van der Waals contacts with rifamycin CGP 4832 atoms are labeled and shown in green. Rifamycin CGP 4832 is presented as a bond model with carbon atoms white, oxygen atoms red and, nitrogen atoms blue.

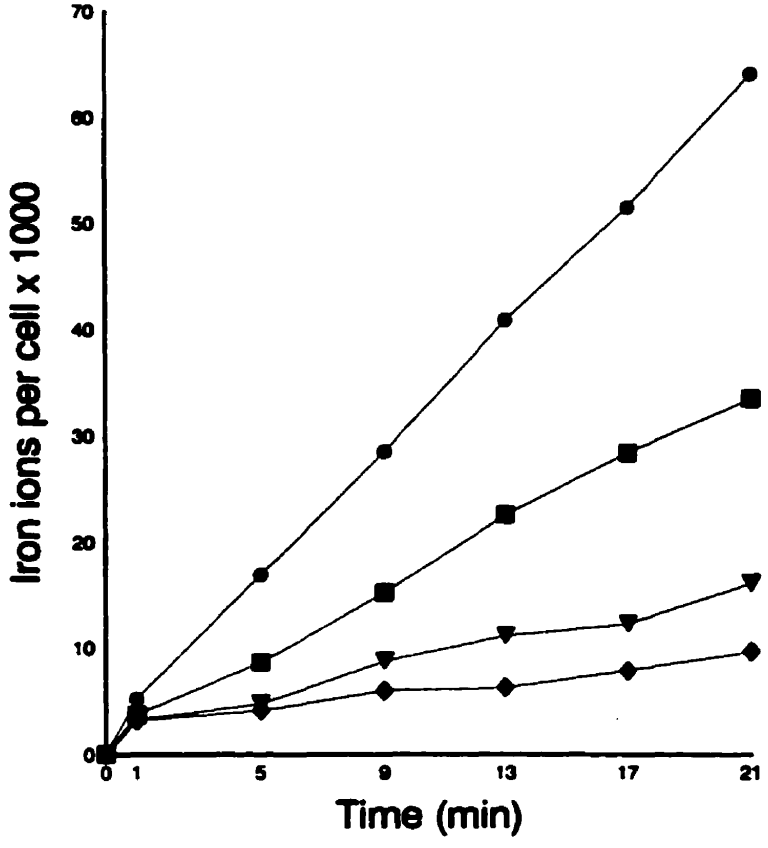

Figure 5. Transport inhibition assays using rifamycin CGP 4832. Transport of radiolabeled [$^{55}Fe^{3+}$]-ferrichrome (2.35 μM) into *E. coli* AB2847 cells in the absence (●), and presence of 10 μg/ml (■), 30 μg/ml (▼), and 100 μg/ml (◆) of CGP 4832.

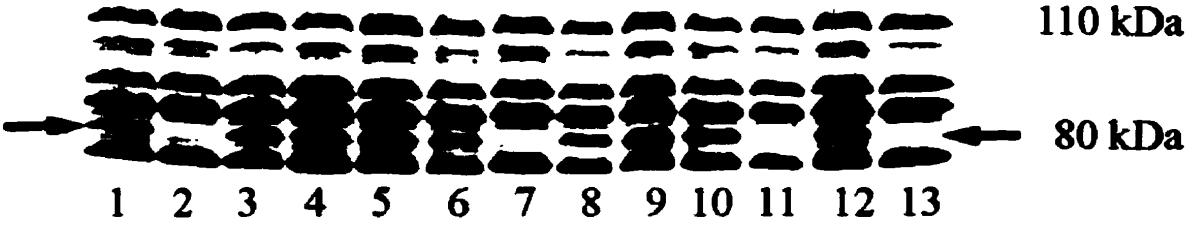

Figure 6. SDS-PAGE of isolated *E. coli* strain AB2847 outer membranes from rifamycin CGP 4832-resistant bacterial mutants. Lanes 1 and 12 represent wild-type outer membranes; lanes 2 and 13 contain purified outer membranes from the FhuA deletion mutant P8; and lanes 3 through 11 contain outer membranes from rifamycin CGP 4832-resistant mutants 5, 10, 15, 25, 48, 55, 60, 84, and 19 (see Table 4 for additional details).

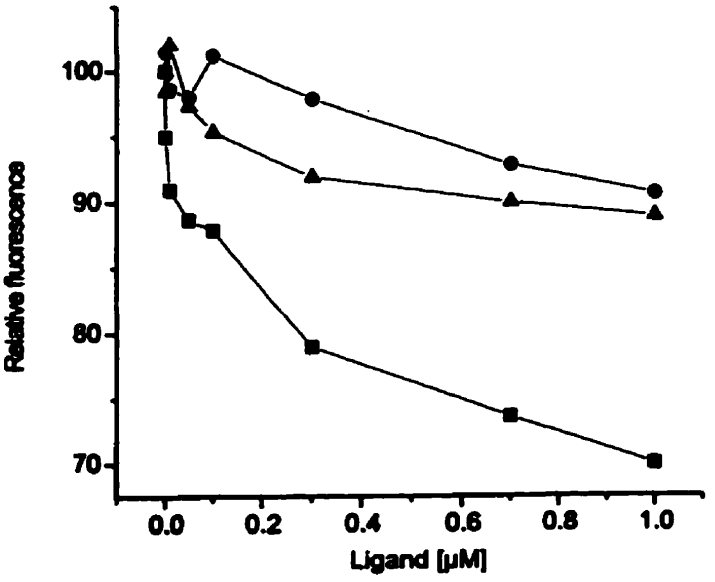
Relative fluorescence
100
90
80
70
0.0
0.2
0.4
0.6
0.8
1.0
Ligand [μM]

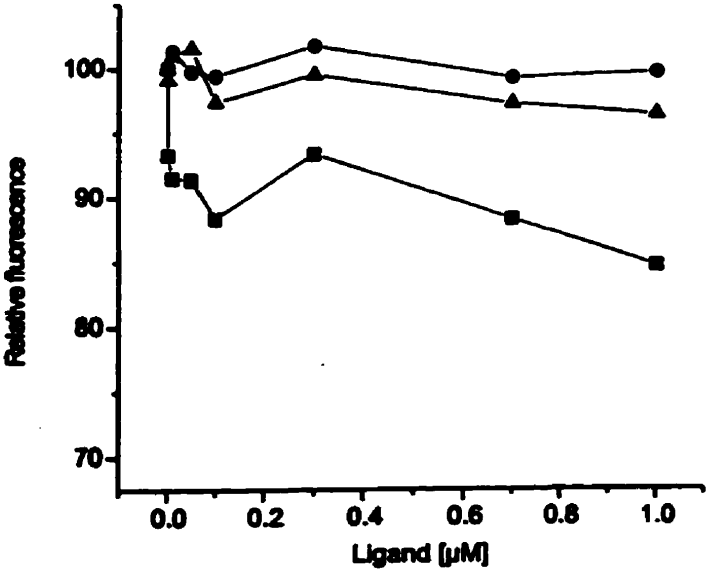
Relative fluorescence
100
90
80
70
0.0
0.2
0.4
0.6
0.8
1.0
Ligand [μM]

Figure 7. Ligand-induced fluorescence quenching [ferrichrome (■), desferriferrichrome (●), and rifamycin CGP 4832 (▲)] of the emitted tryptophan fluorescence of (**A**) FhuA, and (**B**) tryptophan containing solutions. The given tryptophan fluorescence values were averaged from three independent experiments in which each spectrum was collected three times. The background fluorescence spectra of all buffers (without added ligand) were subtracted from the collected experimental spectra. The emitted tryptophan fluorescence of FhuA was taken as 100%.

Acknowledgements

We gratefully acknowledge M. Degano at the X-ray diffraction beam line at ELETTRA (Trieste, Italy) for his assistance during data collection and R. Naef at Noravtis-Pharma for providing rifamycin CGP 4832. The Deutsche Forschungsgemeinschaft (to V.B. and W.W.) and the Medical Research Council of Canada (to J.W.C.) supported this work. A.D.F. is the recipient of a Deutscher Akademischer Austauschdienst Grant for Study and Research and a Medical Research Council of Canada Doctoral Research Award.

References

Bonhivers, M., Ghazi, A., Boulanger, P., and Letellier, L. (1996). FhuA, a transporter of the *Escherichia coli* outer membrane is converted into a channel upon the binding of bacteriophage T5. *EMBO J.* 15, 1850-1856.

Bös, C, Lorenzen, D., and Braun, V. (1998). Specific in vivo labeling of cell surface exposed protein loops: reactive cysteines in the predicted gating loop mark a ferrichrome binding site and a ligand-induced conformational change of the *Escherichia coli* FhuA protein. *J. Bacteriol.* 180, 605-613.

Braun, V., Günthner, K., Hantke, K., and Zimmermann, L. (1983). Intracellular activation of albomycin in *Escherichia coli* and *Salmonella typhimurium*. *J. Bacteriol.* 156, 308-315.

Brünger, A.T., Adams, P.D., Clore, G.M., DeLano, W.L., Gros, P., Grosse-Kunstleve, R.W., Jiang, J.-S. Kuszewski, J., Nilges, M., Pannu, N.S., Read, R.J., Rice, L.M., Simonson, T., and Warren, G.L. (1998). Crystallography & NMR system: A new software suite for macromolecular structure determination. *Acta Cryst. D* 54, 905-921.

Chopra, I. (1999). Research and development of antibacterial agents. *Curr. Opin. Microbiol.* 1, 495-501.

Curtis, N.A., Eisenstadt, R.L., Turner, K.A., and White, A.J. (1985). Porin-mediated cephalosporin resistance in *Escherichia coli* K-12. J. *Antimicrobial. Chemother.* 15, 642-644.

Ferguson, A.D., Hofmann, E., Coulton, J.W., Diederichs, K., and Welte, W. (1998a). Siderophore-mediated iron transport: Crystal structure of FhuA with bound lipopolysaccharide. *Science* 282, 2215-2220.

Ferguson, A.D., Breed, J., Diederichs, K., Welte, W., and Coulton, J.W. (1998b). An internal affinity-tag for purification and crystallization of the siderophore receptor FhuA, integral outer membrane protein from *Escherichia coli* K-12. *Prot. Sci.* 7, 1636-1638.

Ferguson, A.D., Braun, V., Fiedler, H.-P., Coulton, J.W., Diederichs, K., and Welte, W. (2000). Crystal structure of the antibiotic albomycin in complex with the outer membrane transporter FhuA. *Prot. Sci.* In press

Hartmann, A., Fiedler, H.-P., and Braun, V. (1979). Uptake and conversion of the antibiotic albomycin by *Escherichia coli* K-12. *Eur. J. Biochem.* 99, 517-524.

Jaffé, A., Chabbert, Y.A., and Derlot, E. (1983). Selection and characterization of beta-lactam-resistant *Escherichia coli* K-12 mutants. *Antimicrobiol. Agents Chemother.* 23, 622-625.

Jones, T.A., Zou, J.Y., Cowan, S.W., and Kjeldgaard, M. (1991). Improved methods for building protein models in electron density maps and the location of errors in these models. *Acta Cryst. A* 47, 110-119.

Kabsch, W. (1988). Evaluation of single crystal X-ray diffraction data from a position sensitive detector. *J. Appl. Crystallogr.* 21, 916-924.

Kadner, R.J., Heller, K., Coulton, J.W., and Braun, V. (1980). Genetic control of hydroxamate-mediated iron uptake in *Escherichia coli*. *J. Bacteriol.* 143, 256-264.

Kadner, R.J. (1990). Vitamin B_{12} transport in *Escherichia coli*: energy coupling between membranes. *Mol. Microbiol.* 4, 2027-2033.

Kraulis, P.J. (1991). MOLSCRIPT: a program to produce both detailed and schematic plots of protein structures. *J. Appl. Crystallogr.* 24, 946-950.

Locher, K.P., and Rosenbusch, J. (1997). Oligomeric states and siderophore binding of ligand-gated FhuA protein that forms channels across *Escherichia coli* outer membranes. *Eur. J. Biochem.* 247, 770-775.

Medeiros, A.A., O'Brien, T.F., Rosenberg, E.Y., and Nikaido, H. (1987). Loss of OmpC porin in a strain of *Salmonella typhimurium* causes increased resistance to cephalosporins during therapy. *J. Infect. Dis.* 156, 751-757.

Merrit, E.A., and Bacon, D.J. (1997). Raster3D photorealistic molecular graphics. *Methods Enzymol.* 277, 505-524.

Miller, J.H. (1972). Experiments in Molecular Genetics: Cold Spring Harbour; New York. Cold Spring Harbour Laboratory Press:

Moeck, G.S., Fazly-Bazzaz, B.S., Gras, M.F., Ravi, T.S., Ratcliffe, M.J.H., and Coulton, J.W. (1994). Genetic insertion and exposure of a reporter epitope in the ferrichrome-iron receptor of *Escherichia coli* K-12. *J. Bacteriol.* 176, 4250-4259.

Moeck, G.S., Tawa, P., Xiang, H., Ismail, A.A., Turnbull, J.L., and Coulton, J.W. (1996). Ligand-induced conformational change in the ferrichrome-iron receptor of *Escherichia coli* K-12. *Mol. Microbiol.* 22, 459-471.

Moeck, G.S. Coulton, J.W., and Postle, K. (1997). Cell envelope signalling in *Escherichia coli*. Ligand binding to the ferrichrome-iron receptor FhuA promotes interaction with the energy-transducing protein TonB. *J. Biol. Chem.* 272, 28391-28397.

Moeck, G.S., and Coulton, J.W. (1998). TonB-dependent iron aquisition: mechanisms of siderophore-mediated active transport. *Mol. Microbiol.* 128, 675-681.

Nikaido, H., and Rosenberg, E.Y. (1990). Cir and Fiu proteins in the outer membrane of *Escherichia coli* catalyze transport of monomeric catechols: study with beta-lactam antibiotics containing catechols and analogous groups. *J. Bacteriol.* 172, 1361-1367.

Pugsley, A.P., Zimmerman, W., and Wehrli, W. (1987). Highly efficient uptake of a rifampicin derivative via the FhuA-TonB-dependent uptake route in *Escherichia coli*. *J. Gen. Microbiol.* 133, 3505-3511.

Schöffler, H., and Braun, V. (1989). Transport across the outer membrane of *Escherichia coli* K12 via the FhuA receptor is regulated by the TonB protein of the cytoplasmic membrane. *Mol. Gen. Genet.* 217, 378-383.

Tuckamn, M., and Osburne, M.S. (1992). *In vivo* inhibition of TonB-dependent processes by a TonB box consensus pentapeptide. *J. Bacteriol.* 174, 320-323.

Vaara, M., Plachy, W.Z., and Nikaido, H. (1990). Partioning of hydrophobic probes into lipopolysaccharide bilayers. *Biochimica et Biophysica Acta.* 1024, 152-158.

Wehrli, W., Zimmermann, W., Kump, W, Tosch W., Vischer, W., and Zak, O. (1987). CGP 4832, a semisynthetic rifamycin derivative highly active against some Gram-negative bacteria. *J. Antibiotics* 40, 1733-1739.

Welte, W., Nestel, U., Wacker, T., and Diederichs, K. (1995). Structure and function of the porin channel. *Kidney Int.* 48, 930-940.

General conclusions and opportunities for research

Prior to the solution of the three-dimensional structure of FhuA, this channel-forming receptor was predicted to form a 32-stranded antiparallel β-barrel (Koebnik & Braun, 1993). One exceptionally long surface-exposed loop, known as the 'gating loop', was believed to mediate the binding of all FhuA-specific ligands, bacteriophages and colicin M (Braun et al., 1998). FepA and BtuB were postulated to have similar topologies and ligand-binding sites (Murphy et al., 1990; Rutz et al., 1992; Lathrop et al., 1995; Newton et al., 1997). By analogy to the constriction loop of porins and their putative mechanism of voltage gating, the gating loops of TonB-dependent receptors were believed to 'gate' the opening and closing of the channel. The energy-transducing protein TonB presumably functions as the 'gate keeper'. This hypothesis lead to the conclusion that TonB-dependent receptors simply function as 'gated porins' (Murphy et al., 1990; Rutz et al., 1992). This widely accepted proposal was supported by the observation that when the linear sequence corresponding to the gating loop was genetically excised, outer membrane receptors form stable nonspecific channels when reconstituted in artificial lipid bilayers (Rutz et al., 1992; Killmann et al., 1993; 1996). However, the idea of large gated porins embedded within the outer membrane ignores (i) outer membrane receptors bind their cognate ligands with high-affinity; (ii) siderophores and vitamin B_{12} are actively pumped into the periplasm of the cell against a concentration gradient; and (iii) the rate of ligand transport by wild-type TonB-dependent receptors at low ligand concentrations is higher than observed with deletion mutants (Reynolds et al., 1980; Killmann et al., 1993).

In contrast to the predicted topological model of FhuA the three-dimensional structure of FhuA revealed that this receptor actually consists of two domains. A 22-stranded antiparallel β-barrel spans the outer membrane; longer extracellular loops and shorter periplasmic turns connect adjacent β-strands. Located inside the β-barrel is a globular domain known as the 'cork'. Three loops of the cork domain extend approximately 20 Å above the plane of the outer membrane to form apex A at Arg81, apex B at Gln100, and apex C at Tyr116. The presence of the cork domain delineates a pair of pockets within the receptor. The extracellular pocket is exposed to the external

medium, while the periplasmic pocket is in direct contact with the periplasm. In the crystallographic structures of FhuA in complex with ferricrocin, phenylferricrocin, albomycin or rifamycin CGP 4832, a single ligand molecule is bound in the extracellular pocket of the receptor. Side-chain residues from the extracellular loops and β-strands of the barrel domain, and apices A, B, and C of the cork domain, form interactions with the ligand. Numerous aromatic side-chain residues line the interior of the extracellular pocket of FhuA, and may function to extract ligand from the external medium; apices A, B, and C form the high-affinity binding site. The binding of hydroxamate-type siderophores to FhuA induces conformational changes in the receptor. Within the ligand-binding site an induced fit mechanism is observed: apices A and B of the cork domain are translated approximately1.5 Å toward the siderophore. This vertical shift is propagated through the outer membrane to the periplasmic pocket of FhuA, culminating in the unwinding of an N-terminal α-helix termed the 'switch helix'. This structural alteration likely signals the liganded conformation of the receptor, and may constitute the structural basis for transmembrane signalling in *E. coli*.

As no significant ion gradient can be maintained across the outer membrane, gram-negative bacteria have developed an intricate method to couple a chemiosmotic gradient that is maintained across the cytoplasmic membrane with ligand uptake (Nikaido & Vaara, 1985; Postle, 1993). The TonB-ExbB-ExbD complex transfers the proton motive force of the cytoplasmic membrane, across the periplasm, to high-affinity outer membrane receptors. All TonB-dependent receptors share one N-terminal segment of conserved primary structure, the 'TonB-box'. This region has been demonstrated to be involved in forming interactions with TonB (Cadieux & Kadner, 1999; Merianos et al., 2000). The liganded status of the receptor and the conformation of TonB influence interactions between these proteins (Larsen et al., 1997; Moeck et al., 1997; Cadieux & Kadner, 1999; Larsen et al., 1999; Merianos et al., 2000). Accordingly, mutations that disrupt the conformation of the TonB-box abrogate TonB-dependent activity (Kadner, 1990). While the structure of TonB-box of FhuA has not been resolved thus far, it has been established that (i) the TonB-box changes its location by approximately 17 Å upon ligand binding; (ii) this segment is localized in the periplasm; and (iii) the accessibility of the TonB-box changes upon the binding of ligand (Ferguson et al., 1998; Locher et al.,

1998). Following the formation of a transient complex, TonB releases its stored conformational energy, by an undefined energy-transduction mechanism, to the outer membrane receptor. The passage of ligand through FhuA is dependent upon the disruption of the high-affinity binding site. When viewed along the barrel axis the extracellular pocket of FhuA is separated from the periplasmic pocket in one region of the barrel by only a thin layer of side-chain residues. This region is referred to as the 'putative channel-forming segment'. Lining the inner barrel wall of the putative channel-forming segment, and extending from the ligand-binding site to the periplasmic pocket of FhuA, are a series of highly conserved side-chain residues. By analogy to the 'greasy slide' of glycoporins, this arrangement of side-chain residues may function as a series of low-affinity ligand-binding sites. A subtle rearrangement of the loops of the cork domain surrounding the putative channel-forming segment of FhuA would suffice to allow for the surface diffusion ligand into the periplasm.

Chapter seven describes the crystallographic structure of FhuA in complex with the rifamycin derivative CGP 4832. While this structurally unrelated antibiotic utilizes the common ligand-binding site within the extracellular pocket of FhuA, the binding of rifamycin CGP 4832 does not promote the unwinding of the switch helix. Paradoxically, FhuA-mediated transport of this antibiotic across the outer membrane of *E. coli* is a TonB-dependent event. This data indicates that although TonB may preferentially interact with outer membrane receptors with unwound switch helices, side-chain residues from one or more periplasmic turns of the β-barrel likely form interactions with TonB of sufficient affinity to allow TonB-dependent transport to occur in the absence of the extended conformation of the TonB-box (Moeck et al., 1997; Braun et al., 1999; Merianos et al., 2000).

The data presented in the experimental chapters of this thesis establishes the three-dimensional structure of a TonB-dependent receptor in the unliganded and various liganded conformations, and has significantly advanced the understanding of the structure-function relationships of FhuA (for a review, see Braun, 1998; Postle, 1999). The crystallographic structure of FhuA and the proposed mechanism for siderophore-mediated iron transport may serve as a model for other TonB-dependent receptors. Information derived from the structures of FhuA in complex with albomycin and

rifamycin CGP 4832 may also be applied to the rational design of novel antibiotics.

The three-dimensional structures of two LPS molecules in complex with FhuA are described in chapter five of this thesis. A conserved LPS-binding motif consisting of four positively charged side-chain residues has been identified on the surfaces of known LPS-binding proteins. This common LPS-binding motif may be used to detect other LPS-binding sites among known crystallographic structures, and may facilitate the design of proteins with altered LPS-binding properties.

The three-dimensional structures of FhuA and FepA now provide a structural foundation from which to better understand the molecular basis of siderophore-mediated iron uptake, and the mechanisms of active transport (Ferguson et al., 1998; Locher et al., 1998; Buchanan et al., 1999). However, crystal structures alone cannot fully reveal the molecular dynamics of these active outer membrane transporters as they undergo energy-dependent conformational changes during the process of ligand transport (Jiang et al., 1997). Insights into the structural determinants of channel formation by FhuA and to assess whether ligand molecules do indeed bind to side-chain residues lining the putative channel-forming segment, could be derived from the three-dimensional structure of FhuA in complex with the bacteriophage tail protein pb5. The binding of bacteriophage T5 to FhuA is regulated by the protein pb5 (Mondigler et al., 1995; 1996). Electrophysiological studies using purified FhuA reconstituted into planar lipid bilayers show that upon pb5-mediated binding of bacteriophage T5, FhuA forms stable high-conductance channels that are presumably identical to those formed *in vivo* (Bonhivers et al., 1996). Accordingly, ferrichrome bound in the ligand-binding site of FhuA is released into the external medium in the absence of TonB (Letellier et al., 1997). The structure of this complex may yield the 'open-channel' conformation of FhuA. Moreover, as observed with the glycoporins, X-ray crystallographic studies may be able 'trap' one or more ligand molecules within a bacteriophage T5-mediated open-channel conformation of FhuA, and thus, confirm the proposed mechanism of ligand transport (Dutzler et al., 1995; Forst et al., 1998).

Given the unexpected results derived from the FhuA-CGP 4832 complex, additional structural data concerning the relationship between the structure of FhuA and its role as the receptor for the cyclic peptide microcin J25 should be collected (Blond et al., 1999).

The determination of this complex would establish whether this structurally and chemically unrelated antibiotic utilizes the common ligand-binding site of FhuA. Could microcin J25 bind to the outer surface of the β-barrel? Does this antibiotic induce FhuA reconstituted in planar lipid bilayers to form channels? Ideally, the structure of FhuA in complex with TonB would provide essential information as to the sites of interactions between these proteins. The introduction of disulphide-bridges, which covalently cross-link FhuA to a C-terminal fragment of TonB, might prove to be useful in the pursuit of this goal (Cadieux & Kadner, 1999).

References

Blond, A., Péduzzi, J., Goulard, C., Chiuchiolo, M.J., Barthélémy, M., Prigent, Y., Salomón, R.A., Farías, R.N., Moreno, F., Rebuffat, S. (1999). The cyclic structure of microcin J25, a 21-residue peptide antibiotic from *Escherichia coli*. *Eur. J. Biochem.* **259**:747-755.

Bonhivers, M., Ghazi, A., Boulanger, P., Letellier, L. (1996). FhuA, a transporter of the *Escherichia coli* outer membrane, is converted into a channel upon binding of bacteriophage T5. *EMBO J.* **15**:1850-1856.

Braun, V., Hantke, K., Köster, W. (1998). Iron transport and storage in microorganisms, plants, and animals. In: A Sigel and H Sigel, (eds.), *Metal Ions in Biological Systems*, Marcel Dekker, New York, pp 67-145.

Braun, V. (1998). Pumping iron through cell membranes. *Science* **282**:2202-2203.

Braun, M., Killmann, H., Braun, V. (1999). The β-barrel domain of FhuAΔ5-160 is sufficient for TonB-dependent FhuA activities of *Escherichia coli*. *Mol. Microbiol.* **33**:1037-1049.

Buchanan, S.K., Smith, B.S., Venkatramani, L., Xia, D., Esser, L., Palnitkar, M., Chakraborty, R., van der Helm, D., Deisenhofer, J. (1999). Crystal structure of the active outer membrane transporter FepA from *Escherichia coli*. *Nature Struct. Biol.* **6**:56-63.

Cadieux, N., Kadner, R.J. (1999). Site-directed disulfide bonding reveals an interaction site between energy-coupling protein TonB and BtuB, the outer membrane cobalamin transporter. *Proc. Natl. Acad. Sci. USA* **96**:10673-10678.

Dutzler, R., Wang, Y-F., Rizkallah, P.J., Rosenbusch, J.P., Schirmer, T. (1995). Crystal structures of various maltooligosaccharides bound to maltoporin reveal a specific sugar translocation pathway. *Structure* **4**:127-134.

Ferguson, A.D., Hofmann, E., Coulton, J.W., Diederichs, K., Welte, W. (1998). Siderophore-mediated iron transport: Crystal structure of FhuA with bound lipopolysaccharide. *Science* **282**:2215-2220.

Ferguson, A.D., Welte, W., Hofmann, E., Lindner, B., Holst, O., Coulton, J.W., Diederichs, K. (2000a). A conserved structural motif for lipopolysaccharide recognition

by procaryotic and eucaryotic proteins. *Structure* In press.

Ferguson, A.D., Braun, V., Fiedler, H-P., Coulton, J.W., Diederichs, K., Welte, W. (2000b). Crystal structure of the antibiotic albomycin in complex with the outer membrane transporter FhuA. *Prot. Science* In press.

Ferguson, A.D., Ködding, J., Coulton, J.W., Diederichs, K., Braun, V., Welte, W. (2000c). Crystal structure of a rifamycin derivative in complex with the active outer membrane transporter FhuA. To be submitted

Feucht, A., Schmid, A., Benz, R., Schwarz, H., Heller, K.J. (1990). Pore formation associated with the tail-tip protein pb2 of bacteriophage T5. *J. Biol. Chem.* **265**:18561-18567.

Forst, D., Welte, W., Wacker, T., Diederichs, K. (1998). Structure of the sucrose-specific porin ScrY from *Salmonella typhimurium* and its complex with sucrose. *Nature Struct. Biol.* **5**:37-46.

Guihard, G., Boulanger, P., Letellier, L. (1992). Involvement of phage T5 proteins and contact sites between the outer and inner membrane of *Escherichia coli* in phage T5 DNA. *J. Biol. Chem.* **267**:3173-3178.

Jiang, X., Payne, M.A., Cao, Z., Foster, S.B., Feix, J.B., Newton, S.M.C., Klebba, P.E. (1997). Ligand-specific opening of a gated porin channel in the outer membrane of living bacteria. *Science* **276**:1261-1264.

Kadner, R.J. (1990). Vitamin B_{12} transport in *Escherichia coli*: energy coupling between membranes. *Mol. Micro.* **4**:2027-2033.

Killmann, H., Benz, R., Braun, V. (1993). Conversion of the FhuA transport protein into a diffusion channel through the outer membrane of *Escherichia coli*. *EMBO J.* **12**:3007-3016.

Killmann, H., Benz, R., Braun, V. (1996). Properties of the FhuA channel in the *Escherichia coli* outer membrane after deletion of FhuA portions within and outside the predicted gating loop. *J. Bacteriol.* **178**:6913-6920.

Koebnik, R., Braun, V. (1993). Insertion derivatives containing segments of up to 16 amino acids identify surface- and periplasm-exposed regions of the FhuA outer membrane receptor of *Escherichia coli* K-12. *J. Bacteriol.* **175**:826-839.

Lathrop, J.T., Wei B.Y., Touchie, G.A., Kadner, R.J. (1995). Sequences of the *Escherichia coli* BtuB protein essential for its insertion and function in the outer membrane. *J. Bacteriol.* **177**:6810-6819.

Larsen, R.A., Foster-Hartnett, D., McIntosh, MA., Postle, K. (1997). Regions of *Escherichia coli* TonB and FepA proteins essential for *in vivo* physical interactions. *J. Bacteriol.* **179**:3213-3221.

Larsen, R.A., Thomas, M.G., Postle, K. (1999). Protonmotive force, ExbB and ligand-bound FepA drive conformational changes in TonB. *Mol. Microbiol.* **31**:1809-1824.

Letellier, L., Locher, K.P., Plançon, L., Rosenbusch, J.P. (1997). Modeling ligand-gated receptor activity. FhuA-mediated ferrichrome efflux from lipid vesicles is triggered by phage T5. *J. Biol. Chem.* **272**:1448-1451.

Locher, K.P., Rees, B., Koebnik, R., Mitschler, A., Moulinier, L., Rosenbusch, R., Moras, D. (1998). Transmembrane signaling across the ligand-gated FhuA receptor: Crystal structures of free and ferrichrome-bound states reveal allosteric changes. *Cell* **95**:771-778.

Merianos, H.J., Cadieux, N., Lin, C.H., Kadner, R.J., Cafiso, D.S. (2000). Substrate-induced exposure of an energy-coupling motif of a membrane transporter. *Nature Struct. Biol.* **7**:205-209.

Moeck, G.S., Coulton, J.W., Postle, K. (1997). Cell envelope signalling in *Escherichia coli*. Ligand binding to the ferrichrome-iron receptor FhuA promotes interaction with the energy-transducing protein TonB. *J. Biol. Chem* **272**: 28391-28397.

Mondigler, M., Vögele, R.T., Heller, K.J. (1995). Overproduced and purified receptor binding protein pb5 of bacteriophage T5 binds to the T5 receptor protein FhuA. *FEMS Lett.* **130**:293-300.

Mondigler, M., Holz, T., Heller, K.J. (1996). Identification of the receptor-binding regions of pb5 proteins of bacteriophage T5 and BF23. *Virology* **219**:19-28.

Murphy, C.K., Kalve, V.I., Klebba, P.E. (1990). Surface topology of the *Escherichia coli* K-12 ferric enterobactin receptor. *J. Bacteriol.* **172**:2736-2746.

Newton, S.H.C., Allen, J.S., Cao, Z., Qi, Z., Jiang, X., Sprencel, C., Igo, J.D., Foster, S.B., Payne, M.A., Klebba, P.E. (1997). Double mutagenesis of a positive charge

cluster in the ligand-binding site of the ferric enterobactin receptor, FepA. *Proc. Natl. Acad. Sci. USA* **94**:4560-4565.

Nikaido, H., Vaara, M. (1985). Molecular basis of bacterial outer membrane permeability. *Microbiol. Rev.* **49**:1-32.

Plançon, L., Chami, M., Letellier, L. (1997). Reconstitution of FhuA, an *Escherichia coli* outer membrane protein, into liposomes. *J. Biol. Chem.* **272**:16868-18872.

Postle, K. (1993). TonB protein and energy transduction between membranes. *J. Bioenerg. Biomemb.* **25**:591-601.

Postle, K. (1999). Active transport by customized β-barrels. *Nature Struct. Biol.* **6**:3-6.

Reynolds, P.R., Mottur, G.P., Bradbeer, C. (1980). Transport of vitamin B_{12} in *Escherichia coli*. Some observations on the role of the gene products of *btuC* and *tonB*. *J. Biol. Chem.* **255**:4313-4319.

Rutz, J.M., Liu, J., Lyons, J.A., Goranson, J., Armstrong, S.K., McIntosh, M.A., Feix, J.B., Klebba, P.E. (1992). Formation of a gated channel by a ligand-specific transport protein in the bacterial outer membrane. *Science* **258**:471-475.